Studying gravitational waves of compact binary systems using post-Newtonian theory

Tanguy Marchand

▶ To cite this version:

Tanguy Marchand. Studying gravitational waves of compact binary systems using post-Newtonian theory. Other [cond-mat.other]. Sorbonne Université, 2018. English. NNT : 2018SORUS121 . tel-02325598

THÈSE DE DOCTORAT
DE L'UNIVERSITÉ SORBONNE UNIVERSITÉ

Spécialité : Physique

École doctorale n°564: Physique en Île-de-France

réalisée

à l'Institut d'Astrophysique de Paris

sous la direction de Luc BLANCHET

présentée par

Tanguy MARCHAND

pour obtenir le grade de :

DOCTEUR DE L'UNIVERSITÉ SORBONNE UNIVERSITÉ

Sujet de la thèse :

Études des ondes gravitationnelles des binaires compactes à l'approximation post-newtonienne.

soutenue le 15 Juin 2018

devant le jury composé de :

Clifford M. WILL	Rapporteur
Edward K. PORTER	Rapporteur
Pierre FAYET	Examinateur
Eric GOURGOULHON	Examinateur
Cristina VOLPE	Examinatrice
David LANGLOIS	Membre invité
Luc BLANCHET	Directeur de thèse

Acknowledgements

In the first place, I would like to thank Luc Blanchet, who has supervised my thesis at the Institut d'Astrophysique de Paris, and has brought me into the field of post-Newtonian theory. I would also like to thank Guillaume Faye, with whom I have closely worked, and who spent a lot of time answering my questions on post-Newtonian theory, on Mathematica and on the different libraries he coded over the years. Besides, I also thank David Langlois, who has co-supervised my thesis, and has provided useful advice and guidance over these three years.

I would also like to thank the different people working on post-Newtonian theory and with whom I have either exchanged or worked with during this thesis: Laura Bernard, Sylvain Marsat, Alejandro Bohé, Alexandre le Tiec and Cliff Will. The formal meetings as well as all the informal discussions I have been able to held with them consequently enhanced my understanding of post-Newtonian theory.

I would also like to thank warmly Eric Gourgoulhon, Cristina Volpe, and Pierre Fayet to be part of my PhD jury, and more particularly Cliff Will and Ed Porter for having accepted to be the referees of this PhD thesis.

Eventually, I would like to thank all the people I have interacted with during this thesis, either for scientific purposes, or for any other reason. In particular, I would like to thank the different PhD students of the Institut d'Astrophysique de Paris.

Contents

Introduction

Less than three years ago, the first direct detection of gravitational waves by the LIGO–Virgo collaboration on the 14^{th} of September 2015, opened a new window on our universe and a new domain in our field of science: gravitational wave astrophysics. This breakthrough is the result of decades of theoretical and experimental research in general relativity. In fact, gravitational waves were mentioned for the first time in 1916 by Albert Einstein, even though the theoretical community were convinced of their existence much later. Experimental efforts to detect them started in the 1960s, and their first detection in 2015 results both from the technological developments made to improve gravitational-wave detectors as well as theoretical research aiming at predicting gravitational waveforms.

Hence, the different tools used to study general relativity and predict gravitational waves from astrophysical events have played a crucial role in this discovery. It is today extremely important to enhance our models and our gravitational wave templates as much as possible as the quality of the science we will produce from gravitational wave astrophysics will depend on them. In fact, the better our templates are, the better the signal-to-noise ratio of our observations are, the more accurate our parameter estimations (masses, spins, distances etc.) of the observed events are. The validity and the robustness of the astrophysical catalogs we might build in the next years and decades highly depend on the effort we spend enhancing our understanding on how extremely accurate predictions from general relativity can be obtained.

In the landscape of formalisms available to understand gravitational waves, the post-Newtonian theory is a method to compute physical quantities in an analytical and perturbative manner. The perturbative parameter used is v/c, where v is the typical velocity of the matter source and c is the speed of light, and a n^{th} post-Newtonian order corresponds to a factor $(v/c)^{2n}$. We are going to use this formalism in this manuscript to study and understand the dynamics and the emission of gravitational waves from compact binary systems, i.e., from systems made of two compact objects (such as black holes or neutron stars). The end result of our formalism is either physical gauge-independent quantities — such as the phase of the gravitational wave signal — that can be used to build templates, or to cross-validate other methods of computation (such as black hole perturbation approaches or numerical relativity). However, most results are given in terms of intermediate gauge-dependent results such as the equations of motion. They are also of interest as they can be compared with other formalisms, modulo coordinate transformations, and corroborate our understanding of the various techniques used in general relativity.

In this thesis, we worked on the study of compact binary systems using the post-Newtonian theory, and in particular the Blanchet-Damour-Iyer formalism, in order to enhance our understanding of the dynamics and the emission of gravitational waves by such systems.

The thesis is organized as follows. Chapter 1 is an introduction to the linearized theory of general relativity and to gravitational waves. Different equations, such as the Einstein quadrupole formulae are provided in order to explain the notion of gravitational waves as well as their effects on matter systems and get rough orders of magnitude.

In chapter 2, we focus on the detection of gravitational waves. In particular, the different possible sources are reviewed and we tackle the design of gravitational wave detectors, the different formalisms used to build templates as well as the data analysis techniques used by the LIGO–Virgo collaboration. These first two chapters are rather introductory and can be skipped by a reader who is already familiar with this field and wants to jump directly into the technical details of post-Newtonian computations.

Chapter 3 is an overall review of the field of post-Newtonian theory describing in particular the state-of-the-art results in that domain. We describe the different relevant quantities that can be computed using post-Newtonian theory and explain the overall goal motivating the different computations done throughout the thesis.

In chapter 4 we describe the multipolar-post-Minkowskian algorithm which is a building block of the Blanchet-Damour-Iyer formalism, and we obtain new results regarding the highly non-linear *third-order tail* effect in the radiative field, in particular we compute the 4.5 post-Newtonian order coefficient of the energy flux of spinless compact binary systems in circular orbits.

Chapter 5 is a rather short but highly technical chapter describing the cornerstone of our framework: the matching procedure. The matching procedure is omnipresent in our formalism and enables to relate the multipolar-post-Minkowskian expansion done in chapter 4 to the near-zone computations of the post-Newtonian field and to the equations of motion done in chapters 6-7-8.

In chapters 6 and 7, we start from the recently derived equations of motion of a spinless compact binary system at the fourth post-Newtonian order, and we compute the last ambiguity parameter in these equations of motion. Then the dynamics of such systems is studied through the computation of the different Noetherian conserved quantities.

Finally, chapter 8 describes the computation of the source moment multipoles and in particular the source mass quadrupole at the fourth post-Newtonian order, linking the dynamics of a compact binary system, to its emission of gravitational waves. This chapter constitutes a major step in the program of computing the radiation field at the fourth post-Newtonian order.

The work done during this thesis has led to several new results described throughout the manuscript: (i) the computation of the third-order tail effect and the coefficient at the 4.5 post-Newtonian order of the energy flux for spinless binary systems in circular orbits detailed in chapter 4, (ii) the computation of the last ambiguity of the Fokker Lagrangian as described in section 6.2.2, completing therefore the first ambiguity free derivation of the fourth post-Newtonian order of the equations of motion of spinless compact bodies from first principles, (iii) the derivation of the different conserved quantities of the fourth post-Newtonian order dynamics detailed in chapter 7 and finally (iv) the preliminary results of the computation of the mass quadrupole at the fourth post-Newtonian order provided in chapter 8.

These results have led to the following publications during this thesis:

1. T. Marchand, L. Blanchet, G. Faye *Gravitational-wave tail effects to quartic non-linear order*, Class. Quant. Grav. **33** (2016) no.24, 244003 [1]

2. T. Marchand, L. Bernard, L. Blanchet, G. Faye *Ambiguity-Free Completion of the Equations of Motion of Compact Binary Systems at the Fourth Post-Newtonian Order* Phys. Rev. D **97** (2018) no.4, 044023 [2]

3. L. Bernard, L. Blanchet, G. Faye, T. Marchand *Center-of-Mass Equations of Motion and Conserved Integrals of Compact Binary Systems at the Fourth Post-Newtonian Order* Phys. Rev. D **97** (2018) no.4, 044037 [3]

Besides, the following paper in preparation will contain the material described in chapter 8:

4. T. Marchand, G. Faye, L. Blanchet, *Hadamard regularization of the mass quadrupole moment of compact binary systems at the fourth post-Newtonian order*, in prep [4]

We should mention that significant parts of the chapters 4, 6 and 7 are directly extracted from the publications listed above.

1 – Introduction to gravitational waves and to the linearized theory of general relativity

1.1 Short history of the theory of gravitational waves

The history of general relativity started in 1915, with the paper of Albert Einstein *Die Grundlage der allgemeinen Relativitätstheorie* (*The Foundation of the General Theory of Relativity*) [5] containing the Einstein field equations and providing the foundations of general relativity. This theory automatically recovers Newton's laws of gravitation in the weak field limit, can explain the previously observed anomalous advance of the perihelion of Mercury and predicts the bending of light rays near massive bodies (this last prediction would be confirmed in 1919 during a solar eclipse by an expedition led by Eddington).

As soon as 1916, using a perturbation of the metric on top of the Minkowski metric [6], Einstein predicted the existence of wave solutions for the metric in vacuum. Two years later, in 1918 [7], he derived the Einstein quadrupole formula for the energy flux, but his proof did not apply to self-gravitating systems. Curiously enough, his result in this paper was wrong by a factor 1/2. A new step was done in 1922 when Eddington [8] isolated the two degrees of freedom of gravitational waves in the transverse and traceless gauge, enhancing the understanding of the physical reality of gravitational waves. However, it was still unclear at that time whether gravitational waves were physical or were just an artifact of a specific choice of a coordinate system. It would be rather long to comprehensively list all the steps in the controversy that occurred at that time regarding the reality of gravitational waves, and we refer to [9] for further readings on that topic. This controversy was solved in the late 1950s [10, 11, 12] when it was shown once for all that gravitational waves carry energy and therefore correspond to a physical reality.

These theoretical breakthroughs were corroborated by the study of the equations of motion in general relativity of N point-particles that started as soon as 1917 by Lorentz and Droste deriving the first order correction in $\left(\frac{v}{c}\right)^2$ to Newton's law of physics [13] (the so-called 1 post-Newtonian equations of motion)[1]. The study of these equations of motion to high post-Newtonian orders are still an active field of research, and a historical review of the different results in that field will be done in detail in chapter 3. Let us just mention here, that

[1] In post-Newtonian theory, a n post-Newtonian term (or a n-PN term) in a formula corresponds to a correction at the $\left(\frac{v}{c}\right)^{2n}$ order where v is the speed of the considered bodies and c the speed of light. In order to be more general, we discard v and define the n^{th} PN order to be a correction at the $\frac{1}{c^{2n}}$ order.

the emission of gravitational waves of a binary system predicted by the Einstein quadrupole formula leads to a loss of energy of the system that explicitly appears in the equations of motion at the 2.5 post-Newtonian order (i.e. at $\mathcal{O}\left[(v/c)^5\right]$), and which was computed for fluids in the early 1970s by Chandrasekar and Esposito [14], Burke and Thorne [15, 16], as well as many others (cf chapter 3 or [17] for a review) and for point-particle later in 1981 by Damour and Deruelle [18].

As we will see in section 1.4, the discovery in 1974 of the pulsar PSR1913+16 by Hulse and Taylor [19], and its study led to the first observational evidence of the loss of energy of a binary system through the emission of gravitational waves. This discovery earned Hulse and Taylor the Nobel Prize in 1993 for "*new type of pulsar, a discovery that has opened up new possibilities for the study of gravitation*".

In parallel, since the 1960s, experimental efforts were conducted to detect directly on Earth these gravitational waves. In the University of Maryland, Joseph Weber developed the first gravitational wave detectors made of resonance bars. While he claimed to have detected some signals, his result could not be reproduced by other teams and no convincing detections were made using resonance bars. In the late 1960s, the idea of using laser interferometry to detect gravitational waves emerged and pioneer works in the US and in Europe led to the construction of different kilometer-scale laser interferometers (cf section 2.1 for a historical review of these detectors). It would have required more than 50 years of experimental and theoretical developments, to do the first direct detections on Earth of these gravitational waves and to start a new era of physics by opening the windows of gravitational astrophysics.

1.2 The linearized theory of general relativity and gravitational waves

This section is an introduction to gravitational waves and the linearized theory of general relativity. It summarizes materials that can be found in a lot of different textbooks. For a more comprehensive derivation of the following results, we refer to a classical textbook in gravitational wave such as the first chapters of [20].

1.2.1 The linearized Einstein equations

In general relativity, the space-time is described by a manifold $\mathcal{M}$ of dimension 4 together with a metric $g_{\mu\nu}$ which is a symmetric and non-degenerate two-rank tensor of signature +2 on that manifold. The Einstein equations, describing how the matter curves the space-time are a set of second-order differential equations of the metric $g_{\mu\nu}$ sourced by the stress-energy tensor $T_{\mu\nu}$

$$R_{\mu\nu}(g,\partial g,\partial\partial g) - \frac{1}{2}g_{\mu\nu}R(g,\partial g,\partial\partial g) = \frac{8\pi G}{c^4}T_{\mu\nu}\,, \tag{1.1}$$

where G is Newton's constant, c the speed of light and the notation $R_{\mu\nu}(g,\partial g,\partial\partial g)$ means that the tensor $R_{\mu\nu}$ depends on the metric and its first and second space-time derivatives. The left-hand side of the Einstein equations (1.1) is called the Einstein tensor $G_{\mu\nu} = R_{\mu\nu} - \frac{1}{2}g_{\mu\nu}R$ and depends on the Ricci tensor $R_{\mu\nu}$ and the scalar curvature R. Both of these quantities are built from the Riemann curvature tensor. In order to be able to write explicitly the Einstein equations in term of the metric, let us provide the expression of the Riemann tensor as a function of the metric

$$R^{\lambda}{}_{\rho\mu\nu} = \partial_\mu \Gamma^{\lambda}_{\rho\nu} - \partial_\nu \Gamma^{\lambda}_{\mu\rho} + \Gamma^{\epsilon}_{\rho\nu}\Gamma^{\lambda}_{\epsilon\mu} - \Gamma^{\epsilon}_{\mu\rho}\Gamma^{\lambda}_{\epsilon\nu} \,. \tag{1.2}$$

There exists different sign conventions in general relativity; the conventions, and the notations used in this manuscript are listed in the appendix A. In particular, greek indices $\alpha, \beta, \ldots$ take their values in $0, \ldots, 3$ while latin indices $i, j, k, \ldots$ take their values in $1, \ldots, 3$. We used the Einstein convention to sum over the indices that are repeated. The symbol $\Gamma^{\alpha}_{\mu\nu}$ represents the Christoffel symbol which is defined as

$$\Gamma^{\mu}_{\nu\rho} = \frac{1}{2} g^{\mu\lambda} \left(\partial_\nu g_{\rho\lambda} + \partial_\rho g_{\nu\lambda} - \partial_\lambda g_{\nu\rho} \right) \,. \tag{1.3}$$

It is worth noticing that unlike all the other quantities presented so far, the Christoffel symbol is not a tensor, as it does not transform like a tensor under diffeomorphisms.

Eventually, the Ricci scalar is defined as $R_{\mu\nu} = R^{\lambda}{}_{\mu\lambda\nu}$ and the curvature scalar as $R = R_{\mu\nu} g^{\mu\nu}$. Plugging equation (1.3) in equation (1.2) we can explicitly express the Einstein equations as a function of the metric. This leads however to quite a cumbersome expression and we only want to look at the linear theory for now. Therefore we are going to develop the Einstein equations around flat space-time and define the trace-reverse variable

$$g_{\mu\nu} = \eta_{\mu\nu} + h_{\mu\nu} \,, \tag{1.4}$$

where $\eta_{\mu\nu} = \mathrm{diag}(-, +, +, +)$ is the Minkowski metric and where $|h_{\mu\nu}| \ll 1$. From now on, all the indices will be raised and lowered using the Minkowski metric $\eta_{\mu\nu}$. Besides, when using the Einstein convention to sum over spatial indices $i, j, k, \ldots$ we may sometime omit to put one of the summed indices up, and the other one down (i.e. h_{ii} is the same quantity than $h^{i}{}_{i}$). Before rewriting the Einstein equations in the linearized theory, it is convenient to define

$$\bar{h}_{\mu\nu} = h_{\mu\nu} - \frac{1}{2}\eta_{\mu\nu} h \,, \tag{1.5}$$

where $h = h_{\mu\nu}\eta^{\mu\nu}$. A rather fastidious but straightforward computation shows that to order $\mathcal{O}(h)$ we have

$$\Box \bar{h}_{\mu\nu} + \eta_{\mu\nu}\partial^\rho \partial^\sigma \bar{h}_{\rho\sigma} - \partial^\rho \partial_\nu \bar{h}_{\mu\rho} - \partial^\rho \partial_\mu \bar{h}_{\nu\rho} = -\frac{16\pi G}{c^4} T_{\mu\nu} \,, \tag{1.6}$$

where $\Box = -\frac{1}{c^2}\frac{\partial^2}{\partial t^2} + \delta^{ij}\frac{\partial}{\partial x^i}\frac{\partial}{\partial x^j} = -\frac{1}{c^2}\frac{\partial^2}{\partial t^2} + \Delta$ is the d'Alembert operator (or the d'Alembertian) and where Δ is known as the Laplace operator. All the terms of order $\mathcal{O}(h^2)$ or higher have been discarded. As h is of order $\mathcal{O}(G)$ (where G is Newton constant) as wee see from solving the equation (1.6), it means that we have discarded terms of order $\mathcal{O}(G^2)$. It is important to keep that fact in mind because it implies that the formulae derived in the following sections are only true up to $\mathcal{O}(G)$.

1.2.2 Gravitational wave solution to the vacuum linearized Einstein equations

Before solving the linearized Einstein equations (1.6), we are going to use the diffeomorphism invariance of general relativity to put ourself in a nice and convenient gauge coordinate system. In fact, under the general diffeomorphism

$$x^\mu \to x'^\mu(x) \,, \tag{1.7}$$

the metric transforms as

$$g_{\mu\nu}(x) \to g'_{\mu\nu}(x') = \frac{\partial x^\rho}{\partial x'^\mu}\frac{\partial x^\sigma}{\partial x'^\nu} g_{\rho\sigma}(x)\,. \tag{1.8}$$

In the case of linear coordinate transformation, we can consider

$$x^\mu \to x'^\mu = x^\mu + \xi^\mu(x)\,, \tag{1.9}$$

with $|\partial\xi^\mu| = \mathcal{O}(h_{\mu\nu}) = \mathcal{O}(\bar{h}_{\mu\nu})$. In that case, using equation (1.8), we can show that $\bar{h}_{\mu\nu}$ transforms as

$$\bar{h}_{\mu\nu} \to \bar{h}'_{\mu\nu} = \bar{h}_{\mu\nu} - (\partial_\mu\xi_\nu + \partial_\nu\xi_\mu - \eta_{\mu\nu}\partial_\rho\xi^\rho)\,. \tag{1.10}$$

Therefore, we have $\partial^\mu\bar{h}_{\mu\nu} \to \partial^\mu\bar{h}_{\mu\nu} - \Box\xi_\nu$ under that coordinate transformation. Hence if $\partial^\mu\bar{h}_{\mu\nu}$ is not vanishing, we can choose a set of functions ξ_μ and perform a coordinate transformation as in equation (1.9) such that we place ourself in a gauge where

$$\partial^\nu\bar{h}_{\mu\nu} = 0\,. \tag{1.11}$$

This kind of gauge transformation will be explicitly done in section 4.1. This specific gauge is the linear case of the harmonic gauge also called the De Donder gauge or the Lorenz gauge[2], which will be the gauge used in chapters 4-5-6-7-8. In fact we will later introduce the quantity[3] $\tilde{h}^{\mu\nu} = \sqrt{-g}g^{\mu\nu} - \eta^{\mu\nu}$ and the harmonic gauge will be obtained by setting $\partial_\mu\tilde{h}^{\mu\nu} = 0$. This is in total consistency with what we are doing in the linearized case as we can show that $\tilde{h}_{\mu\nu} \equiv \tilde{h}^{\alpha\beta}\eta_{\alpha\mu}\eta_{\beta\nu} = -\bar{h}_{\mu\nu} + \mathcal{O}(\bar{h}^2)$. In that gauge, equation (1.6) becomes

$$\Box\bar{h}_{\mu\nu} = -\frac{16\pi G}{c^4}T_{\mu\nu}\,. \tag{1.12}$$

Considering solutions of gravitational waves in vacuum we can set $T_{\mu\nu} = 0$

$$\Box\bar{h}_{\mu\nu} = 0\,. \tag{1.13}$$

We are going to use again the coordinate transformation (1.9) to simplify the result. In fact, as long as $\Box\xi^\mu = 0$, according to equation (1.10), the equation (1.13) remains unchanged. This provides us 4 degrees of freedom that we can kill using the four functions ξ_μ ($\mu = 0, 1, 2,$ or 3). Said otherwise, we can set 4 new constraints. Let us first set $\bar{h} = 0$, which automatically implies that $h_{\mu\nu} = \bar{h}_{\mu\nu}$. We will from now on drop the bar symbol on top of $h_{\mu\nu}$. We can set the three following constraints $h^{0i} = 0$ (we recall that $i = 1, 2$ or 3). According to harmonic gauge condition, we automatically have that $\partial^0 h_{00} = 0$. As we are looking for gravitational waves on top of a background (here the flat background), we can drop any constant term in $h_{\mu\nu}$. Adding up everything we mentioned, and taking into account the components of $h_{\mu\nu}$ that vanish, we have to solve the following system

$$\Box h_{\mu\nu} = 0,\; h^{0\mu} = 0,\; \partial^i h_{ij} = 0,\; h^i{}_i = 0,\; h_{ij} = h_{ji}\,. \tag{1.14}$$

[2]This gauge is called the *Lorenz* gauge after the Danish physicist Ludvig Valentin Lorenz (1829-1891) and not the *Lorentz* gauge after the Dutch physicist Hendrik Antoon Lorentz (1853-1928). The latter gave his name to the Lorentz transformation, the electromagnetic Lorentz force but not to the Lorenz gauge. This confusion is quite common in the literature.

[3]This quantity will be denoted h in the chapters 4-5-6-7-8, but we denote it $\tilde{h}$ here to avoid any confusion.

The gauge we introduced by imposing $h^{\mu}{}_{\mu} = 0$ and $\partial^{\mu} h_{\mu\nu} = 0$ is called the transverse-traceless gauge, which is often abbreviated as the TT-gauge. We will refer to that gauge by using the notation $h^{TT}_{\mu\nu}$. The general solution of this set of equations will be a sum (or, in Fourier space an integral) of elementary solutions corresponding to a gravitational wave. The elementary solution of (1.14) corresponding to a gravitational wave of frequency $\omega/(2\pi)$ and propagating along a direction $\boldsymbol{z}$[4] is

$$h^{TT}_{\mu\nu}(\boldsymbol{x}, \boldsymbol{y}, \boldsymbol{z}) = \begin{pmatrix} 0 & 0 & 0 & 0 \\ 0 & h_+ & h_\times & 0 \\ 0 & h_\times & -h_+ & 0 \\ 0 & 0 & 0 & 0 \end{pmatrix} , \tag{1.15}$$

where $h_+ = A_+ \cos(\omega[t - z/c] + \varphi_+)$ and $h_\times = A_\times \cos(\omega[t - z/c] + \varphi_\times)$, where $A_{+,\times}$ and $\varphi_{+,\times}$ are constant. We can see from (1.15) that a gravitational wave has two polarizations that are denoted h_+ and $h_\times$ with amplitudes A_+ and $A_\times$ and phases φ_+ and $\varphi_\times$. One could wonder whether these two polarizations are physical or if one of them can be removed by a new change of coordinate. This will be the purpose of the next section.

1.2.3 Effect of gravitational waves on matter

Indeed, it is always important to keep in mind that in general relativity, only observables correspond to physical quantities and that a feature in the metric does not automatically correspond to a physical effect but could be only due to a coordinate artifact. It is therefore crucial, in order to interpret equation (1.15), to see the response of test masses to this metric.

Let us consider a test mass A moving on the wordline $X^{\alpha}_{A}(\tau)$. The wordline X^{α}_{A} is determined in general relativity by the following geodesic equation

$$\frac{\mathrm{d}^2 X^{\alpha}_{A}}{\mathrm{d}\tau^2} + \Gamma^{\alpha}_{\mu\nu} \frac{\mathrm{d}X^{\mu}_{A}}{\mathrm{d}\tau} \frac{\mathrm{d}X^{\nu}_{A}}{\mathrm{d}\tau} = 0 \,. \tag{1.16}$$

Let us assume that the mass A is at $\tau = \tau_0$ at rest. Then $\frac{\mathrm{d}X^{i}_{A}}{\mathrm{d}\tau}(\tau_0) = 0$ and $\frac{\mathrm{d}X^{0}_{A}}{\mathrm{d}\tau}(\tau_0) = c$ and for $\alpha = i$ the geodesic equation (1.16) at $\tau = \tau_0$ becomes

$$\frac{\mathrm{d}^2 X^{i}_{A}}{\mathrm{d}\tau^2} + \Gamma^{i}_{00} c^2 = 0 \,. \tag{1.17}$$

However, by using the definition of the Christoffel symbol (1.3) and the harmonic gauge condition we find $\Gamma^{i}_{00} = \mathcal{O}(h^2)$. Therefore, at linear order, a test mass at rest in the TT frame, remains at rest. Let us consider two nearby masses A and B at rest in the TT frame. Their coordinates are $X^{0}_{A}(\tau) = c\tau$, $X^{i}_{A}(\tau) = x^{i}_{A}$ which is constant, and $X^{0}_{B}(\tau) = c\tau$, $X^{i}_{A}(\tau) = x^{i}_{B}$ which is also constant. Let us denote $L^i = x^{i}_{B} - x^{i}_{A}$ and $L = \sqrt{L^i L_i}$. At a given time τ, the distance between the points A and B can be inferred from the square root of the following interval quantity $\Delta = \sqrt{\mathrm{d}s^2}$

$$\mathrm{d}s^2 = g_{\mu\nu} \mathrm{d}x^{\mu} \mathrm{d}x^{\nu} \,. \tag{1.18}$$

[4] $\boldsymbol{z}$ is the direction corresponding to the space index $i = 3$. Similarly $\boldsymbol{x}$ and $\boldsymbol{y}$ are the direction corresponding to the space indices $i = 1$ and $i = 2$.

By considering a general linear metric in the TT-gauge, we obtain to linear order

$$\Delta = L + h_{ij}^{TT}\frac{L_i L_j}{2L}\,. \tag{1.19}$$

Considering the gravitational waves propagating along $\boldsymbol{z}$ at the frequency $\frac{\omega}{2\pi}$ described in the equation (1.15), the distance Δ between two nearby point becomes

$$\Delta = L\left[1 + \frac{A_+\cos\left(\omega[t-z/c]+\varphi_+\right)(L_x^2 - L_y^2) - 2A_\times\cos\left(\omega[t-z/c]+\varphi_\times\right)L_x L_y}{2L^2}\right]\,, \tag{1.20}$$

where we have used the notations $L_x = L^{i=1}$ and $L_y = L^{i=2}$.

It is important to keep in mind that this distance is an observable. In fact, let us assume that an observer with a clock device at the point A sends a light ray at the time τ to the point B, which is reflected and sent back and reaches the point A at the time $\tau+\delta\tau$. As long as the distance between A and B is small with respect to the gravitational wavelength, the proper distance between the point A and B will be given by $\Delta = c\delta\tau/2$. As $\delta\tau$ can be measured by an observer at the point A, so can Δ. We can now assert that the gravitational wave solution described in the previous section has a real physical effect that can be measured, and contains two different polarizations. The geometrical effect of these polarizations is described in the figure 1.1.

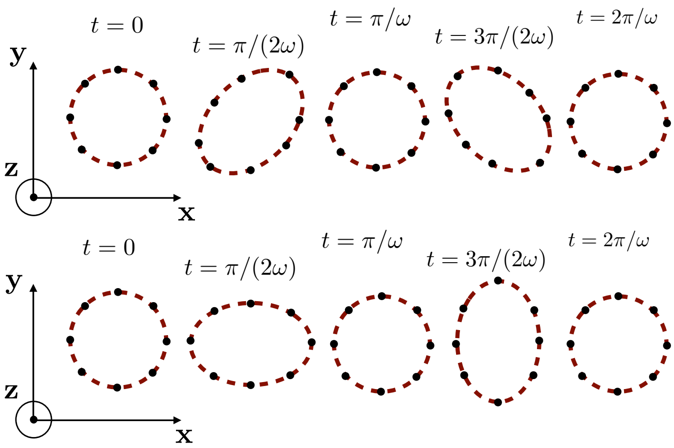

Figure 1.1: Effect of a gravitational wave of pulsation ω propagating along the $\boldsymbol{z}$ direction on test particles. Top: polarization $h_\times$. Bottom: polarization h_+.

1.3 The Einstein quadrupole formulae

Now that we have understood how gravitational waves propagate and interact with matter in the linearized theory of general relativity, we are going to relate the emission of gravitational waves at linear order to the *mass quadrupole* of a source. For that we need to go back to equation (1.12)

$$\Box\bar{h}_{\mu\nu} = -\frac{16\pi G}{c^4}T_{\mu\nu} + \mathcal{O}(\bar{h}^2)\,. \tag{1.21}$$

We recall that $\Box = -\frac{1}{c^2}\frac{\partial^2}{\partial t^2} + \delta^{ij}\frac{\partial}{\partial x^i}\frac{\partial}{\partial x^j} = -\frac{1}{c^2}\frac{\partial^2}{\partial t^2} + \Delta$ is the *flat* d'Alembert operator. We want to solve (1.21) in the case of an isolated source imposing the non-incoming radiation condition. This means, that no gravitational wave should arrive from infinity to the source. This is done by applying the *retarded* d'Alembert operator and leads to:

$$\bar{h}_{\mu\nu}(t,\boldsymbol{x}) = \frac{4G}{c^4}\int \mathrm{d}^3\boldsymbol{x}'\frac{T_{\mu\nu}(t-\frac{|\boldsymbol{x}-\boldsymbol{x}'|}{c},\boldsymbol{x}')}{|\boldsymbol{x}-\boldsymbol{x}'|}\,. \tag{1.22}$$

By doing a multipolar expansion of the right-hand side of (1.22), we can express the metric as a function of the mass quadrupole of the source. This derivation is done in detail in a lot of different textbook (see for example [20]), and reads in TT coordinate:

$$h_{ij}^{TT}(t,\boldsymbol{x}) \approx \frac{2G}{c^4 r}\Lambda_{ij}{}^{kl}\frac{\mathrm{d}^2 I_{kl}}{\mathrm{d}t^3}\left(t-\frac{r}{c}\right)\,, \tag{1.23}$$

where $\Lambda_{ij,kl}$ is the TT-projector defined by $\Lambda_{ij,kl} = P_{ik}P_{jl} - \frac{1}{2}P_{ij}P_{kl}$ where $P_{ij}(\boldsymbol{x}) = \delta_{ij} - n_i n_j$, where $n_i = x_i/r$ and where x_i is the vector $\boldsymbol{x}$. I_{ij} represent the symmetric trace-free (STF) part of the mass quadrupole. It is defined at linear order by

$$I_{ij} = \int \mathrm{d}^3\boldsymbol{x}\rho(\boldsymbol{x})x_{<i}x_{j>}\,, \tag{1.24}$$

where ρ is the mass density of the source, and the brackets $<\cdot>$ represent the STF operator: $x_{<i}x_{j>} = \frac{1}{2}(x_i x_j + x_j x_i) - \frac{1}{3}r^2\delta_{ij}$.

1.3.1 Einstein quadrupole formulae for the energy and angular momentum fluxes

The gravitational waves emitted by an isolated source, and given by (1.23) at linear order, carry energy as well as angular momentum. The derivations of their fluxes at the leading order are done in different textbooks (such as [20]), and we are going to extend them to much higher orders in chapter 4 (cf in particular equation (4.122)). Therefore, we are going to provide them at linear order here, without further proof. The energy flux $\mathcal{F}$ and the angular momentum flux $\mathcal{G}_i$ of an isolated source emitted gravitational waves are given by

$$\mathcal{F} = \frac{G}{c^5}\left[\frac{1}{5}\frac{\mathrm{d}^3 I_{ab}}{\mathrm{d}t^3}\frac{\mathrm{d}^3 I_{ab}}{\mathrm{d}t^3} + \mathcal{O}\left(\frac{1}{c^2}\right)\right]\,, \tag{1.25}$$

$$\mathcal{G}_i = \frac{G}{c^5}\left[\frac{2}{5}\epsilon_{iab}\frac{\mathrm{d}^2 I_{ac}}{\mathrm{d}t^2}\frac{\mathrm{d}^3 I_{bc}}{\mathrm{d}t^3} + \mathcal{O}\left(\frac{1}{c^2}\right)\right]\,, \tag{1.26}$$

where ϵ_{abc} is the Levi-Civita symbol ($\epsilon_{123} = 1$). We recall that we used the Einstein convention to sum over repeated indices. When these indices are space-time indices, as the background metric is the Minkowski metric, we do not systematically raise one of the repeated indices.

For a binary system, this loss of energy and angular momentum has two consequences. First of all, the separation of the two companion objects will slowly decrease and they may end up merging eventually. Secondly, if a binary system has some eccentricity e (i.e. if its orbit is not circular), we will see in section 1.3.2 that these fluxes lead to decrease the eccentricity and circularize the orbit. Therefore, the usual gravitational wave source that we are often going to consider is made of two masses orbiting each other on circular orbits, getting closer and closer and eventually merging.

1.3.2 Some applications of the Einstein quadrupole formulae and orders of magnitude

Magnitude of gravitational waves Let us consider a system of two masses of equal mass M orbiting around each other at a distance r_{12}. If we drop all the numerical coefficients in order to just study the order of magnitude of the metric $h = |h_{ij}^{TT}|$ we have from equation (1.23)

$$h \sim \frac{1}{r} \frac{G^2 M^2}{c^4 r_{12}} \,. \tag{1.27}$$

For a source of size a and of mass M we define the compactness as $\Xi = \frac{GM}{ac^2}$. The compactness of a source is a dimensionless number who is smaller than $\frac{1}{2}$ and whose value is $\frac{1}{2}$ for a non-spinning black hole in Schwarzschild coordinates. Therefore, for a system of two black holes of masses $M/2$ and a separation r_{12} orbiting each other and eventually merging, the value of Ξ of the binary system will be $\Xi = \frac{GM}{r_{12}c^2}$. This value of Ξ will slowly increase as the two black holes get closer and will reach $\frac{1}{2}$ when the two objects merge into a final black hole. For a single isolated neutron star, $\Xi \sim 0.2$, for a white dwarf $\Xi \sim 10^{-4} - 10^{-3}$, for the Sun $\Xi \sim 2\ 10^{-6}$ and for the Earth $\Xi \sim 7\ 10^{-10}$. By using this notation (1.27) becomes

$$h \sim 10^{-20}\ \Xi \left(\frac{M}{M_\odot}\right)\left(\frac{1\mathrm{Mpc}}{r}\right) , \tag{1.28}$$

where $M_\odot = 2\ 10^{30}$ kg is the mass of the Sun and 1Mpc = 1Megaparsec. Hence if we observe two black holes of 10 $M_\odot$ merging at 100 Mpc, the order of magnitude of the signal during the last cycles before the merger will be 10^{-21}. According to our discussion in section 1.2.3 on the effect of gravitational waves on matter, this means that the distance between free falling objects on Earth are modified by a factor 10^{-21} when such an event occurs.

h is proportional to the compactness of the source Ξ, and the compactness of a binary system is smaller than the compactness of the bodies forming the binary system. Therefore, we will from now on only consider compact binary systems, i.e., binary systems made of compact objects such as neutron stars, or black holes.

Lifetime of a binary system Let us use the Einstein quadrupole formulae for the flux to estimate the lifetime of a compact binary system of two bodies of masses M_1 and M_2 on circular orbits with a separation of r_{12}. The Newtonian mechanical energy E_m of such a system is composed of the kinetic energy and the gravitational potential energy. Its value is

$$E_m = -\frac{GM\nu}{2r_{12}} \,. \tag{1.29}$$

Where $M = M_1 + M_2$ is the total mass of the system and $\nu = \frac{M_1 M_2}{(M_1+M_2)^2}$ is the symmetric mass ration ($0 \leq \nu \leq 1/4$ with $\nu = 1/4$ for equal mass system). Let us consider that this system evolves as a succession of circular orbits of radius $r_{12}(t)$. We can computed the energy flux of this system using the equation (1.25) and we obtain

$$\mathcal{F} = \frac{32}{5} \frac{c^5 \nu^2}{G} \left(\frac{GM}{r_{12}c^2}\right)^5 \,. \tag{1.30}$$

By stating the balance equation for the energy at Newtonian order

$$\frac{\mathrm{d}E_m}{\mathrm{d}t} = -\mathcal{F}\,, \tag{1.31}$$

we obtain the following differential equation for r_{12}

$$\dot{r}_{12} = -\frac{K}{r_{12}^3}\,, \tag{1.32}$$

with $K = \frac{64}{5}\frac{G^3M^3\nu}{c^5}$. The solution of this equation is $r_{12}(t) = \left(r_{12}(t_0)^4 - 4K(t-t_0)\right)^{1/4}$. Therefore, the lifetime Δt (defined as $\Delta t \equiv t_f - t_0$ where $r_{12}(t_f) = 0$) of such a system before its coalescence can be roughly estimated as

$$\Delta t = \frac{5}{256}\frac{r_{12}^4c^5}{G^3M^3\nu}\,. \tag{1.33}$$

If we consider two equal-masses black holes (of masses $M/2$) separated by N Schwarzschild radii (i.e. $r_{12} = \frac{NGM}{c^2}$) we have

$$\Delta t \sim \left(\frac{N}{20}\right)^4 \left(\frac{M}{10M_\odot}\right) 0.6 \text{ sec}\,. \tag{1.34}$$

As we will see in the next chapter, ground-based detectors can detect gravitational waves from frequencies starting around 30 Hz. This corresponds to an orbital frequency of the binary system of 15 Hz. Using Kepler's law of physics we can compute the separation r_{12} between the two bodies as a function of their orbital frequency Ω as $r_{12} = \left(\frac{GM}{\Omega^2}\right)^{1/3}$. Hence we find that the lifetime of a binary of orbital frequency Ω is

$$\Delta t = 268 \text{ sec} \left(\frac{15\ Hz}{\Omega}\right)^{8/3} \left(\frac{20M_\odot}{M}\right)^{5/3}\,. \tag{1.35}$$

The two equations (1.34) and (1.35) provide estimates that are one or two orders of magnitude above the coalescence times observed in the gravitational wave detection during the last two years. The main reason of this over-estimation is because close to the merger, the velocity of the source becomes a high percentage of the speed of light and the gravitational field that one body feels from its companion becomes strong. Therefore, the accuracy of our post-Newtonian computation that we did at the 0^{th} order (i.e. at newtonian order) gets worse and worse as we get close to the merger. We could improve this accuracy either by going to higher order in post-Newtonian expansion, or by using numerical relativity to solve directly the full Einstein equations. Also note that we are computing the time remaining before r_{12} reaches 0 while the merger actually occurs when r_{12} is of the order of the radius of the compact objects.

Circularization of the orbit Let us now focus on a system whose eccentricity e is not zero. We are going to average the balance equation (1.31) over one period P of the system and we will consider the following quantity

$$<\mathcal{F}>(t) \equiv \frac{1}{P}\int_{s=t}^{t+P} \mathrm{d}s\mathcal{F}(s) = \frac{32}{5}\frac{c^5}{G}\nu^2\left(\frac{GM}{r_{12}^{\max}c^2}\right)^5 f(e)\,, \tag{1.36}$$

where $r_{12}^{\max}$ is twice the semi-major axis and $f(e) = \frac{1+\frac{73}{24}e^2+\frac{37}{96}e^4}{(1-e^2)^{7/2}}$ is the Peters-Mathews enhancement factor due to the average done over one eccentric orbit. Similarly

$$< \mathcal{G} > (t) \equiv \frac{1}{P}\int_{s=t}^{t+P} \mathrm{d}s\mathcal{G}(s) = -\frac{32\nu^2}{5c^5}\sqrt{\frac{G^7M^9}{(r_{12}^{\max})^7}}f_{\mathcal{G}}(e)\,, \tag{1.37}$$

with $f_{\mathcal{G}}(e) = \frac{1+\frac{7}{8}e^2}{(1-e^2)^2}$. Note that the functions $f(e)$ and $f_{\mathcal{G}}(e)$ are increasing functions of e: the more eccentric a system is, the more it looses energy and angular momentum through gravitational wave radiation!

Now, using the average balance equation $\frac{\mathrm{d}E}{\mathrm{d}t} = - < \mathcal{F} >$ and $\frac{\mathrm{d}J}{\mathrm{d}t} = - < \mathcal{G} >$ we can find coupled differential equations governing the evolution of $r_{12}^{\max}(t)$ and $e(t)$. While these equations does not have a simple analytical solution, we can use them to express $r_{12}^{\max}$ as a function of e and find that

$$r_{12}^{\max}(e) = \kappa\frac{e^{12/19}}{1-e^2}\left(1+\frac{121}{304}e^2\right)^{870/2299}\,, \tag{1.38}$$

where κ depends on the initial conditions.

A careful study of the right-hand side of the equation (1.38) shows that $r_{12}^{\max}(e)$ is an increasing function of e. Therefore, as the semi-major axis of a binary system decreases, the orbit gets more circular. For any reasonable value of e (i.e. e not extremely close to 1), the eccentricity of a compact binary system will become relatively small by the time of the coalescence.

Let us take the example of the binary pulsar PSR1916+13 described in the next section. Today, this binary system has a semi-major axis $r_{12}^{\max}/2 \sim 2\ 10^9$m and an eccentricity of $e \sim 0.6$. This pulsar is made of two objects of radii of order $r \sim 10$ km (cf next section). Therefore, it is interesting to compute the eccentricity during the last orbits before coalescence, for example when the two objects will enter the bandwidth of current ground-based detectors. This will occur when the orbital frequency will roughly reach 15 Hz which corresponds to $r_{12}^{\max} = 1000$ km. Using (1.38) we get for this system $\kappa = 3.4\ 10^9$ m. Using that value of κ we can infer that for $r_{12}^{\max} = 100r = 1000$km we have $e = 2\ 10^{-6}$ which is indeed extremely small.

Once the orbit of a compact binary system is circular, we expect it to remain circular. This is consistent with the fact that for circular orbit of radius r_{12}, the angular momentum $J = \sqrt{J_iJ_i}$ is

$$J = \nu\sqrt{GM^3r_{12}}\,. \tag{1.39}$$

If we consider the consecutive circular orbits governed by equation (1.32), we have

$$\frac{\mathrm{d}J}{\mathrm{d}t} = \nu\sqrt{GM^3}\frac{\dot{r}_{12}}{2\sqrt{r_{12}}} = -\frac{32Mc^2\nu^2}{5}\left(\frac{G^7M^7}{r_{12}^7c^{14}}\right)^{1/2}\,. \tag{1.40}$$

Computing $\mathcal{G} = \sqrt{\mathcal{G}_i\mathcal{G}_i}$ from equation (1.26) we find

$$\mathcal{G} = \frac{32Mc^2\nu^2}{5}\left(\frac{G^7M^7}{r_{12}^7c^{14}}\right)^{1/2}\,. \tag{1.41}$$

Thus

$$\frac{\mathrm{d}J}{\mathrm{d}t} = -\mathcal{G}\,. \tag{1.42}$$

The balance equations for the energy and the angular momentum at linear order are therefore satisfied for consecutive circular orbits. More detailed studies of the stability of circular orbits, such as the one carried in [21], corroborate the fact that circular binaries stay on circular orbits until their coalescence.

1.4 The confirmation with radio-astronomy of the Einstein quadrupole formulae

The discovery and the study of the binary pulsar system PSR B1913+16 was the first observational confirmation of the loss of energy of a binary system through the emission of gravitational waves. The observation of this pulsar over several decades is in perfect agreement with the computation performed using the linearization of the Einstein equations as well as the Einstein quadrupole formula. This is therefore a huge argument confirming the validity of perturbative computation in general relativity.

1.4.1 Neutron stars, pulsars, and pulsar binary systems

A neutron star is a compact object (of compactness $\Xi \sim 0.2$) that can result from the core-collapse of a massive star at the end of its life. Known neutron stars have masses roughly in the range between $1M_\odot$ and $2M_\odot$, and based on different models, we expect them to have radii of the order of $10 - 15$km (this uncertainty is due to the unknown composition of the core and the unknown neutron star equation of state). They are called neutron stars because the main component of these objects are believed to be a fluid of neutrons.

Neutron stars can be highly magnetized, and their fields can lead to two opposite electromagnetic jets. Besides they rotate on themselves along an axis which is not specifically aligned with their jets. Therefore, if the jet of a neutron star turns out to be pointed toward the Earth once per rotation, we receive periodic signal from it. We call such a neutron star a pulsar.

It turns out that pulsars are extremely interesting objects for three main reasons. First of all, they are compact objects, so they constitute a nice laboratory to study relativistic effects. Secondly, the time of arrival of the pulse from a pulsar can be extremely stable. In fact due to the conservation of angular momentum, the rotational speeds of these objects are regular — except for the energy loss due to the radiation of their extreme electromagnetic field (as well as possibly a small emission of gravitational wave, cf section 2.2.6). Therefore, once one has fitted the decrease of the rotational period due to radiation, the time arrival of the pulse can be used as an extremely precise clock that can compete with atomic clocks on Earth. Last but not least, they emit at radio wavelength so we can observe them using large radio interferometer arrays which can have an angular precision down to milli-arcseconds. So to summarize, studying pulsars means studying relativistic objects with an extreme time and angular accuracy.

A huge breakthrough occurred in 1974 with the discovery by Hulse and Taylor of a pulsar within a binary system whose secondary object is thought to be a neutron star [19]. Based on what we previously said, it has therefore been possible to extensively study the trajectory (with high accuracy both in time and in space) of such a system and to use it to test the Einstein quadrupole formula.

1.4.2 Evolution of the orbits

In order to test the Einstein quadrupole formula, we first need to know the masses of the two objects as well as the semi-major axis of their orbits. This latter parameter cannot be directly measured because we do not know the inclination under which we see the orbital plane of the binary.

These three parameters can be inferred directly from the Einstein parameter γ, the periastron advance $< \dot{\omega} >$ of the system together with the orbital period P of the system. The Einstein parameter γ is a change of the pulse arrival time due to the perturbation of a clock that would be on the pulsar because of the gravity field generated by its companion, i.e., the gravitational redshift (the Einstein effect) as well as its own relativistic speed (i.e. the second order doppler effect). The periastron advance $< \dot{\omega} >$ is due to the fact that at linear order in general relativity, the trajectory of the bodies in a binary system are not closed ellipses. This is exactly the same effect that than the famous 43 arc-seconds per century advance of the perihelion of Mercury. Both of these two relativistic effects depends on a combination of the masses and on the period P of the system. Once they have been measured, the masses are fully determined and their current values are $m_p = 1.4389(2) \pm 0.0002 M_\odot$ for the pulsar and $m_c = 1.3886 \pm 0.0002 M_\odot$ for the companion [22].

Now that the two masses have been computed, the semi-major axis can be deduced from its Newtonian value

$$a = \left(G[m_p + m_c]\right)^{1/3} \left(\frac{P}{2\pi}\right)^{2/3} . \tag{1.43}$$

The eccentricity of this binary can be directly measured from the observation and is $e = 0.6171334(5)$ [22]. Now, we can compute using equation (1.36) the energy loss of the system and therefore the change of its orbital period $\dot{P}$. The change of its orbital period will affect the time at which the orbit reach its periastron. This is this shift of the periastron time that has been measured over the years and is in perfect agreement with the predictions made by perturbative computations in general relativity as shown in figure 1.2 extracted from [22].

The study of pulsar binary systems with radio telescope has provided us some crucial information. It is an evidence for the existence of gravitational waves (or at least for the loss of energy through gravitational wave radiation). Besides, the perfect fitting between observations and computations done using the Einstein quadrupole formula corroborates the validity of using perturbation theory to make predictions in general relativity.

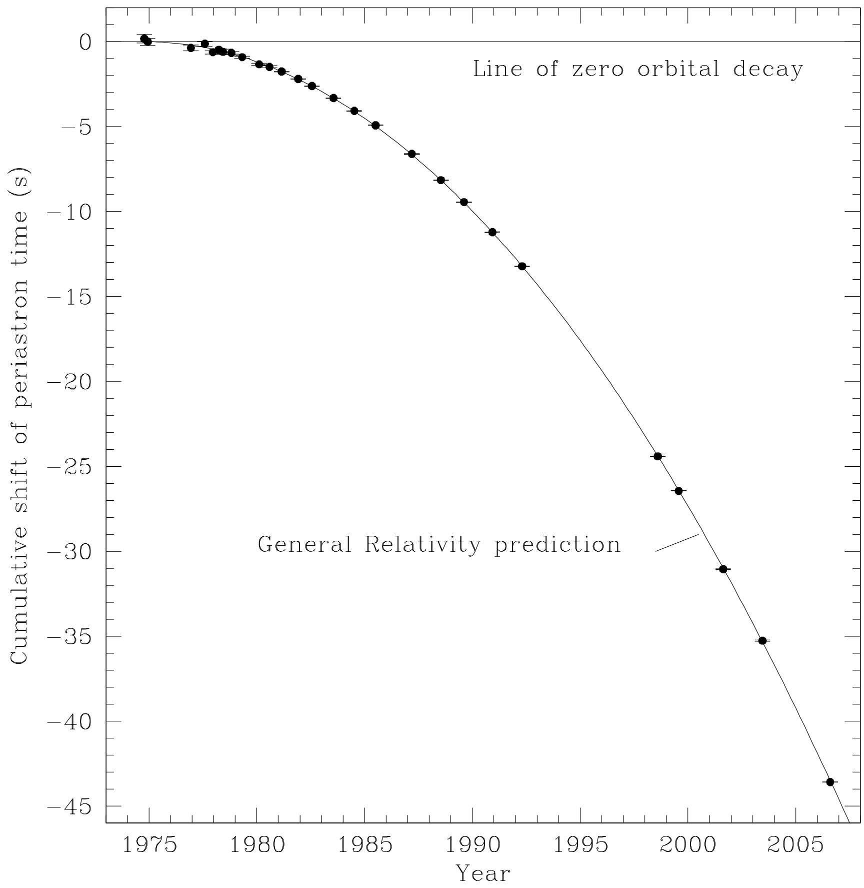

Figure 1.2: The orbital decay of the binary PSRB1916+13 measured through the cumulative shift of its periastron time. The black line is the prediction from general relativity using the Einstein quadrupole formula while the dots correspond to the observations. Figure extracted from [22]

2 – Detection of gravitational waves

2.1 Detection of GW with laser interferometry

2.1.1 History: from the Weber bars to the interferometer detectors.

The first gravitational wave detectors built were resonant bars designed by Joseph Weber in the 1960s in the University of Maryland. These bars are cylinders with a length of 2 meters and a diameter of 1 meter and their resonance frequencies are around $f_r = 10^3$ Hz. The closer the frequency of the gravitational wave is to f_c, the more sensitive the device is. Therefore, resonant bars have quite a narrow frequency bandwidth (of the order of $[f_r - 100\text{Hz}; f_r + 100\text{Hz}]$). While Weber claimed to have detected an interesting signal at multiple times [23, 24], his results could not be reproduced nor confirmed by the rest of the community and no convincing detection was made.

Meanwhile, other scientists in the US and in Europe started to work in the late 1960s on the design and construction of a kilometer-scale interferometer. After more than two decades, the project LIGO was finally confirmed and funded by the NSF and the construction of two laser interferometers in Hanford and Livingston (US) started in the mid-1990s. The Initial LIGO detectors ran from 2002 to 2010 but no detection was made. From 2010 to 2015, the LIGO detectors were upgraded into the *advanced LIGO detectors* which started to take data in 2015.

In Europe, the British and German project GEO started in 1989 and the construction of the GEO 600 interferometer in Germany near Hannover began in 1995. Meanwhile, a European interferometer detector led by France and Italy and called *Virgo* started to be built in 1996. Different observing runs of the initial VIRGO detector took place between 2007 and 2011 and after an upgrading phase, the *advanced VIRGO detector* starting to take data in 2017.

2.1.2 Ground-based interferometry

The principle of an interferometer is shown in the figure 2.1 describing the LIGO detectors. A laser is emitted by a laser source and split in two different beams by a beam splitter. Each beam enters a 4 km long arm at the end of which stands a *free falling test mass*[1] which is a mirror suspended and isolated through different layers of pendula. The two laser beams are then recombined, and their interference is measured by a photodetector. Besides, other mirrors are placed at the beginning of the 4 km arms, so the device is actually a *Fabry-Perot* interferometer. The interferometer is configured in such a way that when no gravitational

[1] The *free falling* properties of these mirrors are only through the horizontal axis.

wave signal is present, the two beams reaching the photodetector have a difference of phase of $\pi/2$ and interfere destructively. Hence the photodetector is at a *black spot*. If a wave passes through the detector, the distances L_x and L_y are modified as explained in section 1.2.3, and the difference of phase between the lasers changes. This change is directly measured by the photodetector. Finally, it is worth mentioning the presence of a recycling power mirror enhancing the total circulating electro-magnetic power in the cavity of the detector. We refer to [25], for a detailed description of the LIGO interferometer.

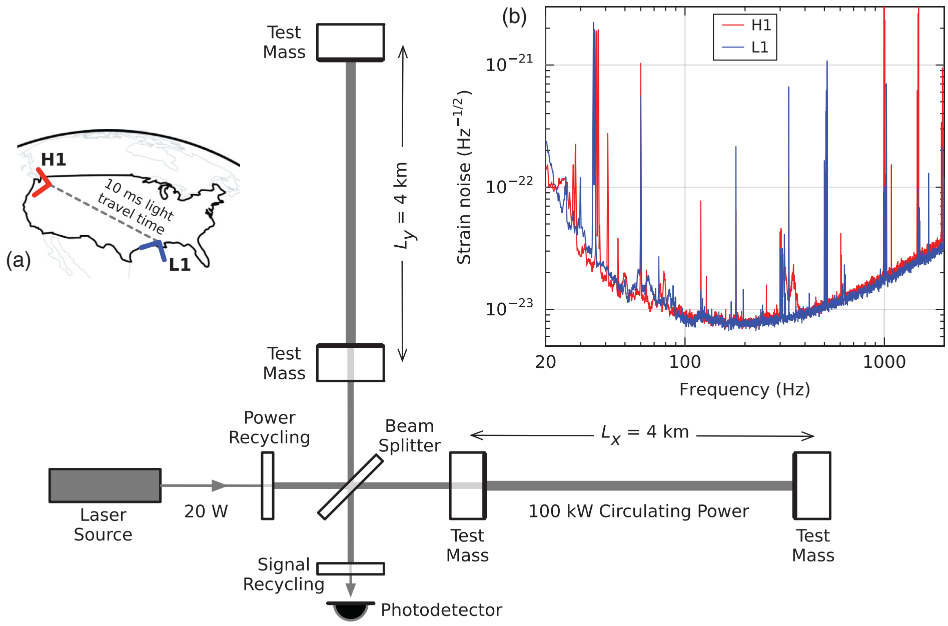

Figure 2.1: a) Schematic representation of the LIGO interferometer detectors. b) Sensitivity curves of the LIGO detectors (as of September 2015). Figure extracted from [26]

The sensitivity of the detector at each frequency is represented by its *spectral strain sensitivity* which is expressed in Hz$^{-1/2}$. Let $s(t)$ be the output signal of the detector. This signal is made of the gravitational wave $h(t)$ that we want to measure as well as all the instrumental and terrestrial noise $n(t)$

$$s(t) = n(t) + h(t)\,. \tag{2.1}$$

The noise $n(t)$ is a stochastic time series that we are going to characterize by its spectral power density. If the noise is stationary, then the Fourier components of the noise at different frequencies are uncorrelated and we define $S_n(f)$ as

$$< \tilde{n}^*(f), \tilde{n}(f') >= \delta(f - f')\frac{S_n(f)}{2}\,, \tag{2.2}$$

where $\tilde{n}(f)$ is the Fourier component of $n(t)$ at the frequency f and $\tilde{n}^*(f)$ is the complex conjugate of $\tilde{n}(f)$. $S_n(f)$ is the relevant quantity to assess the strength of the noise as it describes how much noise is contained for each frequency

$$< n(t)^2 >= \int_0^\infty \mathrm{d}f S_n(f)\,. \tag{2.3}$$

The *spectral strain density* of the noise, or the *strain noise* is defined to be $S_n(f)^{-1/2}$ and is expressed in $\mathrm{Hz}^{1/2}$. We will see in section 2.3.1 how to relate the signal-to-noise ratio of a signal to the strain noise. The strain noise of the advanced LIGO detector is shown in figure 2.1. As we can see, the bandwidth of the detector is roughly $15-200$Hz with the strain noise containing peaks at some specific frequencies: these frequencies correspond for example to resonance frequencies of some components of the detector.

The general shape of the strain noise is due to the different sources of noise [27]: (i) the *Newtonian noise*, present at low frequency, due to changes of the local gravitational potential because of the variation of the mass distribution surrounding the detector; (ii) the seismic noise (also at low frequency); (iii) the thermal noise mainly due to the suspensions, the test masses and the coating (note that current interferometer detectors are at room temperature while it is planned to use cryogeny to reduce the thermal noise of the next generation of ground-based detectors such as the Japanese KAGRA detector under construction [28]); (iv) finally, at high frequency, the noise is dominated by *the shot noise* of the laser: the number of photons hitting the photodetector fluctuates due to the quantum properties of the laser and affect the measurement.

2.1.3 LISA and space-based interferometry

The LISA project is a space-based gravitational detector project led by the ESA together with NASA[2]. In its current design [29], this detector is made of 3 spacecraft forming a triangle with sides of 2.5 millions of kilometers. Each spacecraft emits two laser beams toward the other ones. This network of six laser beams enables to measure with great precision the distance between the spacecraft. Besides each spacecraft contains one free-falling mass (i.e. a cube inside the spacecraft that does not touch any part of the spacecraft). The exact position with respect to the spacecraft of each test mass is also measured internally through interferometry. Therefore, we end up measuring the distances between test masses 2.5 millions of kilometers apart.

Such a mission will be sensitive at much lower frequencies than the ground-based detectors because of the size of its arms. LISA is expected to be sensitive in the range of [0.1mHz, 1Hz].

In 2015, the *LISA pathfinder* mission was launched. It put in orbit two free falling masses in a spacecraft and measured the relative acceleration between them. The accuracy obtained was way better than what was required, and the mission was a success [30]. Therefore, the community is today optimistic on the realization of this mission and its launch is planned in the 2030s.

2.1.4 Summary of the current and future network of GW observatories

The current network of gravitational wave detectors contains today 4 working ground-based interferometers: the two advanced LIGO 4-km long detectors in Livingston (US) and Hanford (US);the 3-km long advanced VIRGO detector in Italy near Pisa; and the 600-meter long GEO600 detector near Hannover in Germany. This latter is mainly use to develop and test new technologies as its sensitivity is below the sensitivities of the advanced LIGO and VIRGO detectors.

[2] From 1997 to 2011, LISA was a joined project of these two agencies. Due to financial constraints, the NASA withdrew its contribution in 2011. In summer 2016 however, NASA decided eventually to participate in this project.

In the next few years, two other ground-based detectors will be built. Another LIGO detector called *LIGO-India* is indeed expected to be constructed in India in the next few years. Additionally in Japan, a 3-km long detector called the *Kamioka Gravitational Wave Detector (KAGRA)* is planned and should be in operation also in the next few years.

In conclusion, we will soon have 5 state-to-the-art ground-based detectors that will be joined in the 2030s by the LISA space-based mission. Besides, both in Europe and in the US, projects of third generation detectors start to emerge, such as the Einstein Telescope in Europe that would be made of three 10-km long arms.

2.2 Possible sources

As we saw in the first chapter, the linear perturbation theory of general relativity tells us that in order to emit gravitational waves, a source needs to have a varying quadrupole moment. Besides, the strength of the emitted gravitational wave depends on how compact the source is. Let us review the main classes of expected gravitational waves that can be detected by the ground-based and space-based detectors.

2.2.1 Continuous compact binary systems

Let us consider the example of the Hulse-Taylor binary system described in section 1.4. It is a binary system of orbital frequency of 3.6 10^{-5} Hz. Today, such a system could not be observed by ground-based (nor space-spaced) detector such as LIGO/Virgo, because its frequency is way too low. Such a system will evolve because of its emission of gravitational waves and enter the ground-based detector bandwidth before its coalescence in few hundreds of millions of years. This introduces a first kind of source: the coalescence of binary systems made of compact objects with masses of the order of solar masses.

2.2.2 Compact binary coalescence (CBC)

By stellar mass CBC, we refer to a binary system made of two compact stellar mass objects (two black holes, two neutron stars, or one black hole and one neutron star)[3] coalescing. All the events detected by the ground-based detectors so far were stellar mass CBC. These binary systems were formed a long time ago and got closer and closer through different astrophysical processes, including in the end gravitational wave emission. As we have seen, the gravitational wave emission of a binary system tends to circularize the orbit, and by the time of the coalescence, we expect the orbits of most of the CBC to be circular as explained in section 1.3.

2.2.2.a) CBC made of two black holes

Among the CBC, the coalescence of a binary black hole (BBH) is the simplest to study theoretically as there is no need to take into account any baryonic matter. The typical signal of a BBH coalescence is shown in figure 2.2 and can be divided in three parts.

The signal starts with the *inspiral*, where the two black holes are still quite far away from each other. The signal received in the detector is essentially a sinusoidal signal whose

[3]Or any other exotic compact object.

amplitude and frequency increase with time as the black holes are getting closer and faster. This part of the signal is quite smooth and regular, and corresponds to relatively small value of v/c. It can be studied using perturbative approaches, namely using post-Newtonian approximation (cf section 2.3.2).

Then the *merger* occurs, where the two black holes merge into one another forming a final bigger black hole. The physics governing this part is highly non-linear and the only way to predict the waveform of the merger itself today is through the use of numerical relativity (cf section 2.3.3).

Finally, during the *ringdown*, the final spinning black hole relaxes and stabilizes. The signal during the ringdown is made of a combination of exponentially damped sinusoidal waves. The frequencies and the damping times associated to the final spinning black hole can be studied using black hole perturbation theory looking at perturbations of Kerr solutions.

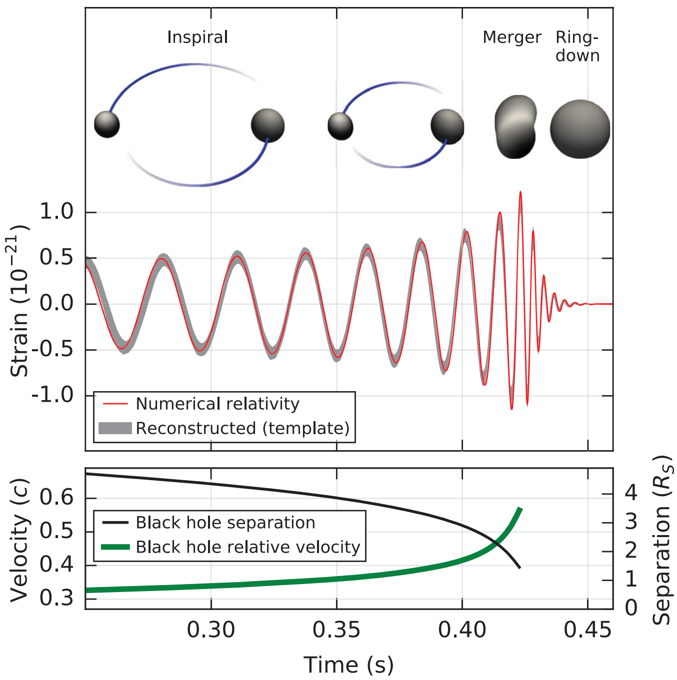

Figure 2.2: Theoretical signal of the binary black hole coalescence corresponding to GW150914. Top: the red curve shows the signal reconstructed using numerical relativity of this event and the grey line the signal reconstructed using phenomenological templates. Bottom: the relative velocity of the black holes (green) and the distance between the two black holes (black). Figure extracted from [26]

2.2.2.b) Binary neutron star (BNS)

The signal expected for coalescence of a BNS is quite similar during the inspiral to the signal of a BBH coalescence. The only noticeable difference is that neutron star have a mass range of $1-2$ solar masses which is smaller than the usual mass range of stellar mass black holes. Therefore the frequency of the coalescence is expected to be in general higher, which means that we can detect them during much more cycles once they enter the ground-based frequency bandwidth. Besides, the spin of neutron star is expected to stay quite low, contrary to the spins of black holes, resulting in less precession of the orbital plane.

The baryonic structure of the neutron star starts to play a role few cycles before the merger were tidal forces deform the two neutron stars. The response of the neutron stars to the tidal forces depends on their structures and in particular on their unknown equation of state. The merger and the post-merger parts of signal are studied using numerical relativity (cf [31] for a review on BNS numerical relativity).

2.2.2.c) Neutron star black hole coalescence

Nothing theoretically prevents a compact binary system to be made of one neutron star and one black hole. However, such a system has not been detected using radio-astronomy and none of the gravitational events detected so far corresponds to a neutron star black hole coalescence.

The inspiral phase of such binary systems is also similar during the inspiral of the signal of a BBH coalescence and, the merger and post-merger part of the signal have been extensively studied using numerical relativity and we refer to the review [32] for further reading on that topic.

2.2.3 Super Massive Black Hole Binary

It is commonly accepted in astrophysics that a supermassive black hole stands in the center of a huge fraction, if not all, of the galaxies [33]. These black holes are between 10^6 and 10^{10} solar masses. As galaxies merge through the evolution of the universe, their central super-massive black holes form binaries (SMBHB) that may end up coalescing. The dynamics of formation of super-massive black hole binaries is an active field of research today, and a huge effort is made to solve the *last parsec problem*: in order to bring the two black hole close enough where the gravitational wave emission starts to be efficient, different frictional mechanisms have to be invoked [34].

Because of the high masses involved, the gravitational wave frequency of such systems should be in the range of 10^{-5}Hz - 10^{-2} Hz by the time of the coalescence, which means that such system could be detected by space-based detectors such as the LISA project. It is worth noticing that the LISA detector might detect SMBHB up to redshift $z \sim 10$, or beyond if they exist. Besides, we expect to be able to localize the host galaxies of the SMBHB detected and measure their redshifts. As the *luminosity distance* D_L of the event can be deduced directly from the gravitational signal, this ensures extremely promising tests of cosmology by having an independent measurement of the redshift-distance relation at high redshift.

2.2.4 Extreme mass ratio inspiral (EMRI)

Stellar mass compact objects in the vicinity of a super-massive black holes constitute another class of interesting sources as they form extreme mass ratio binary systems. The inspiral phase of such systems is expected to last during $N \sim 10^5$ cycles. Classical post-Newtonian theory cannot track with an accuracy good enough the gravitational phase of such a signal and another approximation framework is used to study such system: the *self-force* theory framework based on black hole perturbation theory (cf section 2.3.5). The typical frequencies of ERMIs are in the range of $10^{-3} - 10^{-2}$ Hz and are expected to be detected by the LISA mission [35].

2.2.5 Supernovae

At the end of their lives, some stars collapse on themselves because of their gravity fields and generate core-collapse supernovae of type Ib, Ic, or II. If this process deviates from spherical symmetry, it can create gravitational waves. The physics of core-collapse supernovae is highly complex and contains a lot of different factors (electromagnetic fields, neutrino physics, relativistic hydrodynamical shock fronts, general relativity effects) and their modeling heavily relies on numerical simulations [36].

2.2.6 Continuous wave

Isolated fast-rotating neutron stars are also a promising source of gravitational waves. In fact, different mechanisms can generate an asymmetrical distribution of the matter within the neutron star. Therefore its fast rotation would lead to a varying mass quadrupole, hence producing gravitational waves. Such a source would produce a continuous quasi single-frequency signal whose frequency only slowly decreases due to the intrinsic *spin-down* due to the rotational energy loss of the source. Thus, even if this signal is weak, it could be detected by collecting data for a long time. No signal of such a system has been found so far by digging into the data collected by the ground-based detectors. However, advanced data analysis algorithms have put interesting upper limits on this process by looking to known pulsars. In particular the *spin-down limit* of J1813-1749, has been beaten [37], i.e., the upper limit on the gravitational wave flux of J1813-1749 is strictly smaller than its rotational energy loss. Said otherwise, its energy loss cannot be solely due to gravitational wave emission.

2.2.7 Stochastic background

The accumulation of *unresolved* sources creates a stochastic background that could be observed. In fact, all the astrophysical gravitational events that cannot be isolated in the data, add up to produce a background whose power spectrum can be predicted. The stochastic background of compact binary systems has not been detected in the ground-based detectors so far, but we expect this background to be observable in the future ground-based detectors as well as in LISA.

2.3 Template building and match filtering

From now on, and until the end of the manuscript, we will only consider gravitational wave signals coming from compact binary systems.

2.3.1 Matched filtering

Let us take the notation introduced in section 2.1.2. The output of the detector is a signal $s(t)$ which is the sum of the noise $n(t)$ and a gravitational wave signal $h(t)$. The amplitude of signal $h(t)$ can be of the same order of magnitude, or even smaller than the magnitude of the noise $n(t)$. Therefore, we cannot always read *by eye* the signal in the output of the detector and a matched filtering process need to be applied. The main strategy is to compute the correlation of the output with templates of different expected signals. When the template corresponds to the real gravitational signal $h(t)$, this correlation will peak.

In order to look for a specific signal $h(t)$ corresponding to the merger of two black holes for example, we are going to create a filter $K(t)$ and define $\hat{s}$ as

$$\hat{s} = \int_{-\infty}^{+\infty} \mathrm{d}t\ s(t)K(t)\,. \tag{2.4}$$

A first guess would be to take $K(t) = h(t)$. However, if we know the strain noise of the detector, there is a better choice for the filter $K(t)$. Indeed, we define the signal-to-noise ratio as S/N where S is the expected value of $\hat{s}$ while N is the variance of $\hat{s}$ when $h(t) = 0$ (i.e. when no signal is present). If $\tilde{h}(f)$ and $\tilde{K}(f)$ are the Fourier components of $h(t)$ and $K(t)$, it can be shown that the signal-to-noise ratio becomes

$$\frac{S}{N} = \frac{\int_{-\infty}^{\infty} \mathrm{d}f\ \tilde{h}(f)\tilde{K}^*(f)}{\sqrt{\frac{1}{2}\int_{-\infty}^{\infty} \mathrm{d}f\ S_n(f)|\tilde{K}(f)|^2}}\,. \tag{2.5}$$

It turns out that the right-hand-side of the equation (2.5) is maximal for $\tilde{K}(f) \propto \tilde{h}(f)/S_n(f)$, and becomes

$$\frac{S}{N} = 2\left(\int_0^{\infty} \mathrm{d}f \frac{|\tilde{h}(f)|^2}{S_n(f)}\right)^{1/2}\,. \tag{2.6}$$

The signal-to-noise ratio depends on the ratio $|\tilde{h}(f)^2|/S_n(f)$, therefore the signal should peak at frequencies where the strain noise $S_n(f)$ is as small as possible in order to be detected.

In practice, a bank of templates covering all the phase space of the kind of signal expected is created. In the case of compact binary systems, the phase space would be made of the masses of the compact objects, their spins, the time of the coalescence, as well as their orientation and position in the sky. Then the correlations between the output of the detector and the different templates is computed using the filter $K(t)$, in order to detect a signal in the output and study its properties. We will not detail the statistical analysis done by the LIGO–Virgo collaboration, but we will just mention that different methods of classical and Bayesian analysis are commonly used to analyze the different runs.

Hence, it is crucial to develop methods that compute with high accuracy the expected signal $h(t)$ in order to build useful banks of templates. In the case of compact binary systems, different means of computations that we are going to present are simultaneously used.

2.3.2 Post-Newtonian theory

The post-Newtonian theory in the case of compact binary systems is the main topic of this thesis and will be extensively studied in the following chapters. In post-Newtonian theory, the Einstein equations are solved perturbatively order by order in v/c where v is the relative velocity of the two compact objects, and c the speed of light. This method is therefore relevant when v/c is a small parameter which is the case in the early phase of the coalescence during the inspiral. In the figure 2.2, we see that in the case of GW150914 $v/c \sim 0.3$ few cycles before the merger and progressively increase up to $v/c \sim 0.6$ just before the merger.

A n^{th} post-Newtonian order effect is a $(v/c)^{2n}$ effect relatively to the leading order. For the equations of motion the leading order is derived using the classical Newtonian laws of physics (hence the terminology *post-Newtonian*). On the other hand, for the energy flux, the leading order contains a factor $1/c^5$ already, and is given by the Einstein quadrupole formula (1.25).

Post-Newtonian results are completely *analytical*, and the PN coefficients can be expressed using rational numbers together with some common irrational numbers. They provide analytical formulae that depend on the parameters of the compact binary system (masses and spins) and can be used for any values of the parameters, regardless of the nature of the compact objects of the binary system (i.e. black holes or neutron stars).

2.3.3 Numerical relativity

The Einstein equations can be solved numerically by computers in order to model compact binary system coalescences. This constitutes a huge field of research containing both theoretical and computational challenges. A breakthrough was achieved in 2005 by Pretorius [38] simulating for the first time the last few orbits before coalescence, followed by equivalent work by Campanelli *et al.* [39] as well as Baker *et al.* [40]. Since then, different numerical schemes have emerged and have successfully simulated such events.

Today, numerical relativity is the only tool to study the merger part of the coalescence and thus plays a major role in the template building process. However, simulating compact binary systems required a lot of computational power and time. Besides, each simulation is done for a specific set of physical parameters and a lot of simulations are required to cover the whole phase space when constructed banks of templates.

The different groups within the numerical relativity community often release banks of simulations (e.g [41]) containing few hundreds of different simulations that can be used for building and calibrating templates.

2.3.4 Studying the ringdown with black hole perturbation

During the final part of the coalescence, the *ringdown*, the final black hole oscillates and stabilizes itself into a stationary Kerr black hole. The field of *black hole perturbation* can provide useful insight on this process. In fact, this part of the signal is composed, in linear approximation in the black hole perturbation, of a sum of exponentially damped sinusoids. The characteristic frequencies and damping times can be computed by studying the so-called *quasi-normal mode* (QNM) of a Kerr black hole using the Teukoslky equation. However, in order to know the amplitude and time-shift of each QNM, one needs the initial conditions usually produced by numerical relativity.

2.3.5 The self-force framework

The *self-force* method, is the perturbative study of binary systems, where the small parameter is the mass ratio of the two objects. It is therefore designed to study the evolution of extreme mass ratio inspirals (EMRI), namely stellar mass black holes plunging into supermassive black holes. At the lowest order, the small object follows a geodesic of the space-time created by the supermassive black hole. However, the presence of this companion changes the metric of the space-time which induces a deviation of the small companion from the initial geodesic. This deviation can be seen as a *self-force* of the small companion on itself.

The self-force framework combines both analytical and numerical approaches. It is today the most promising way to create accurate templates for EMRIs, and is an extremely active field of research motivated by the future space-based mission such as LISA.

2.3.6 Building the template with Effective-One-Body and IMRPhenomD

The different methods described previously are tools to study the dynamics of CBC as well as their gravitational wave emissions. On top of these frameworks, there are two main methods in order to create templates for the data analysis of the LIGO–Virgo collaboration. These methods use results from different frameworks previously described and create ready-to-use templates.

2.3.6.a) Effective-One-Body

The Effective-One-Body (EOB) method is an ingenious formalism developed by Damour and Buonanno in 1999 [42]. In this framework, the two-body problem is reformulated and described as one effective body on an effective metric, whose dynamics is described by an effective Hamiltonian. This framework heavily uses post-Newtonian results together with *resummation techniques* consisting of re-writing in a factorized form the post-Newtonian development used. The effective-one-body method also uses numerical relativity results to inform and adjust certain parameters, especially during the merger and the ringdown phases.

2.3.6.b) IMRPhenom

The second family of templates used are phenomenological templates usually called *IMR-Phenom* templates (IMR standing for Inspiral-Merger-Ringdown). These templates are built in the Fourier space and parametrize the signal with a set of coefficients that are determined either using post-Newtonian results (for the inspiral), black hole perturbation (for the ring-down) or by calibration to numerical relativity (for the merger). Besides, they contain extra coefficients used to describe phenomenologically the intermediate phase between the inspiral and the merger.

2.4 First detections

2.4.1 Runs O1 and O2

During the first run O1, which started on the 12th of September 2015 and ended on the 19th of January 2016, only the Advanced LIGO detectors were turned on. Two black hole binary coalescence detections were confirmed with a significance higher than 5.3σ (GW150914 and GW151226) and one binary black hole coalescence candidate was detected but could not be claimed as a detection due to its low significance of 1.7σ and its high false alarm rate of $0.37\ \text{year}^{-1}$. During the second run 02 (from the 30th of November 2016 to the 25th of August 2017 for the Advanced LIGO detectors, with the Advanced Virgo detector joining the run on the 1st of August 2017), 3 BBH coalescences (GW170104, GW170608, GW170814) and one BNS coalescence (GW170817) were detected. In particular, GW170814 and GW170817 were analyzed with the data from both the Advanced LIGO detectors and the Advanced Virgo detector.

2.4.2 The first direct detection of gravitational waves: GW150914

2.4.2.a) The storyline

Two days after the beginning of the first run, on 14 September 2015, the LIGO detectors were still in engineering mode, and were not yet turned into the research mode. However, the whole chain of detection was fully operational and at 09 : 50 : 45 UTC, a chirp signal of about 0.2s corresponding to a BBH coalescence was observed. Only few minutes afterward, at 09 : 54 UTC, an automatic alert was triggered and was very quickly read by the scientists working at Hannover, Germany [26]. This triggered a series of meticulous analyses and checks. Once the signal was analyzed in-depth and the LIGO–Virgo collaboration had made sure that the data was free of glitch, the first detection of gravitational waves was announced on the 11th of February, 2016.

2.4.2.b) The signal

The output recorded by the LIGO detectors is shown in figure 2.3. The last row of figure 2.3 shows the power density contained in the signal in a time-frequency diagram. Similarly, we can see *by eye* the characteristic chirp expected in the case of a compact binary coalescence.

The signal received corresponds to a BBH with initial masses of $m_1 = 36.2^{+5.2}_{-3.8} M_\odot$ and $m_2 = 29.1^{+3.7}_{-4.4} M_\odot$, with a final black hole of $m_f = 62.3^{+3.7}_{-3.1} M_\odot$. During this coalescence, $3.0^{+0.5}_{-0.4} M_\odot c^2$ of energy were radiated. This corresponds to a peak luminosity of $3.6^{+0.5}_{-0.4}\ 10^{56}$ erg s^{-1} which made GW150914 at the day of its detection, the brightest astrophysical event (in any kind of radiation) ever recorded [26].

2.4.2.c) Electromagnetic counterpart

Two days after the event, the LIGO–Virgo collaboration sent to their partners a first localization map of the event. This map has been refined by different offline analyses and a final map with a 90% credible region with area 630 deg^2[4] was given to the electromagnetic partners of the LIGO–Virgo collaboration. 25 different observational teams covering the whole range of the electromagnetic spectrum (Gamma-ray, X-ray, Optical, IR and radio) reported their observations. A weak signal was found by the Fermi GBM instrument 0.4s after GW150914 but nothing was found neither by the INTEGRAL SPI-ACS instrument nor by AGILE [43]. Apart from the Fermi signal, no other observational team has reported any electromagnetic counterpart that could be linked to GW150914. For a BBH, we do not expect any electromagnetic counterpart as we do not expect large amount of baryonic matter around the binary system. This conclusion is so far corroborated by the 4 other BBH detections for which no electromagnetic counterpart has been found.

[4] To give an order of magnitude, the angular surface of the moon is around 0.2 deg^2.

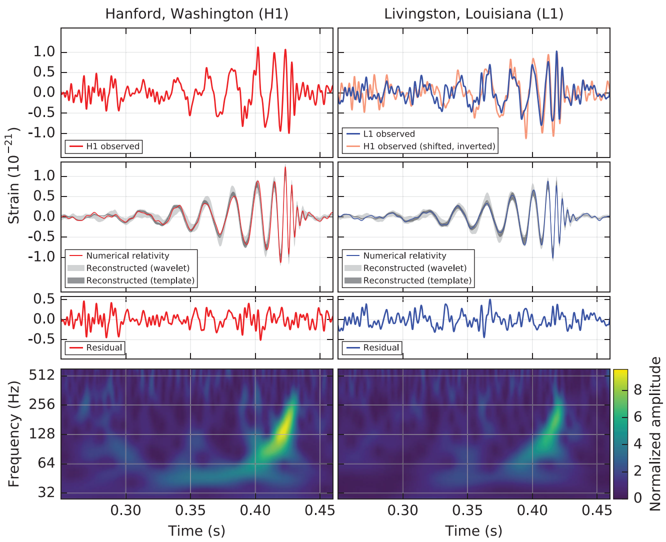

Figure 2.3: From top to bottom: (i) the signal received by the LIGO detectors; (ii) the templates and numerical simulation corresponding to the best parameter fit; (iii) the residual noise once the best template fit is subtracted to the signal (iv) the time-frequency power spectrum of the signal, clearly showing distinctive chirps.

2.4.2.d) Consequences

This first detection by the LIGO–Virgo collaboration is of major importance and corresponds to a huge scientific breakthrough rewarding decades of experimental and theoretical research. In particular, this detection constitutes: (i) the first direct detection of gravitational waves; (ii) the first direct observation of black holes; (iii) the first direct observation of BBH; (iv) and finally the confirmation that binary black holes merge within a Hubble time.

2.4.3 The first detection of NS-NS coalescence: GW170817

2.4.3.a) Detection, and sky localization

On the 17th of August, 2017, a signal consistent with a BNS coalescence with initial masses between $0.86M_\odot$ and $2.26M_\odot$ at a luminosity distance of 40^{+8}_{-14}Mpc was observed by the LIGO–Virgo detectors with a coalescence time of 12 : 41 : 04 UTC [44]. Using the combination of data from the three detectors, the 90% credible region of the localization of the BNS was reduced down to 28 deg^2 only. As we do expect electromagnetic counterpart coming from BNS coalescence, and as this detection was in coincidence with a detection of a gamma-ray burst GRB 170817A received at 12 : 41 : 06 UTC, a circular was sent to the partners of the LIGO–Virgo collaboration the same day at 13 : 21 : 42 UTC.

2.4.3.b) Electro-magnetic counterpart

Thanks to the precision of the localization map provided by the LIGO and Virgo collaboration and to the extensive observing campaign, an optical transient was found associated with the galaxy NGC 4993 less than 11 hours after the merger by the One-Meter Two-Hemisphere

(1M2H) team. In the next few hours, this transient was subsequently and independently observed by five different teams, namely the Dark Energy Camera, the Distance Less Than 40Mpc Survey, Las Cumbres Observatory, the Visible and Infrared Survey Telescope for Astronomy, and Master. This transient is identified as a kilonova linked to GRB 170817A, providing therefore an extremely precise localization of this event. This has enabled to do an extensive study across all the electromagnetic spectrum during the following days and weeks.

2.4.3.c) The signal

As the masses of the neutron stars are smaller than the masses of the black holes of GW150914, the frequency of the signal just before the merger is higher. Therefore, the signal enters the bandwidth of the advanced LIGO–Virgo detectors a long time before the merger. In the case of GW170817, more than 3000 cycles were observed for more than one minute. This signal is the perfect illustration of the need of post-Newtonian theory as high accuracy is required to keep track of the phase of this signal for such a long time.

2.4.3.d) Astrophysical consequences

The discovery a this new type of gravitational source, constitutes another major scientific breakthrough. The existence of binaries made of neutron stars was already known through pulsar binaries observed with radio-astronomy. Besides we already knew that some of these pulsars should normally merge within a Hubble time.

However, this is the confirmation that neutron star coalescences are the seed of at least a part of the short gamma-ray bursts. Besides, as the redshift of the host galaxy has been measured, and as the luminosity distance of the event can be measured using the gravitational wave signal, we can make an independent computation of the Hubble constant at low redshift. Doing so we obtain $H_0 = 70^{+12}_{-8}$km s^{-1}Mpc^{-1} which is consistent with the value measured from the Planck mission $H_0 = 67.90 \pm 0.55$km s^{-1}Mpc^{-1} [44]. Last but not least, the first gamma-ray reached Earth 1.7 s after the gravitational wave, which implies new constraints on the difference between the speed of light and the speed of propagation of gravitational waves, on Lorentz invariance violations and on the equivalence principle.

2.4.4 Summary

To conclude, these first detections constitute a major breakthrough in theoretical physics and started a new field of astrophysics by opening a new window on the universe. The science that we will be able to produce in the next few years and decades depends on the number of events detected and on our abilities to analyze properly the output of the detectors and estimate the parameters of the observed events. This requires templates as accurate as possible covering the whole parameter phase space. As these templates rely on different methods such as post-Newtonian theory or numerical relativity, it is highly crucial to pursue our effort in each of these frameworks.

3 – Introduction to post-Newtonian theory

In this short chapter, we first introduce the different quantities that we are going to consider in post-Newtonian theory. Then, we provide a historical review as well as a state-of-the-art review of the results regarding the spinless equations of motions on one hand, and the spin effects on the other hand. Finally, we explain the 4.5PN project that motivated the different works performed during this thesis, and provide the outline of the following chapters.

3.1 Introduction to post-Newtonian theory

The post-Newtonian formalism is a framework that computes the effects of general relativity perturbatively using analytic tools. The small parameter in our situation is v/c where v is the relative speed of the compact objects and c the speed of light. In order to be more general, we consider the small parameter indexing the post-Newtonian order to be $1/c$. In particular, a n^{th} post-Newtonian order, or a n-PN order, corresponds to a factor $1/c^{2n}$ beyond the leading order. In this thesis, we use post-Newtonian framework to study compact binary systems where we model the compact bodies by point particles.

They are different quantities that interest us in the study of compact binary system.

Equations of motion First of all, we want to compute the equations of motion of the two bodies. These equations start at linear order by the Newton equations of motion, and have their first relativistic corrections at the first post-Newtonian order in $1/c^2$. In the equations of motion, two different contributions have to be distinguished: the conservative part starting at Newtonian order (i.e. at 0PN) and contributing at *even* post-Newtonian order (i.e. 1PN, 2PN, 3PN and 4PN etc.), and the dissipative part due to the loss of energy of the system by the emission of gravitational waves. The dissipative part starts at the 2.5PN order, which is a direct consequence of the $1/c^5$ coefficient in the Einstein quadrupole formula (1.26), and then contributes at the 3.5PN order and at the 4PN order. The latter contribution is due to the non-local *tail* effects. The methods used to compute the conservative and the dissipative parts are often different. For example the Fokker Lagrangian method described in chapter 6 will only compute the conservative part, and the dissipative terms will have to be added to the final result (as done in chapter 7).

Conserved quantities From the conservative part of the equations of motion, we can define conserved quantities that correspond to the invariance with respect to the Poincaré group: the energy, the angular momentum, and the linear momentum of the compact binary system. Of course, due to the dissipative terms in the equations of motion, these quantities are not totally conserved in the full dynamics, and balance equations can be written between the time derivatives of the conserved quantities and their fluxes carried by gravitational waves.

Radiative field, fluxes, and waveform Once the dynamics of the compact binary system is known, the next step is to study how the gravitational waves are emitted, and travel from the source to the detectors on Earth. In practice, the compact binary system is studied in an asymptotically flat spacetime (imposing a condition of no-incoming radiation from other sources located at infinity) and we look at the gravitational wave behavior at future null infinity $\mathcal{I}^+$. There are two particular quantities that we are interesting in. First, we can compute the gravitational waveform which corresponds to the transverse-traceless part of the metric near $\mathcal{I}^+$. These waveforms are usually given through their two polarizations $h_\times$ and h_+. Furthermore the polarizations are usually decomposed into modes that corresponds to spin-weighted spherical harmonics of weight -2. The other relevant quantity that is computed at $\mathcal{I}^+$ is the energy flux of the gravitational waves.

The leading order of the energy flux, corresponding to the Einstein quadrupole formula, has a $1/c^5$ factor. Therefore the n^{th} post-Newtonian order of the flux corresponds to a factor $1/c^{2n}$ above the Einstein quadrupole formula, hence to an absolute order of $1/c^{2n+5}$.

The phase of the signal For data-analysis purposes, one of the most useful results of post-Newtonian theory is the phase evolution of the signal. In order to compute this phase at high-order, we can use an adiabatic approach where we consider that the binary system follows consecutive circular orbits of energy E, with an energy flux $\mathcal{F}$. If both the energy and the flux of the system are known as functions of the orbital frequency of the circular orbits Ω, we can state the following balance equation

$$\frac{\mathrm{d}E}{\mathrm{d}t}(\Omega) = -\mathcal{F}(\Omega)\,. \tag{3.1}$$

If both sides of the equation (3.1) are known at the n^{th} post-Newtonian order, then the evolution of the phase ϕ of the system can be deduced at the n^{th} post-Newtonian. In fact we have

$$\phi = \int \Omega \mathrm{d}t = -\int \mathrm{d}\Omega \frac{\mathcal{F}(\Omega)}{\frac{\mathrm{d}E}{\mathrm{d}\Omega}} \tag{3.2}$$

Today, this phase evolution has been computed at the 3 PN order for general eccentric orbits [45], and many spin effects were included up to the 3PN and the 4PN order (cf section 3.3). For spinless circular orbits, this phase evolution is known at the 3.5PN order. When expressed with the 1PN dimensionless variable $x \equiv \left(\frac{Gm\Omega}{c^3}\right)^{2/3} = \mathcal{O}(1/c^2)$ (we recall that Ω is the orbital frequency), it reads

$$\phi = -\frac{x^{-5/2}}{32\nu}\bigg\{1 + \left(\frac{3715}{1008} + \frac{55}{12}\nu\right)x - 10\pi x^{3/2}$$

$$
\begin{aligned}
&+\left(\frac{15293365}{1016064}+\frac{27145}{1008}\nu+\frac{3085}{144}\nu^2\right)x^2+\left(\frac{38645}{1344}-\frac{65}{16}\nu\right)\pi x^{5/2}\ln\left(\frac{x}{x_0}\right)\\
&+\left[\frac{12348611926451}{18776862720}-\frac{160}{3}\pi^2-\frac{1712}{21}\gamma_{\mathrm{E}}-\frac{856}{21}\ln(16\,x)\right.\\
&\qquad\left.+\left(-\frac{15737765635}{12192768}+\frac{2255}{48}\pi^2\right)\nu+\frac{76055}{6912}\nu^2-\frac{127825}{5184}\nu^3\right]x^3\\
&+\left(\frac{77096675}{2032128}+\frac{378515}{12096}\nu-\frac{74045}{6048}\nu^2\right)\pi x^{7/2}+\mathcal{O}\left(\frac{1}{c^8}\right)\Bigg\}\,,
\end{aligned}
\tag{3.3}
$$

where x_0 is a constant of integration that depends on the time arrival of the gravitational wave, and where $\nu=\frac{m_1m_2}{(m_1+m_2)^2}$ is the symmetric mass ratio.

3.2 The equations of motion: a historical review

3.2.1 1PN, 2PN and 2.5PN

The first derivation of the equations of motion of self-interacting bodies in general relativity started as soon as 1917 by the work of Lorentz and Droste computing at 1PN the dynamics of N point particles [13]. This result was confirmed 20 years later by another derivation by Einstein, Infeld and Hoffmann using surface-integral method [46]. In this method, surfaces surrounding the compact bodies (outside of the bodies) are considered and the equations of motion are derived using only the Einstein equations in the vacuum. Therefore, the Einstein-Infeld-Hoffmann technique works automatically for any compact objects. At the same time, Fock [47] obtained in 1939 the equations of motion of the centers of mass of compact objects, at 1PN order, described by fluid balls, in agreement with the previous derivations.

At the 1PN order, the dynamics is known for an arbitrary number N of particles. This dynamics is rather short and reads (for particles labeled by $A, B, C, \dots$)

$$
\begin{aligned}
\frac{\mathrm{d}\boldsymbol{v}_A}{\mathrm{d}t}=&-\sum_{B\neq A}\frac{Gm_B}{r_{AB}^2}\boldsymbol{n}_{AB}\left[1-4\sum_{C\neq A}\frac{Gm_C}{c^2r_{AC}}-\sum_{D\neq B}\frac{Gm_2}{c^2r_{BD}}\left(1-\boldsymbol{n}_{AB}\cdot\boldsymbol{n}_{BD}\frac{r_{AB}}{r_{BD}}\right)\right.\\
&\left.+\frac{1}{c^2}\left(\boldsymbol{v}_A\boldsymbol{v}_A+2\boldsymbol{v}_B\boldsymbol{v}_B-4\boldsymbol{v}_A\boldsymbol{v}_B-\frac{3}{2}\boldsymbol{v}_B\cdot\boldsymbol{n}_{AB}\right)\right]\\
&+\sum_{B\neq A}\frac{Gm_B}{c^2r_{AB}^2}\boldsymbol{v}_{AB}\left[\boldsymbol{n}_{AB}\cdot(3\boldsymbol{v}_B-4\boldsymbol{v}_A)\right]-\frac{7}{2}\sum_{B\neq A}\sum_{D\neq B}\frac{G^2m_Bm_D}{c^2r_{AB}r_{BD}^3}\boldsymbol{n}_{BD}\,.
\end{aligned}
\tag{3.4}
$$

The extension of the equations of motion to the second post-Newtonian order was done only 30 years later. It started with the work of Ohta et al. in 1973-1974 [48, 49, 50, 51] using an Hamiltonian approach, but their results were not totally complete. In 1981-1983, the work of Damour and Deruelle led to the 2PN and 2.5PN equations of motion for two particles [52, 53, 54, 55, 56]. Let us mention other derivations of the 2PN equations of motion that were done later and independently: first of all, the work from Kopeikin et al. in 1985-1986 [57, 58] who derived this result by taking into account the internal structure of the bodies and checked explicitly that the dynamics does not depend on it at that order. Secondly, in 1998 Blanchet et al. [59] recovered these equations of motion in harmonic coordinates and computed also, for the first time, the near-zone metric. Then, Itoh, Futamase and Asada in 2000-2001 [60, 61] used a surface-integral (in the same spirit than the Einstein-Infeld-Hoffmann method, but technically much simpler) to recover the 2PN dynamics. Let us also mention the different work using extended fluids ball by Pati and Will such as [62] that recovers the 2PN-2.5PN equations of motion as well as the 3.5PN reaction radiation terms (cf the last paragraph of section 3.2.2 below).

3.2.2 3PN and 3.5PN

Different derivations including both the 3PN and the 3.5PN term have then been performed, such as the ADM-Hamiltonian formalism, done by Jaranowski and Schäfer joined later by Damour in 1997-2000 [63, 64, 65, 66, 67, 68, 69, 70, 71], using point-particle approximation for the compact bodies, and providing the result in the ADM-gauge.

Another method that have been used, was performed by Blanchet and Faye in 2000-2001 [72, 73, 74, 75], together with de Andrade [76] and Iyer [77]. It is based on solving directly the equations of motion in harmonic coordinates, iteratively order by order.

In 2003-2004, Itoh and Futamase applied the method they used at 2PN, and extended it at 3PN and 3.5PN [78, 79, 80]. As usual, this method encapsulates the compact bodies with surfaces, and only the Einstein equations in the vacuum are used.

More recently in 2011, an Effective-Field-Theory approach developed by Goldberger and Rothstein, was used by Foffa and Sturani [81] to find the 3PN Lagrangian, also in harmonic coordinates.

Let us also mention another series of publication focusing on the 3.5PN (and 4.5PN) dissipative terms, corresponding to a 1PN (and 2PN) relative correction of the dissipative effect occurring at 2.5PN. This effect has been computed in 1993-1995 by Iyer and Will [82, 83]. This works is based on balance equation between the conservative part and the energy flux emitted by the system. In 1996, Will and Wiseman obtained the second post-Newtonian correction in the flux, and obtained also from first principles the 2.5PN and 3.5PN coefficients in the equations of motion [84]. Latter works not relying on a specific balance equation, confirmed the 3.5PN term from first principles such as the derivation from Pati and Will done in 2002 [62] using their own DIRE (Direct Integration of relaxed Einstein equations) method developed in 1999-2000 [85, 86].

3.2.3 4PN and 4.5PN

Out of the different methods mentioned above at 3PN, three techniques have been used so far at 4PN.

The ADM approach was used in 2012-2014 by Jaranowski and Schäfer [87, 88, 89] joined later by Damour [90, 91]. They obtained the full 4PN dynamics and Hamiltonian except for one *ambiguity* parameter that needs to be fitted to self-force computations.

In 2016-2017, the work by Bernard-Bohé-Blanchet-Faye-Marsat [92], used the Fokker Lagrangian method, to derive the dynamics at 4PN in harmonic coordinates. While a first result of this latter work was in disagreement with the ADM approach result and the comparison with self-force computations, a better treatment of the infra-red regularization and the tail effects, enabled to get rid of that discrepancy and find from first principle the 4PN dynamics without any ambiguity[93, 94, 2]. This work will be explained in detail in chapter 6.

Finally, preliminary results have been published between 2013-2017 by Foffa *et al.* together with Sturani, Galley, Leibovich, Porto, Ross, using the Effective-Field-Theory approach [81, 95, 96, 97, 98]. While, the full dynamics is not computed yet, the main difficulties and caveats appearing at 4PN seemed to have already been solved, and this method might recover and confirm the first two results soon.

3.3 Spins

3.3.1 Formalism

So far, we have only reviewed work dealing with spinless bodies, i.e. neglecting the effect of the angular momentum of the compact bodies. However, a significant part of the compact bodies, and in particular the black holes, that we are going to detect can be spinning very fast. Some of the black holes may even be close to maximally spinning Kerr black holes. It is therefore crucial to take into account the effects of the spins on the dynamics and on the radiation of compact binary systems. As the work during this thesis did not tackle spins at all, we are just going to review the state-of-the-art results in that field here. Apart from this section, we will not mention the spins in the rest of the manuscript.

In PN theory, the spins are often described by the spin variable S defined as

$$S \equiv S_{\text{physical}} c \,, \tag{3.5}$$

where S_{physical} is the physical angular momentum of the compact body. In order to deal with dimensionless variables, we define χ such that $S \equiv m^2 G \chi$, where χ is equal to one for maximally spinning Kerr black hole. The usual way to count the post-Newtonian order of a spin effect, is to count the power of c when the result is expressed with the variable χ. This will give the magnitude of the spin effect in the worst case where the spin is maximal, i.e., $\chi = 1$.

The computation of the spin effect is based on the pole-dipole approximation: in the spinless case, particles are just monopole quantities characterized by their mass. In the pole-dipole approximation, they are characterized by two quantities: their mass and their spin. However, there is a variety of formalisms to deal with this pole-dipole approximation. For example, in some works, the contribution of the spins to the energy-impulsion tensor of the particles is given by [99, 100, 101, 102, 103] [1]

$$T_S^{\mu\nu}(t, \boldsymbol{x}) = -\frac{1}{c} \sum_A \nabla_\rho \left[S_A^{\rho(\mu} v_A^{\nu)} \frac{\delta(\boldsymbol{x} - \boldsymbol{y}_A)}{\sqrt{-(g)_A}} \right] \,, \tag{3.6}$$

where the particles are labelled by A, $S_A^{\mu\nu}$ is the spin tensor, $\boldsymbol{y}_A$ and v_A^μ are the position and the velocity of particle A and where $(g)_A$ is the determinant of the metric at the point $\boldsymbol{y}_A$. The spin tensor is an antisymmetric 4-rank tensor describing only the 3 degrees of freedom of the angular momentum of a compact body. Therefore, additional constraints called *supplementary spin condition (SSC)* have to imposed[2]. The dynamics of the particles is then described by the so-called Mathisson-Papapetrou equation.

[1] Cf the energy-impulsion tensor of spinless point-particle given by equation (6.16).

[2] The SSC corresponds to the choice of the point within the compact body from which we define the angular momentum.

3.3.2 State-of-the-art

As for the equations of motion, the effect of the spins have been computed by different methods: the ADM-Hamiltonian method, the post-Newtonian iteration scheme in harmonic coordinates (PNISH), and the effective-field theory framework (EFT). We need here to distinguish the effect of the spins in the equations of motion, and in the radiative field.

Regarding the equations of motion, the spin-orbit (SO) interaction starts at 1.5PN. It has been computed at 3.5PN (i.e. at *next-to-next-to-leading order*) within the ADM Hamiltonian method [104, 105, 106] and the PNISH formalism [107, 108, 109], while this effect has been computed only at 2.5PN (*next-to-leading order*) within the Effective-Field-Theory framework [110, 111]. The spin-spin interaction (SS) starts at 2PN and has now been computed at 3PN within the PNISH [112], ADM and EFT formalism [113, 114, 115]. Besides, the *crossed interaction* between the spins of each body $S_1 S_2$ has been determined by the ADM formalism at 4PN [116, 117]. For the spin-spin-spin (SSS) interaction, both the ADM [118] and the PNISH [119] formalism have computed it at the 3.5PN order.

The effects of the spins to the radiative field and the energy flux have been mainly tackled by the PNISH (with few partial results also provided by the EFT [120, 121]). Within the PNISH, for circular orbits, the SO contribution is known at 4PN [122, 123, 124], the SS [112] and the SSS [119] at 3PN. As both the dynamics and the energy flux are fully known at 3PN for the spins, the contribution of the spins to the phase at 3PN for circular orbit has been fully computing.

However, it turns out that the gravitational waveform polarizations are only known so far at 2PN [125, 126]. It is worth mentioning that all the results presented in this section take into account the work done for the spinless case. This means that the different effects are derived in such a way that we only have to add these effects on top of the spinless results.

3.4 The 4.5PN Project

The work done during this thesis is motivated by the project to compute the phase of the gravitational wave signal at 4.5PN for spinless compact binary in circular orbits, hence extending the equation (3.3).

In this thesis, the framework used is referred to as the *Blanchet-Damour-Iyer* formalism. In this framework, the field exterior to the source is studied using a multipolar-post-Minkowskian expansion of the metric, and is parametrized by a set of source multipole moments. A matching equation is used to connect the exterior field to the PN expansion of the field inside the source. This enables to obtain the expression of the source multipole moments as a function of the interior metric. Then conservative part of the dynamics is computed using a post-Newtonian expansion of the metric in harmonic coordinate. At the end of the day, we obtain the phase evolution as shown in equation (3.3)

The following chapters of this manuscript tackle the different steps mentioned above. In chapter 4, the multipolar-post-Minkowskian algorithm is explained in great detail. Then, chapter 5 deals with the matching procedure between the far-zone and the near-zone. The conservative part of the equations of motion at 4PN is obtained in chapter 6 using the Fokker Lagrangian, and the conserved quantities at 4PN are derived in chapter 7. Finally, chapter

8 explains how the multipole source moments are computing, dealing in particular with the computation of the mass quadrupole moment at 4PN.

While the phase is the most relevant and useful quantity for the analysis of the gravitational wave signal, this 4.5PN project will also enable to compute other interesting quantities such as the waveform and the polarizations at 4.5PN.

4 – The far-zone radiative field and the gravitational wave flux

The goal of this chapter is to study the gravitational field outside of the source through the use of the multipolar post-Minkowskian (MPM) algorithm. In this algorithm, the MPM expansion of the *far-zone* field is parametrized by a set of functions called the *source multipolar moments*. As we are going to see, non-local terms called *tails* enter this MPM expansion at the second post-Minkowskian iteration as well as at higher iterations. The main result of this chapter (equation (4.106)) correspond to the *tails* entering the fourth post-Minkowskian order of the metric. This result depends on the source mass quadrupole M_{ij}. The expression of M_{ij} as well as the expressions of all the other source multipole moments are derived thanks to a matching equation between the *far zone* and the *near zone*, which is the topic of chapter 5.

Using the equation (4.106) and the explicit value of M_{ij} at the 3PN order given by equation (4.123) (as well as other source multipolar moments provided by the equations (4.125)), we can compute the 4.5PN coefficient of the energy flux for spinless binary systems in circular orbits, as shown in the equation (4.137). This requires a few technical steps, such as the radiative coordinate transformation that is detailed in section 4.3.1.

4.1 The multipolar post-Minkowskian algorithm

4.1.1 The Einstein multipolar post-Minkowskian equations

In this section, we want to study the propagation of the gravitational waves from the source to the detectors. We consider a compact source of matter emitting gravitational waves in an asymptotically flat spacetime, and study the propagation of these waves from the source to the future null infinity $\mathcal{I}^+$. Therefore we want to find the most general solution to the Einstein equations in the *vacuum*, outside of a generic source, imposing the *non-incoming radiation* boundary condition[1]. We study such a solution by performing its Multipolar and post-Minkowskian (MPM) expansion.

We start by defining the deviation of the gothic metric to Minkowski's metric

$$h^{\alpha\beta} \equiv \sqrt{-g}g^{\alpha\beta} - \eta^{\alpha\beta}\,, \tag{4.1}$$

[1]This means that we are considering an isolated system emitting gravitational waves without any incoming gravitational waves coming from $\mathcal{I}^-$.

where g is the determinant of the metric $g_{\mu\nu}$, and $\mathfrak{g}^{\alpha\beta} \equiv \sqrt{-g}g^{\alpha\beta}$ is commonly referred to as the gothic metric. Besides, we impose the harmonic coordinate condition

$$\partial_\mu h^{\mu\nu} = 0\,. \tag{4.2}$$

In all this chapter, the background metric is the Minkowskian metric, and all the indices are lowered and raised with $\eta_{\mu\nu} = \mathrm{diag}(-1,+1,+1,+1)$ (except when explicitly specified). The Einstein equations can be written in the following form

$$\Box h^{\alpha\beta} = \frac{16\pi G}{c^4}\tau^{\alpha\beta}\,, \tag{4.3}$$

where $\Box = -\frac{1}{c^2}\frac{\partial^2}{\partial t^2} + \delta^{ij}\frac{\partial}{\partial x^i}\frac{\partial}{\partial x^j}$ is the flat d'Alembertian operator, and $\tau^{\alpha\beta}$ is the stress-energy pseudo tensor that takes into account both the matter and the non-linearities of the Einstein equations

$$\tau^{\alpha\beta} = |g|T^{\alpha\beta} + \frac{c^4}{16\pi G}\Lambda^{\alpha\beta}\,. \tag{4.4}$$

$T^{\alpha\beta}$ is the energy-impulsion tensor of the matter and can be set to zero ($T^{\alpha\beta} = 0$) throughout the rest of the chapter as we are considering solutions valid outside the source. $\Lambda^{\alpha\beta}$ takes into account the non-linearities of the Einstein equations and is given by

$$\begin{aligned}\Lambda^{\alpha\beta} = &-h^{\mu\nu}\partial^2_{\mu\nu}h^{\alpha\beta} + \partial_\mu h^{\alpha\nu}\partial_\nu h^{\beta\mu} + \frac{1}{2}g^{\alpha\beta}g_{\mu\nu}\partial_\lambda h^{\mu\tau}\partial_\tau h^{\nu\lambda}\\ &- g^{\alpha\mu}g_{\nu\tau}\partial_\lambda h^{\beta\tau}\partial_\mu h^{\nu\lambda} - g^{\beta\mu}g_{\nu\tau}\partial_\lambda h^{\alpha\tau}\partial_\mu h^{\nu\lambda} + g_{\mu\nu}g^{\lambda\tau}\partial_\lambda h^{\alpha\mu}\partial_\tau h^{\beta\nu}\\ &+ \frac{1}{8}\left(2g^{\alpha\mu}g^{\beta\nu} - g^{\alpha\beta}g^{\mu\nu}\right)\left(2g_{\lambda\tau}g_{\epsilon\pi} - g_{\tau\epsilon}g_{\lambda\pi}\right)\partial_\mu h^{\lambda\pi}\partial_\nu h^{\tau\epsilon}\,.\end{aligned} \tag{4.5}$$

In the previous equation (4.5), the indices of the metric $g_{\mu\nu}$ are raised with $g_{\mu\nu}$ itself (i.e. $g^{\mu\nu}g_{\mu\rho} = \delta^\nu_\rho$). There is no closed-form expression expressing $\Lambda^{\alpha\beta}$ as a function of $h^{\mu\nu}$ but one can always use equation (4.5) to expand $\Lambda^{\alpha\beta}$ up to any order n of $h^{\mu\nu}$ (neglecting terms of order $\mathcal{O}[h^{n+1}]$). For example

$$\Lambda^{\mu\nu} = N^{\mu\nu}(h^{\alpha\beta},h^{\alpha\beta}) + M^{\mu\nu}(h^{\alpha\beta},h^{\alpha\beta},h^{\alpha\beta}) + L^{\mu\nu}(h^{\alpha\beta},h^{\alpha\beta},h^{\alpha\beta},h^{\alpha\beta}) + \mathcal{O}(h^5)\,. \tag{4.6}$$

Because we set $T^{\alpha\beta} = 0$, the harmonic condition (4.2) implies

$$\partial_\mu\Lambda^{\mu\nu} = 0\,. \tag{4.7}$$

As we mentioned, we are going to find a Multipolar and Post-Minkowskian solution for $h^{\mu\nu}$. For that, we first define the following post-Minkowskian expansion

$$h^{\mu\nu} = Gh^{\mu\nu}_{(1)} + G^2h^{\mu\nu}_{(2)} + \cdots = \sum_{n\geq 1}G^n h^{\mu\nu}_{(n)}\,, \tag{4.8}$$

where G is Newton's constant. If we inject the expansion (4.8) into the Einstein equations (4.3) and look at each power of G we obtain the following set of equations, called the *multipolar post-Minkowskian Einstein vacuum equations* (for $n \geq 1$)

$$\Box h^{\mu\nu}_{(n)} = \Lambda^{\mu\nu}_{(n)}\left(h^{\alpha\beta}_{(1)}, h^{\alpha\beta}_{(2)}, \ldots, h^{\alpha\beta}_{(n-1)}\right)\,, \tag{4.9a}$$

$$\partial_\mu h^{\mu\nu}_{(n)} = 0\,, \tag{4.9b}$$

where $\Lambda^{\mu\nu}_{(1)} = 0$ and $\Lambda^{\mu\nu}_{(n)}$ corresponds to the coefficient in G^n in the source $\Lambda^{\mu\nu}$. This coefficient only depends on the solutions of lower post-Minkowskian orders, i.e., on $\{h^{\alpha\beta}_{(1)}, h^{\alpha\beta}_{(2)}, \dots, h^{\alpha\beta}_{(n-1)}\}$. In the following sections, we are going to explicitly solve (4.9) outside the source. Said otherwise, we will look for a solution for all $(t, \boldsymbol{x})$ such that $r = |\boldsymbol{x}| > a$ where a is bigger than the size of the source. However, in practice, we will find a formal vacuum solution valid for any $r > 0$ in a form of a multipolar expansion.

For convenience, we set $c = 1$ in the following sections. We will restore explicitly the powers of c in the equation (4.112).

4.1.2 Solving the MPM Einstein equations in the linear case

4.1.2.a) The MPM solution at linear order

Let us start by looking at the linear case of the set of equations (4.9)

$$\Box h^{\mu\nu}_{(1)} = 0\,, \tag{4.10a}$$

$$\partial_\mu h^{\mu\nu}_{(1)} = 0\,. \tag{4.10b}$$

We are looking for the most general solution of this set of equations outside of the source ($r > a$) that is past-stationary and is respecting the non-incoming wave boundary conditions. This means that there exists $\mathcal{T}$ such that $h^{\mu\nu}_{(1)}(t, \boldsymbol{x}) = h^{\mu\nu}_{(1)}(\boldsymbol{x})$ for $t \leq -\mathcal{T}$, hence the field is stationary for $t \leq -\mathcal{T}$ (and even for $t + r/c \leq \mathcal{T}$). Such a solution is known since the work of Thorne in 1980 [127]. It depends on six sets of functions $\{I_L, J_L, W_L, X_L, Y_L, Z_L\}$ that we will call the *multipolar source moments*. Here, L is a short-hand notation denoting ℓ space dummy indices. I.e. $L \equiv i_1 i_2 \dots i_\ell$ with $\{i_1, i_2, \dots, i_\ell\} \in \{1, 2, 3\}^\ell$. Similarly, $aL-1$ denotes the set of indices $aL - 1 = ai_1 \dots i_{\ell-1}$. We summarize all our notations in the appendix A. The functions $\{I_L, J_L, W_L, X_L, Y_L, Z_L\}$ are symmetric and trace-free (STF) with respect with all their indices. Besides they are all stationary in the past: for $t \leq -\mathcal{T}$, $I_L(t)$, $J_L(t)$, $W_L(t)$, $X_L(t)$, $Y_L(t)$ as well as $Z_L(t)$ are constant. With this notation we have [127]

$$h^{\alpha\beta}_{(1)} = k^{\alpha\beta}_{(1)} + \partial^\alpha \varphi^\beta_{(1)} + \partial^\beta \varphi^\alpha_{(1)} - \eta^{\alpha\beta}\partial_\mu \varphi^\mu_{(1)}\,. \tag{4.11}$$

With $k^{\alpha\beta}_{(1)}$ defined as:

$$k^{00}_{(1)} = -\frac{4}{c^2}\sum_{\ell\geqslant 0}\frac{(-1)^\ell}{\ell!}\partial_L\left(\frac{1}{r}\mathrm{I}_L(u)\right)\,, \tag{4.12a}$$

$$k^{0i}_{(1)} = \frac{4}{c^3}\sum_{\ell\geqslant 1}\frac{(-1)^\ell}{\ell!}\left\{\partial_{L-1}\left(\frac{1}{r}\mathrm{I}^{(1)}_{iL-1}(u)\right) + \frac{\ell}{\ell+1}\epsilon_{iab}\partial_{aL-1}\left(\frac{1}{r}\mathrm{J}_{bL-1}(u)\right)\right\}\,, \tag{4.12b}$$

$$k^{ij}_{(1)} = -\frac{4}{c^4}\sum_{\ell\geqslant 2}\frac{(-1)^\ell}{\ell!}\left\{\partial_{L-2}\left(\frac{1}{r}\mathrm{I}^{(2)}_{ijL-2}(u)\right) + \frac{2\ell}{\ell+1}\partial_{aL-2}\left(\frac{1}{r}\epsilon_{ab(i}\mathrm{J}^{(1)}_{j)bL-2}(u)\right)\right\}\,. \tag{4.12c}$$

And $\varphi^\alpha_{(1)}$ defined as

$$\varphi^0_{(1)} = \frac{4}{c^3}\sum_{\ell\geqslant 0}\frac{(-1)^\ell}{\ell!}\partial_L\left(\frac{1}{r}\mathrm{W}_L(u)\right)\,, \tag{4.13a}$$

$$\varphi^i_{(1)} = -\frac{4}{c^4}\sum_{\ell\geqslant 0}\frac{(-1)^\ell}{\ell!}\partial_{iL}\left(\frac{1}{r}\mathrm{X}_L(u)\right) \tag{4.13b}$$

$$-\frac{4}{c^4}\sum_{\ell\geqslant 1}\frac{(-1)^\ell}{\ell!}\left\{\partial_{L-1}\left(\frac{1}{r}\mathrm{Y}_{iL-1}(u)\right)+\frac{\ell}{\ell+1}\epsilon_{iab}\partial_{aL-1}\left(\frac{1}{r}\mathrm{Z}_{bL-1}(u)\right)\right\}. \tag{4.13c}$$

Where ϵ_{abc} is the Levi-Civita symbol, $u = t - r$ is the retarded time and $I^{(n)}_L(u)$ and $J^{(n)}_L(u)$ denotes the n^{th} time derivative of the functions $I_L(u)$ and $J_L(u)$.

4.1.2.b) Interpretation of the functions $\{I_L, J_L, W_L, X_L, Y_L, Z_L\}$: the multipole source moments

So far, the functions $\{I_L, J_L, W_L, X_L, Y_L, Z_L\}$ have not been specified. The only constraint is that they are stationary in the past in order to satisfy the non-incoming radiation condition. They depend on the physical properties of the source that is enclosed in the world-tube $r < a$. Using the matching equation (5.40) derived in the next chapter, we will be able to provide explicit expressions for these functions at the section 5.4. But for now, we are just going to provide a physical interpretation of them.

According to the equation (4.11), the function $\varphi_{(1)}$ only plays the role of a gauge transformation: it plays a role similar to gauge transformation parametrized by ξ^μ in the section 1.2.2, equation (1.10). Therefore let us focus first on the quantity $k^{\mu\nu}_{(1)}$ and on the physical interpretation of I_L and J_L.

The functions I_L are called the ℓ^{th}*-order mass multipole source moments*. Indeed it turns out that for $\ell = 0$, I is the ADM-mass of the source and is a constant function of time. Similarly for $\ell = 1$, I_i is proportional to the center of mass position and depends linearly on the time t. By imposing the stationary of the solution in the past, we obtain the fact that I_i is also constant. More generally, I_L is the ℓ^{th}-order mass multipole moment of the source, and at Newtonian order is given by

$$I_L(t) = \int \mathrm{d}^3\boldsymbol{x}\rho(\boldsymbol{x})\hat{x}_L + \mathcal{O}\left(\frac{1}{c^2}\right), \tag{4.14}$$

where $\rho(\boldsymbol{x})$ is the mass density at the position $\boldsymbol{x}$, where $\hat{x}_L \equiv x_{<i_1}\dots x_{i_\ell>}$ and where $<\cdot>$ means that we take the STF part of the indices. Of course, at Newtonian order, the quadrupole mass source moments I_{ij} corresponds to the multipole moments introduced in chapter 1 in equation (1.24).

The functions J_L are called the ℓ^{th}*-order current multipole source moments* with J_i being the total angular moment ($J_i = \text{const}$). At newtonian order

$$J_L(t) = \int \mathrm{d}^3\boldsymbol{x}\epsilon_{abi_\ell}\rho(\boldsymbol{x})x_{<i_1\dots i_{\ell-1}>a}v^b(\boldsymbol{x}) + \mathcal{O}\left(\frac{1}{c^2}\right), \tag{4.15}$$

where $v^b(\boldsymbol{x})$ is the velocity of the matter at the position $\boldsymbol{x}$.

The rest of the source multipole moments $\{W_L, X_L, Y_L, Z_L\}$ does not play a physical role at the first post-Minkowskian order because they can be removed by a change of gauge such as (1.10). However, they become physically relevant at higher post-Minkowskian orders, so it is crucial to keep them. One could show that the full MPM solution parametrized by the sets of moments $\{I_L, J_L, W_L, X_L, Y_L, Z_L\}$ is physically equivalent to the solution parametrized by the sets $\{M_L, S_L, 0, 0, 0, 0\}$ where M_L and S_L differs from I_L and J_L from 2.5-PN order and are called the *canonical source multipole moments* (respectively the *canonical source mass multipole moments* and the *canonical source current multipole moments*). For example [128]

$$\begin{aligned}
M_{ij} = I_{ij} &+ \frac{4G}{c^5}\left[W^{(2)}I_{ij} - W^{(1)}I^{(1)}_{ij}\right] \\
&+ \frac{4G}{c^7}\bigg[\frac{4}{7}W^{(1)}_{a\langle i}I^{(3)}_{j\rangle a} + \frac{6}{7}W_{a\langle i}I^{(4)}_{j\rangle a} - \frac{1}{7}I_{a\langle i}Y^{(3)}_{j\rangle a} - Y_{a\langle i}I^{(3)}_{j\rangle a} - 2XI^{(3)}_{ij} - \frac{5}{21}I_{ija}W^{(4)}_a \\
&\qquad + \frac{1}{63}I^{(1)}_{ija}W^{(3)}_a - \frac{25}{21}I_{ija}Y^{(3)}_a - \frac{22}{63}I^{(1)}_{ija}Y^{(2)}_a + \frac{5}{63}Y^{(1)}_a I^{(2)}_{ija} + 2W_{ij}W^{(3)} \\
&\qquad + 2W^{(1)}_{ij}W^{(2)} - \frac{4}{3}W_{\langle i}W^{(3)}_{j\rangle} + 2Y_{ij}W^{(2)} - 4W_{\langle i}Y^{(2)}_{j\rangle} \\
&\qquad + \varepsilon_{ab\langle i}\left(\frac{1}{3}I_{j\rangle a}Z^{(3)}_b + \frac{4}{9}J_{j\rangle a}W^{(3)}_b - \frac{4}{9}J_{j\rangle a}Y^{(2)}_b + \frac{8}{9}J^{(1)}_{j\rangle a}Y^{(1)}_b + Z_a I^{(3)}_{j\rangle b}\right)\bigg] \\
&+ \left(\frac{1}{c^8}\right) .
\end{aligned} \tag{4.16}$$

4.1.3 The MPM algorithm at any order n

We are now going to show that we can integrate the MPM Einstein equations (4.9) through the use of the MPM algorithm at each order n (the order $n = 1$ being already solved in the previous section). Let us assume that the solution of $h^{\mu\nu}$ is known up to G^{n-1}, i.e. that $\{h^{\mu\nu}_{(1)}, \ldots, h^{\mu\nu}_{(n-1)}\}$ are known as functions of $\{I_L, J_L, W_L, X_L, Y_L, Z_L\}$, and we focus on the following equations

$$\Box h^{\mu\nu}_{(n)} = \Lambda^{\mu\nu}_n\big(h^{\alpha\beta}_{(1)}, h^{\alpha\beta}_{(2)}, \ldots, h^{\alpha\beta}_{(n-1)}\big) , \tag{4.17a}$$

$$\partial_\mu h^{\mu\nu}_{(n)} = 0 . \tag{4.17b}$$

4.1.3.a) The operator $\mathrm{FP}_B\,\Box^{-1}_{\mathrm{ret}}\left[\left(\frac{r}{r_0}\right)^B \cdot\ \right]$

The first step is to use some inverse d'Alembertian operator $\Box^{-1}$ on the source $\Lambda_{(n)}$. As we are imposing the non-incoming radiation condition, we need to to use the retarded propagator $\Box^{-1}_{\mathrm{ret}}$ as we did in chapter 1. So a first try would be to define

$$u^{\mu\nu}_{(n)}(t,\boldsymbol{x}) \overset{?}{\equiv} \Box^{-1}_{\mathrm{ret}}\Lambda^{\mu\nu}_{(n)}(t,\boldsymbol{x}) = -\frac{1}{4\pi}\int \mathrm{d}^3\boldsymbol{x}'\,\frac{\Lambda^{\mu\nu}_{(n)}(t - \frac{|\boldsymbol{x}'-\boldsymbol{x}|}{c}, \boldsymbol{x}')}{|\boldsymbol{x}'-\boldsymbol{x}|} . \tag{4.18}$$

However, such a solution is ill-defined. In fact, $h^{\mu\nu}_{(1)}$ is singular when $r \to 0$, therefore $\Lambda^{\mu\nu}_{(2)}(h^{\alpha\beta}_{(1)}, h^{\alpha\beta}_{(1)})$ (and $h^{\mu\nu}_{(2)}$ etc.) are also singular when $r \to 0$. In particular, we see that if $\Lambda^{\alpha\beta}_{(n)} \sim_{r\to 0} r^k$ with $k \leq -3$, then the equation (4.18) is not convergent. This is an ultra-violet (UV) divergence that we are going to deal with using the Finite Part regularization.

The first step is to multiply the source by $\left(\frac{r}{r_0}\right)^B$ where B is a complex number and r_0 is a constant that we introduce by hand. This constant is not physical and should disappear at the end of the day when we express physical observables, but can stay in intermediate results. Let us $k_{\max}$ be an integer such that $\Lambda^{\alpha\beta}_{(n)} =_{r\to 0} \mathcal{O}(r^{k_{\max}})$. One could argue that if we consider the formal infinite multipolar sums of equations (4.12)–(4.13), we could not find such a $k_{\max}$. However, in practice, our computation will be truncated to a finite multipolar order, so the degree of divergency of the source at $r \to 0$ will be finite. Now, for B such that $\Re(B) > k_{\max} - 3$, we define

$$\begin{aligned} I^{\mu\nu}_{(n)}(B) &\equiv \Box^{-1}_{\text{ret}} \left[\left(\frac{r}{r_0} \right)^B \Lambda^{\mu\nu}_{(n)} \right] \\ &= -\frac{1}{4\pi} \int \mathrm{d}^3\boldsymbol{x}' \frac{\left(\frac{r}{r_0}\right)^B \Lambda^{\mu\nu}_{(n)}(t - \frac{|\boldsymbol{x}'-\boldsymbol{x}|}{c}, \boldsymbol{x}')}{|\boldsymbol{x}' - \boldsymbol{x}|} \,. \end{aligned} \tag{4.19}$$

As long as $\Re(B) > k_{\max} - 3$, $I^{\mu\nu}_{(n)}(B)$ is well-defined and is a analytic function of $B \in \mathbb{C}$. This latter assertion will not be proved here but can be checked by studying the mathematical structure of the source $\Lambda^{\mu\nu}_{(n)}$ as done in [129]. By *analytic continuation*, this function is uniquely defined over all the complex plane except possibly some isolated poles (in particular except for $B = 0$ very often). In the neighborhood of $B = 0$ we are going to perform a *Laurent expansion* of $I^{\mu\nu}_{(n)}(B)$

$$I^{\mu\nu}_{(n)}(B) \underset{B\to 0}{=} \sum_{k \geq p_0} B^k \iota^{\mu\nu}_{(k)} \,. \tag{4.20}$$

Now, if we apply the d'Alembertian operator $\Box$ on both sides of equation (4.20), the left-hand side becomes

$$\begin{aligned} \left(\frac{r}{r_0} \right)^B \Lambda^{\mu\nu}_{(n)} &\underset{B\to 0}{=} \left[1 + B \ln\left(\frac{r}{r_0}\right) + \frac{B^2}{2!} \ln^2\left(\frac{r}{r_0}\right) + \dots \right] \Lambda^{\mu\nu}_{(n)} \\ &= \left[1 + \sum \frac{B^q}{q!} \ln^q\left(\frac{r}{r_0}\right) \right] \Lambda^{\mu\nu}_{(n)} \,. \end{aligned} \tag{4.21}$$

By applying the d'Alembertian operator on each side of equation (4.20) and equating the different powers of B we obtain that

$$\Box \iota^{\mu\nu}_{(k)} = 0 \text{ for } k < 0 \,, \tag{4.22a}$$
$$\Box \iota^{\mu\nu}_{(0)} = \Lambda^{\mu\nu}_{(n)} \,, \tag{4.22b}$$
$$\Box \iota^{\mu\nu}_{(k)} = \frac{1}{k!} \ln^k\left(\frac{r}{r_0}\right) \Lambda^{\mu\nu}_{(n)} \text{ for } k \geq 1 \,. \tag{4.22c}$$

Therefore, we are interested in the function $\iota^{\mu\nu}_{(0)}$ which is called the Finite Part of $I^{\mu\nu}_{(n)}(B)$ when $B \to 0$ and denoted $\mathrm{FP}_B\, I^{\mu\nu}_{(n)}(B)$. Hence, instead of the definition (4.18), we define $u^{\mu\nu}_{(n)}$ by

$$u^{\mu\nu}_{(n)} = \underset{B}{\mathrm{FP}}\, \Box^{-1}_{\text{ret}} \left[\left(\frac{r}{r_0} \right)^B \Lambda^{\mu\nu}_{(n)} \right] . \tag{4.23}$$

Based on what we previously said, $u^{\mu\nu}_{(n)}$ is well-defined and we have

$$\Box u^{\mu\nu}_{(n)} = \Lambda^{\mu\nu}_{(n)} \,. \tag{4.24}$$

4.1.3.b) Going to the harmonic gauge

In the previous section, we find a way to solve the equation (4.17a) but there is no reason why $u^{\mu\nu}_{(n)}$ should be divergence-free. So we have not yet solved the equation (4.17b). Let us define $w^{\mu}_{(n)} \equiv \partial_\nu u^{\mu\nu}_{(n)}$. We want to find a function $v^{\mu\nu}_{(n)}$ such that $\Box v^{\mu\nu}_{(n)} = 0$ and $\partial_\nu v^{\mu\nu}_{(n)} = -w^\mu$. As we are dealing with multipolar-expanded quantities, we can find four sets of functions $\{N_L, P_L, Q_L, R_L\}$ such that [129, 130]

$$w^0_{(n)} = \sum_{l=0}^{+\infty} \partial_L \left[r^{-1} N_L(u)\right] , \tag{4.25a}$$

$$\begin{aligned} w^i_{(n)} = &\sum_{l=0}^{+\infty} \partial_{iL} \left[r^{-1} P_L(u)\right] \\ &+ \sum_{l=1}^{+\infty} \left\{\partial_{L-1} \left[r^{-1} Q_{iL-1}(u)\right] + \epsilon_{iab}\partial_{aL-1} \left[r^{-1} R_{bL-1}(u)\right]\right\} , \end{aligned} \tag{4.25b}$$

where we recall that $u = t - r$ is the retarded time. Using these functions, let us define $v^{\mu\nu}_{(n)}$ by [130]

$$v^{00}_{(n)} = -r^{-1}N^{(-1)} + \partial_a \left[r^{-1} \left(-N_a^{(-1)} + C_a^{(-2)} - 3P_a\right)\right] , \tag{4.26a}$$

$$v^{0i}_{(n)} = r^{-1} \left(-Q_i^{(-1)} + 3P_i^{(1)}\right) - \epsilon_{iab}\partial_a \left[r^{-1} R_b^{(-1)}\right] - \sum_{l=2}^{+\infty} \partial_{L-1} \left[r^{-1} N_{iL-1}\right] , \tag{4.26b}$$

$$v^{ij}_{(n)} = -\delta_{ij} r^{-1} P + \sum_{l=2}^{+\infty}\Big\{2\delta_{ij}\partial_{L-1} \left[r^{-1} P_{L-1}\right] - 6\partial_{L-2(i} \left[r^{-1} P_{j)L-2}\right] \tag{4.26c}$$

$$+ \partial_{L-2} \left[r^{-1}(N^{(1)}_{ijL-2} + 3P^{(2)}_{ijL-2} - Q_{ijL-2})\right] - 2\partial_{aL-2} \left[r^{-1}\epsilon_{ab(i} R_{j)bL-2}\right]\Big\} . \tag{4.26d}$$

Here $N_a^{(-n)}$ is the n^{th} primitive of N_a, that vanishes in the past[2].

Now, all the terms in $v^{\mu\nu}_{(n)}$ are on the form $\partial_L \frac{F(u)}{r} = \partial_L \frac{F(t-r)}{r}$, so we have automatically $\Box v^{\mu\nu}_{(n)} = 0$. Besides, it is fastidious but straightforward to show (using the decomposition (4.25)) that $\partial_\nu v^{\mu\nu}_{(n)} = -w^\mu_{(n)}$.

Now, if we define $h^{\mu\nu}_{(n)} = v^{\mu\nu}_{(n)} + u^{\mu\nu}_{(n)}$, we obtain a solution for the equations (4.17a)–(4.17b), and the procedure presented above, called the *MPM algorithm* enables us to compute at each order n the MPM expansion of the metric $h^{\mu\nu}$ in harmonic coordinates.

The choice of $v^{\mu\nu}_{(n)}$ defined by the equation (4.26) is arbitrary[3]. We could have chosen another solution of $v^{\mu\nu}_{(n)}$ with the same properties. If we did so, the MPM expansion that we would have obtained would have differed: it would have been a different function of the multipole source moments $\{I_L, J_L, W_L, X_L, Y_L, Z_L\}$. But we can show that this difference can be absorbed by a redefinition of the multipole source moments. Therefore, when we derive the explicit expressions of the multipole source moments (cf equation (5.50)), it is crucial to keep in mind the arbitrary choice of $v^{\mu\nu}_{(n)}$ that we made in order to obtain the expressions of $\{I_L, J_L, W_L, X_L, Y_L, Z_L\}$ consistently with that specific choice.

[2] More precisely, as all the physical quantities we are dealing with are zero (or constant) for all $t \leq -\mathcal{T}$, we have $N_a^{(-n)}(u) = \int_{-\mathcal{T}}^{u} N_a^{(-n+1)}(s)\mathrm{d}s$ for $u \geq -\mathcal{T}$ and $N_a^{(-n)}(u) = 0$ for $u < -\mathcal{T}$.

[3] For example, its definition has slightly changed between [129] and [130].

4.1.4 A useful notation

Let us introduce a useful notation that we are going to use throughout the chapter to list all the terms appearing in the MPM expansion of the metric. The linear metric $h^{\mu\nu}_{(1)}$ depends in a linear way on the sets of functions $\{I_L, J_L, W_L, X_L, Y_L, Z_L\}$. We are going to use the notation $h^{\mu\nu}_{(1)I_L}$ to denote the term of $h^{\mu\nu}_{(1)}$ that depends on I_L and so on. For example, using the definition (4.11)

$$h^{00}_{(1)I_{kl}} = -\frac{2}{c^4}\partial_{ab}\left[\frac{1}{r}I_{ab}(u)\right], \tag{4.27a}$$

$$h^{0i}_{(1)I_{kl}} = \frac{2}{c^3}\partial_{a}\left[\frac{1}{r}I^{(1)i}_{a}(u)\right], \tag{4.27b}$$

$$h^{ij}_{(1)I_{kl}} = -\frac{2}{c^4}\frac{1}{r}I^{(2)ij}(u)\,. \tag{4.27c}$$

$h^{\mu\nu}_{(1)I_{kl}}$ corresponds to the contribution of the mass multipole of the source to the first post-Minkowskian order of the metric. Now, each term appearing at the n^{th} post-Minkowskian order of the metric can be identified by a list of n multipole source moments and corresponds to the contribution of the interactions of these moments to the metric at the n^{th} post-Minkowskian order.

For example, the interaction between the masse quadrupole I_{ij} and the current quadrupole J_{ij} appearing in the second post-Minkowskian order is noted $h^{\mu\nu}_{(2)I_{kl}\times J_{mn}}$ and is the solution constructed with the previously described MPM algorithm of the following equations

$$\Box h^{\mu\nu}_{(2)I_{kl}\times J_{mn}} = \Lambda^{\mu\nu}_{(2)}(h^{\alpha\beta}_{(1)I_{kl}}, h^{\alpha\beta}_{(1)J_{mn}})\,, \tag{4.28a}$$

$$\partial_\nu h^{\mu\nu}_{(2)I_{kl}\times J_{mn}} = 0\,. \tag{4.28b}$$

4.2 An explicit computation of the tails

For the rest of the chapter, we are going to use for convenience the canonical source multipole moments M_L and S_L. As we explained above, those multipole moments only differ from I_L and J_L at the 2.5PN order (cf equation (4.16)).

We are going to compute the following terms: $h^{\mu\nu}_{(2)M\times M_{ij}}$, $h^{\mu\nu}_{(3)M^2\times M_{ij}}$ and $h^{\mu\nu}_{(4)M^3\times M_{ij}}$. The first is known since 1992 from Blanchet and Damour [131] and contributes at the 1.5PN order in the gravitational wave energy flux. The second term $h^{\mu\nu}_{(3)M^2\times M_{ij}}$ has been computed asymptotically (i.e. when $r\to\infty$) in 1998 by Blanchet [132] and contributes at 3PN order in the flux. This latter term has then been fully computed during this thesis in [1], alongside with the asymptotic value of $h^{\mu\nu}_{(4)M^3\times M_{ij}}$ that was required to compute the flux at 4.5PN.

In a first section, we are going to derive steps by steps, the explicit propagators used to compute $h^{\mu\nu}_{(2)M\times M_{ij}}$, and we will discuss the non-local terms called *tails* appearing already at the second post-Minkowskian order. Then, we will provide all the useful formulae found in [1], that are required to compute $h^{\mu\nu}_{(3)M^2\times M_{ij}}$ and the asymptotic value of $h^{\mu\nu}_{(4)M^3\times M_{ij}}$.

This section 4.2 is rather long and technical, as all the formulae required to get the asymptotic value of $h^{\mu\nu}_{(4)M^3\times M_{ij}}$ are derived. Its final result, i.e., the asymptotic value of $h^{\mu\nu}_{(4)M^3\times M_{ij}}$ is then provided at the end of the section in 4.2.6.

4.2.1 A computation step by step of $h^{\mu\nu}_{(2)M\times M_{ij}}$

To begin with, let us provide the value of $h^{\mu\nu}_{(1)M}$ as well as $h^{\mu\nu}_{(1)M_{ij}}$ (posing $c=1$):

$$h^{00}_{(1)M}(t,\boldsymbol{x}) = -4r^{-1}M\,, \tag{4.29a}$$
$$h^{0i}_{(1)M}(t,\boldsymbol{x}) = 0\,, \tag{4.29b}$$
$$h^{ij}_{(1)M}(t,\boldsymbol{x}) = 0\,. \tag{4.29c}$$

For further use we also provide

$$h^{00}_{(2)M^2}(t,\boldsymbol{x}) = -7r^{-2}M^2\,, \tag{4.30a}$$
$$h^{0i}_{(2)M^2}(t,\boldsymbol{x}) = 0\,, \tag{4.30b}$$
$$h^{ij}_{(2)M^2}(t,\boldsymbol{x}) = -n_{ij}r^{-2}M^2\,, \tag{4.30c}$$

and

$$h^{00}_{(3)M^3}(t,\boldsymbol{x}) = -8r^{-3}M^3\,, \tag{4.31a}$$
$$h^{0i}_{(3)M^3}(t,\boldsymbol{x}) = 0\,, \tag{4.31b}$$
$$h^{ij}_{(3)M^3}(t,\boldsymbol{x}) = 0\,. \tag{4.31c}$$

The vector n^i is defined as $n^i = x^i/r$, and $n_{i_1\dots i\ell} = n_{i_1}\dots n_{i_\ell}$. While the equations (4.30) and (4.31) could be computed through the use of the MPM algorithm, $h^{\alpha\beta}_{(n)M^n}$ can be easily and quickly obtained by expanding up to power G^n the Schwarzschild metric in harmonic coordinates. Finally we have

$$h^{00}_{(1)M_{ij}}(t,\boldsymbol{x}) = -2\hat{n}_{ab}r^{-3}\left[3M_{ab}(t-r) + 3rM^{(1)}_{ab}(t-r) + r^2M^{(2)}_{ab}(t-r)\right]\,, \tag{4.32a}$$
$$h^{0i}_{(1)M_{ij}}(t,\boldsymbol{x}) = -2\hat{n}_{a}r^{-2}\left[M^{(1)}_{ai}(t-r) + rM^{(2)}_{ai}(t-r)\right]\,, \tag{4.32b}$$
$$h^{ij}_{(1)M_{ij}}(t,\boldsymbol{x}) = -2r^{-1}M^{(2)}_{ij}(t-r)\,. \tag{4.32c}$$

This last equation is equivalent to the example provided in section 4.1.4 equation (4.27), but the derivative ∂_L have been explicitly computed. The hat symbol on top of $n_{i_1\dots i\ell}$ means that we should take the STF part of it. If we inject these values in the quadratic source in order to compute $\Lambda^{\mu\nu}_{(2)}(h^{\alpha\beta}_{(1)M}, h^{\alpha\beta}_{(1)M_{ij}})$, and multiply the source by the regularization factor $\left(\frac{r}{r_0}\right)^B$ all the terms of the source can be written in the following form

$$\left(\frac{r}{r_0}\right)^B \Lambda^{\mu\nu}_{(2)M\times M_{ij}} \sim \sum \left(\frac{r}{r_0}\right)^B \frac{\hat{n}_L F(t-r)}{r^k}\,, \tag{4.33}$$

where F is a function that is zero or constant for $t \leq -\mathcal{T}$. In order to perform the MPM algorithm, we first need to find an expression for $\mathrm{FP}\Box^{-1}_{\mathrm{ret}}\left[\left(\frac{r}{r_0}\right)^B \frac{\hat{n}_L}{r^k}F(t-r)\right]$ for any $\ell \geq 0$ and $k \geq 2$.

Computing $\Box^{-1}_{\mathrm{ret}}\left[\left(\frac{r}{r_0}\right)^B \frac{\hat{n}_L}{r^k} F(t-r)\right]$

Let us focus first on the retarded propagator without taking the Finite Part yet and compute $\Box^{-1}_{\mathrm{ret}}\left[\left(\frac{r}{r_0}\right)^B \frac{\hat{n}_L}{r^k} F(t-r)\right]$.

$\Box^{-1}_{\mathrm{ret}}$ is the operator defined by equation (4.18), but this definition is not very adapted to our multipolar decomposition of the source. In fact, if a source can be written as $S(t,\boldsymbol{x}) = \hat{n}_L \tilde{S}(r, t-r)$, and satisfy some regularity conditions when $r \to 0$[4] ,then we have [129]

$$\Box^{-1}_{\mathrm{ret}} S(t,\boldsymbol{x}) = \int_{-\infty}^{t-r} \mathrm{d}s \hat{\partial}_L \left(\frac{R\left[\frac{t-r-s}{2}, s\right] - R\left[\frac{t+r-s}{2}, s\right]}{r} \right) , \tag{4.34}$$

where R is defined as

$$R(r,s) \equiv r^\ell \int_0^r \mathrm{d}y \frac{(r-y)^\ell}{\ell!} \left(\frac{2}{y}\right)^{\ell-1} \tilde{S}(y,s) . \tag{4.35}$$

If we use (4.34) for the source $S(t,\boldsymbol{x}) = \left[\left(\frac{r}{r_0}\right)^B \frac{\hat{n}_L}{r^k} F(t-r)\right]$ we get after few algebra steps including some integration by parts

$$\begin{aligned}\Box^{-1}_{\mathrm{ret}}\left[\left(\frac{r}{r_0}\right)^B \frac{\hat{n}_L}{r^k} F(t-r)\right] &= \frac{2^{k-3}}{(2r_0)^B (B-k+2)(B-k+1)\cdots(B-k-\ell+2)} \\ &\times \int_r^{+\infty} ds\, F(t-s) \hat{\partial}_L \left\{ \frac{(s-r)^{B-k+\ell+2} - (s+r)^{B-k+\ell+2}}{r} \right\} . \end{aligned} \tag{4.36}$$

Case $k=2$: $\mathrm{FP}\Box^{-1}_{\mathrm{ret}}\left[\left(\frac{r}{r_0}\right)^B \frac{\hat{n}_L}{r^2} F(t-r)\right]$

For $k=2$, equation (4.36) becomes

$$\Box^{-1}_{\mathrm{ret}}\left[\left(\frac{r}{r_0}\right)^B \frac{\hat{n}_L}{r^2} F(t-r)\right] = \frac{1}{2(2r_0)^B B(B-1)\cdots(B-\ell)} \tag{4.37}$$

$$\times \int_r^{+\infty} ds\, F(t-s) \hat{\partial}_L \left\{ \frac{(s-r)^{B+\ell} - (s+r)^{B+\ell}}{r} \right\} . \tag{4.38}$$

Now, in order to take the Finite Part when $B \to 0$ we need to do a Laurent expansion of the right-hand side. For that, we will use the fact that $(s-r)^B = 1 + B\ln(s-r) + \mathcal{O}(B^2)$ and $(s+r)^B = 1 + B\ln(s+r) + \mathcal{O}(B^2)$. Therefore, by taking into account the pole in $1/B$ appearing in the pre-factor of (4.37), we find that

$$\begin{aligned}\mathrm{FP}\Box^{-1}_{\mathrm{ret}}\left[\left(\frac{r}{r_0}\right)^B \frac{\hat{n}_L}{r^2} F(t-r)\right] &= \frac{(-1)^\ell}{2} \int_r^{+\infty} ds\, F(t-s) \\ &\times \hat{\partial}_L \left\{ \frac{(s-r)^\ell \ln(s-r) - (s+r)^\ell \ln(s+r)}{\ell! r} \right\} . \end{aligned} \tag{4.39}$$

[4] Cf [129] for the mathematical properties that should satisfy S when $r \to 0$. In practice, as we are going to multiply S by $(r/r_0)^B$, these conditions will be automatically satisfied.

To obtain (4.39), we have used the following [129]:

$$\hat{\partial}_L \left[\frac{(s-r)^k - (s+r)^k}{r} \right] = 0 \text{ for } k = 0, \dots, 2\ell \,. \tag{4.40}$$

As shown in [131], this result can be written as

$$\mathrm{FP}\Box^{-1}_{\mathrm{ret}} \left[\left(\frac{r}{r_0}\right)^B \frac{\hat{n}_L}{r^2} F(t-r) \right] = -\frac{\hat{n}_L}{r} \int_r^{+\infty} ds F(t-s) Q_\ell \left(\frac{s}{r}\right) \ , \tag{4.41}$$

where Q_ℓ is the Legendre function of second kind defined by

$$Q_\ell(x) = \frac{1}{2} P_\ell(x) \ln \left(\frac{x+1}{x-1}\right) - \sum_{j=1}^{\ell} \frac{1}{j} P_{\ell-j}(x) P_{j-1}(x) \ , \tag{4.42}$$

and where P_ℓ are the Legendre polynomials. For further use, note that the asymptotic behavior of Q_l is given by

$$Q_\ell(y) = -\frac{1}{2} \ln \left(\frac{y-1}{2}\right) - H_\ell + \mathcal{O}(y-1) \,, \tag{4.43}$$

where $H_\ell = \sum_{j=1}^{\ell} \frac{1}{j}$ denotes the usual harmonic number.

Equation (4.41) is a closed analytical form that enables us to integrate all the terms with $k = 2$ in the source $\Lambda^{\mu\nu}_{(2)M\times M_{ij}}$.

Integrate the quartic source when $k \geq 3$

When $k \geq 3$, the equation (4.36) is still valid. Starting from there, we can integrate $k-2$ times by part the integral along s. This leads to an integral that is similar to the case $k = 2$ in addition to some boundary terms. Doing so, we obtain [130]

$$\begin{aligned} \Box^{-1}_{\mathrm{ret}} \left[\left(\frac{r}{r_0}\right)^B \frac{\hat{n}_L}{r^k} F(t-r) \right] &= \left(\frac{r}{r_0}\right)^B \sum_{i=0}^{k-3} \alpha_i(B) \hat{n}_L \frac{F^{(i)}(t-r)}{r^{k-i-2}} \\ &\quad + \beta(B) \Box^{-1}_{\mathrm{ret}} \left[\left(\frac{r}{r_0}\right)^B \frac{\hat{n}_L}{r^2} F^{(k-2)}(t-r) \right] \ , \end{aligned} \tag{4.44}$$

where the coefficient α_i and β are given by

$$\alpha_i(B) = \frac{2^i (B-k+2+i)..(B-k+3)}{(B-k+2-\ell+i)..(B-k+2-\ell)(B-k+3+\ell+i)..(B-k+3+\ell)} \ , \tag{4.45a}$$

$$\beta(B) = \frac{2^{k-2} B(B-1)..(B-\ell)}{(B-k+2)..(B-k-\ell+2)(B+\ell)..(B-k+\ell+3)} \ . \tag{4.45b}$$

When $3 \geq k \geq \ell+2$, $\beta(B) = 0$ and $\alpha_i(B)$ does not have any $1/B$ pole. Therefore the result is simply [130]

$$\underset{B=0}{\mathrm{FP}} \, \Box^{-1}_{\mathrm{ret}} \left[\left(\frac{r}{r_0}\right)^B \frac{\hat{n}_L}{r^k} F(t-r) \right] = -\frac{2^{k-3}(k-3)!(\ell+2-k)!}{(\ell+k-2)!} \hat{n}_L$$

$$\times \sum_{j=0}^{k-3} \frac{(\ell+j)!}{2^j j!(\ell-j)!} \frac{F^{(k-3-j)}(t-r)}{r^{j+1}} \,. \tag{4.46}$$

In the case $k \geq \ell+3$, α_i has a pole and $\beta(B)$ is finite. Thus we obtain [130]

$$\begin{aligned}
&\mathop{\mathrm{FP}}_{B=0} \Box^{-1}_{\mathrm{ret}}\left[\left(\frac{r}{r_0}\right)^B \frac{\hat{n}_L}{r^k} F(t-r)\right] \\
&\quad = \sum_{i=0}^{k-3} \tilde{\alpha}_i \hat{n}_L \frac{F^{(i)}(t-r)}{r^{k-i-2}} + \frac{(-1)^{k+\ell} 2^{k-2}(k-3)!}{(k+\ell-2)!(k-\ell-3)!} \\
&\quad \times \left\{ \frac{(-1)^\ell}{2} \ln\left(\frac{r}{r_0}\right) \hat{\partial}_L \left(\frac{F^{(k-\ell-3)}(t-r)}{r}\right) + \mathrm{FP}_{B=0} \Box^{-1}_{\mathrm{ret}}\left[\frac{\hat{n}_L}{r^2} F^{(k-2)}(t-r)\right]\right\} \,.
\end{aligned} \tag{4.47}$$

Explicit expression of $h_{(2)M\times M_{ij}}$

Using the previous integration formulae, the mass-quadrupole metric appearing at the second post-Minkowskian order can be explicitly computed. As explained in section 4.1.3, we proceed in two steps. First we compute $u^{\mu\nu}_{(2)M\times M_{ij}}$ using the integration formulae presented above. Then we compute $v^{\mu\nu}_{(2)M\times M_{ij}}$ using the prescription given in 4.1.3.b). The final result is therefore $h^{\mu\nu}_{(2)M\times M_{ij}} = u^{\mu\nu}_{(2)M\times M_{ij}} + v^{\mu\nu}_{(2)M\times M_{ij}}$. However it happens that in that specific case $v^{\mu\nu}_{(2)M\times M_{ij}} = 0$ and we get

$$\begin{aligned}
M^{-1} h^{00}_{(2)M\times M_{pq}} &= n_{ab} r^{-4}\left\{-21 M_{ab} - 21 r M^{(1)}_{ab} + 7 r^2 M^{(2)}_{ab} + 10 r^3 M^{(3)}_{ab}\right\} \\
&+ 8 n_{ab} \int_1^{+\infty} dx Q_2(x) M^{(4)}_{ab}(t-rx) \,,
\end{aligned} \tag{4.48a}$$

$$\begin{aligned}
M^{-1} h^{0i}_{(2)M\times M_{pq}} &= n_{iab} r^{-3}\left\{-M^{(1)}_{ab} - r M^{(2)}_{ab} - \frac{1}{3} r^2 M^{(3)}_{ab}\right\} \\
&+ n_a r^{-3}\left\{-5 M^{(1)}_{ai} - 5 r M^{(2)}_{ai} + \frac{19}{3} r^2 M^{(3)}_{ai}\right\} \\
&+ 8 n_a \int_1^{+\infty} dx Q_1(x) M^{(4)}_{ai}(t-rx) \,,
\end{aligned} \tag{4.48b}$$

$$\begin{aligned}
M^{-1} h^{ij}_{(2)M\times M_{pq}} &= n_{ijab} r^{-4}\left\{-\frac{15}{2} M_{ab} - \frac{15}{2} r M^{(1)}_{ab} - 3 r^2 M^{(2)}_{ab} - \frac{1}{2} r^3 M^{(3)}_{ab}\right\} \\
&+ \delta_{ij} n_{ab} r^{-4}\left\{-\frac{1}{2} M_{ab} - \frac{1}{2} r M^{(1)}_{ab} - 2 r^2 M^{(2)}_{ab} - \frac{11}{6} r^3 M^{(3)}_{ab}\right\} \\
&+ n_{a(i} r^{-4}\left\{6 M_{j)a} + 6 r M^{(1)}_{j)a} + 6 r^2 M^{(2)}_{j)a} + 4 r^3 M^{(3)}_{j)a}\right\} \\
&+ r^{-4}\left\{-M_{ij} - r M^{(1)}_{ij} - 4 r^2 M^{(2)}_{ij} - \frac{11}{3} r^3 M^{(3)}_{ij}\right\} \\
&+ 8 \int_1^{+\infty} dx Q_0(x) M^{(4)}_{ij}(t-rx) \,.
\end{aligned} \tag{4.48c}$$

In the equations (4.48), the quadrupole M_{ij} and its derivative $M^{(n)}_{ij}$ are evaluated at the retarded time $u = t - r$ in all the instantaneous terms (for which the dependence is not written explicitly), while they are evaluated at $t - rx$ in the non-local terms.

4.2.2 Non-locality: the appearance of the tails

Equation (4.48) shows two kinds of terms: local terms and non-local terms. At linear order in G — as gravitational waves travel at the speed of light — the metric $h^{\mu\nu}_{(1)}(t, \boldsymbol{x})$ due to a source whose wordline is along the origin only depends on that source at the time $u = t - r/c$. However, starting from the second post-Minkowskian order, terms like $8n_{ab}\int_1^{+\infty} dx Q_2(x) M^{(4)}_{ab}(t - rx)$ depend on the quadrupole of the source along its past history up to $t - r/c$. This non-local effect is called a tail effect and is due to the non-linearities of the Einstein field equations. It can be interpreted as the gravitational waves emitted by the varying quadrupole of the source, being scattered by the background metric curved by the mass of the source. It is therefore in that case a mass-quadrupole interaction. The figure 4.1, provides further clarifications of this non-local effect.

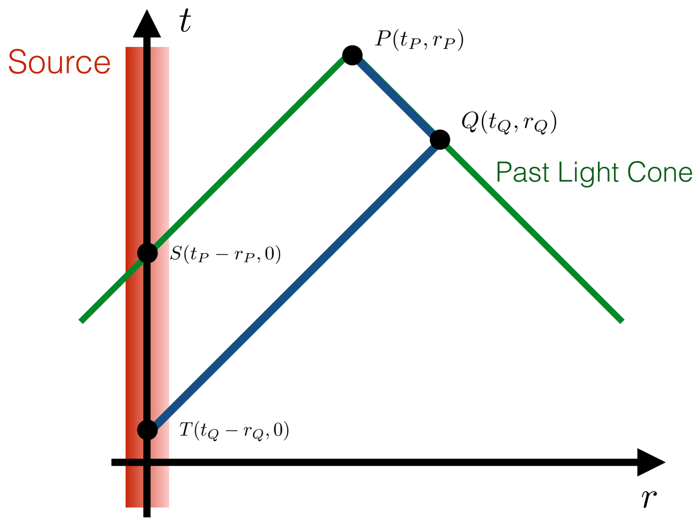

Figure 4.1: Schematic representation of the tail effect. The linear metric at point $P(t_P, r_P)$ only depends on the source at the point $S(t_p - r_p, 0)$ which represents the intersection of the past light cone of P with the wordline of the source. At the second post-Minkowskian order, the metric at the point P depends on the linear metric on the past light cone of P, for example on the point Q. However, the linear metric at the point Q depends on the source at the point T. Therefore, the second post-Minkowskian metric at the point P depends on the source at the point T and more generally on all the past of the source. This effect constitutes a non-local term in the metric called a *tail*.

4.2.3 Computation of the tails-of-tails and the tails-of-tails-of-tails

Now that $h^{\mu\nu}_{(2)M\times M_{ij}}$ is fully known, we can compute the source $\Lambda^{\mu\nu}_{(3)M\times M\times M_{ij}}$. This source contains all the interactions between: $h^{\mu\nu}_{(1)M}$ and $h^{\mu\nu}_{(2)M\times M_{ij}}$, $h^{\mu\nu}_{(2)M^2}$ and $h^{\mu\nu}_{(1)M_{ij}}$, and finally between $h^{\mu\nu}_{(1)M}$, $h^{\mu\nu}_{(1)M}$ and $h^{\mu\nu}_{(1)M_{ij}}$. Using the notation introduced in equation (4.6), we have

$$\Lambda^{\mu\nu}_{(3)M\times M\times M_{ij}} = N^{\mu\nu}[h^{\alpha\beta}_{(1)M}, h^{\alpha\beta}_{(2)M\times M_{ij}}] + N^{\mu\nu}[h^{\alpha\beta}_{(2)M^2}, h^{\alpha\beta}_{(1)M_{ij}}]$$

$$+ M^{\mu\nu}[h^{\alpha\beta}_{(1)M}, h^{\alpha\beta}_{(1)M}, h^{\alpha\beta}_{(1)M_{ij}}]\,. \tag{4.49}$$

We recall that $h^{\mu\nu}_{(2)M^2}$ is provided by the equation (4.30). The integration of (4.49) was investigated by Blanchet in 1998 [132] and $h_{(3)M^2\times M_{ij}}$ was found asymptotically when $r \to \infty$ with $u = t - r/c$ constant. This result has been extended by our work [1] where we developped formulae to fully integrate equation (4.49). Once $h^{\mu\nu}_{(3)M^2\times M_{ij}}$ is computed we have been able to compute the quartic source $\Lambda^{\mu\nu}_{(4)M^3\times M_{ij}}$ and to integrate it asymptotically, which means that we computed $h^{\mu\nu}_{(4)M^3\times M_{ij}}$ for $r \to \infty$ with $u = t - r/c$ constant.

Based on the form of $h^{\mu\nu}_{(2)M\times M_{ij}}$ we see that $\Lambda^{\mu\nu}_{(3)M^2\times M_{ij}}$ contains two kinds of terms: instantaneous terms that can be integrated with the formulae presented in section 4.2.1, and non-local terms coming from the tails. These non-local terms are always of the form

$$\hat{n}_L\, r^{-k} \int_1^{+\infty} \mathrm{d}y\, V_m(y) F(t - ry)\,, \tag{4.50}$$

where $V_m(y)$ is a kernel function that can be expressed by means of polynomials and Legendre functions of second kind $Q_l(y)$, and F is usually a time-derivative of the mass quadrupole M_{ij}. Therefore, the goal of the following section 4.2.4 is to provide explicit formulae to integrate (4.50), i.e., to find the solution of (4.51).

Once this is done, we can compute $\Lambda^{\mu\nu}_{(4)M^3\times M_{ij}}$ which depends on $h^{\mu\nu}_{(1)M}$, $h^{\mu\nu}_{(2)M^2}$, $h^{\mu\nu}_{(3)M^3}$, $h^{\mu\nu}_{(1)M_{ij}}$, $h^{\mu\nu}_{(2)M\times M_{ij}}$ and finally $h^{\mu\nu}_{(3)M^2\times M_{ij}}$. If we do so, we notice that $\Lambda^{\mu\nu}_{(4)M^3\times M_{ij}}$ also contains both instantaneous terms and non-local terms of the form (4.50), but with kernel functions $V_m(y)$ much more complicated this time. So we will only be able to provide formulae to integrate them asymptotically.

4.2.4 Explicit closed-form representations of the solution

We are looking for the retarded solution of a d'Alembertian equation whose source term is non-local

$$\Box \underset{k,m}{\Psi}_L = \hat{n}_L\, r^{-k} \int_1^{+\infty} \mathrm{d}y\, V_m(y) F(t - ry)\,, \tag{4.51}$$

where $F(u)$ is a smooth function of the retarded time that is identically zero in the remote past, i.e., $F \in \mathcal{C}^\infty(\mathbb{R})$ and $F(u) = 0$ for $u \leqslant -\mathcal{T}$ (with $-\mathcal{T}$ being a fixed instant in the past), and where $V_m(y)$ is a generic function belonging to the following m-dependent class

$$\begin{aligned}\mathscr{V}_m = \Big\{ & V(y) \in \mathcal{C}^\infty(]1,+\infty[) | \exists\ a \geqslant 0,\ b \geqslant 0 \text{ such that} \\ & V(y) \underset{y\to+\infty}{=} \mathcal{O}\left[y^{-(m+1)} \ln^a(y)\right] \text{ and } V(y) \underset{y\to 1^+}{=} \mathcal{O}\left[\ln^b(y-1)\right]\Big\}\,.\end{aligned} \tag{4.52}$$

We see that the integer m basically specifies the behavior of our $\mathscr{V}_m$-type functions when $y \to +\infty$, while those functions are assumed to be integrable when $y \to 1^+$. A typical function belonging to the class $\mathscr{V}_m$ is the Legendre function of the second kind $Q_m(y)$, defined by (4.42). Then, for $V_m \in \mathscr{V}_m$, we define the retarded multipolar solution of (4.51) as

$$\underset{k,m}{\Psi}_L = \underset{B=0}{\mathrm{FP}}\, \Box^{-1}_{\mathrm{ret}} \left[\hat{n}_L \left(\frac{r}{r_0}\right)^B r^{-k} \int_1^{+\infty} \mathrm{d}y\, V_m(y) F(t - ry)\right]. \tag{4.53}$$

Following the prescriptions presented in 4.1.3.a), this solution is defined by analytic continuation in $B \in \mathbb{C}$ as the finite part (FP) in the Laurent expansion when $B \to 0$ of the usual inverse retarded integral $\Box^{-1}_{\mathrm{ret}}$ acting on the source regularized by means of the inserted factor $(r/r_0)^B$.

We shall now present explicit forms for the general solution (4.53), i.e., analytic closed-form representations for ${}_{k,m}\Psi_L$. In order to get the full cubic metric $h^{\mu\nu}_{(3)M^2\times M_{ij}}$, we need to distinguish several cases.

4.2.4.a) Case where $k=1$, $\ell \geqslant 0$ and $m \geqslant 0$

This case has been already investigated in Ref. [132] when $V_m = Q_m$ is the Legendre function of the second kind. The result extends naturally to all $V_m \in \mathscr{V}_m$

$$\underset{1,m}{\Psi}_L = \hat{n}_L \int_1^{+\infty} \mathrm{d}s F^{(-1)}(t-rs) \left[Q_\ell(s) \int_1^s \mathrm{d}y\, V_m(y)\, \frac{\mathrm{d}P_\ell}{\mathrm{d}y}(y) + P_\ell(s) \int_s^{+\infty} \mathrm{d}y\, V_m(y)\, \frac{\mathrm{d}Q_\ell}{\mathrm{d}y}(y)\right]. \tag{4.54}$$

Since $F(u)$ is identically zero in the past (before some given finite instant $-\mathcal{T}$), we define $F^{(-1)}(u)$ to be the anti-derivative of F that is also identically zero in the past. Here, $P_\ell(y)$ is the usual Legendre polynomial.

4.2.4.b) Case where $k=2$, $\ell \geqslant 0$ and $m \geqslant 0$

For $k=2$, and still $V_m \in \mathscr{V}_m$ with $m \geqslant 0$, we start with the formula (D5) of Appendix D in Ref. [129], which yields, for the case at hands

$$\underset{2,m}{\Psi}_L = -\frac{\hat{n}_L}{2r} \int_{-\infty}^{t-r} \mathrm{d}\xi \int_{\frac{t-r-\xi}{2}}^{\frac{t+r+\xi}{2}} \frac{\mathrm{d}w}{w} \int_1^{+\infty} \mathrm{d}x\, V_m(x)\, F[\xi-(x-1)w] \times P_\ell\left[1 - \frac{(t-r-\xi)(t+r-\xi-2w)}{2rw}\right]. \tag{4.55}$$

Now, we define new variables $(\xi, w) \to (y, z)$ by $\xi - (x-1)w = t - ry$ and $z = 1 - \frac{(t-r-\xi)(t+r-\xi-2w)}{2rw}$. With these variables we get

$$\underset{2,m}{\Psi}_L = -\frac{\hat{n}_L}{2} \int_1^{+\infty} \mathrm{d}x\, V_m(x) \int_1^{+\infty} \mathrm{d}y\, F(t-ry) \times \int_{-1}^{1} \mathrm{d}z\, \frac{P_\ell(z)}{\sqrt{(xy-z)^2-(x^2-1)(y^2-1)}}. \tag{4.56}$$

By virtue of the mathematical formula (A.5) of [132][5] we obtain

$$\underset{2,m}{\Psi}_L = -\hat{n}_L \int_1^{+\infty} \mathrm{d}s\, F(t-rs) \left[Q_\ell(s) \int_1^s \mathrm{d}y\, V_m(y) P_\ell(y)\right.$$

[5]Namely,

$$\frac{1}{2}\int_{-1}^{1} \frac{\mathrm{d}z\, P_\ell(z)}{\sqrt{(xy-z)^2-(x^2-1)(y^2-1)}} = \begin{cases} P_\ell(x)\, Q_\ell(y) & \text{when} \quad 1 < x \leqslant y\,, \\ P_\ell(y)\, Q_\ell(x) & \text{when} \quad 1 < y \leqslant x\,. \end{cases}$$

$$+P_\ell(s)\int_s^{+\infty}\mathrm{d}y\,V_m(y)Q_\ell(y)\Bigg]\,, \tag{4.57}$$

which has a structure similar to that of the solution (4.54).

4.2.4.c) Case where $k \geqslant 2$, $\ell \geqslant k-2$ and $m \geqslant k-2$

To deal with this case, it is convenient to introduce, given some positive integer p and some function $V_m \in \mathscr{V}_m$, the p-th anti-derivative $V_m^{(-p)}(y)$ of V_m that vanishes when $y=1$, together with all its derivatives of orders smaller than p. Namely, we define

$$V_m^{(-p)}(y) = \int_1^y \mathrm{d}x\,V_m(x)\,\frac{(y-x)^{p-1}}{(p-1)!}\,, \tag{4.58}$$

and adopt the convention that $V_m^{(0)}(y) = V_m(y)$. Such a choice is indeed meaningful for functions V_m that satisfy the characteristic properties of the class $\mathscr{V}_m$.

Let us show that, for any $\ell \geqslant k-2$, $m \geqslant k-2$, and for any $V_m \in \mathscr{V}_m$,

$$\begin{aligned}\underset{k,m}{\Psi}{}_L = &-\hat{n}_L\int_1^{+\infty}\mathrm{d}s\,F^{(k-2)}(t-rs)\\ &\times\left[Q_\ell(s)\int_1^s\mathrm{d}y\,V_m^{(-k+2)}(y)P_\ell(y)+P_\ell(s)\int_s^{+\infty}\mathrm{d}y\,V_m^{(-k+2)}(y)Q_\ell(y)\right],\end{aligned} \tag{4.59}$$

where $V_m^{(-k+2)}(y)$ is the $(k-2)$-th anti-derivative of $V_m(y)$ defined by the equation (4.58). We will proceed by induction over the integer k. The initial case $k=2$ corresponds to the equation (4.57). Let us thus assume that (4.59) is valid up to $k-1$ with $k \geqslant 3$, and let us show that it is then valid for k. By definition, we have

$$\underset{k,m}{\Psi}{}_L = \underset{B=0}{\mathrm{FP}}\,\Box^{-1}_{\mathrm{ret}}\left[\hat{n}_L\left(\frac{r}{r_0}\right)^B r^{-k}\int_1^{+\infty}\mathrm{d}y\,V_m(y)F(t-ry)\right], \tag{4.60}$$

which we can integrate by part, for $V_m \in \mathscr{V}_m$ and $m \geqslant k-2$. We find

$$\underset{k,m}{\Psi}{}_L = \underset{B=0}{\mathrm{FP}}\,\Box^{-1}_{\mathrm{ret}}\left[\hat{n}_L\left(\frac{r}{r_0}\right)^B r^{-k+1}\int_1^{+\infty}\mathrm{d}y\,V_m^{(-1)}(y)F^{(1)}(t-ry)\right], \tag{4.61}$$

where $V_m^{(-1)}(y) = \int_1^y \mathrm{d}x\,V_m(x)$ in agreement with (4.58). As $m \geqslant 1$ (because $k \geqslant 3$), $\alpha_m = \int_1^{+\infty}\mathrm{d}y\,V_m(y)$ is a convergent integral. Posing $\tilde{V}_{m-1}(y) = V_m^{(-1)}(y) - \alpha_m$, we rewrite (4.61) as

$$\begin{aligned}\underset{k,m}{\Psi}{}_L = &\,\alpha_m\,\underset{B=0}{\mathrm{FP}}\,\Box^{-1}_{\mathrm{ret}}\left[\hat{n}_L\left(\frac{r}{r_0}\right)^B r^{-k}F(t-r)\right]\\ &+\underset{B=0}{\mathrm{FP}}\,\Box^{-1}_{\mathrm{ret}}\left[\hat{n}_L\left(\frac{r}{r_0}\right)^B r^{-k+1}\int_1^{+\infty}\mathrm{d}y\,\tilde{V}_{m-1}(y)\,F^{(1)}(t-ry)\right].\end{aligned} \tag{4.62}$$

The point now is that $\tilde{V}_{m-1} \in \mathscr{V}_{m-1}$, so that we can make use of the equation (4.59) (which is our induction hypothesis) to obtain

$$\underset{k,m}{\Psi}{}_L = \alpha_m\,\underset{B=0}{\mathrm{FP}}\,\Box^{-1}_{\mathrm{ret}}\left[\hat{n}_L\left(\frac{r}{r_0}\right)^B r^{-k}F(t-r)\right] - \hat{n}_L\int_1^{+\infty}\mathrm{d}s\,F^{(k-2)}(t-rs)$$

$$\times \left[Q_\ell(s) \int_1^s \mathrm{d}y\, \tilde{V}_{m-1}^{(-k+3)}(y) P_\ell(y) + P_\ell(s) \int_s^{+\infty} \mathrm{d}y\, \tilde{V}_{m-1}^{(-k+3)}(y) Q_\ell(y) \right]. \quad (4.63)$$

The first term is instantaneous and, keeping in mind that $\ell \geqslant k-2$, it may be integrated by means of the formula (4.46). Since we have $\tilde{V}_{m-1}^{(-k+3)}(y) = V_m^{(-k+2)}(y) - \alpha_m \frac{(y-1)^{k-3}}{(k-3)!}$, we obtain exactly the result ${}_{k,m}\Psi_L$ given by (4.59) that we wanted to prove, with however the following additional term

$$\underset{k,m}{\delta \Psi}_L = \alpha_m \, \hat{n}_L \int_1^{+\infty} \mathrm{d}s\, F^{(k-2)}(t - rs)$$
$$\times \left[\mathcal{A}_\ell^{k-3}(s) - \frac{2^{k-3}(k-3)!(\ell+2-k)!}{(\ell+k-2)!} \sum_{j=0}^{k-3} \frac{(\ell+j)!\,(s-1)^j}{2^j(\ell-j)!(j!)^2} \right], \quad (4.64)$$

in which we have introduced the following combination

$$\mathcal{A}_\ell^{k-3}(s) = Q_\ell(s) \int_1^s \mathrm{d}y\, P_\ell(y)\, \frac{(y-1)^{k-3}}{(k-3)!} + P_\ell(s) \int_s^{+\infty} \mathrm{d}y\, Q_\ell(y)\, \frac{(y-1)^{k-3}}{(k-3)!}. \quad (4.65)$$

We are now going to prove that the additional term (4.64) is actually zero, because the quantity in the square brackets of (4.64) is in fact identically zero (for any $s \in]1, +\infty[$). To this end, we notice that the two integrals appearing in (4.65) are of the same type, namely

$$\mathcal{I}_\ell^p(s) = \int_a^s \mathrm{d}y\, f_\ell(y)\, \frac{(y-1)^p}{p!}, \quad (4.66)$$

where we have posed $p = k-3$ for simplicity sake. The lower boundary is $a=1$ or $a=+\infty$ according to the integral in (4.65) we are considering. The function $f_\ell(y)$ represents either the Legendre polynomial $P_\ell(y)$ for $a=1$ or the Legendre function $Q_\ell(y)$ for $a=+\infty$. In both cases, the integral is well-defined. Using the fact that $f_\ell(y)$ satisfies the usual Legendre differential equation[6] and performing two integrations by parts, we obtain the following recursive relation

$$\mathcal{I}_\ell^p(s) = \frac{1}{(\ell-p)(\ell+p+1)} \left[\Big(f_\ell(s)\big[(\ell-p)s - p\big] - \ell f_{\ell-1}(s) \Big) \frac{(s-1)^p}{p!} + 2p\, \mathcal{I}_\ell^{p-1}(s) \right]. \quad (4.67)$$

It nicely translates, when inserted into (4.65), into the simple recurrence equation

$$\mathcal{A}_\ell^p(s) = \frac{1}{(\ell-p)(\ell+p+1)} \left[\frac{(s-1)^p}{p!} + 2p\, \mathcal{A}_\ell^{p-1}(s) \right], \quad (4.68)$$

[6] Namely,

$$\frac{\mathrm{d}}{\mathrm{d}y}\left[(1-y^2) \frac{\mathrm{d}f_\ell(y)}{\mathrm{d}y} \right] + \ell(\ell+1) f_\ell(y) = 0\,.$$

We remind also the following properties of Legendre functions that are used in our computation

$$(1-y^2)\frac{\mathrm{d}f_\ell(y)}{\mathrm{d}y} = \ell \Big[f_{\ell-1}(y) - y f_\ell(y) \Big],$$
$$P_\ell(y) Q_{\ell-1}(y) - P_{\ell-1}(y) Q_\ell(y) = \frac{1}{\ell}\,.$$

whose solution is straightforwardly found to be

$$\mathcal{A}_\ell^p(s) = \frac{2^p p!(\ell-p-1)!}{(\ell+p+1)!}\sum_{j=0}^{p}\frac{(\ell+j)!\,(s-1)^j}{2^j(\ell-j)!(j!)^2}\,. \tag{4.69}$$

To arrive at the latter expression, we need the readily checked relation $A_\ell^0(s) = \frac{1}{\ell(\ell+1)}$, which plays the role of normalization condition. The result (4.69) shows that the additional term (4.64) is indeed zero, which completes our proof of the equation (4.59).

To conclude, for any $\ell \geqslant k-2$ and $m \geqslant k-2$, we have shown that the solution ${}_{k,m}\Psi_L$ is given by

$$\underset{k,m}{\Psi}_L = -\hat{n}_L\int_1^{+\infty}\mathrm{d}s\,F^{(k-2)}(t-rs)\Big[Q_\ell(s)\int_1^s\mathrm{d}y\,V_m^{(-k+2)}(y)P_\ell(y) \\ + P_\ell(s)\int_s^{+\infty}\mathrm{d}y\,V_m^{(-k+2)}(y)Q_\ell(y)\Big]\,, \tag{4.70}$$

which appears to be an interesting generalization of (4.57) corresponding to the case $k=2$. Notice, however, that the latter formula (4.70) is not valid in the case $k=1$. This case has to be treated separately using the result (4.54).

Stricto sensu, we are not allowed to use the equation (4.70) when $m=0$, $k=3$, $\ell=2$, which corresponds to one of the non-local terms appearing in the source $\Lambda^{\mu\nu}_{(3)M^2\times M_{ij}}$. However, it happens to be valid also in this case. Indeed, the proof leading to (4.57) still holds for $m=-1$ as all integrals are convergent. Then, to derive the formula for $m=0$, $k=3$, $\ell=2$, we proceed similarly to the recursion presented previously, by performing an integration by parts and choosing for $V_0^{(-1)}(y)$ the anti-derivative that vanishes for $y=1$ (see the equation (4.61)).

4.2.4.d) Case $\ell = 0$, $k \geqslant 3$ and $m \geqslant k-2$

As it turned out, one (and only one) term of the cubic source does not fall into the previous cases. For this term, corresponding to the values $\ell=0$, $k=3$ and $m=2$, we need to find another formula. To find it, we notice that, for the proof of the case where $\ell=0$, $k=3$ and $m=2$, all the reasonings in the previous section 4.2.4.c) remain valid for $\ell=0$ up to (4.63), which is actually true as soon as $m \geqslant 1$. Now, the equation (4.47) tells us that

$$\underset{B=0}{\mathrm{FP}}\,\Box^{-1}_{\mathrm{ret}}\Big[\Big(\frac{r}{r_0}\Big)^B r^{-3}F(t-r)\Big] \\ = -\Big[\ln\Big(\frac{r}{r_0}\Big)+1\Big]\frac{F(t-r)}{r} + 2\int_1^{+\infty}\mathrm{d}s\,F^{(1)}(t-rs)Q_0(s)\,. \tag{4.71}$$

Inserting (4.71) into (4.63) for $k=3$, we find

$$\underset{3,m}{\Psi}_{L=0} = -\Big[\ln\Big(\frac{r}{r_0}\Big)+1\Big]\frac{F(t-r)}{r}\int_1^{+\infty}\mathrm{d}y\,V_m(y) \\ + \int_1^{+\infty}\mathrm{d}s\,F^{(1)}(t-rs)\Big(Q_0(s)\int_1^s\mathrm{d}y\,(y+1)V_m(y) \\ + \int_s^{+\infty}\mathrm{d}y\,\Big[(y+1)Q_0(y)+\ln\Big(\frac{y-1}{s-1}\Big)\Big]V_m(y)\Big)\,, \tag{4.72}$$

where we recall that $Q_0(y) = \frac{1}{2}\ln(\frac{y+1}{y-1})$. Observe the first appearance of the logarithm of r, in the first term of (4.72), due to the presence of a pole in the original integral when $B \to 0$. As a result the formula (4.72) explicitly depends on the arbitrary scale r_0, but this gauge constant should disappear in any final result expressing physical observables. With the equation (4.72), we have in hands enough material to integrate explicitly all the cubic hereditary source terms.

We found a generalization to the case where $\ell = 0$, $k \geqslant 3$ and $m \geqslant k-2$, even if such terms do not appear in $\Lambda^{\mu\nu}_{(3)M^2\times M_{ij}}$. Indeed, for $\ell = 0$, $k \geqslant 3$ and $m \geqslant k-2$

$$\begin{aligned}\underset{k,m}{\Psi}{}_{L=0} =& \frac{(-1)^k}{(k-2)!}\Bigg\{\left[\ln\left(\frac{r}{r_0}\right)+H_{k-2}\right]\frac{F^{(k-3)}(t-r)}{r}\int_1^{+\infty}\mathrm{d}y\, V_m(y)\varphi_{k-2}(y)\\ &-\int_1^{+\infty}\mathrm{d}s\, F^{(k-2)}(t-rs)\bigg(Q_0(s)\int_1^s\mathrm{d}y\, V_m(y)\,(y+1)^{k-2}\\ &\qquad+\int_s^{+\infty}\mathrm{d}y\, V_m(y)\left[(y+1)^{k-2}Q_0(y)+\varphi_{k-2}(y)\ln\left(\frac{y-1}{s-1}\right)\right]\bigg)\\ &-\sum_{i=1}^{k-3}(-1)^{k+i}\frac{(k-3-i)!}{r^{k-1-i}}\int_1^{+\infty}\mathrm{d}y\, V_m(y)\,\varphi_i(y)\,F^{(i-1)}(t-ry)\Bigg\}\,,\end{aligned} \tag{4.73}$$

where we have posed $\varphi_i(y) = \frac{1}{2}[(y+1)^i-(y-1)^i]$, to ease the notation, and $H_{k-2} = \sum_{j=1}^{k-2}\frac{1}{j}$. Notice the last term in (4.73), which is absent from (4.72) and constitutes an additional contribution here for $k \geqslant 4$.

The proof of equation (4.73), differs from the proof we just presented for $k=3$, and goes as follows. First, according to equation (4.34), we have

$$\underset{k,m}{\Psi}{}_{L=0} = \frac{1}{r}\,\underset{B}{\mathrm{FP}}\int_{-\infty}^{t-r}\mathrm{d}s\left[R_B\left(\frac{t-r-s}{2},s\right)-R_B\left(\frac{t+r-s}{2},s\right)\right]\,, \tag{4.74}$$

where R_B is given by (4.35)

$$R_B(r,s) = \frac{1}{2}\int_0^r\mathrm{d}x\left(\frac{x}{r_0}\right)^B x^{-k+1}\int_1^{+\infty}\mathrm{d}y\, V_m(y)F[s-x(y-1)]\,. \tag{4.75}$$

Let us call A_1 the first term in the equation (4.74), actually a retarded homogeneous solution of the wave equation, and A_2 the second term, which is made of a mixture of retarded and advanced times. By construction, we have ${}_{k,m}\Psi_{L=0} = A_1 + A_2$.

We inject (4.75) into A_1 and define the new variable $u = \frac{t-r-s}{2}$, thereby expressing A_1 in terms of the new set of variables (u,x,y). Next, after commuting the x and u integrals, we explicitly integrate over u. Once this is done, we perform $k-1$ integrations by part with respect to x and apply the Finite Part procedure to get

$$\begin{aligned}A_1 =& \frac{(-1)^k}{2(k-2)!}\frac{1}{r}\int_0^{+\infty}\mathrm{d}x\left[\ln\left(\frac{x}{r_0}\right)+H_{k-2}\right]\\ &\int_1^{+\infty}\mathrm{d}y\, V_m(y)\,(y+1)^{k-1}\,F^{(k-2)}\left[t-r-x(y+1)\right]\,.\end{aligned} \tag{4.76}$$

The same treatment is applied to the second term A_2 but the computation is longer, as some boundary terms arise. We find that

$$
\begin{aligned}
A_2 = &-\frac{(-1)^k}{2(k-2)!}\frac{1}{r}\int_r^{+\infty}\mathrm{d}x\left[\ln\left(\frac{x}{r_0}\right)+H_{k-2}\right]\int_1^{+\infty}\mathrm{d}y\,V_m(y)\,(y+1)^{k-1}\,F^{(k-2)}[t+r-x(y+1)]\\
&-\frac{(-1)^k}{2(k-2)!}\frac{1}{r}\int_0^{r}\mathrm{d}x\left[\ln\left(\frac{x}{r_0}\right)+H_{k-2}\right]\int_1^{+\infty}\mathrm{d}y\,V_m(y)\,(y-1)^{k-1}\,F^{(k-2)}[t-r-x(y-1)]\\
&+\frac{(-1)^k}{(k-2)!}\frac{1}{r}\left[\ln\left(\frac{r}{r_0}\right)+H_{k-2}\right]\int_1^{+\infty}\mathrm{d}y\,V_m(y)\,\varphi_{k-2}(y)\,F^{(k-3)}(t-ry)\\
&-\sum_{i=1}^{k-3}\frac{(-1)^i}{(k-2)\cdots(k-2-i)}\frac{1}{r^{k-i-1}}\int_1^{+\infty}\mathrm{d}y\,V_m(y)\,\varphi_i(y)\,F^{(i-1)}(t-ry)\,,
\end{aligned}
\tag{4.77}
$$

where $\varphi_i(y)=\frac{1}{2}[(y+1)^i-(y-1)^i]$. Then, we make the change of variable $t-rs=t-r-x(y+1)$ in (4.76), as well as the changes $t-rs=t+r-x(y+1)$ in the first line of (4.77) and $t-rs=t-r-x(y-1)$ in the second line of (4.77). Finally, with these new variables, after exchanging the integrations, simplifications occur, yielding the formula (4.73).

4.2.4.e) Results: the tails-of-tails

All the formulae presented above enabled us to explicitly compute $h^{\mu\nu}_{(3)M^2\times M_{ij}}$. For that we first compute $u^{\mu\nu}_{(3)m^2\times M_{ij}}$ using the integration formulae provided above and then $v^{\mu\nu}_{(3)M\times M_{ij}}$ as prescribed in section 4.1.3.b). Then we pose $h^{\mu\nu}_{(3)M\times M_{ij}}\equiv u^{\mu\nu}_{(3)M\times M_{ij}}+v^{\mu\nu}_{(3)M\times M_{ij}}$. While the result is too long to be display here, we can however, take the limit of $h^{\mu\nu}_{(3)M^2\times M_{ij}}$ when $r\to\infty$, with $u=t-r/c$ constant. By doing so, we retrieve the results derived in [132]

$$
\begin{aligned}
M^{-2}h^{00}_{(3)M^2\times M_{pq}} = &\frac{n_{ab}}{r}\int_0^{+\infty}d\tau M^{(5)}_{ab}\left\{-4\ln^2\left(\frac{\tau}{2r}\right)-4\ln\left(\frac{\tau}{2r}\right)\right.\\
&\left.+\frac{116}{21}\ln\left(\frac{\tau}{2r_0}\right)-\frac{7136}{2205}\right\}+o\left(r^{\varepsilon_0-2}\right)\,,
\end{aligned}
\tag{4.78a}
$$

$$
\begin{aligned}
M^{-2}h^{0i}_{(3)M^2\times M_{pq}} = &\frac{\hat{n}_{iab}}{r}\int_0^{+\infty}d\tau M^{(5)}_{ab}\left\{-\frac{2}{3}\ln\left(\frac{\tau}{2r}\right)-\frac{4}{105}\ln\left(\frac{\tau}{2r_0}\right)-\frac{716}{1225}\right\}\\
&+\frac{n_a}{r}\int_0^{+\infty}d\tau M^{(5)}_{ai}\left\{-4\ln^2\left(\frac{\tau}{2r}\right)-\frac{18}{5}\ln\left(\frac{\tau}{2r}\right)\right.\\
&\left.+\frac{416}{75}\ln\left(\frac{\tau}{2r_0}\right)-\frac{22724}{7875}\right\}+o\left(r^{\varepsilon_0-2}\right)\,,
\end{aligned}
\tag{4.78b}
$$

$$
\begin{aligned}
M^{-2}h^{ij}_{(3)M^2\times M_{pq}} = &\frac{\hat{n}_{ijab}}{r}\int_0^{+\infty}d\tau M^{(5)}_{ab}\left\{-\ln\left(\frac{\tau}{2r}\right)-\frac{191}{210}\right\}\\
&+\delta_{ij}\frac{n_{ab}}{r}\int_0^{+\infty}d\tau M^{(5)}_{ab}\left\{-\frac{80}{21}\ln\left(\frac{\tau}{2r}\right)-\frac{32}{21}\ln\left(\frac{\tau}{2r_0}\right)-\frac{296}{35}\right\}\\
&+\frac{\hat{n}_{a(i}}{r}\int_0^{+\infty}d\tau M^{(5)}_{j)a}\left\{\frac{52}{7}\ln\left(\frac{\tau}{2r}\right)+\frac{104}{35}\ln\left(\frac{\tau}{2r_0}\right)+\frac{8812}{525}\right\}\\
&+\frac{1}{r}\int_0^{+\infty}d\tau M^{(5)}_{ij}\left\{-4\ln^2\left(\frac{\tau}{2r}\right)-\frac{24}{5}\ln\left(\frac{\tau}{2r}\right)\right.
\end{aligned}
$$

$$+\frac{76}{15}\ln\left(\frac{\tau}{2r_0}\right)-\frac{198}{35}\Big\}+o\left(r^{\varepsilon_0-2}\right). \tag{4.78c}$$

ε_0 is an arbitrary small positive number and we used the notation $o\left(r^{\varepsilon_0-2}\right)$ to take into account logarithmic powers that could appear at $1/r^2$: $\ln^p(r)r^{-2}=o\left(r^{\varepsilon_0-2}\right)$.

We can see that $h^{\mu\nu}_{(3)M^2\times M_{ij}}$, also contains non-local terms: there are called *tails-of-tails* or *second order tails* as they correspond to the mass-mass-quadrupole interaction.

4.2.5 Formulae to integrate the tails-of-tails-of-tails

We can now compute $\Lambda^{\mu\nu}_{(4)M^3\times M_{ij}}$ which, using the notation from equation (4.6), is given by

$$\begin{aligned}\Lambda^{\mu\nu}_{(4)M^3\times M_{ij}} &= N^{\mu\nu}(h^{\alpha\beta}_{(3)M^2\times M_{ij}},h^{\alpha\beta}_{(1)M})+N^{\mu\nu}(h^{\alpha\beta}_{(2)M\times M_{ij}},h^{\alpha\beta}_{(2)M^2})\\ &+N^{\mu\nu}(h^{\alpha\beta}_{(1)M_{ij}},h^{\alpha\beta}_{(3)M^3})+M^{\mu\nu}(h^{\alpha\beta}_{(1)M},h^{\alpha\beta}_{(1)M},h^{\alpha\beta}_{(2)M\times M_{ij}})\\ &+M^{\mu\nu}(h^{\alpha\beta}_{(1)M},h^{\alpha\beta}_{(2)M^2},h^{\alpha\beta}_{(1)M_{ij}})+L^{\mu\nu}(h^{\alpha\beta}_{(1)M},h^{\alpha\beta}_{(1)M},h^{\alpha\beta}_{(1)M},h^{\alpha\beta}_{(1)M_{ij}}).\end{aligned} \tag{4.79}$$

As we mentioned in the section (4.2.3), the source $\Lambda^{\mu\nu}_{(4)M^3\times M_{ij}}$ contains both local terms of the form $\frac{\hat{n}_L F(t-r)}{r^k}$ as well as non-local terms of the form given by the equation (4.50), but this time, the kernel functions V_m are much more complicated. Hence, we will not try to fully integrate $\Lambda^{\mu\nu}_{(4)M^3\times M_{ij}}$ but we will only compute the asymptotic values of $h^{\mu\nu}_{(4)M^3\times M_{ij}}$.

For that purpose, we will now present other formulae, going beyond those investigated in Ref. [132], for studying the leading order in the asymptotic expansion when $r\to+\infty$ with $t-r$ constant, of $h^{\mu\nu}_{(4)M^3\times M_{ij}}$. As done previously, we still define

$$\Box \underset{k,m}{\Psi}_L=\hat{n}_L\, r^{-k}\int_1^{+\infty}\mathrm{d}y\, V_m(y)F(t-ry)\,, \tag{4.80}$$

with $V_m\in\mathscr{V}_m$. For the cases 4.2.5.a), 4.2.5.b) and 4.2.5.c) below, our results is just an adaptation of the results presented in the appendix of [132]. In fact, in this appendix, the same formulae are derived for $V_m=Q_m$ where Q_m still represents the Legendre Functions of second kind. But all the proofs from that appendix stands if we formally replace Q_m by a generic function $V_m\in\mathscr{V}_m$. The situation is different for the case 4.2.5.d), where we provide a more detailed proof.

4.2.5.a) Case $k=1$, $m\geqslant 0$ and $\ell\geqslant 0$

From the result (4.54) it is straightforward to see (*cf* (A.7) of [132]) that, to leading order at future null infinity ($r\to+\infty$ with $t-r=\text{const}$)

$$\underset{1,m}{\Psi}_L=\frac{\hat{n}_L}{r}\int_0^{+\infty}\mathrm{d}\tau\, F^{(-1)}(t-r-\tau)\int_{1+\tau/r}^{+\infty}\mathrm{d}x\, V_m(x)\frac{\mathrm{d}Q_\ell}{\mathrm{d}x}(x)+\mathcal{O}\left(\frac{1}{r^{2-\epsilon_0}}\right). \tag{4.81}$$

We remind that the neglected terms in $\mathcal{O}(r^{\epsilon_0-2})$ also include possible powers of the logarithm of r.

4.2.5.b) Case $k \geqslant 2$, $\ell \geqslant k-2$, $m \geqslant 0$

The formulae (A.10)–(A.17) of [132] can be extended to any function $V_m \in \mathscr{V}_m$ by means of the same procedure that was used to get them in [132]. We find in that case that

$$\underset{k,m}{\Psi}_L = - \underset{k,m}{\alpha}_\ell \, \frac{\hat{n}_L}{r} \, F^{(k-3)}(t-r) + \mathcal{O}\left(\frac{1}{r^2}\right) . \tag{4.82}$$

The coefficients are given by the following explicit although involved expressions

$$\underset{k,m}{\alpha}_\ell = \sum_{i=0}^{k-2} C_{\ell,i}^{k-2} \int_1^{+\infty} \mathrm{d}y \, V_m(y) Q_{\ell-k+2+2i}(y) \, , \tag{4.83a}$$

$$\text{where} \quad C_{\ell,i}^{k-2} = (-1)^i \binom{k-2}{i} \frac{(2\ell-2k+3+2i)!!}{(2\ell+1+2i)!!} (2\ell-2k+5+4i) \, , \tag{4.83b}$$

with $\binom{k-2}{i}$ denoting the usual binomial coefficient. One can check that the remaining integral is convergent for any $V_m \in \mathscr{V}_m$ as long as $\ell \geqslant k-2$, since $Q_\ell(y) \sim y^{-\ell-1}$ when $y \to +\infty$. Interestingly, the expression (4.83a) for the ${}_{k,m}\alpha_\ell$'s may be recast into the more compact form

$$\underset{k,m}{\alpha}_\ell = (-1)^k \int_1^{+\infty} \mathrm{d}y \, V_m(y) Q_\ell^{(-k+2)}(y) \, , \tag{4.84}$$

where $Q_\ell^{(-k+2)}(y)$ is the $(k-2)$-th anti-derivative of $Q_\ell(y)$ that vanishes at $y = +\infty$ with all its derivatives, i.e.,

$$Q_\ell^{(-k+2)}(y) = - \int_y^{+\infty} \mathrm{d}z \, Q_\ell(z) \, \frac{(y-z)^{k-3}}{(k-3)!} \, , \tag{4.85}$$

for $k \geqslant 3$, and $Q_\ell^{(0)}(y) \equiv Q_\ell(y)$.

4.2.5.c) Case $k \geqslant \ell+3$ and $m \geqslant k-\ell-2$

Adapting the equations (A.19)–(A.21) from [132] we readily get

$$\underset{k,m}{\Psi}_L = - \frac{\hat{n}_L}{r} \int_0^{+\infty} \mathrm{d}\tau \, F^{(k-2)}(t-r-\tau) \left[\underset{k,m}{\beta}_\ell \ln\left(\frac{\tau}{2r_0}\right) + \underset{k,m}{\gamma}_\ell \right] + \mathcal{O}\left(\frac{1}{r^2}\right) , \tag{4.86}$$

with the explicit coefficients

$$\underset{k,m}{\beta}_\ell = \frac{1}{2} \int_1^{+\infty} \mathrm{d}x \, V_m(x) \int_{-1}^{1} \mathrm{d}z \, \frac{(z-x)^{k-3}}{(k-3)!} P_\ell(z) \, , \tag{4.87a}$$

$$\underset{k,m}{\gamma}_\ell = \frac{1}{2} \int_1^{+\infty} \mathrm{d}x \, V_m(x) \int_{-1}^{1} \mathrm{d}z \, \frac{(z-x)^{k-3}}{(k-3)!} P_\ell(z) \left[- \ln\left(\frac{x-z}{2}\right) + H_{k-3} \right] . \tag{4.87b}$$

4.2.5.d) Case $k=4$, $\ell=0$ and $m=0$

So far, we have just extended in a natural way the integration formulae of [132]. However, in our computation, one extra case must still be dealt with, corresponding to the values $k=4$, $\ell=0$ and $m=0$. Because m vanishes, the function $V_0 \in \mathscr{V}_0$ does not go to zero fast enough when $y \to +\infty$ to ensure the convergence of the coefficients (4.87). Therefore, we need to go back to the equations (4.34)–(4.35). In fact (as mentioned in the lemma 7.2 of [129]), it turns out that the $1/r$ behavior of the equation (4.34) comes only from the first term in $R\left(\frac{t-r-s}{2}\right)$. Thus we define

$$R(r,s) = \frac{1}{2r_0^B}\int_0^r \mathrm{d}x\, x^{B-3}\int_1^{+\infty}\mathrm{d}y\, V_0(y)\, F[s-x(y-1)]\,. \tag{4.88}$$

We can then write the leading term of the asymptotic expansion of the solution at infinity, for any $V_0 \in \mathscr{V}_0$, as

$$\underset{4,0}{\Psi}_{L=0} = \frac{1}{r}\,\underset{B=0}{\mathrm{FP}}\int_{-\infty}^{t-r}\mathrm{d}s\, R\left(\frac{t-r-s}{2}, s\right) + \mathcal{O}\left(\frac{1}{r^{2-\epsilon_0}}\right)\,. \tag{4.89}$$

Inserting (4.88) into (4.89) we get

$$\underset{4,0}{\Psi}_{L=0} = \frac{1}{2r}\,\underset{B=0}{\mathrm{FP}}\int_{-\infty}^{t-r}\mathrm{d}s\int_0^{\frac{t-r-s}{2}}\mathrm{d}x\,\frac{x^{B-3}}{r_0^B}\int_1^{+\infty}\mathrm{d}y\, V_0(y)\, F[s-x(y-1)] + \mathcal{O}\left(\frac{1}{r^{2-\epsilon_0}}\right)\,. \tag{4.90}$$

After the convenient change of variable $s \to z = \frac{t-r-s}{2}$, we can integrate explicitly over z. Furthermore, we integrate three times by part the remaining integral over x so as to make the pole $\propto 1/B$ appear. Those operations result in

$$\underset{4,0}{\Psi}_{L=0} = \underset{B=0}{\mathrm{FP}}\left\{\frac{1}{2B(B-1)(B-2)}\left(\frac{r}{r_0}\right)^B\int_1^{+\infty}\mathrm{d}s\, F^{(2)}(t-rs)(s-1)^B\int_1^{+\infty}\mathrm{d}y\,\frac{V_0(y)}{(y+1)^{B-2}}\right\}$$
$$+\,\mathcal{O}\left(\frac{1}{r^{2-\epsilon_0}}\right)\,. \tag{4.91}$$

The above equation enables us to integrate all the terms that are not covered by the previous formulae. Notice that the integral

$$I_0(B) = \int_1^{+\infty}\mathrm{d}y\,\frac{V_0(y)}{(y+1)^{B-2}} \tag{4.92}$$

in (4.91) diverges when $B=0$, since the function $V_0(y)$ only behaves like y^{-1} when $y\to+\infty$. However, this divergence is "protected" by the analytic continuation in B and it is even possible to perform a Laurent expansion of $I_0(B)$ as B goes to zero. To this aim, let us consider the expansion of $V_0(y)$ in powers of the variable $y+1$ at infinity. For the actual source we are interested in, it turns out that

$$V_0(y) = \frac{V_{-1}}{y+1} + \frac{V_{-2}}{(y+1)^2} + \frac{V_{-3}}{(y+1)^3} + \frac{V_{-3}^{\log}\ln(y+1)}{(y+1)^3} + \delta V_{-4}(y)\,, \tag{4.93}$$

where V_{-1}, V_{-2}, V_{-3} and $V_{-3}^{\log}$ are numerical constants, whereas the function $\delta V_{-4}(y)$ behaves like some power of $\ln(y-1)$ near $y=1$ and is $o(1/y^3)$ near $y\to+\infty$. Thus, we have at first order in B

$$\int_1^{+\infty}\mathrm{d}y\,\frac{\delta V_{-4}(y)}{(y+1)^{B-2}} = \int_1^{+\infty}\mathrm{d}y\,(y+1)^2\delta V_{-4}(y)\left[1-B\ln(y+1)\right] + \mathcal{O}\left(B^2\right)\,. \tag{4.94}$$

Substituting to $V_0(y)$ its expansion (4.93) in the equation (4.92), we find

$$I_0(B) = \frac{2^{2-B}V_{-1}}{B-2} + \frac{2^{1-B}V_{-2}}{B-1} + \frac{2^{-B}V_{-3}}{B} + 2^{-B}V_{-3}^{\log}\left(\frac{\ln 2}{B} + \frac{1}{B^2}\right) + \int_1^{+\infty} \mathrm{d}y\, (y+1)^2 \delta V_{-4}(y) \left[1 - B\ln(y+1)\right] + \mathcal{O}\left(B^2\right) . \tag{4.95}$$

Each time that we have to apply (4.91), we use the above truncated expression for the integral $I_0(B)$, which is readily expanded up to the first order in B, and take the Finite Part when $B=0$ as defined in (4.91).

4.2.5.e) Integrating the instantaneous logarithmic terms

Finally, the quartic source also contains terms that are instantaneous, and thus simpler than the previous hereditary terms, but involve the logarithm of r. These instantaneous logarithmic terms are not covered by the solution (4.53). The problem amounts to finding an explicit representation of

$$\underset{k}{\chi}_L = \underset{B=0}{\mathrm{FP}}\, \Box^{-1}_{\mathrm{ret}}\left[\hat{n}_L \left(\frac{r}{r_0}\right)^B \ln\left(\frac{r}{r_0}\right) r^{-k}\, F(t-r)\right] = \underset{B=0}{\mathrm{FP}}\, \frac{\mathrm{d}}{\mathrm{d}B}\left\{\Box^{-1}_{\mathrm{ret}}\left[\hat{n}_L \left(\frac{r}{r_0}\right)^B r^{-k}\, F(t-r)\right]\right\} . \tag{4.96}$$

Notice that for all those terms the scale r_0 entering the instantaneous logarithms $\ln(r/r_0)$ is the same as the one of our MPM algorithm.

Case $k=2$ According to the equation (4.37) we have (for any $B\in\mathbb{C}$)

$$\Box^{-1}_{\mathrm{ret}}\left[\hat{n}_L \left(\frac{r}{r_0}\right)^B r^{-2}\, F(t-r)\right] = \frac{1}{K_\ell(B)}\int_r^{+\infty} \mathrm{d}s\, F(t-s)\, \hat{\partial}_L\left[\frac{(s-r)^{B+\ell} - (s+r)^{B+\ell}}{r}\right] , \tag{4.97}$$

with $K_\ell(B) = 2(2r_0)^B B(B-1)\cdots(B-\ell)$. Let us inject (4.97) into (4.96), apply the differentiation with respect to B, perform the Laurent expansion when $B\to 0$, and look for the Finite Part coefficient. This leads to

$$\underset{2}{\chi}_L = \frac{(-1)^\ell}{4\ell!}\int_r^{+\infty} \mathrm{d}s\, F(t-s)\, \hat{\partial}_L\left[\frac{(s-r)^\ell\left(\ln\left(\frac{s-r}{2r_0}\right) + H_\ell\right)^2 - (s+r)^\ell\left(\ln\left(\frac{s+r}{2r_0}\right) + H_\ell\right)^2}{r}\right] , \tag{4.98}$$

where $H_\ell = \sum_{j=1}^{\ell}\frac{1}{j}$ is the ℓ-th harmonic number. Note that we have used equation (4.40) to obtain the result (4.98). An alternative, simpler representation of the right-hand side of (4.98) involving the Legendre function reads

$$\underset{2}{\chi}_L = -\frac{\hat{n}_L}{2r}\int_r^{+\infty} \mathrm{d}s\, F(t-s)\, Q_\ell\left(\frac{s}{r}\right)\left[\ln\left(\frac{s^2-r^2}{4r_0^2}\right) + 2H_\ell\right] . \tag{4.99}$$

To prove it, we have verified that the above function satisfies the requested d'Alembertian equation and has the same leading behavior at infinity as the expression (4.98) of χ_{2L}. As a result, the $1/r$ coefficient when $r \to +\infty$ with $t-r$ constant can be computed from (4.99), by inserting the expansion (4.43) of the Legendre function $Q_\ell(y)$ when $y \to 1^+$. We get

$$\underset{2}{\chi}_L = \frac{\hat{n}_L}{4r}\int_0^{+\infty} \mathrm{d}\tau\, F(t-r-\tau)\Big[\left(\ln\left(\frac{\tau}{2r_0}\right)+2H_\ell\right)^2 - \ln^2\left(\frac{r}{r_0}\right)\Big] + \mathcal{O}\left(\frac{1}{r^{2-\epsilon}}\right). \quad (4.100)$$

Case $3 \leqslant k \leqslant \ell+2$ According to the equation (4.44) we have in this case

$$\Box^{-1}_{\mathrm{ret}}\left[\hat{n}_L\left(\frac{r}{r_0}\right)^B r^{-k}\,F(t-r)\right] = \left(\frac{r}{r_0}\right)^B \sum_{i=0}^{k-3}\alpha_i(B)\,\hat{n}_L\frac{F^{(i)}(t-r)}{r^{k-i-2}} + \beta(B)\,\Box^{-1}_{\mathrm{ret}}\left[\hat{n}_L\left(\frac{r}{r_0}\right)^B r^{-2}\,F^{(k-2)}(t-r)\right]. \quad (4.101)$$

The B-dependent coefficients $\alpha_i(B)$ and $\beta(B)$ are given by the equation (4.45). However, for $3 \leqslant k \leqslant l+2$, $\alpha_i(B)$ does not have any pole when $B \to 0$, and the expansion of $\beta(B)$ starts at the first order in B, i.e., $\beta(B) = B + \mathcal{O}(B^2)$. As the retarded integral of a source term whose radial dependence is r^{-2} (with any power of the logarithm of r) does not have any pole either, we find

$$\underset{k}{\chi}_L = \frac{1}{r}\left[\alpha_{k-3}(0)\ln\left(\frac{r}{r_0}\right)+\alpha'_{k-3}(0)\right]\hat{n}_L\,F^{(k-3)}(t-r) + \beta'(0)\,\underset{B=0}{\mathrm{FP}}\,\Box^{-1}_{\mathrm{ret}}\left[\hat{n}_L\left(\frac{r}{r_0}\right)^B r^{-2}\,F^{(k-2)}(t-r)\right] + \mathcal{O}\left(\frac{1}{r^{2-\epsilon}}\right), \quad (4.102)$$

where $\alpha'_{k-3}(0)$ and $\beta'(0)$ denote the B-derivative, evaluated at $B=0$, of the coefficients $\alpha_{k-3}(B)$ and $\beta(B)$. For completeness, let us point out that

$$\alpha_{k-3}(0) = -\frac{2^{k-3}(k-3)!(\ell-k+2)!}{(k-3-\ell)!(k-2+\ell)!}, \quad (4.103a)$$

$$\alpha'_{k-3}(0) = \alpha_{k-3}(0)\Big[H_{k+\ell-2}-H_{k-3}-2H_\ell+H_{\ell-k+2}\Big], \quad (4.103b)$$

with $\beta(0)=0$ and $\beta'(0)=2\alpha_{k-3}(0)$. The equation (4.102) is sufficient for our purposes as we can compute the last term thanks to the identity (4.97).

Case $k \geqslant \ell+3$ In that case, (4.101) is still valid, but $\alpha_{k-3}(B)$ has now a simple pole while $\beta(B)$ has no polar part. Let us then write $\alpha_{k-3}(B) = a_{-1}B^{-1}+a_0+a_1B+\mathcal{O}(B^2)$, so that $\alpha'_{k-3}(B) = -a_{-1}B^{-2}+a_1+\mathcal{O}(B)$; similarly, $\beta(B) = b_0+b_1B+\mathcal{O}(B^2)$ and $\beta'(B) = b_1+\mathcal{O}(B)$. When computing the Finite Part of (4.97) we are allowed to commute the Finite Part operation with the evaluation of $\beta(B=0)=b_0$ and $\beta'(B=0)=b_1$ since the retarded integral of a source term $\propto r^{-2}$ is convergent. The solution χ_{kL} may then be put in the form

$$\underset{k}{\chi}_L = \frac{1}{r}\left[\frac{a_{-1}}{2}\ln^2\left(\frac{r}{r_0}\right)+a_0\ln\left(\frac{r}{r_0}\right)+a_1\right]\hat{n}_L\,F^{(k-3)}(t-r) + b_1\,\underset{B=0}{\mathrm{FP}}\,\Box^{-1}_{\mathrm{ret}}\left[\hat{n}_L\left(\frac{r}{r_0}\right)^B r^{-2}\,F^{(k-2)}(t-r)\right]$$

$$+ b_0 \underset{B=0}{\mathrm{FP}}\, \Box^{-1}_{\mathrm{ret}}\Big[\hat{n}_L \left(\frac{r}{r_0}\right)^B \ln\left(\frac{r}{r_0}\right) r^{-2}\, F^{(k-2)}(t-r)\Big] + \mathcal{O}\left(\frac{1}{r^{2-\epsilon}}\right) , \tag{4.104}$$

where

$$a_{-1} = \frac{(-1)^{k+\ell} 2^{k-3}(k-3)!}{(k-3-\ell)!(k-2+\ell)!} , \tag{4.105a}$$

$$a_0 = a_{-1}\Big[H_{k-3-\ell} - H_{k-3} - 2H_\ell + H_{k-2+\ell}\Big] , \tag{4.105b}$$

$$a_1 = \frac{a_0^2}{2a_{-1}} + \frac{a_{-1}}{2}\Big[H_{k-3-\ell,2} - H_{k-3,2} + H_{k-2+\ell,2}\Big] , \tag{4.105c}$$

together with $b_0 = 2a_{-1}$ and $b_1 = 2a_0$; here $H_{p,2} = \sum_{j=1}^{p} \frac{1}{j^2}$ denotes the second harmonic number. The formula (4.104) is also sufficient for our purposes, as the asymptotic form of the last two terms can be computed with the help of the equations (4.97)–(4.98).

4.2.6 Result

With the help of the formulae derived in section 4.2.5, we can now integrate the source $\Lambda^{\mu\nu}_{(4)M^3\times M_{ij}}$ to get the $1/r$ asymptotic value of $u^{\mu\nu}_{(4)M^3\times M_{ij}}$. Then we compute asymptotically $v^{\mu\nu}_{(4)M^3\times M_{ij}}$ by adapting the prescription of section 4.1.3.b) to the asymptotic case ($r \to \infty$, $t-r$ constant) as done in [132]. This new result was published in [1] and reads

$$\begin{aligned} h^{00}_{(4)M^3\times M_{ij}} = \frac{M^3 \hat{n}_{ab}}{r}\int_0^{+\infty} \mathrm{d}\tau\, M^{(6)}_{ab} \bigg\{ &-\frac{8}{3}\ln^3\left(\frac{\tau}{2r}\right) + \frac{148}{21}\ln^2\left(\frac{\tau}{2r}\right) + \frac{232}{21}\ln\left(\frac{r}{r_0}\right)\ln\left(\frac{\tau}{2r}\right) \\ &+ \frac{1016}{2205}\ln\left(\frac{\tau}{2r}\right) + \frac{104}{15}\ln\left(\frac{r}{r_0}\right) + \frac{16489}{1575} - \frac{232\pi^2}{63}\bigg\} + \mathcal{O}\left(\frac{1}{r^{2-\epsilon_0}}\right) , \end{aligned} \tag{4.106a}$$

$$\begin{aligned} h^{0i}_{(4)M^3\times M_{ij}} = \frac{M^3 \hat{n}_{abi}}{r}\int_0^{+\infty} \mathrm{d}\tau\, M^{(6)}_{ab} \bigg\{ &-\frac{26}{35}\ln^2\left(\frac{\tau}{2r}\right) - \frac{8}{105}\ln\left(\frac{\tau}{2r}\right)\ln\left(\frac{r}{r_0}\right) \\ &-\frac{6658}{11025}\ln\left(\frac{\tau}{2r}\right) + \frac{178}{315}\ln\left(\frac{r}{r_0}\right) - \frac{59287}{33075} + \frac{8\pi^2}{315}\bigg\} \\ + \frac{M^3 \hat{n}_{a}}{r}\int_0^{+\infty} \mathrm{d}\tau\, M^{(6)}_{ai} \bigg\{ &-\frac{8}{3}\ln^3\left(\frac{\tau}{2r}\right) + \frac{562}{75}\ln^2\left(\frac{\tau}{2r}\right) + \frac{832}{75}\ln\left(\frac{\tau}{2r}\right)\ln\left(\frac{r}{r_0}\right) \\ &+\frac{926}{1125}\ln\left(\frac{\tau}{2r}\right) + \frac{1154}{175}\ln\left(\frac{r}{r_0}\right) + \frac{212134}{18375} - \frac{832\pi^2}{225}\bigg\} + \mathcal{O}\left(\frac{1}{r^{2-\epsilon_0}}\right) , \end{aligned} \tag{4.106b}$$

$$\begin{aligned} h^{ij}_{(4)M^3\times M_{ij}} = \frac{M^3 \hat{n}_{abij}}{r}\int_0^{+\infty} \mathrm{d}\tau\, M^{(6)}_{ij} \bigg\{ &-\ln^2\left(\frac{\tau}{2r}\right) - \frac{4}{5}\ln\left(\frac{\tau}{2r}\right) + \frac{107}{105}\ln\left(\frac{r}{r_0}\right) - \frac{30868}{11025}\bigg\} \\ + 2\frac{M^3 \hat{n}_{a(j}}{r}\int_0^{+\infty} \mathrm{d}\tau\, M^{(6)}_{i)a} \bigg\{ &\frac{234}{35}\ln^2\left(\frac{\tau}{2r}\right) + \frac{104}{35}\ln\left(\frac{\tau}{2r}\right)\ln\left(\frac{r}{r_0}\right) \\ &+\frac{58694}{3675}\ln\left(\frac{\tau}{2r}\right) - \frac{598}{735}\ln\left(\frac{r}{r_0}\right) + \frac{1487812}{77175} - \frac{104\pi^2}{105}\bigg\} \\ + \frac{M^3 \hat{n}_{ab}\delta_{ij}}{r}\int_0^{+\infty} \mathrm{d}\tau\, M^{(6)}_{ab} \bigg\{ &-\frac{48}{7}\ln^2\left(\frac{\tau}{2r}\right) - \frac{64}{21}\ln\left(\frac{\tau}{2r}\right)\ln\left(\frac{r}{r_0}\right) \end{aligned}$$

$$
\begin{aligned}
&-\frac{7108}{441}\ln\left(\frac{\tau}{2r}\right)+\frac{1756}{2205}\ln\left(\frac{r}{r_0}\right)-\frac{4508029}{231525}+\frac{64\pi^2}{63}\Bigg\} \\
&+\frac{M^3}{r}\int_0^{+\infty}\mathrm{d}\tau\, M_{ij}^{(6)}\left\{-\frac{8}{3}\ln^3\left(\frac{\tau}{2r}\right)+\frac{16}{3}\ln^2\left(\frac{\tau}{2r}\right)+\frac{152}{15}\ln\left(\frac{\tau}{2r}\right)\ln\left(\frac{r}{r_0}\right)\right. \\
&\left.-\frac{2332}{525}\ln\left(\frac{\tau}{2r}\right)+\frac{3608}{525}\ln\left(\frac{r}{r_0}\right)+\frac{286408}{55125}-\frac{152\pi^2}{45}\right\}+\mathcal{O}\left(\frac{1}{r^{2-\epsilon_0}}\right).
\end{aligned}
\tag{4.106c}
$$

We remind again that the neglected terms in $\mathcal{O}(r^{\epsilon_0-2})$ also include possible powers of the logarithm of r. The quadrupole moments inside the integrals are evaluated at time $t-r-\tau$. Note that, at this stage, the logarithms involve both the radial distance r to the source and the constant r_0 coming from the MPM algorithm. As we can see, $h^{\mu\nu}_{(4)M^3\times M_{ij}}$ contains also non-local terms: they are *third order tails* or *tails-of-tails-of-tails*.

4.3 Going to radiative coordinates and flux derivation

4.3.1 Going to radiative coordinates

We shall now extract the relevant physical information from the metric provided in equation (4.106) as viewed at future null infinity, in the form of the so-called radiative quadrupole moment U_{ij} [127] — not to be confused of course with the source type quadrupole moment M_{ij}. So far, we have performed all our computations in harmonic coordinates x^μ. However, this choice of coordinates has the well-known disadvantage that the coordinate cones $t-r$ (where $r=|x^i|$) deviate by powers of the logarithm of r from the true space-time characteristics or light cones. As a result, the $1/r$ expansion of the metric (as $r\to+\infty$ with $t-r=$ const) involves powers of logarithms. For example, it is clear from (4.106), that (for $r\to+\infty$ with $t-r=$ const)

$$
h^{\mu\nu}_{(4)M^3\times M_{ij}} \sim \frac{\ln^3 r}{r}+\mathcal{O}\left(\frac{1}{r^{2-\epsilon}}\right). \tag{4.107}
$$

We get rid of these logarithms by going to radiative coordinates X^μ for which the associated coordinate cones $T-R$ (where $R=|X^i|$) become asymptotically tangent to the true light cones at future null infinity. As in previous works [132], this is achieved by applying the coordinate transformation $X^\mu=x^\mu+\xi^\mu(x)$, where ξ^μ is defined by

$$
\xi^0=-2GM\ln\left(\frac{r}{b_0}\right), \tag{4.108a}
$$

$$
\xi^i=0, \tag{4.108b}
$$

with b_0 denoting an arbitrary scale that is *a priori* different from the scale r_0. Let us show that this simple coordinate change is sufficient to remove all the log-terms from our quartic metric (4.106). Keeping only the $1/R$ terms and consistently taking into account all the $M^3\times M_{ij}$ interactions, one can check that the metric in radiative coordinates $H^{\mu\nu}_{(4)M^3\times M_{ij}}$ differs from the metric $h^{\mu\nu}_{(4)M^3\times M_{ij}}$ in harmonic-coordinates by

$$
H^{\mu\nu}_{(4)M^3\times M_{ij}}=h^{\mu\nu}_{(4)M^3\times M_{ij}}-\xi^\lambda\partial_\lambda h^{\mu\nu}_{(3)M^2\times M_{ij}}+\frac{1}{2}\xi^\lambda\xi^\sigma\partial^2_{\lambda\sigma}h^{\mu\nu}_{(2)M\times M_{ij}}
$$

$$- \frac{1}{6}\xi^\lambda\xi^\sigma\xi^\rho\partial^3_{\lambda\sigma\rho}h^{\mu\nu}_{(1)M_{ij}} + \mathcal{O}\left(\frac{1}{R^2}\right) \,, \tag{4.109}$$

where both sides are evaluated at the same dummy coordinate point, say X^μ. Injecting in this relation the results found for $h^{\mu\nu}_{(4)M^3\times M_{ij}}$, $h^{\mu\nu}_{(3)M^2\times M_{ij}}$, $h^{\mu\nu}_{(2)M\times M_{ij}}$ and $h^{\mu\nu}_{(1)M_{ij}}$, with ξ^μ given by (4.108), we indeed observe that all the logarithms of R vanish. More precisely, we obtain

$$\begin{aligned} H^{00}_{(4)M^3\times M_{ij}} &= \frac{M^3\hat{N}_{ab}}{R}\int_0^{+\infty}\mathrm{d}\tau\, M^{(6)}_{ab}\bigg\{-\frac{8}{3}\ln^3\left(\frac{\tau}{2b_0}\right) - 4\ln^2\left(\frac{\tau}{2b_0}\right) + \frac{232}{21}\ln\left(\frac{\tau}{2b_0}\right)\ln\left(\frac{\tau}{2r_0}\right) \\ &\qquad -\frac{14272}{2205}\ln\left(\frac{\tau}{2b_0}\right) + \frac{104}{15}\ln\left(\frac{\tau}{2r_0}\right) + \frac{16489}{1575} - \frac{232\pi^2}{63}\bigg\} + \mathcal{O}\left(\frac{1}{R^2}\right) \,, \end{aligned} \tag{4.110a}$$

$$\begin{aligned} H^{0i}_{(4)M^3\times M_{ij}} &= \frac{M^3\hat{N}_{abi}}{R}\int_0^{+\infty}\mathrm{d}\tau\, M^{(6)}_{ab}\bigg\{-\frac{2}{3}\ln^2\left(\frac{\tau}{2b_0}\right) - \frac{8}{105}\ln\left(\frac{\tau}{2b_0}\right)\ln\left(\frac{\tau}{2r_0}\right) \\ &\qquad -\frac{1432}{1225}\ln\left(\frac{\tau}{2b_0}\right) + \frac{178}{315}\ln\left(\frac{\tau}{2r_0}\right) - \frac{59287}{33075} + \frac{8\pi^2}{315}\bigg\} \\ &\quad + \frac{M^3\hat{N}_a}{R}\int_0^{+\infty}\mathrm{d}\tau\, M^{(6)}_{ai}\bigg\{-\frac{8}{3}\ln^3\left(\frac{\tau}{2b_0}\right) - \frac{18}{5}\ln^2\left(\frac{\tau}{2b_0}\right) + \frac{832}{75}\ln\left(\frac{\tau}{2b_0}\right)\ln\left(\frac{\tau}{2r_0}\right) \\ &\qquad -\frac{45448}{7875}\ln\left(\frac{\tau}{2b_0}\right) + \frac{1154}{175}\ln\left(\frac{\tau}{2r_0}\right) + \frac{212134}{18375} - \frac{832\pi^2}{225}\bigg\} \\ &\quad + \mathcal{O}\left(\frac{1}{R^2}\right) \,, \end{aligned} \tag{4.110b}$$

$$\begin{aligned} H^{ij}_{(4)M^3\times M_{ij}} &= \frac{M^3\hat{N}_{abij}}{R}\int_0^{+\infty}\mathrm{d}\tau\, M^{(6)}_{ab}\bigg\{-\ln^2\left(\frac{\tau}{2b_0}\right) - \frac{191}{105}\ln\left(\frac{\tau}{2b_0}\right) + \frac{107}{105}\ln\left(\frac{\tau}{2r_0}\right) - \frac{30868}{11025}\bigg\} \\ &\quad + 2\frac{M^3\hat{N}_{a(j}}{R}\int_0^{+\infty}\mathrm{d}\tau\, M^{(6)}_{i)a}\bigg\{\frac{26}{7}\ln^2\left(\frac{\tau}{2b_0}\right) + \frac{104}{35}\ln\left(\frac{\tau}{2b_0}\right)\ln\left(\frac{\tau}{2r_0}\right) \\ &\qquad +\frac{8812}{525}\ln\left(\frac{\tau}{2b_0}\right) - \frac{598}{735}\ln\left(\frac{\tau}{2r_0}\right) + \frac{1487812}{77175} - \frac{104\pi^2}{105}\bigg\} \\ &\quad + \frac{M^3\hat{N}_{ab}\delta_{ij}}{R}\int_0^{+\infty}\mathrm{d}\tau\, M^{(6)}_{ab}\bigg\{-\frac{80}{21}\ln^2\left(\frac{\tau}{2b_0}\right) - \frac{64}{21}\ln\left(\frac{\tau}{2b_0}\right)\ln\left(\frac{\tau}{2r_0}\right) \\ &\qquad -\frac{592}{35}\ln\left(\frac{\tau}{2b_0}\right) + \frac{1756}{2205}\ln\left(\frac{\tau}{2r_0}\right) - \frac{4508029}{231525} + \frac{64\pi^2}{63}\bigg\} \\ &\quad + \frac{M^3}{R}\int_0^{+\infty}\mathrm{d}\tau\, M^{(6)}_{ij}\bigg\{-\frac{8}{3}\ln^3\left(\frac{\tau}{2b_0}\right) - \frac{24}{5}\ln^2\left(\frac{\tau}{2b_0}\right) + \frac{152}{15}\ln\left(\frac{\tau}{2b_0}\right)\ln\left(\frac{\tau}{2r_0}\right) \\ &\qquad -\frac{396}{35}\ln\left(\frac{\tau}{2b_0}\right) + \frac{3608}{525}\ln\left(\frac{\tau}{2r_0}\right) + \frac{286408}{55125} - \frac{152\pi^2}{45}\bigg\} + \mathcal{O}\left(\frac{1}{R^2}\right) \,, \end{aligned} \tag{4.110c}$$

where $N_i = X_i/R$, and where the quadrupole moments are evaluated at time $T_R - \tau$ in the past, with $T_R = T - R$ denoting the retarded time in radiative coordinates.

4.3.2 The radiative multipole moments

By definition, the radiative mass and current multipole moments $U_L(T_R)$ and $V_L(T_R)$ are the multipolar coefficients that parameterize the transverse-tracefree (TT) projection of the spatial metric in radiative coordinates, at retarded radiative time T_R, i.e.,

$$H_{ij}^{\mathrm{TT}}(U,\boldsymbol{x}) = \frac{4G}{c^2R}\mathcal{P}_{ijab}(\boldsymbol{N})\sum_{\ell=2}^{+\infty}\frac{1}{c^\ell \ell!}\left\{N_{L-2}\mathrm{U}_{abL-2}(U) - \frac{2\ell}{c(\ell+1)}N_{cL-2}\epsilon_{cd(a}\mathrm{V}_{b)dL-2}(U)\right\} + \mathcal{O}\left(\frac{1}{R^2}\right). \tag{4.111}$$

We have explicitly put back the power of c and G in (4.111). The TT projection operator is given by $\mathcal{P}_{ijkl} = \mathcal{P}_{ik}\mathcal{P}_{jl} - \frac{1}{2}\mathcal{P}_{ij}\mathcal{P}_{kl}$ where $\mathcal{P}_{ij} = \delta_{ij} - N_iN_j$ represents the projector onto the plane transverse to the unit direction $N_i = X_i/R$ from the source to the observer.

Adding the contribution of $h^{\mu\nu}_{(1)M_{ij}}$, $h^{\mu\nu}_{(2)M\times M_{ij}}$, $h^{\mu\nu}_{(3)M^2\times M_{ij}}$ and $h^{\mu\nu}_{(4)M^3\times M_{ij}}$ to the radiative mass quadrupole U_{ij} we obtain

$$\begin{aligned}
U_{ij}(T_R) = M_{ij}^{(2)}(T_R) &+ \frac{GM}{c^3}\int_0^{+\infty}\mathrm{d}\tau\, M_{ij}^{(4)}(T_R-\tau)\left[2\ln\left(\frac{c\tau}{2b_0}\right) + \frac{11}{6}\right] \\
&+ \frac{G^2M^2}{c^6}\int_0^{+\infty}\mathrm{d}\tau\, M_{ij}^{(5)}(T_R-\tau)\left[2\ln^2\left(\frac{c\tau}{2b_0}\right) + \frac{11}{3}\ln\left(\frac{c\tau}{2b_0}\right)\right. \\
&\qquad\left. -\frac{214}{105}\ln\left(\frac{c\tau}{2r_0}\right) + \frac{124627}{22050}\right] \\
&+ \frac{G^3M^3}{c^9}\int_0^{+\infty}\mathrm{d}\tau\, M_{ij}^{(6)}(T_R-\tau)\left[\frac{4}{3}\ln^3\left(\frac{c\tau}{2b_0}\right) + \frac{11}{3}\ln^2\left(\frac{c\tau}{2b_0}\right)\right. \\
&\qquad + \frac{124627}{11025}\ln\left(\frac{c\tau}{2b_0}\right) - \frac{428}{105}\ln\left(\frac{c\tau}{2b_0}\right)\ln\left(\frac{c\tau}{2r_0}\right) \\
&\qquad\left. -\frac{1177}{315}\ln\left(\frac{c\tau}{2r_0}\right) + \frac{129268}{33075} + \frac{428}{315}\pi^2\right] + \mathcal{O}\left(\frac{1}{c^{12}}\right).
\end{aligned} \tag{4.112}$$

Equation (4.112) is the final result of this section. We have restored the powers of c to show that the tails-of-tails-of-tails represent a 4.5PN effect in the waveform. They correspond to the most difficult interaction between multipole moments to be computed up to the 4.5PN level.

In order to compute the contributions of the tails to the flux at 4.5PN, we need the following radiative moments. These radiative multipole moments are computed similarly to U_{ij} by using the MPM algorithm. Because of the $1/c$ factors contained in equation (4.122), these radiative multipole moments have to be known to a lower order and have already been computed in [133].

$$\begin{aligned}
U_{ijk}(T_R) = M_{ijk}^{(3)}(T_R) &+ \frac{GM}{c^3}\int_0^{+\infty}\mathrm{d}\tau\, M_{ijk}^{(5)}(T_R-\tau)\left[2\ln\left(\frac{c\tau}{2b_0}\right) + \frac{97}{30}\right] \\
&+ \frac{G^2M^2}{c^6}\int_0^{+\infty}\mathrm{d}\tau\, M_{ijk}^{(6)}(T_R-\tau)\left[2\ln^2\left(\frac{c\tau}{2b_0}\right) + \frac{97}{15}\ln\left(\frac{c\tau}{2b_0}\right)\right. \\
&\qquad\left. -\frac{26}{21}\ln\left(\frac{c\tau}{2r_0}\right) + \frac{13283}{4410}\right] + \mathcal{O}\left(\frac{1}{c^9}\right),
\end{aligned} \tag{4.113a}$$

$$V_{ij}(T_R) = S_{ij}^{(2)}(T_R) + \frac{GM}{c^3}\int_0^{+\infty}\mathrm{d}\tau\, S_{ij}^{(4)}(T_R-\tau)\left[2\ln\left(\frac{c\tau}{2b_0}\right) + \frac{7}{3}\right]$$

$$+\frac{G^2M^2}{c^6}\int_0^{+\infty}\mathrm{d}\tau\, S^{(5)}_{ij}(T_R-\tau)\left[2\ln^2\left(\frac{c\tau}{2b_0}\right)+\frac{14}{3}\ln\left(\frac{c\tau}{2b_0}\right)\right.$$
$$\left.-\frac{214}{105}\ln\left(\frac{c\tau}{2r_0}\right)-\frac{26254}{11025}\right]+\mathcal{O}\left(\frac{1}{c^9}\right)\,, \tag{4.113b}$$
$$U_{ijkl}(T_R)=M^{(4)}_{ijkl}(T_R)+\frac{GM}{c^3}\int_0^{+\infty}\mathrm{d}\tau\, M^{(6)}_{ijkl}(T_R-\tau)\left[2\ln\left(\frac{c\tau}{2b_0}\right)+\frac{59}{15}\right]\,, \tag{4.113c}$$
$$V_{ijk}(T_R)=S^{(3)}_{ijk}(T_R)+\frac{GM}{c^3}\int_0^{+\infty}\mathrm{d}\tau\, S^{(5)}_{ijk}(T_R-\tau)\left[2\ln\left(\frac{c\tau}{2b_0}\right)+\frac{10}{3}\right]\,, \tag{4.113d}$$
$$U_{ijklm}(T_R)=M^{(5)}_{ijklm}(T_R)+\frac{GM}{c^3}\int_0^{+\infty}\mathrm{d}\tau\, M^{(7)}_{ijklm}(T_R-\tau)\left[2\ln\left(\frac{c\tau}{2b_0}\right)+\frac{464}{105}\right]\,, \tag{4.113e}$$
$$V_{ijkl}(T_R)=S^{(4)}_{ijkl}(T_R)+\frac{GM}{c^3}\int_0^{+\infty}\mathrm{d}\tau\, S^{(6)}_{ijkl}(T_R-\tau)\left[2\ln\left(\frac{c\tau}{2b_0}\right)+\frac{119}{30}\right]\,. \tag{4.113f}$$

4.3.3 Deriving the equation for the flux

In this section, we are going to express the energy flux carried by gravitational waves as a function of the radiative multipole moments U_L and V_L. In particular, we will recover at the Newtonian order the Einstein quadrupole formula (1.25) that we used in chapter 1. The energy contained in the spacetime is described by the 00 component of the *energy-impulsion pseudo-tensor* $\tau^{\mu\nu}$ divided by c^2 where $\tau^{\mu\nu}$ is defined in equation (6.8)

$$\tau^{00}=|g|T^{00}+\frac{c^4}{16\pi G}\Lambda^{00}\,, \tag{4.114}$$

where the first term $|g|T^{00}$ describes the energy of the matter and the second term $\frac{c^4}{16\pi G}\Lambda^{00}$ describes the energy contained in the gravitational field. Therefore, the energy flux $\mathcal{F}$ can be defined as

$$\mathcal{F}=-\frac{\mathrm{d}}{\mathrm{d}t}\int\mathrm{d}^3x\frac{\tau^{00}}{c^2}\,. \tag{4.115}$$

According to the harmonicity condition we have $\partial_\mu\tau^{\mu\nu}=0$. Applying this equation for $\nu=0$ we get

$$\frac{1}{c}\partial_t\tau^{00}=-\partial_i\tau^{0i}\,. \tag{4.116}$$

Let us integrate over d^3x the equation (4.116), and divide it by c:

$$\mathcal{F}=-\frac{\mathrm{d}}{\mathrm{d}t}\int\mathrm{d}^3x\frac{\tau^{00}}{c^2}=\frac{1}{c}\int\mathrm{d}^3x\partial_i\tau^{0i}\,. \tag{4.117}$$

By using the *Gauss*'s theorem we can transform the right-hand side of (4.117) into a 2-dimensional integral at infinity. Therefore, it becomes relevant to use the radiative coordinate (T,X^i) and we obtain

$$\mathcal{F}=\lim_{R\to\infty}\frac{1}{c}\int\mathrm{d}\Omega\; N^iR^2\tau^{0i}(H^{\mu\nu})\,, \tag{4.118}$$

where $\mathrm{d}\Omega$ is a solid angle interval. It turns out that $\tau^{\mu\nu}$ is at least quadratic in $H^{\mu\nu}$, and $H^{\mu\nu}\sim_{R\to\infty}1/R$. Thus, we only need to consider the $1/R^2$ terms in τ^{0i}, that comes from the quadratic part of Λ^{0i} noted N^{0i}

$$\Lambda^{0i}=N^{0i}(H^{\alpha\beta},H^{\alpha\beta})+\mathcal{O}\left(\frac{1}{R^3}\right)\,, \tag{4.119}$$

where $N^{\mu\nu}$ is defined in equation (4.6). We find after a tedious but straightforward computation that

$$\mathcal{F} = \frac{1}{32\pi G c} \int \mathrm{d}\Omega \; R^2 \mathcal{P}_{ijkl} \dot{H}^{TT}_{ij} \dot{H}^{TT}_{kl} \,, \tag{4.120}$$

where $\mathcal{P}_{ijkl}$ is the TT projector defined after the equation (4.111) and where the dots denote time-derivatives. Now, the last step is to inject into (4.120) the equation (4.111) and integrate over the angle $\mathrm{d}\Omega$. This requires the extensive use of the following two formulae

$$\int \mathrm{d}\Omega N_{i_1} \dots N_{i_{2p+1}} = 0 \,, \tag{4.121a}$$

$$\int \mathrm{d}\Omega N_{i_1} \dots N_{i_{2p}} = \frac{4\pi}{(2p+1)!!} \delta_{\{i_1 i_2 \dots} \delta_{i_{2p-1} i_{2p}\}} \,. \tag{4.121b}$$

We can also use the fact that $\int \mathrm{d}\Omega \hat{N}_L = 0$ if $\ell \geq 1$. Doing so, a lot of simplifications occur, and the final result turns to be

$$\mathcal{F} = \sum_{\ell=2}^{+\infty} \frac{G}{c^{2\ell+1}} \left\{ \frac{(\ell+1)(\ell+2)}{(\ell-1)\ell\ell!(2\ell+1)!!} \mathrm{U}^{(1)}_L \mathrm{U}^{(1)}_L + \frac{4\ell(\ell+2)}{c^2(\ell-1)(\ell+1)!(2\ell+1)!!} \mathrm{V}^{(1)}_L \mathrm{V}^{(1)}_L \right\} . \tag{4.122}$$

We can check that at the Newtonian order, we recover the Einstein quadrupole formula. In fact, we have at the linear order $U_{ij} = M^{(2)}_{ij} + \mathcal{O}\left(\frac{1}{c^2}\right)$ and $\mathcal{F} = \frac{G}{5c^5} U^{(1)}_{ij} U^{(1)}_{ij} + \mathcal{O}\left(\frac{1}{c^7}\right)$, so the equation (1.25) is the Newtonian limit of the equation (4.122).

4.3.4 The flux at 4.5PN for circular orbits

In this section we derive, based on the quartic radiative mass quadrupole moment (4.112), as well as the higher order radiative multipole moments listed in section 4.3.1 , the complete 4.5PN coefficient of the gravitational-wave energy flux (4.122), in the case of binary systems of non-spinning compact objects moving on circular orbits. We thus extend the circular energy flux known at the 3.5PN order [134, 132, 77, 135] by including the 4.5PN coefficient, while the determination of the 4PN coefficient is left to future work. The test mass limit of our new 4.5PN coefficient turns out to be in perfect agreement with the prediction from black hole perturbation theory [136, 137, 138].

The reason why we are able to control the 4.5PN order without knowing the complete 4PN field (since the source moments are known only up to the 3.5PN order [45, 128, 133][7]) is the fact that for half-integral PN orders, i.e., $\frac{n}{2}$PN orders where n is an *odd* integer, any instantaneous term is zero in the energy flux for circular orbits. This can be shown by a simple dimensional argument (see the discussion in Sec. II of [139]).

In addition to tail terms and instantaneous terms, there is a third class of term occurring in the MPM algorithm called *semi-hereditary* terms. They are linked to memory effects and correspond to integral along the past of the source. The time derivative of such memory effects turns out to be an instantaneous term. Therefore, these memory effects do not arise at half-integral PN orders, because of the time derivative acting on the radiative moments in the flux equation (4.122).

Hence, at the 4.5PN order, it is therefore sufficient to control the occurrence of such non-linear tail interactions between multipole moments. For that purpose, it is very useful

[7] Cf chapter 8 for preliminary results on the 4PN mass quadrupole moment.

to apply some "selection rules" that permit one to determine all the possible multipole interactions occurring at a given PN order [45, 128, 133]. According to those selection rules, in order to control the 4.5PN order for circular orbits, we need only the contributions of (i) quadratic multipole tails, of the form $M \times M_L$ or $M \times S_L$, with $2 \leqslant \ell \leqslant 5$ for mass moments M_L and $2 \leqslant \ell \leqslant 4$ for current moments S_L, (ii) the quartic quadrupole tails-of-tails-of-tails $M^3 \times M_{ij}$ (with $\ell = 2$ in this case), and (iii) the double product between the quadratic quadrupole tails $M \times M_{ij}$ and the cubic quadrupole tails-of-tails $M^2 \times M_{ij}$.

The cubic tails-of-tails $M^2 \times M_{ij}$ by themselves contribute to the circular energy flux, starting at the 3PN order [132]. The 4PN order correction will be given in (4.132). Moreover, from the point (iii) above, we see that the cubic tails-of-tails also contribute at the 4.5PN order through their interactions with the quadrupole tails $M \times M_{ij}$.

4.3.4.a) Required quantities

The computation of quadratic tails for circular compact binaries only requires at the 4.5PN order, the mass quadrupole moment at 3PN order, since 4.5PN means 3PN beyond the dominant quadrupole tail at the 1.5PN order. In chapter 8, we will explain how to derive explicit formulae for the source multipole moment, and in particular for the mass quadrupole moment M_{ij}. At 3PN, this quantity is known for a long time (see e.g., Ref. [45]) and reads

$$M_{ij} = m\,\nu\left(A\,x^{\langle ij\rangle} + B\,\frac{r^2}{c^2}v^{\langle ij\rangle} + \frac{48}{7}\frac{G^2m^2\nu}{c^5 r}x^{\langle i}v^{j\rangle}\right) + \mathcal{O}\left(\frac{1}{c^7}\right)\,. \tag{4.123}$$

Here x^i and v^i denote the orbital separation and relative velocity of the two particles (and the angular brackets refer to the STF projection). The mass parameters are the total mass $m = m_1 + m_2$ and the symmetric mass ratio $\nu = \frac{m_1 m_2}{(m_1+m_2)^2}$. A and B are given by

$$\begin{aligned}
A &= 1 + \gamma\left(-\frac{1}{42} - \frac{13}{14}\nu\right) + \gamma^2\left(-\frac{461}{1512} - \frac{18395}{1512}\nu - \frac{241}{1512}\nu^2\right) + \gamma^3\left(\frac{395899}{13200}\right.\\
&\quad \left.-\frac{428}{105}\ln\left(\frac{r}{r_0}\right) + \left[\frac{3304319}{166320} - \frac{44}{3}\ln\left(\frac{r}{r'_0}\right)\right]\nu + \frac{162539}{16632}\nu^2 + \frac{2351}{33264}\nu^3\right)\,, && (4.124a)\\
B &= \frac{11}{21} - \frac{11}{7}\nu + \gamma\left(\frac{1607}{378} - \frac{1681}{378}\nu + \frac{229}{378}\nu^2\right)\\
&\quad + \gamma^2\left(-\frac{357761}{19800} + \frac{428}{105}\ln\left(\frac{r}{r_0}\right) - \frac{92339}{5544}\nu + \frac{35759}{924}\nu^2 + \frac{457}{5544}\nu^3\right)\,. && (4.124b)
\end{aligned}$$

The harmonic-coordinates PN parameter is $\gamma = \frac{Gm}{rc^2}$, where $r = |x^i|$ represents the radial harmonic-coordinates separation.

In order to compute the contribution of the tails to the flux, we also require the following source multipole moments that have been computed in [140, 45]

$$\begin{aligned}
\mathrm{M}_{ijk} = -\nu\, m\, \Delta\, \Bigg\{ & x_{\langle ijk\rangle}\left[1 - \gamma\nu - \gamma^2\left(\frac{139}{330} + \frac{11923}{660}\nu + \frac{29}{110}\nu^2\right)\right]\\
& + \frac{r^2}{c^2}\,x_{\langle i}v_{jk\rangle}\left[1 - 2\nu - \gamma\left(-\frac{1066}{165} + \frac{1433}{330}\nu - \frac{21}{55}\nu^2\right)\right]\\
& + \frac{196}{15}\,\frac{r}{c}\,\gamma^2\,\nu\, x_{\langle ij}v_{k\rangle}\Bigg\} + \mathcal{O}\left(\frac{1}{c^5}\right)\,, && (4.125a)
\end{aligned}$$

$$
\begin{aligned}
\mathrm{S}_{ij} &= -\nu\, m\, \Delta \left\{ \epsilon_{ab\langle i} x_{j\rangle a} v_b \left[1 + \gamma \left(\frac{67}{28} - \frac{2}{7}\nu \right) + \gamma^2 \left(\frac{13}{9} - \frac{4651}{252}\nu - \frac{1}{168}\nu^2 \right) \right] \right. \\
&\quad \left. - \frac{188}{35}\, \frac{r}{c}\, \gamma^2\, \nu\, \epsilon_{ab\langle i} v_{j\rangle a} x_b \right\} + \mathcal{O}\left(\frac{1}{c^5}\right) , \qquad (4.125b) \\
\mathrm{M}_{ijkl} &= \nu\, m \left\{ x_{\langle ijkl\rangle} \left[1 - 3\nu + \gamma \left(\frac{3}{110} - \frac{25}{22}\nu + \frac{69}{22}\nu^2 \right) \right. \right. \qquad (4.125c) \\
&\quad \left. + \gamma^2 \left(-\frac{126901}{200200} - \frac{58101}{2600}\nu + \frac{204153}{2860}\nu^2 + \frac{1149}{1144}\nu^3 \right) \right] \qquad (4.125d) \\
&\quad \left. + \frac{r^2}{c^2}\, x_{\langle ij} v_{kl\rangle} \left[\frac{78}{55}(1 - 5\nu + 5\nu^2) \right] \right\} + \mathcal{O}\left(\frac{1}{c^4}\right) , \\
\mathrm{S}_{ijk} &= \nu\, m \left\{ \epsilon_{ab\langle i} x_{jk\rangle a} v_b \left[1 - 3\nu + \gamma \left(\frac{181}{90} - \frac{109}{18}\nu + \frac{13}{18}\nu^2 \right) \right] \right. \\
&\quad \left. + \frac{r^2}{c^2}\, \epsilon_{ab\langle i} x_a v_{jk\rangle b} \left[\frac{7}{45} \left(1 - 5\nu + 5\nu^2 \right) + \right] \right\} + \mathcal{O}\left(\frac{1}{c^4}\right) , \qquad (4.125e) \\
\mathrm{M}_{ijklm} &= -\nu\, m\, \Delta x_{\langle ijklm\rangle} \left(1 - 2\nu\right) + \mathcal{O}\left(\frac{1}{c^2}\right) , \qquad (4.125f) \\
\mathrm{S}_{ijkl} &= -\nu\, m\, \Delta \epsilon_{ab\langle i} x_{jkl\rangle a} v_b \left(1 - 2\nu\right) + \mathcal{O}\left(\frac{1}{c^2}\right) . \qquad (4.125g)
\end{aligned}
$$

Where Δ is defined as $\Delta \equiv (m_1 - m_2)/(m_1 + m_2)$. Notice the two scales entering the logarithmic terms at the 3PN order in the source mass quadrupole: one is the length scale r_0 coming from the MPM algorithm (see Sec. 4.1), while the other scale r'_0 is the logarithmic barycenter of two gauge constants r'_1 and r'_2 which appear in the 3PN equations of motion in harmonic coordinates. These constants are defined later in chapters 6 and 7 (cf equation (7.10) for the definition of r'_0). In order to compute the flux at 4.5PN for circular orbits, we need the circular equations of motion at 3PN. We will just provide them directly here all these results will be generalized to 4PN in the chapter 7. The circular equations of motion at 3PN in the center of mass is

$$
\boldsymbol{a} = -\omega^2 \boldsymbol{x} \qquad (4.126)
$$

where ω is the orbital frequency. Its value as a function of $\gamma = \frac{Gm}{rc^2}$ is given by

$$
\begin{aligned}
\omega^2 = \frac{Gm}{r^3} \Bigg\{ & 1 + (-3 + \nu)\gamma + \left(6 + \frac{41}{4}\nu + \nu^2 \right) \gamma^2 \\
& + \left(-10 + \left[-\frac{75707}{840} + \frac{41}{64}\pi^2 + 22 \ln\left(\frac{r}{r'_0}\right) \right] \nu + \frac{19}{2}\nu^2 + \nu^3 \right) \gamma^3 + \mathcal{O}\left(\frac{1}{c^8}\right) \Bigg\} . \qquad (4.127)
\end{aligned}
$$

The latter expression can be inverted in order to express γ as a function of the *quasi-invariant* PN parameter x defined by $x = (\frac{Gm\omega}{c^3})^{2/3}$ where ω stands for the orbital frequency, related to r by (4.127). A scalar such as the circular energy flux is *quasi-invariant* when expressed in terms of x, in the sense that it stays invariant under the class of coordinate transformations that are asymptotically Minkowskian at infinity.

$$
\begin{aligned}
\gamma = x \Bigg\{ & 1 + \left(1 - \frac{\nu}{3} \right) x + \left(1 - \frac{65}{12}\nu \right) x^2 \\
& + \left(1 + \left[-\frac{2203}{2520} - \frac{41}{192}\pi^2 - \frac{22}{3} \ln\left(\frac{r}{r'_0}\right) \right] \nu + \frac{229}{36}\nu^2 + \frac{1}{81}\nu^3 \right) x^3 + \mathcal{O}\left(\frac{1}{c^8}\right) \Bigg\} . \qquad (4.128)
\end{aligned}
$$

Here, we do not consider the 2.5PN radiation reaction term in the equations of motion, since it generates some contribution at the 4PN order but not at the 4.5PN order. To summarize, there are three arbitrary length scales in the problem: r_0, r_0', as well as b_0 which originates from our choice of radiative type coordinate system through (4.108). It is non trivial to check that these three scales cancel out in the final gauge invariant expression of the energy flux for circular orbits.

Another important step of the calculation is the reduction of the tail integrals to circular orbits. As usual, those integrals are to be computed proceeding as if the world-lines in the integrands obeyed the current circular dynamics, which amounts to neglecting the evolution in the past by radiation reaction. The influence of the past evolution would be to correct the dominant 1.5PN tail integral by a 2.5PN radiation reaction term, and would thus be of order 4PN, but not 4.5PN. From (4.112), we see that, at the 4.5PN order, we also need some integration formulae involving up to three powers of logarithms. Those are [141]

$$\int_0^{+\infty} \mathrm{d}\tau\, \ln\left(\frac{\tau}{\tau_0}\right) e^{-\mathrm{i}\Omega\tau} = \frac{\mathrm{i}}{\Omega}\left(\ln(\Omega\tau_0) + \gamma_\mathrm{E} + \mathrm{i}\frac{\pi}{2}\right), \tag{4.129a}$$

$$\int_0^{+\infty} \mathrm{d}\tau\, \ln^2\left(\frac{\tau}{\tau_0}\right) e^{-\mathrm{i}\Omega\tau} = -\frac{\mathrm{i}}{\Omega}\left[\left(\ln(\Omega\tau_0) + \gamma_\mathrm{E} + \mathrm{i}\frac{\pi}{2}\right)^2 + \frac{\pi^2}{6}\right], \tag{4.129b}$$

$$\begin{aligned}\int_0^{+\infty} \mathrm{d}\tau\, \ln^3\left(\frac{\tau}{\tau_0}\right) e^{-\mathrm{i}\Omega\tau} = \frac{\mathrm{i}}{\Omega}\Bigg[&\left(\ln(\Omega\tau_0) + \gamma_\mathrm{E} + \mathrm{i}\frac{\pi}{2}\right)^3 \\ &+\frac{\pi^2}{2}\left(\ln(\Omega\tau_0) + \gamma_\mathrm{E} + \mathrm{i}\frac{\pi}{2}\right) + 2\zeta(3)\Bigg].\end{aligned} \tag{4.129c}$$

Here, Ω denotes a multiple of the orbital frequency ω. The constant τ_0 is arbitrary, and related either to r_0, r_0' or b_0. We denote by $\gamma_\mathrm{E} \simeq 0.577$ the Euler constant, whereas $\zeta(3) \simeq 1.202$ is the Apéry constant (ζ being the usual notation for the Riemann zeta function).

4.3.4.b) Results

In order to compute the tail contributions to the energy flux of circular binaries at 4.5PN, we need first to inject the source multipole moments (equations (4.123), and (4.125)) into the radiative multipole moments (equations (4.112) and (4.113)). Then, we need to inject these results into the equation (4.122), and use the prescription defined by the equations (4.129) to compute the non-local terms.

As we can see in (4.122), the energy flux depends on the square value of the radiative multipole moments: $\left(U_L^{(1)}\right)^2$ and $\left(V_L^{(1)}\right)^2$, therefore in order to keep track of the different terms, we will decompose the result using the explicit dependence on G of each terms

$$\mathcal{F}_\mathrm{tail} = \mathcal{F}_\mathrm{quadratic} + \mathcal{F}_\mathrm{cubic} + \mathcal{F}_\mathrm{quartic} + \mathcal{O}\left(G^5\right), \tag{4.130}$$

where $\mathcal{F}_\mathrm{quadratic} = \mathcal{O}(G^2)$, $\mathcal{F}_\mathrm{cubic} = \mathcal{O}(G^3)$ and $\mathcal{F}_\mathrm{quartic} = \mathcal{O}(G^4)$. The quadratic tails correspond to multipole interactions. In particular, we need the full 3PN precision for the mass quadrupole moment, as in (4.123)–(4.124). The higher order moments require some lower PN precision as provided in the equations (4.125). The result in term of the PN parameter $\gamma = Gm/(rc^2)$ up to the 4.5PN order reads (factorizing out the Newtonian flux as usual)

$$
\begin{aligned}
\mathcal{F}_{\text{quadratic}} = \frac{32c^5}{5G}\nu^2\gamma^5\Big\{ & 4\pi\gamma^{3/2} \\
& + \left(-\frac{25663}{672} - \frac{125}{8}\nu\right)\pi\gamma^{5/2} + \left(\frac{90205}{576} + \frac{505747}{1512}\nu + \frac{12809}{756}\nu^2\right)\pi\gamma^{7/2} \\
& + \left(\frac{9997778801}{106444800} - \frac{6848}{105}\ln\left(\frac{r}{r_0}\right) + \left[-\frac{8058312817}{2661120} + \frac{287}{32}\pi^2 + \frac{572}{3}\ln\left(\frac{r}{r'_0}\right)\right]\nu \right.\\
& \left. \quad -\frac{12433367}{13824}\nu^2 - \frac{1026257}{266112}\nu^3\right)\pi\gamma^{9/2} + \mathcal{O}\left(\frac{1}{c^{11}}\right)\Big\}. \qquad (4.131)
\end{aligned}
$$

In contrast to the quadratic tails, the cubic tails-of-tails contribute to integral PN approximations, starting at the 3PN order [132]. At the next 4PN order they involve the contribution of the mass quadrupole moment (to be computed with 1PN precision), as well as that of the mass octupole and current quadrupole moments. Furthermore, at the same level of the cubic tails, we must include in the flux the square of the quadratic tails. Those various contributions have all been computed. For their sum, we obtain, extending (5.9) of [132],

$$
\begin{aligned}
\mathcal{F}_{\text{cubic}} = \frac{32c^5}{5G}\nu^2\gamma^5\Big\{ & \left(-\frac{116761}{3675} + \frac{16}{3}\pi^2 - \frac{1712}{105}\gamma_{\text{E}} - \frac{856}{105}\ln(16\gamma) + \frac{1712}{105}\ln\left(\frac{r}{r_0}\right)\right)\gamma^3 \\
& + \left(\frac{12484937}{30870} - \frac{4040}{63}\pi^2 + \frac{86456}{441}\gamma_{\text{E}} + \frac{43228}{441}\ln(16\gamma) - \frac{86456}{441}\ln\left(\frac{r}{r_0}\right)\right. \\
& \quad + (1-4\nu)\left[\frac{670000393}{7408800} + \frac{445}{42}\pi^2 - \frac{56731}{4410}\gamma_{\text{E}} - \frac{56731}{8820}\ln(16\gamma)\right. \\
& \quad \left.\left. + \frac{133771}{4410}\ln 2 - \frac{47385}{1568}\ln 3 + \frac{56731}{4410}\ln\left(\frac{r}{r_0}\right)\right]\right)\gamma^4 + \mathcal{O}\left(\frac{1}{c^{10}}\right)\Big\}. \qquad (4.132)
\end{aligned}
$$

The constant b_0 disappears, as expected. However, $\mathcal{F}_{\text{cubic}}$ still contains r_0. The point is that these cubic tails at the 3PN and 4PN orders are not the only contributions to the full coefficients, since the flux also contains many instantaneous terms (i.e. not tail terms) that depend on the source multipole moments, and notably the 4PN quadrupole. After the moments have been replaced by their explicit expressions, those terms should cancel out the remaining constants r_0 in (4.132). Thus, since the 4PN instantaneous contributions are not known, we shall ignore henceforth the 4PN coefficient in the flux except for the partial result (4.132).

In addition, there are other tail contributions at the 4PN order (but not at the 4.5PN order) that we have not yet taken into account. We can mention for instance the 2.5PN effect corresponding to the past evolution of the binary source due to radiation reaction. It should affect the computation of the 1.5PN tail integral at the 4PN order. We also recall the non-local 4PN tail term entering the equations of motion (cf chapter 6), which will have to be included when performing the order reduction of accelerations coming from the time derivatives of the Newtonian quadrupole moment. All these contributions will have to be systematically included in future work.

Let us next focus on the computation of the quartic-order tails in the flux. One contribution is directly due to the quartic tail term at the 4.5PN order in the radiative mass quadrupole moment (4.112). However, there is another contribution coming from a double product between the quadratic quadrupole tail at the 1.5PN order and the cubic quadrupole tail-of-tail at the 3PN order — recall that the energy flux contains the square of the time derivative of (4.112). It turns out that important cancellations occur between these two terms, notably all the logarithms squared and cubed disappear, leaving only a term linear in the logarithm. The constant b_0 cancels out as expected, but a dependence of r_0 is left out at this stage. In the end, we find that

$$\mathcal{F}_{\text{quartic}} = \frac{32c^5}{5G}\nu^2\gamma^5\left\{\left(-\frac{467044}{3675} - \frac{3424}{105}\ln(16\gamma) + \frac{6848}{105}\ln\left(\frac{r}{r_0}\right) - \frac{6848}{105}\gamma_{\text{E}}\right)\pi\gamma^{9/2} + \mathcal{O}\left(\frac{1}{c^{11}}\right)\right\}. \tag{4.133}$$

Finally we are in a position to control the half-integral PN approximations (or so-called "odd" PN terms) in the energy flux for circular orbits, as they are entirely due to tail integrals. The "odd" part of the flux in this case is

$$\mathcal{F}\Big|_{\text{odd}} = \mathcal{F}_{\text{tail}}\Big|_{\text{odd}} = \Big(\mathcal{F}_{\text{quadratic}} + \mathcal{F}_{\text{quartic}}\Big)\Big|_{\text{odd}} + \mathcal{O}\left(G^5\right). \tag{4.134}$$

We do not include the cubic tail part (4.132) since it is "even" in the PN sense. Therefore, we need only to sum up (4.131) and (4.133). We gladly discover that the scale r_0 cancels out from the sum, thereby obtaining

$$\begin{aligned}\mathcal{F}\Big|_{\text{odd}} = \frac{32c^5}{5G}\nu^2\gamma^5\Big\{&4\pi\gamma^{3/2} \\ &+\left(-\frac{25663}{672} - \frac{125}{8}\nu\right)\pi\gamma^{5/2} + \left(\frac{90205}{576} + \frac{505747}{1512}\nu + \frac{12809}{756}\nu^2\right)\pi\gamma^{7/2} \\ &+\bigg(-\frac{24709653481}{745113600} - \frac{6848}{105}\gamma_{\text{E}} - \frac{3424}{105}\ln(16\gamma) \\ &\quad+\left[-\frac{8058312817}{2661120} + \frac{287}{32}\pi^2 + \frac{572}{3}\ln\left(\frac{r}{r'_0}\right)\right]\nu \\ &\quad-\frac{12433367}{13824}\nu^2 - \frac{1026257}{266112}\nu^3\bigg)\pi\gamma^{9/2} + \mathcal{O}\left(\frac{1}{c^{11}}\right)\Big\}.\end{aligned} \tag{4.135}$$

Still there remains a dependence on the scale r'_0 coming from the equations of motion, but that is merely due to our use of the harmonic-coordinates PN parameter γ. Eliminating γ in favor of the quasi-invariant frequency-related PN parameter $x = (Gm\omega/c^3)^{2/3}$ with the help of (4.127) yields then our final result

$$\begin{aligned}\mathcal{F}\Big|_{\text{odd}} = \frac{32c^5}{5G}\nu^2x^5\Big\{&4\pi x^{3/2} \\ &+\left(-\frac{8191}{672} - \frac{583}{24}\nu\right)\pi x^{5/2} + \left(-\frac{16285}{504} + \frac{214745}{1728}\nu + \frac{193385}{3024}\nu^2\right)\pi x^{7/2} \\ &+\bigg(\frac{265978667519}{745113600} - \frac{6848}{105}\gamma_{\text{E}} - \frac{3424}{105}\ln(16x) + \left[\frac{2062241}{22176} + \frac{41}{12}\pi^2\right]\nu \\ &\quad-\frac{133112905}{290304}\nu^2 - \frac{3719141}{38016}\nu^3\bigg)\pi x^{9/2} + \mathcal{O}\left(\frac{1}{c^{11}}\right)\Big\}.\end{aligned} \tag{4.136}$$

We insist that the latter odd part of the flux, although it has been computed only from tail contributions, represents the full PN-odd part of the complete flux, in the case of circular orbits.

Our result can be compared with those derived from black hole perturbation theory in the small mass ratio limit $\nu \to 0$. Black hole perturbations have been expanded for this problem at the 1.5PN order [142], then extended up to the 5.5PN order in [143, 144, 145, 136], and more recently, using the method [146, 147, 148], up to extremely high PN orders [137, 138]. In this framework, a test-particle follows a geodesic on a Schwarzschild metric and the energy radiated by this particle is computed through a post-Newtonian expansion. When we take $\nu \to 0$ (i.e. $m_1/m_2 \to 0$ with constant total mass $m = m_1 + m_2$), our new 4.5PN result in (4.136) perfectly reproduces the latter works (see (3.1) in [136]). Last but not least, more recently, Messina and Nagar [149] confirmed fully our result within the EOB formalism by recovering the coefficients of the equation (4.136).

For consistency, let us provide the full known flux up to 4.5PN where only the 4PN coefficients (which are not yet fully computed) are missing. This result includes not only the tail effects, but also all the instantaneous terms. Up to 3.5PN, this formula was already known for a long time and the 4.5PN coefficient (computed above) is therefore a new term extended this result. In fact, we recall that at 4.5PN, only tail effects contribute to the flux for circular orbits. Hence we have

$$\begin{aligned}\mathcal{F}_{\text{total}} = \frac{32c^5}{5G}\nu^2 x^5\Bigg\{ & 1 + \left(-\frac{1247}{336} - \frac{35}{12}\nu\right)x + 4\pi x^{3/2} + \left(-\frac{44711}{9072} + \frac{9271}{504}\nu + \frac{65}{18}\nu^2\right)x^2 \\ & + \left(-\frac{8191}{672} - \frac{583}{24}\nu\right)\pi x^{5/2} + \bigg[\frac{6643739519}{69854400} + \frac{16}{3}\pi^2 - \frac{1712}{105}\gamma_E \\ & - \frac{856}{105}\ln(16x) + \left(-\frac{134543}{7776} + \frac{41}{48}\pi^2\right)\nu - \frac{94403}{3024}\nu^2 - \frac{775}{324}\nu^3\bigg]x^3 \\ & + \left(-\frac{16285}{504} + \frac{214745}{1728}\nu + \frac{193385}{3024}\nu^2\right)\pi x^{7/2} + (\text{unknown coefficients})x^4 \\ & + \Big(\frac{265978667519}{745113600} - \frac{6848}{105}\gamma_{\text{E}} - \frac{3424}{105}\ln(16x) + \left[\frac{2062241}{22176} + \frac{41}{12}\pi^2\right]\nu \\ & - \frac{133112905}{290304}\nu^2 - \frac{3719141}{38016}\nu^3\Big)\pi x^{9/2} + \mathcal{O}(x^5)\Bigg\}\,. \end{aligned} \tag{4.137}$$

The computation of the remaining unknown coefficients at the 4PN order is one of the main goal of the 4.5PN project. The computation of the equation of motions at the 4PN order in chapter 6 as well as the computation of the source mass quadrupole at the 4PN order in chapter 8 constitute crucial steps in the determination of these unknown coefficients.

5 – The matching equation and its consequences

The goal of this chapter is to derive a matching equation relating, on the one hand, the far-zone multipolar post-Minkowskian (MPM) expansion done in the previous chapter, and on the other hand the near-zone post-Newtonian results that we are going to compute in chapters 6-7-8. This chapter is rather technical, and its main results are the equations (5.40)–(5.41). The two major consequences of this matching equation are: (i) the derivation of the multipole source moments entering the MPM algorithm as explained in section 5.4; (ii) the effect of the *tails* in the conservative part of the dynamics at the fourth post-Newtonian order as explained in chapter 6 section 6.1.5.

5.1 Near zone, far zone, buffer zone and notations

As usual, $h^{\mu\nu}$ is the deviation of the gothic metric to Minkowski

$$h^{\mu\nu} = \sqrt{-g}g^{\mu\nu} - \eta^{\mu\nu}\,. \tag{5.1}$$

Using $h^{\mu\nu}$, the Einstein equations are

$$\Box h^{\alpha\beta} = \frac{16\pi G}{c^4}\tau^{\alpha\beta}\,, \tag{5.2}$$

where $\Box = -\frac{1}{c^2}\frac{\partial^2}{\partial t^2} + \delta^{ij}\frac{\partial}{\partial x^i}\frac{\partial}{\partial x^j}$ is the flat d'Alembertian operator, and $\tau^{\alpha\beta}$ is the stress-energy pseudo tensor

$$\tau^{\alpha\beta} = |g|T^{\alpha\beta} + \frac{c^4}{16\pi G}\Lambda^{\alpha\beta}\,, \tag{5.3}$$

where $T^{\alpha\beta}$ is the energy-impulsion tensor of the matter and $\Lambda^{\alpha\beta}$ takes into account the non-linearities of the Einstein equations and is given by equation (4.5). It is important to keep in mind that $h^{\mu\nu}$ has not been post-Newtonian expanded, or multipolar expanded so far and that the equation (5.2) represents the full Einstein equations without any approximation or asymptotical expansion and is valid everywhere, outside and inside the source. In the rest of this chapter, we will denote by an overbar a post-Newtonian expansion, and by $\mathcal{M}$ a multipolar expansion.

The **far zone** is defined as the region $r >> a$ where a is the size of the source. In the far zone, the multipolar expansion of the metric noted $\mathcal{M}(h^{\mu\nu})$ is well-defined and is equal to the real value of the exterior metric

$$h^{\mu\nu}_{\text{ext}} = \mathcal{M}(h^{\mu\nu})\,. \tag{5.4}$$

In the **near-zone**, defined as the region $r \leq \lambda$ where λ is the gravitational wavelength, the post-Newtonian expansion of the metric is well-defined and converges to the actual value of the metric

$$h^{\mu\nu}_{\text{int}} = \overline{h^{\mu\nu}} \,. \tag{5.5}$$

If the source is post-Newtonian, then the gravitational wavelength is much larger than the size of the source: $\lambda \gg a$. Therefore there exists an intermediate region, or buffer region where $a << r << \lambda$, overlapping the near-zone and the far-zone. In this region, both the multipolar expansion and the post-Newtonian expansion of the metric are well-defined and converge to the true value

$$h^{\mu\nu}_{\text{buffer}} = \mathcal{M}(h^{\mu\nu}) = \overline{h}^{\mu\nu} \,. \tag{5.6}$$

In the buffer-zone, $\overline{h}^{\mu\nu}$ is also equal at its own multipolar expansion: $\overline{h}^{\mu\nu} = \mathcal{M}(\overline{h}^{\mu\nu})$. Similarly, the multipolar expansion of the metric $\mathcal{M}(h^{\mu\nu})$ can be post-Newtonian expanded and $\mathcal{M}(h^{\mu\nu}) = \overline{\mathcal{M}(h^{\mu\nu})}$. This leads to the matching equation in the buffer zone (for $a \leq r \leq \lambda$)

$$\overline{\mathcal{M}(h^{\mu\nu})} = \mathcal{M}\left(\overline{h}^{\mu\nu}\right) \,. \tag{5.7}$$

Actually, the equation (5.7) should not be seen as a numerical equality valid solely in the buffer zone. Instead, the matching equation states that (5.7) as to be seen as *functional identity* true everywhere in the sense that the coefficients of the formal expansion of both side of (5.7) are equal.

The matching equation extends naturally to the energy-impulsion pseudo tensor $\tau^{\mu\nu}$. As $\tau^{\mu\nu} = \frac{16\pi G}{c^4}\Lambda^{\mu\nu}$ when $r \geq a$, $\mathcal{M}\left(\tau^{\mu\nu}\right) = \frac{c^4}{16\pi G}\mathcal{M}\left(\Lambda^{\mu\nu}\right)$. Therefore the matching equation for the source is

$$\overline{\mathcal{M}\left(\Lambda^{\mu\nu}\right)} = \mathcal{M}(\overline{\Lambda}^{\mu\nu}) = \frac{16\pi G}{c^4}\mathcal{M}\left(\overline{\tau}^{\mu\nu}\right) \,. \tag{5.8}$$

Indeed, $\mathcal{M}(T^{\mu\nu}) = 0$ since $T^{\mu\nu}$ has a compact support.

5.2 The Finite Part regularization and propagators

5.2.1 Finite Part

The matching procedure that we are going to present heavily relies on the Finite Part regularization. We have already seen the Finite Part regulator in section 4.1.3.a) in order to treat ultra-violet divergences. We will extend this regulator to deal with any kind of divergence.

Let us $F(\boldsymbol{x})$ be a function smooth everywhere except potentially at $r = 0$ such that there exist $(p, q) \in \mathbb{Z}^2$ such that $F(\boldsymbol{x}) = \mathcal{O}(r^p)$ when $r \to 0$ and $F(\boldsymbol{x}) = \mathcal{O}(r^q)$ when $r \to \infty$. Basically, we do not want F to have exponential divergences at $r = 0$ or at infinity. We define the Finite Part of the integral of F to be

$$I \equiv \underset{B}{\text{FP}} \int \mathrm{d}^3\boldsymbol{x} \left(\frac{|\boldsymbol{x}|}{r_0}\right)^B F(\boldsymbol{x}) \equiv I_1 + I_2 \,, \tag{5.9}$$

where

$$I_1 \equiv \underset{B}{\text{FP}} \int_{r \leq R} \mathrm{d}^3\boldsymbol{x} \left(\frac{|\boldsymbol{x}|}{r_0}\right)^B F(\boldsymbol{x}) \,, \tag{5.10}$$

$$I_2 \equiv \underset{B}{\mathrm{FP}} \int_{r>R} \mathrm{d}^3\boldsymbol{x} \left(\frac{|\boldsymbol{x}|}{r_0}\right)^B F(\boldsymbol{x})\,, \tag{5.11}$$

where $R > 0$ is an arbitrary cut-off and B a complex number used to build the Finite Part procedure.

The computation of I_1, is similar to what was done in 4.1.3.a): for $\Re B > -p-3$, the integral $\int_{r\leq R} \mathrm{d}^3\boldsymbol{x} \left(\frac{|\boldsymbol{x}|}{r_0}\right)^B F(\boldsymbol{x})$ is well-defined and can under some regularity conditions on F (cf [129]) be extended by analytical continuation to all the complex plane except isolated poles. Then I_1 is defined as the Finite Part (i.e. the zeroth power of B) of the Laurent's expansion of the result when $B \to 0$. For I_2, the integral $\int_{r>R} \mathrm{d}^3\boldsymbol{x} \left(\frac{|\boldsymbol{x}|}{r_0}\right)^B F(\boldsymbol{x})$ is well-defined for $\Re B < -q-3$ and can similarly be extended as a function of B to all the complex plane except isolated pole by analytical continuation. I_2 is also defined as the Finite Part of the Laurent's expansion of this result when $B \to 0$. It can be shown that the result $I_1 + I_2$ does not depend on the arbitrary choice of R, but it can depend of course, on r_0.

Hence, the Finite Part regularization can deal with both Ultra-Violet ($r \to 0$) and Infra-Red ($r \to \infty$) divergences.

5.2.2 $\widetilde{\Box^{-1}_{\mathrm{ret}}}$, $\widetilde{\Delta^{-k}}$ and $\widetilde{I^{-1}}$

Let us define here the three operators that we are going to use in this chapter. Here, F is a function which is smooth everywhere except at the origin where it can diverge. The behavior of F when $r \to 0$ (and when $r \to \infty$) is always of the order of $\mathcal{O}(r^N)$ with $N \in \mathbb{Z}$, which means that there exists a part of the complex plane for B such that $\left(\frac{r}{r_0}\right)^B F$ decreases fast enough at $r \to 0$ (or at $r \to \infty$) for the following integrals to be convergent. The retarded-propagator $\Box^{-1}_{\mathrm{ret}}$ has already been extensively used in the chapter 4. Let us introduce here a new notation and define $\widetilde{\Box^{-1}_{\mathrm{ret}}}$ as the propagator $\Box^{-1}_{\mathrm{ret}}$ combined with the Finite Part regularization procedure:

$$\begin{aligned}\widetilde{\Box^{-1}_{\mathrm{ret}}}\,[F]\,(t,\boldsymbol{x}) &\equiv \underset{B}{\mathrm{FP}}\,\Box^{-1}_{\mathrm{ret}}\left[\left(\frac{r}{r_0}\right)^B F\right] \\ &= -\frac{1}{4\pi}\,\underset{B}{\mathrm{FP}} \int \mathrm{d}^3\boldsymbol{x}' \left(\frac{|\boldsymbol{x}'|}{r_0}\right)^B \frac{F\left(t-\frac{|\boldsymbol{x}-\boldsymbol{x}'|}{c},\boldsymbol{x}'\right)}{|\boldsymbol{x}-\boldsymbol{x}'|}\,.\end{aligned} \tag{5.12}$$

Now, let us define a similar propagator in order to invert the Laplacian operator Δ. For $F(t,\boldsymbol{x})$ a smooth function decreasing fast enough at spatial infinity, we define Δ^{-1} as

$$\Delta^{-1}F \equiv -\frac{1}{4\pi}\int \mathrm{d}^3\boldsymbol{x}' \frac{F(t,\boldsymbol{x}')}{|\boldsymbol{x}-\boldsymbol{x}'|}\,. \tag{5.13}$$

In order to extend this operator to any smooth function F which behaves as $\mathcal{O}(r^N)$ when $r \to \infty$ we use the Finite Part regularization and define

$$\widetilde{\Delta^{-1}}F \equiv \underset{B}{\mathrm{FP}}\left[\left(\frac{r}{r_0}\right)^B \Delta^{-1}F\right]\,. \tag{5.14}$$

A similar reasoning than the one done in 4.1.3.a) shows that $\Delta\left[\widetilde{\Delta^{-1}}F\right] = F$. We can generalize the $\widetilde{\Delta^{-1}}$ operator to $\widetilde{\Delta^{-k-1}}$ by defining

$$\widetilde{\Delta^{-k-1}}F \equiv \underset{B}{\mathrm{FP}}\left[\Delta^{-k-1}\left(\frac{r}{r_0}\right)^B F\right] \tag{5.15}$$

$$= -\frac{1}{4\pi}\underset{B}{\mathrm{FP}}\int \mathrm{d}^3\boldsymbol{x}'\left(\frac{|\boldsymbol{x}'|}{r_0}\right)^B |\boldsymbol{x}-\boldsymbol{x}'|^{2k-1}F(t,\boldsymbol{x}')\,. \tag{5.16}$$

Of course, we have $\Delta^{k+1}\left[\widetilde{\Delta^{-k-1}}F\right] = F$.

Finally, we are going to define the instantaneous inverse d'Alembertian propagator by

$$\widetilde{I^{-1}}F \equiv \sum_{k=0}^{\infty}\left(\frac{\partial}{c\partial t}\right)^{2k}\widetilde{\Delta^{-k-1}}F\,. \tag{5.17}$$

We can show that $\Box\left[\widetilde{I^{-1}}F\right] = F$. This definition is motivated by the following formal expansion

$$\frac{1}{\Box} = \frac{1}{\Delta - \frac{\partial^2}{c^2\partial t^2}} = \Delta^{-1}\frac{1}{1-\frac{\partial^2}{c^2\partial t^2}\Delta} = \Delta^{-1}\left(1+\frac{\partial^2}{c^2\partial t^2}\Delta^{-1}+\left(\frac{\partial^2}{c^2\partial t^2}\Delta^{-1}\right)^2+\dots\right) \tag{5.18}$$

$$= \sum_{k=0}^{\infty}\left(\frac{\partial}{c\partial t}\right)^{2k}\Delta^{-k-1}\,. \tag{5.19}$$

To conclude this section, note that we can also define the advanced inverse d'Alembertian operator as

$$\Box^{-1}_{\mathrm{adv}}F = -\frac{1}{4\pi}\int \mathrm{d}^3\boldsymbol{x}'\frac{F\left(t+\frac{|\boldsymbol{x}-\boldsymbol{x}'|}{c},\boldsymbol{x}'\right)}{|\boldsymbol{x}-\boldsymbol{x}'|}\,. \tag{5.20}$$

Then it is interesting to notice that while I^{-1} and $\frac{\Box^{-1}_{\mathrm{ret}}+\Box^{-1}_{\mathrm{adv}}}{2}$ are two similar-looking operators, they are not equal (cf [150] for a discussion on the link between these two operators).

5.3 The matching equation

The exterior metric

The exterior metric has been built in chapter 4, through the use of the multipolar-post-Minkowskian algorithm where we iteratively computed the n^{th} post-Minkowskian order of the metric in the form of a multipole expansion. At each step n, we first computed $\widetilde{\Box^{-1}_{\mathrm{ret}}}\left[\Lambda^{\mu\nu}_{(n)}\right]$ (equation (4.23)), then we added a homogeneous solution in order to satisfy the harmonic gauge condition (equation (4.26)). Besides, the first post-Minkowskian order was given by a generic homogeneous solution (4.11). Based on that construction, we can easily show (cf [151] for a formal demonstration) that the exterior metric can be written as

$$h^{\mu\nu}_{\mathrm{ext}} \equiv \mathcal{M}(h^{\mu\nu}) = \widetilde{\Box^{-1}_{\mathrm{ret}}}\left[\mathcal{M}(\Lambda^{\mu\nu})\right] + \sum_{\ell=0}^{\infty}\hat{\partial}_L\left(\frac{\mathcal{X}^{\mu\nu}_L(t-r/c)}{r}\right)\,, \tag{5.21}$$

where the functions $\mathcal{X}_L^{\mu\nu}$ come from the first post-Minkowskian solution as well as the different homogeneous solutions added throughout the MPM algorithm. These functions are not known yet and the goal of this section is to find an explicit formula for them.

The interior metric

Let us find an equation similar to (5.21) for the interior metric $h_{\text{int}}^{\mu\nu}$. First, we are going to do a post-Newtonian expansion of each quantity entering the integrated Einstein equations (5.2). Therefore, we expand $h^{\mu\nu}$ as

$$\overline{h}^{\mu\nu} = \sum_{n\geq 1} \frac{1}{c^{2n}} \overline{h}^{\mu\nu}_{\{n\}}(t, \boldsymbol{x}, \ln c)\,, \tag{5.22}$$

where the $\overline{h}^{\mu\nu}_{\{n\}}$ does not contain any factor c^n but may contain power of $\ln c$. Similarly, the pseudo energy-impulsion tensor can be expanded as

$$\overline{\tau}^{\mu\nu} = \sum_{n\geq -1} \frac{1}{c^{2n}} \overline{\tau}^{\mu\nu}_{\{n\}}(t, \boldsymbol{x}, \ln c)\,. \tag{5.23}$$

This expansion starts with a factor c^2. This is consistent with the overall factor $\frac{16\pi G}{c^4}$ in the equation (5.2). If we inject the post-Newtonian expansions (5.22)–(5.23) into the integrated Einstein equations (5.2), and equal each order of c we obtain for $n \geq 2$

$$\Delta \overline{h}^{\mu\nu}_{\{n\}} = 16\pi G \overline{\tau}^{\mu\nu}_{\{n-2\}} + \frac{\partial^2}{\partial t^2} \overline{h}^{\mu\nu}_{\{n-1\}}\,. \tag{5.24}$$

The set of equations (5.24) can be solved iteratively order by order in n. Assuming that the metric is known up to the $(n-1)^{\text{th}}$ post-Newtonian order (i.e. $\overline{h}^{\mu\nu}_{\{2\}}, \ldots, \overline{h}^{\mu\nu}_{\{n-1\}}$ are known), we can compute the right-hand side of equation (5.24) and find a particular solution $\overline{h}^{\mu\nu}_{\{n\},\text{part}}$ such that

$$\overline{h}^{\mu\nu}_{\{n\},\text{part}} = 16\pi G \widetilde{\Delta^{-1}} \left[\overline{\tau}^{\mu\nu}_{\{n-2\}}\right] + \frac{\partial^2}{\partial t^2} \widetilde{\Delta^{-1}} \left[\overline{h}^{\mu\nu}_{\{n-1\}}\right]\,. \tag{5.25}$$

We can add a homogeneous (with respect to the Δ operator) solution to $\overline{h}^{\mu\nu}_{\{n\},\text{part}}$ in order to obtain the most general solution of (5.24). As the post-Newtonian expansion of the metric is smooth everywhere, the most general homogeneous solution that we can add is of the form

$$\overline{h}^{\mu\nu}_{\{n\},\text{hom}} = \sum_{\ell\geq 0} B^{\mu\nu}_{L\{n\}}(t)\hat{x}_L\,, \tag{5.26}$$

where $B^{\mu\nu}_{L\{n\}}$ are unspecified functions of the variable t. Now, the n^{th} post-Newtonian order metric $\overline{h}^{\mu\nu}_{\{n\}}$ is defined as

$$\overline{h}^{\mu\nu}_{\{n\}} = \overline{h}^{\mu\nu}_{\{n\},\text{part}} + \overline{h}^{\mu\nu}_{\{n\},\text{hom}}\,. \tag{5.27}$$

Now, if we recursively substitute the value of $\overline{h}^{\mu\nu}_{\{n-1\}}$ in equation (5.25) by $\overline{h}^{\mu\nu}_{\{n-1\}} = \overline{h}^{\mu\nu}_{\{n-1\},\text{part}} + \overline{h}^{\mu\nu}_{\{n-1\},\text{hom}}$, and take into account that $\Delta\overline{h}^{\mu\nu}_{\{1\}} = 16\pi G\overline{\tau}^{\mu\nu}_{\{-1\}}$ (as $\overline{h}^{\mu\nu}_{\{0\}} = 0$), we can see that

$$\overline{h}^{\mu\nu}_{\{n\}} = 16\pi G \sum_{k=0}^{n-1} \frac{\partial^{2k}}{\partial t^{2k}} \widetilde{\Delta^{-k-1}} \left[\overline{\tau}^{\mu\nu}_{\{n-2-k\}}\right] + \sum_{\ell\geq 0}\sum_{k=0}^{n-1} B^{\mu\nu(2k)}_{L\{n-k\}} \widetilde{\Delta^{-k}} \left[\hat{x}_L\right]\,. \tag{5.28}$$

If we sum (5.28) for all $n \geq 2$ and divide each term by c^{2n}, the first term of the right hand side becomes

$$\sum_{k\geq 0} \frac{\partial^{2k}}{c^{2k}\partial t^{2k}} \widetilde{\Delta^{-k-1}} \left[\overline{\tau}^{\mu\nu}\right] = \widetilde{I}^{-1} \left[\overline{\tau}^{\mu\nu}\right] . \tag{5.29}$$

Therefore, the general solution of the post-Newtonian metric can be written as a particular solution that is built with the propagator $\widetilde{I^{-1}}$ and a homogeneous solution which is regular at $r = 0$ and can be parametrized by a set of functions that we will call $\mathcal{A}_L^{\mu\nu}$ (cf [151] for a formal proof, and for the relation between $\mathcal{A}_L^{\mu\nu}$ and $\mathcal{B}_{L(n)}^{\mu\nu}$)

$$h_{\text{int}}^{\mu\nu} \equiv \bar{h}^{\mu\nu} = \frac{16\pi G}{c^4} \widetilde{I^{-1}} \left[\overline{\tau}^{\mu\nu}\right] + \sum_{\ell=0}^{\infty} \hat{\partial}_L \left(\overline{\frac{\mathcal{A}_L^{\mu\nu}(t-r/c) - \mathcal{A}_L^{\mu\nu}(t+r/c)}{2r}} \right) . \tag{5.30}$$

The equation (5.30) is analogous to equation (5.21), and the functions $\mathcal{A}_L^{\mu\nu}$ are unspecified at that point, and will be determined thanks to the matching equation. We recall that the bar on top of an expression means that this expression is expanded when $r/c \to 0$, for example

$$\overline{\frac{\mathcal{A}_L^{\mu\nu}(t-r/c) - \mathcal{A}_L^{\mu\nu}(t+r/c)}{2r}} = \sum_{i=\ell}^{\infty} \frac{\hat{\partial}_L(r^{2i})}{(2i+1)!} \frac{\mathcal{A}_L^{\mu\nu(2i+1)}}{c^{2i+1}} . \tag{5.31}$$

5.3.1 Two useful lemmas

In order to fully determine the interior and the exterior metrics, we need to determine explicitly the values of the functions $\mathcal{A}_L^{\mu\nu}$, and $\mathcal{X}_L^{\mu\nu}$ parametrizing the homogeneous parts of the metrics. This will be done by using the two following lemmas that are at the core of the matching procedure

Lemma 1 [150, 152, 153, 151]

$$\overline{\widetilde{\Box_{\text{ret}}^{-1}} \left[\mathcal{M}(\Lambda^{\mu\nu})\right]} = \widetilde{I^{-1}} \left[\overline{\mathcal{M}(\Lambda^{\mu\nu})}\right] - \frac{4G}{c^4} \sum_{\ell\geq 0} \frac{(-1)^\ell}{\ell!} \hat{\partial}_L \left(\overline{\frac{\mathcal{R}_L^{\mu\nu}(t-r/c) - \mathcal{R}_L^{\mu\nu}(t+r/c)}{2r}} \right) , \tag{5.32}$$

with

$$\mathcal{R}_L^{\mu\nu} = \underset{B}{\text{FP}} \int \mathrm{d}^3\boldsymbol{x} \left(\frac{|\boldsymbol{x}|}{r_0}\right)^B \hat{x}_L \int_1^\infty \gamma_\ell(z) \mathcal{M}(\tau^{\mu\nu})(t - z\boldsymbol{x}/c, \boldsymbol{x}) , \tag{5.33}$$

where $\gamma_\ell(z) = (-1)^{\ell+1} \frac{(2\ell+1)!!}{2^\ell \ell!} (z^2-1)^\ell$.

Lemma 2 [151]

$$\mathcal{M}\left[\widetilde{I^{-1}}(\overline{\tau^{\mu\nu}})\right] = \widetilde{I^{-1}} \left[\mathcal{M}(\overline{\tau^{\mu\nu}})\right] - \frac{1}{4\pi} \sum_{\ell\geq 0} \frac{(-1)^\ell}{\ell!} \left(\frac{\mathcal{F}_L^{\mu\nu}(t-r/c) + \mathcal{F}_L^{\mu\nu}(t+r/c)}{2r} \right) , \tag{5.34}$$

with

$$\mathcal{F}_L^{\mu\nu} = \underset{B}{\text{FP}} \int \mathrm{d}^3\boldsymbol{x} \left(\frac{|\boldsymbol{x}|}{r_0}\right)^B \hat{x}_L \int_{-1}^1 \mathrm{d}z \delta_\ell(z) \overline{\tau}^{\mu\nu}(t - z\boldsymbol{x}/c, \boldsymbol{x}) , \tag{5.35}$$

where $\delta_\ell(z) = \frac{(2\ell+1)!!}{2^{(\ell+1)}\ell!} (1-z^2)^\ell$.

Note that $\gamma_\ell(z) = -2\delta_\ell(z)$. These two notations are motivated by the fact that $\int_1^\infty \mathrm{d}z \gamma_\ell(z) = \int_{-1}^1 \mathrm{d}z \delta_\ell(z) = 1$ (the latter equality is only true by analytical continuation in ℓ).

These two technical lemmas are proven in the appendices of [151], using the properties of the operators $\widetilde{\Box^{-1}_{\text{ret}}}$ and $\widetilde{I^{-1}}$ as well as the mathematical structure of the multipolar and post-Newtonian expansions of the field $h^{\mu\nu}$ together with mathematical properties of the Finite Part regularization. We can see that they express somehow the commutators between the operators $\widetilde{I^{-1}}$ (and $\widetilde{\Box^{-1}_{\text{ret}}}$) with the multipolar and the post-Newtonian expansions of the metric. These commutators are then expressed with the functions $\mathcal{R}_L^{\mu\nu}$ and $\mathcal{F}_L^{\mu\nu}$ which are integrals of respectively the multipolar and the post-Newtonian expansions of the energy-impulsion pseudo-tensor $\tau^{\mu\nu}$.

5.3.2 The matching equation and its consequences

5.3.2.a) The main result

We are now able to fully exploit the matching equation. We recall that this equation reads

$$\overline{\mathcal{M}(h^{\mu\nu})} = \mathcal{M}(\overline{h^{\mu\nu}}) \,. \tag{5.36}$$

Injecting (5.21) and (5.30) into (5.36), we obtain that

$$\begin{aligned} &\overline{\widetilde{\Box^{-1}}_{\text{ret}} \left[\mathcal{M}(\Lambda^{\mu\nu})\right]} + \overline{\sum_{\ell=0}^{\infty} \hat{\partial}_L \left(\frac{\mathcal{X}_L^{\mu\nu}(t-r/c)}{r}\right)} \\ &= \frac{16\pi G}{c^4}\mathcal{M}\left(\widetilde{I^{-1}}\left[\bar{\tau}^{\mu\nu}\right]\right) + \sum_{\ell=0}^{\infty} \hat{\partial}_L \left(\frac{\mathcal{A}_L^{\mu\nu}(t-r/c) - \mathcal{A}_L^{\mu\nu}(t+r/c)}{2r}\right) . \end{aligned} \tag{5.37}$$

Now if we inject (5.32) and (5.34) into (5.37), and simplify the result using the relation (5.8) we obtain

$$\begin{aligned} &-\frac{4G}{c^4}\sum_{\ell\geq 0}\frac{(-1)^\ell}{\ell!}\hat{\partial}_L\left(\frac{\mathcal{R}_L^{\mu\nu}(t-r/c) - \mathcal{R}_L^{\mu\nu}(t+r/c)}{2r}\right) + \sum_{\ell=0}^{\infty}\hat{\partial}_L\left(\frac{\mathcal{X}_L^{\mu\nu}(t-r/c)}{r}\right) \\ &= -\frac{4G}{c^4}\sum_{\ell\geq 0}\frac{(-1)^\ell}{\ell!}\left(\frac{\mathcal{F}_L^{\mu\nu}(t-r/c) + \mathcal{F}_L^{\mu\nu}(t+r/c)}{2r}\right) \\ &\quad + \sum_{\ell=0}^{\infty}\hat{\partial}_L\left(\frac{\mathcal{A}_L^{\mu\nu}(t-r/c) - \mathcal{A}_L^{\mu\nu}(t+r/c)}{2r}\right) . \end{aligned} \tag{5.38}$$

Therefore

$$\mathcal{A}_L^{\mu\nu} = -\frac{4G}{c^4}\frac{(-1)^\ell}{\ell!}\left[\mathcal{F}_L^{\mu\nu} + \mathcal{R}_L^{\mu\nu}\right] , \tag{5.39a}$$

$$\mathcal{X}_L^{\mu\nu} = -\frac{4G}{c^4}\frac{(-1)^\ell}{\ell!}\mathcal{F}_L^{\mu\nu} . \tag{5.39b}$$

This enables us to provide the final result of this section, that corresponds to the full expression of the interior and exterior metrics, taking into account the matching equation.

Theorem The exterior metric $h^{\mu\nu}_{\text{ext}}$ and the interior metric $h^{\mu\nu}_{\text{int}}$ are given by

$$h^{\mu\nu}_{\text{ext}} \equiv \mathcal{M}(h^{\mu\nu}) = \widetilde{\Box^{-1}_{\text{ret}}}\left[\mathcal{M}(\Lambda^{\mu\nu})\right] - \frac{4G}{c^4}\sum_{\ell=0}^{\infty}\hat{\partial}_L\left(\frac{\mathcal{F}^{\mu\nu}_L(t-r/c)}{r}\right), \tag{5.40}$$

$$\begin{aligned} h^{\mu\nu}_{\text{int}} \equiv \bar{h}^{\mu\nu} = \widetilde{I^{-1}}\left[\bar{\tau}^{\mu\nu}\right] &- \frac{4G}{c^4}\sum_{\ell=0}^{\infty}\hat{\partial}_L\left(\frac{\mathcal{F}^{\mu\nu}_L(t-r/c)-\mathcal{F}^{\mu\nu}_L(t+r/c)}{2r}\right)\\ &- \frac{4G}{c^4}\sum_{\ell=0}^{\infty}\hat{\partial}_L\left(\frac{\mathcal{R}^{\mu\nu}_L(t-r/c)-\mathcal{R}^{\mu\nu}_L(t+r/c)}{2r}\right), \end{aligned} \tag{5.41}$$

with $\mathcal{R}^{\mu\nu}_L$ and $\mathcal{F}^{\mu\nu}_L$ given by the equations (5.33) and (5.35).

5.3.2.b) Interpretation

The second term of the right-hand side of (5.40) will lead to explicit formulae to compute the source multipole moments $\{I_L, J_L, W_L, X_L, Y_L, Z_L\}$ used in the previous chapter 4. We detail this in section 5.4.

Regarding the interior metric, we see that it is constructed using the instantaneous propagator $\widetilde{I^{-1}}$ together with two homogeneous terms depending on $\mathcal{F}^{\mu\nu}_L$ and $\mathcal{R}^{\mu\nu}_L$. These two terms are associated with the radiation reactions. In particular, $\mathcal{F}^{\mu\nu}_L$ corresponds to the dissipative radiative effects due to the emission of gravitational waves. This term starts at 2.5PN (and then contributes at 3.5PN, 4.5PN etc.) in the equations of motion. The second term including the functions $\mathcal{R}^{\mu\nu}_L$ depends on the multipole expansion of the field, and therefore is related to the exterior field. In fact, this term corresponds to the effect of the non-local *tails* being back-scattered into the source. This effect appears at 4PN and will have to be taken into account in the conservative part of the equations of motion at 4PN (cf section 6.1.5).

It can be shown (cf [151]) that the radiation reactions terms $\mathcal{F}^{\mu\nu}_L$ can be directly computed if we use the retarded propagator $\widetilde{\Box^{-1}_{\text{ret}}}$ (as defined in equation the (5.12)) instead of the instantaneous one $\widetilde{I^{-1}}$:

$$h^{\mu\nu}_{\text{int}} \equiv \bar{h}^{\mu\nu} = \widetilde{\Box^{-1}_{\text{ret}}}\left[\bar{\tau}\right] - \frac{4G}{c^4}\sum_{\ell=0}^{\infty}\hat{\partial}_L\left(\frac{\mathcal{R}^{\mu\nu}_L(t-r/c)-\mathcal{R}^{\mu\nu}_L(t+r/c)}{2r}\right). \tag{5.42}$$

In practice, the first term of equation (5.42) is computed through the potentials (such as V, V_i, W_{ij} etc.) that we will later introduce to parametrize the PN metric (cf equations (6.13) and (6.14)), while the second term has to be computed separately as done in section 6.1.5.

5.4 Explicit expressions of the source moment multipoles

In this section, we show how the matching equation (5.40) lead to explicit formulae for the multipole source moments $\{I_L, J_L, W_L, X_L, Y_L, Z_L\}$. The following proof is done in full detail in [153], and we just show the main steps here in order to provide a general understanding of the derivation of that result. Let us call $u^{\mu\nu}$ the first term of (5.40)

$$u^{\mu\nu} \equiv \Box^{-1}_{\text{ret}}\widetilde{\left[\mathcal{M}(\Lambda^{\mu\nu})\right]}. \tag{5.43}$$

As $h^{\mu\nu}$ is divergenceless, so is $\mathcal{M}(h^{\mu\nu})$ and therefore

$$\partial_\nu u^{\mu\nu} = \frac{4G}{c^4}\partial_\nu \left[\sum_{\ell=0}^{\infty} \hat{\partial}_L \left(\frac{\mathcal{F}_L^{\mu\nu}(t-r/c)}{r}\right)\right], \tag{5.44}$$

with $\mathcal{F}_L^{\mu\nu}$ given by equation (5.35). Using the properties of the Finite Part regularization together with (5.35), one can show that (5.44) leads to [153]

$$\partial_\nu u^{\mu\nu} = \frac{4G}{c^4}\partial_\nu \left[\sum_{\ell=0}^{\infty} \hat{\partial}_L \left(\frac{\mathcal{G}_L^{\mu\nu}(t-r/c)}{r}\right)\right], \tag{5.45}$$

with

$$\mathcal{G}_L^{\mu}(u) = \underset{B}{\mathrm{FP}} \int \mathrm{d}^3\boldsymbol{x} B \left(\frac{|\boldsymbol{x}|}{r_0}\right)^B |\boldsymbol{x}|^{-2} x_i \hat{x}_L \int_{-1}^{+1} \mathrm{d}x \delta_l(z) \overline{\tau}^{\mu i}(\boldsymbol{x}, u + z|\boldsymbol{x}|/c)\,. \tag{5.46}$$

Now that the divergence of $u^{\mu\nu}$ has been decomposed multipolarly using the functions $\mathcal{G}_L^{\mu}$ we can use the trick done in equation (4.26) to build a homogeneous solution (for the d'Alembert operator) that kills the divergence of $u^{\mu\nu}$. Therefore we define $v^{\mu\nu}$ such that $\Box v^{\mu\nu} = 0$ and $\partial_\mu v^{\mu\nu} = -\partial_\mu u^{\mu\nu}$ [153]:

$$v^{00} = \frac{4G}{c^4}\left\{-\frac{c}{r}\mathcal{G}^{0(-1)} + \partial_a\left(\frac{1}{r}\left[c\mathcal{G}_a^{0(-1)} + c^2\mathcal{G}^{a(-2)} - \mathcal{G}_{ab}^{b}\right]\right)\right\}, \tag{5.47a}$$

$$\begin{aligned} v^{0i} = \frac{4G}{c^4}\Bigg\{&-\frac{1}{r}\left[c\mathcal{G}^{i(-1)} - \frac{1}{c}\mathcal{G}_{ai}^{a(1)}\right] + \frac{c}{2}\partial_a\left(\frac{1}{r}\left[\mathcal{G}_a^{i(-1)} - \mathcal{G}_i^{a(-1)}\right]\right) \\ &- \sum_{\ell\geq 2}\frac{(-1)^\ell}{\ell!}\partial_{L-1}\left(\frac{1}{r}\mathcal{G}_{iL-1}^{0}\right)\Bigg\}, \end{aligned} \tag{5.47b}$$

$$\begin{aligned} v^{ij} = \frac{4G}{c^4}\Bigg\{&\frac{1}{r}\mathcal{G}^{(i}{}_{j)} + 2\sum_{\ell\geq 3}\frac{(-1)^\ell}{\ell!}\partial_{L-3}\left(\frac{1}{rc^2}\mathcal{G}_{ijaL-3}^{a(2)}\right) \\ &+ \sum_{\ell\geq 2}\frac{(-1)^\ell}{\ell!}\Bigg[\partial_{L-2}\left(\frac{1}{rc}\mathcal{G}_{ijL-2}^{0(1)}\right) + \partial_{aL-2}\left(\frac{1}{r}\mathcal{G}_{ijL-2}^{a}\right) + 2\delta_{ij}\partial_{L-1}\left(\frac{1}{r}\mathcal{G}_{aL-1}^{a}\right) \\ &-4\partial_{L-2(i}\left(\frac{1}{r}\mathcal{G}_{j)aL-2}^{a}\right) - 2\partial_{L-1}\left(\frac{1}{r}\mathcal{G}^{(i}{}_{j)L-1}\right)\Bigg]\Bigg\}. \end{aligned} \tag{5.47c}$$

Now if we define

$$G h_{\text{part},1}^{\mu\nu} \equiv -\frac{4G}{c^4}\sum_{\ell=0}^{\infty}\hat{\partial}_L\left(\frac{\mathcal{F}_L^{\mu\nu}(t-r/c)}{r}\right) - v^{\mu\nu}, \tag{5.48}$$

then we have

$$\Box h_{\text{part},1}^{\mu\nu} = 0\,, \tag{5.49a}$$

$$\partial_\mu h_{\text{part},1}^{\mu\nu} = 0\,, \tag{5.49b}$$

which means that $h_{\text{part},1}^{\mu\nu}$ can be decomposed with a set of unspecified functions $\{\tilde{I}_L, \tilde{J}_L, \tilde{W}_L, \tilde{X}_L, \tilde{Y}_L, \tilde{Z}_L\}$ in a similar way than what is done in equation (4.11). Now, it can be shown that if we start our MPM algorithm with $h_{\text{part},1}^{\mu\nu}$, then we obtain exactly the same result than the general MPM solution described in section 4.1.3. Said differently: $\{\tilde{I}_L, \tilde{J}_L, \tilde{W}_L, \tilde{X}_L, \tilde{Y}_L, \tilde{Z}_L\} = \{I_L, J_L, W_L, X_L, Y_L, Z_L\}$. By injecting (5.46) into (5.47) and then (5.47) into (5.48), we can obtain an explicit expression for $h_{\text{part},1}$. By decomposing this explicit expression into the set of multipoles $\{I_L, J_L, W_L, X_L, Y_L, Z_L\}$ (this requires several algebra steps detailed in [153]), we obtain the following expressions

$$\begin{aligned}\mathrm{I}_L(u) = \underset{B}{\mathrm{FP}} \int \mathrm{d}^3\boldsymbol{x} \left(\frac{|\boldsymbol{x}|}{r_0}\right)^B \int_{-1}^{1} \mathrm{d}z \Big\{ \delta_\ell \hat{x}_L \Sigma - \frac{4(2\ell+1)}{c^2(\ell+1)(2\ell+3)} \delta_{\ell+1} \hat{x}_{iL} \Sigma_i^{(1)} \\ + \frac{2(2\ell+1)}{c^4(\ell+1)(\ell+2)(2\ell+5)} \delta_{\ell+2} \hat{x}_{ijL} \Sigma_{ij}^{(2)} \Big\}, \end{aligned} \tag{5.50a}$$

$$\mathrm{J}_L(u) = \underset{B}{\mathrm{FP}} \int \mathrm{d}^3\boldsymbol{x} \left(\frac{|\boldsymbol{x}|}{r_0}\right)^B \int_{-1}^{1} \mathrm{d}z\, \epsilon_{ab\langle i_\ell} \Big\{ \delta_\ell \hat{x}_{L-1\rangle a} \Sigma_b - \frac{2\ell+1}{c^2(\ell+2)(2\ell+3)} \delta_{\ell+1} \hat{x}_{L-1\rangle ac} \Sigma_{bc}^{(1)} \Big\}, \tag{5.50b}$$

$$\begin{aligned}\mathrm{W}_L(u) = \underset{B}{\mathrm{FP}} \int \mathrm{d}^3\boldsymbol{x} \left(\frac{|\boldsymbol{x}|}{r_0}\right)^B \int_{-1}^{1} \mathrm{d}z \Big\{ \frac{2\ell+1}{(\ell+1)(2\ell+3)} \delta_{\ell+1} \hat{x}_{iL} \Sigma_i \\ - \frac{2\ell+1}{2c^2(\ell+1)(\ell+2)(2\ell+5)} \delta_{\ell+2} \hat{x}_{ijL} \Sigma_{ij}^{(1)} \Big\}, \end{aligned} \tag{5.50c}$$

$$\mathrm{X}_L(u) = \underset{B}{\mathrm{FP}} \int \mathrm{d}^3\boldsymbol{x} \left(\frac{|\boldsymbol{x}|}{r_0}\right)^B \int_{-1}^{1} \mathrm{d}z \Big\{ \frac{2\ell+1}{2(\ell+1)(\ell+2)(2\ell+5)} \delta_{\ell+2} \hat{x}_{ijL} \Sigma_{ij} \Big\}, \tag{5.50d}$$

$$\begin{aligned}\mathrm{Y}_L(u) = \underset{B}{\mathrm{FP}} \int \mathrm{d}^3\boldsymbol{x} \left(\frac{|\boldsymbol{x}|}{r_0}\right)^B \int_{-1}^{1} \mathrm{d}z \Big\{ -\delta_\ell \hat{x}_L \Sigma_{ii} + \frac{3(2\ell+1)}{(\ell+1)(2\ell+3)} \delta_{\ell+1} \hat{x}_{iL} \Sigma_i^{(1)} \\ - \frac{2(2\ell+1)}{c^2(\ell+1)(\ell+2)(2\ell+5)} \delta_{\ell+2} \hat{x}_{ijL} \Sigma_{ij}^{(2)} \Big\}, \end{aligned} \tag{5.50e}$$

$$\mathrm{Z}_L(u) = \underset{B}{\mathrm{FP}} \int \mathrm{d}^3\boldsymbol{x} \left(\frac{|\boldsymbol{x}|}{r_0}\right)^B \int_{-1}^{1} \mathrm{d}z\, \epsilon_{ab\langle i_\ell} \Big\{ - \frac{2\ell+1}{(\ell+2)(2\ell+3)} \delta_{\ell+1} \hat{x}_{L-1\rangle bc} \Sigma_{ac} \Big\}, \tag{5.50f}$$

where

$$\Sigma = \frac{\overline{\tau}^{00} + \overline{\tau}^{ii}}{c^2}, \tag{5.51a}$$

$$\Sigma_i = \frac{\overline{\tau}^{0i}}{c}, \tag{5.51b}$$

$$\Sigma_{ij} = \overline{\tau}^{ij}, \tag{5.51c}$$

and where we recall that $\delta_\ell(z) = \frac{(2\ell+1)!!}{2^(\ell+1)\ell!}(1-z^2)^\ell$. The functions Σ, Σ_i and Σ_{ij} are to be evaluated at the spatial point $\boldsymbol{x}$ and at time $u + zr/c$ (as done in (5.46) for $\overline{\tau}^{\mu i}$).

6 – Ambiguity-free equations of motion at the 4PN order

The goal of this chapter is to obtain the conservative part of the 4PN dynamics for spinless compact binary systems using a Fokker Lagrangian, in harmonic coordinates. This chapter is divided in two parts.

1. The section 6.1 explains the method used by Bernard, Blanchet, Bohé, Faye and Marsat, that provided a first result in 2016 [92] parametrized by an *ambiguity* parameter α, that was adjusted in order to agree with the conserved energy of circular orbit computing by self-force in the small mass ratio limit. As we are going to explain in section 6.1.5, the origin of this ambiguity came from the normalization of the logarithm parametrizing the *tails* effect contributing in the conservative dynamics at the 4PN order. This result however, was not in agreement with the computation done by Damour-Jaranowski-Schäfer [90], which also contained a similar ambiguity parameter C that was adjusted using the conserved energy of circular orbit in the small mass ratio limit. Besides, this result does not agree with the periastron advance predicted by self-force in the limit of circular orbit, and for small mass ratio [94], while the result from Damour-Jaranowski-Schäfer [90] is in perfect agreement.

   However, it has been shown [93, 154] that the discrepancy between these two results can be parametrized by only two coefficients δ_1 and δ_2 (depending on the value of α), and that this discrepancy was probably due to the choice of the regularization for the IR divergences.

2. In the section 6.2 — based on [93, 94, 2]— we see how the systematic use of dimensional regularization cures that discrepancy. In 6.2.1, we first tackle the difference between the Finite Part regularization and dimensional regularization to cure the IR divergences of the instantaneous terms. Then in 6.2.2, we compute the effect of the tails in the conservative part of the dynamics, in dimensional regularization. Adding all these contributions [94, 2], we obtain from *first principles* the 4PN dynamics —i.e. without fitting some coefficients to results coming from other frameworks.

The particular contribution of this thesis to the results derived in this chapter corresponds to the computation in d dimensions of the *tails* presented in the section 6.2.2 determining the last ambiguity.

6.1 Presentation of the Fokker Lagrangian method

6.1.1 The method

In this section, we are going to construct a *generalized Lagrangian* L that depends on the positions $\boldsymbol{y}_A(t)$ and the velocities $\boldsymbol{v}_A(t)$ of the two bodies ($A = 1$ or $A = 2$) as well as on the accelerations and higher derivatives of the accelerations ($\boldsymbol{a}_A(t)$, $\boldsymbol{b}_A(t) \equiv \frac{\mathrm{d}\boldsymbol{a}_A}{\mathrm{d}t}$, ...), yielding to an action $S = \int \mathrm{d}t L$ such that the generalized Euler-Lagrange equations of motion

$$\frac{\delta S}{\delta \boldsymbol{y}_A} = 0 \Leftrightarrow \frac{\partial L}{\partial \boldsymbol{y}_A} - \frac{\mathrm{d}}{\mathrm{d}t}\left(\frac{\partial L}{\partial \boldsymbol{v}_A}\right) + \frac{\mathrm{d}^2}{\mathrm{d}t^2}\left(\frac{\partial L}{\partial \boldsymbol{a}_A}\right) - \frac{\mathrm{d}^3}{\mathrm{d}t^3}\left(\frac{\partial L}{\partial \boldsymbol{b}_A}\right) + \cdots = 0\,, \tag{6.1}$$

correspond to the conservative equations of motion at the 4^{th} post-Newtonian order. The equation (6.1) will not contain any dissipative terms, because it comes from a Lagrangian method. Such terms (appearing at 2.5PN, 3.5PN and for non-local terms at 4PN) will have to be added by hand to the final equations of motion.

To obtain such a result, L. Bernard, L. Blanchet, A. Bohé, G. Faye and S. Marsat used a Fokker Lagrangian method [92] that we are going to present.

To do so, we consider the following action

$$S = S_g + S_m\,, \tag{6.2}$$

where S_g is the Landau-Lifshitz form of the Einstein-Hilbert action containing a gauge-fixing term

$$S_g = \frac{c^3}{16\pi G}\int \mathrm{d}^4x\,\sqrt{-g}\left[g^{\mu\nu}\left(\Gamma^\rho_{\mu\lambda}\Gamma^\lambda_{\nu\rho} - \Gamma^\rho_{\mu\nu}\Gamma^\lambda_{\rho\lambda}\right) - \frac{1}{2}g_{\mu\nu}\Gamma^\mu\Gamma^\nu\right]. \tag{6.3}$$

Here, $\Gamma^\mu \equiv g^{\alpha\beta}\Gamma^\mu_{\alpha\beta}$ and $-\frac{1}{2}g_{\mu\nu}\Gamma^\mu\Gamma^\nu$ is a gauge-fixing term in order to place ourself in harmonic coordinates. S_m is the usual matter action for 2 point-particles ($A \in \{1, 2\}$)

$$S_m = -\sum_A m_A c^2 \int \mathrm{d}t\sqrt{-(g_{\mu\nu})_A\, v^\mu_A v^\nu_A/c^2}\,, \tag{6.4}$$

where $v^\mu_A = (c, \boldsymbol{v}_A)$ and $y^\mu_A = (ct, \boldsymbol{y}_A)$ and where $(g_{\mu\nu})_A$ means that the metric is evaluated at the location of the particle A (which will required a UV regularization technique as described in 6.1.2). As we can see in the equation (6.3), the gravitational part of the action is of the form

$$S_g = \int \mathrm{d}t L_g = \int \mathrm{d}t\mathrm{d}^3\boldsymbol{x}\mathcal{L}_g\,, \tag{6.5}$$

where $\mathcal{L}_g$ is called a *Lagrangian density.*

As done in chapter 4, we define $h^{\mu\nu}$ to be the deviation of the gothic metric to Minkowski

$$h^{\mu\nu} \equiv \sqrt{-g}g^{\mu\nu} - \eta^{\mu\nu}\,. \tag{6.6}$$

Then the generalized Euler-Lagrange equations of (6.3)–(6.4) (i.e. $\delta S = 0$) yield

$$\Box h^{\alpha\beta} = \frac{16\pi G}{c^4}\tau^{\alpha\beta}\,, \tag{6.7a}$$

$$\partial_\mu h^{\mu\nu} = 0\,. \tag{6.7b}$$

where $\Box = -\frac{1}{c^2}\frac{\partial^2}{\partial t^2} + \delta^{ij}\frac{\partial}{\partial x^i}\frac{\partial}{\partial x^j}$ is the flat d'Alembertian operator, and $\tau^{\alpha\beta}$ is the stress-energy pseudo tensor

$$\tau^{\alpha\beta} = |g|T^{\alpha\beta} + \frac{c^4}{16\pi G}\Lambda^{\alpha\beta}(h^{\mu\nu})\,, \tag{6.8}$$

where

$$T^{\mu\nu} = \frac{2}{\sqrt{-g}}\frac{\delta S_m}{\delta g_{\mu\nu}}\,, \tag{6.9}$$

corresponds to the stress-energy tensor of the matter in the space-time and $\Lambda^{\alpha\beta}(h^{\mu\nu})$ corresponds to the non-linearities of the Einstein equations and describes the stress-energy contained in the gravitational field.

To define the Fokker Lagrangian, we first solve (6.7) in order to express the metric $h^{\alpha\beta}$ as a functional of the particle positions, velocities, accelerations and higher-derivatives of the accelerations

$$h^{\mu\nu} = h^{\mu\nu}(\boldsymbol{y}_A(t), \boldsymbol{v}_A(t), \boldsymbol{a}_A(t), \boldsymbol{b}_A(t), \dots)\,. \tag{6.10}$$

Once this is done, we can inject (6.10) into the gravitational and matter parts of the action (6.3)–(6.4) in order to obtain an action that depends only on the positions, velocities, accelerations (and higher time-derivatives of the accelerations) of the particles

$$\begin{aligned} S_{\mathrm{F}}\left[\boldsymbol{y}_B(t), \boldsymbol{v}_B(t), \cdots\right] &= \int \mathrm{d}t \int \mathrm{d}^3\boldsymbol{x}\, \mathcal{L}_g\left[\boldsymbol{x}; \boldsymbol{y}_B(t), \boldsymbol{v}_B(t), \cdots\right] \\ &\quad - \sum_A m_A c^2 \int \mathrm{d}t \sqrt{-g_{\mu\nu}\left(\boldsymbol{y}_A(t); \boldsymbol{y}_B(t), \boldsymbol{v}_B(t), \cdots\right) v_A^\mu v_A^\nu / c^2}\,. \end{aligned} \tag{6.11}$$

Then, the Euler-Lagrange equations of (6.11) provide the expected equations of motion.

6.1.1.a) The n+2 method

As we want to obtain the post-Newtonian expansion of the equations of motion, we are going to inject into the Fokker Lagrangian a post-Newtonian expansion of a solution of the metric (6.10). Before doing so, we should ask ourself whether this approach is legitimate, and at which post-Newtonian order we should compute the metric (6.10) in order to obtain the equations of motion at the 4^{th} post-Newtonian order. Both of these questions are answered in details in [92].

Indeed, as discussed in [92], we are allowed to inject a post-Newtonian solution of the metric $\overline{h}^{\mu\nu}$ in order to obtain the Fokker Lagrangian. By doing so, we get a post-Newtonian expansion of the Lagrangian density, which we have to integrate over the whole space. This leads to infra-red divergences that will have to be cured by a regularization scheme (cf section 6.1.4). This procedure yields the correct equations of motion as long as we stay under the 5.5 post-Newtonian order.

Now, let us assume we want to compute the equations of motion at the n^{th} post-Newtonian order (with $n < 5.5$), at which post-Newtonian order should we compute the metric $\overline{h}^{\alpha\beta}$ that we inject in equations (6.3)–(6.4)? The post-Newtonian metric is composed of local terms that can be derived directly by solving the Einstein equations (6.7), and a non-local term called a *tail term* which is computed by using the matching equation. This tail term will be computed in details in section 6.1.5, and we will focus in this section on the instantaneous terms only. To state at which PN order we need to compute the instantaneous part of the metric, it is convenient to define $\overline{h}^{00ii} \equiv \overline{h}^{00} + \overline{h}^{ii}$. As shown in [92], thanks to non-trivial cancellations between the gravitational part and the matter part of the action, in order to obtain the equations of motion at nPN, we have to inject the metric in the Fokker Lagrangian at

$$\overline{h} = (\overline{h}^{00ii}, \overline{h}^{0i}, \overline{h}^{ij}) \;\; \text{up to order} \;\; \begin{cases} (1/c^{n+2}, 1/c^{n+1}, 1/c^{n+2}) & \text{when } n \text{ is even}\,, \\ (1/c^{n+1}, 1/c^{n+2}, 1/c^{n+1}) & \text{when } n \text{ is odd}\,. \end{cases} \tag{6.12}$$

For $n = 4$, such a metric can be parametrized at this order by a set of potentials:

$$\overline{h}^{00ii} = -\frac{4}{c^2}V - \frac{8}{c^4}V^2 - \frac{8}{c^6}\left[2\hat{X} + V\hat{W} + \frac{4}{3}V^3\right] + \mathcal{O}\left(\frac{1}{c^8}\right)\,, \tag{6.13a}$$

$$\overline{h}^{0i} = -\frac{4}{c^3}V_i - \frac{4}{c^5}\left(2\hat{R}_i + 3VV_i\right) + \mathcal{O}\left(\frac{1}{c^7}\right)\,, \tag{6.13b}$$

$$\overline{h}^{ij} = -\frac{4}{c^4}\left(\hat{W}_{ij} - \frac{1}{2}\delta_{ij}\hat{W}\right) - \frac{16}{c^6}\left(\hat{Z}_{ij} - \frac{1}{2}\delta_{ij}\hat{Z}\right) + \mathcal{O}\left(\frac{1}{c^8}\right)\,. \tag{6.13c}$$

Where $\hat{W} \equiv \hat{W}_{ii}$ and $\hat{Z} \equiv \hat{Z}_{ii}$, and where the potentials V, $\hat{X}$, V_i, $\hat{R}_i$, $\hat{W}_{ij}$, and $\hat{Z}_{ij}$ are defined by

$$\Box V = -4\pi G\,\sigma\,, \tag{6.14a}$$

$$\Box\hat{X} = -4\pi G V\sigma_{ii} + \hat{W}_{ij}\,\partial^2_{ij}V + 2V_i\,\partial_t\partial_i V + V\partial_t^2 V + \frac{3}{2}\,(\partial_t V)^2 - 2\partial_i V_j\,\partial_j V_i\,, \tag{6.14b}$$

$$\Box V_i = -4\pi G\,\sigma_i\,, \tag{6.14c}$$

$$\Box\hat{R}_i = -4\pi G\left[V\sigma_i - V_i\,\sigma\right] - 2\,\partial_k V\partial_i V_k - \frac{3}{2}\,\partial_t V\partial_i V\,, \tag{6.14d}$$

$$\Box\hat{W}_{ij} = -4\pi G\left(\sigma_{ij} - \delta_{ij}\,\sigma_{kk}\right) - \partial_i V\partial_j V\,, \tag{6.14e}$$

$$\begin{aligned}\Box\hat{Z}_{ij} = &-4\pi G\,V\left(\sigma_{ij} - \delta_{ij}\,\sigma_{kk}\right) - 2\,\partial_t V_{(i}\,\partial_{j)}V + \partial_i V_k\,\partial_j V_k + \partial_k V_i\,\partial_k V_j \\ &- 2\partial_k V_{(i}\,\partial_{j)}V_k - \delta_{ij}\,\partial_k V_m\,(\partial_k V_m - \partial_m V_k) - \frac{3}{4}\,\delta_{ij}\,(\partial_t V)^2\,.\end{aligned} \tag{6.14f}$$

where

$$\sigma \equiv \frac{T^{00} + T^{ii}}{c^2},\;\; \sigma_i \equiv \frac{T^{0i}}{c},\;\; \sigma_{ij} \equiv T^{ij}\,. \tag{6.15}$$

As we are not allowed to replace the accelerations by their values in the Fokker Lagrangian, the computations of the potentials V, $\hat{X}$, V_i, $\hat{R}_i$, $\hat{W}_{ij}$, and $\hat{Z}_{ij}$ should be done without replacing the value of the accelerations. This will not be the case for the potentials used in the chapter 8, where we will automatically replace the accelerations by their explicit values.

6.1.1.b) Summary

Let us summarize the different steps required in order to obtain a Lagrangian giving the equations of motion at the 4$^{\text{th}}$ post-Newtonian order:

1. Compute the instantaneous metric at the $\overline{h} = (\overline{h}^{00ii}, \overline{h}^{0i}, \overline{h}^{ij}) = (1/c^6, 1/c^5, 1/c^6)$ order by computing the different potentials V, V_i etc. This metric is parametrized by the trajectory of the particles $(\boldsymbol{y}_A(t), \boldsymbol{v}_A(t), \boldsymbol{a}_A(t), \boldsymbol{b}_A(t), \dots)$. The chapter 8 will provide more details on how these potentials are computed. Let us just point out here that these potentials were already known at the required PN order.

2. Inject the post-Newtonian metric into the gravitational and the matter parts of the action $S = S_g + S_m$ defined in equation (6.3)–(6.4).

3. Integrate over d^3x the Lagrangian density $\mathcal{L}$ obtained in order to get the Fokker Lagrangian L. This integration requires a regularization scheme for the ultra-violet divergences due to the point particle approximation (cf section 6.1.2) as well as another regularization scheme for the infra-red divergences due to the post-Newtonian expansion of the metric (cf section 6.1.4).

4. Compute separately the terms due to the non-local part of the metric (*tails*). This is done in section (6.1.5).

6.1.2 UV regularization using Hadamard partie finie regularization

6.1.2.a) Point particle approximation and UV divergences

The ultra-violet (UV) divergences that appear in this section are due to the *point-particle approximation* done in our formalism. In fact, the two compact objects are described by Dirac delta functions in the energy-impulsion tensor $T^{\mu\nu}$

$$T^{00} = \tilde{\mu}_1 \delta^{(3)}[\boldsymbol{x} - \boldsymbol{y}_1(t)] + \tilde{\mu}_2 \delta^{(3)}[\boldsymbol{x} - \boldsymbol{y}_2(t)]\,, \tag{6.16a}$$

$$T^{0i} = \mu_1 \delta^{(3)}[\boldsymbol{x} - \boldsymbol{y}_1(t)] v_1^i + \mu_2 \delta^{(3)}[\boldsymbol{x} - \boldsymbol{y}_2(t)] v_2^i\,, \tag{6.16b}$$

$$T^{ij} = \mu_1 \delta^{(3)}[\boldsymbol{x} - \boldsymbol{y}_1(t)] v_1^i v_1^j + \mu_2 \delta^{(3)}[\boldsymbol{x} - \boldsymbol{y}_2(t)] v_2^i v_2^j\,. \tag{6.16c}$$

where

$$\mu_A = m_A c \frac{1}{\sqrt{-(g_{\mu\nu})_A v_A^\mu v_A^\nu}} \frac{1}{\sqrt{-(g)_A}}\,, \tag{6.17}$$

$$\tilde{\mu}_A = \left(1 + \frac{v_{Ai} v_{Ai}}{c^2}\right) \mu_A\,, \tag{6.18}$$

where $v_A^\mu = (c, \boldsymbol{v}_A)$, where $(g_{\mu\nu})_A$ is the metric evaluated at the point A and where $(g)_A$ is the determinant of the metric at the point A. At the Newtonian order, we have $\mu_1 = \tilde{\mu}_1 = m_1$ and $\mu_2 = \tilde{\mu}_2 = m_2$. This point-particle energy-tensor impulsion generates divergences that would not appear if we modeled our compact bodies by extended spheres.

To get more insight on this UV divergence, let us consider the case of Newtonian gravity. In classical physics, the gravitational potential U_N created by two masses m_1 and m_2 with position $\boldsymbol{y}_1$ and $\boldsymbol{y}_2$ is given by

$$U_N(\boldsymbol{x}) = \frac{m_1}{|\boldsymbol{x} - \boldsymbol{y_1}|} + \frac{m_2}{|\boldsymbol{x} - \boldsymbol{y_2}|}\,, \tag{6.19}$$

and the acceleration of the particle 1 is given by

$$\boldsymbol{a}_1 = \left[\boldsymbol{\nabla} U_N\right]_{\boldsymbol{x}=\boldsymbol{y}_1} . \tag{6.20}$$

Injecting, (6.19) into (6.20), we see that the first term of (6.19) leads to a divergence due to the point-particle approximation. It is solved by saying that the particle 1 does not feel its own field (due to the action-reaction principle) so only the second term of (6.19) should be injected in (6.20). Said otherwise, if we have taken extended fluids balls to model our two bodies, because of the third law of Newton, the overall contribution of the potential generated by the first body on its own acceleration would exactly cancel out: *the body m_1 does not feel its own field* (cf for example the discussions made on that matter in the book [155]).

In general relativity, the non-linearities of the theory prevent us from such an interpretation. In fact, at the Newtonian order, the potential V is the same as the Newtonian gravitational potential U_N. However, as can be seen in equation (6.32), the metric will depends on higher power of V such as V^2. V^2 will contains different terms diverging at the point 1, and in particular crossed-term $\sim \frac{m_1 m_2}{|\boldsymbol{x}-\boldsymbol{y}_1||\boldsymbol{x}-\boldsymbol{y}_2|}$ that corresponds to the interaction between the fields generated by each bodies. It is therefore non-trivial to compute how such interaction terms affect the motion of the first body, and this is the reason why we need regularization techniques that will provide explicit formulae to deal with these divergences.

In the case of the Fokker Lagrangian, these divergences appear when we perform the spatial integration of the density Lagrangian in order to obtain the ordinary Fokker Lagrangian. I.e. the integral

$$L_F(t) = \int \mathrm{d}^3\boldsymbol{x} \mathcal{L}(t, \boldsymbol{x}) , \tag{6.21}$$

diverges when $\boldsymbol{x} \to \boldsymbol{y}_A$. Note that these divergences also appear in the matter part of the action since the matter part contains terms of the form $F(\boldsymbol{x})\delta^{(3)}(\boldsymbol{x} - \boldsymbol{y}_A)$, where $F(\boldsymbol{x})$ is divergent in $\boldsymbol{y}_A$.

6.1.2.b) Hadamard partie finie regularization

In this section, we present a first regularization technique, called the *Hadamard partie finie regularization*. Let us assume that we want to integrate the function $F(\boldsymbol{x})$ which is a smooth and well-defined function everywhere except at the positions of the two particles $\boldsymbol{y}_1$ and $\boldsymbol{y}_2$ where it may show poles, and let us compute

$$I = \mathrm{Pf} \int F(\boldsymbol{x}) \mathrm{d}^3\boldsymbol{x} , \tag{6.22}$$

where Pf denotes the Hadamard partie finie regularization that we are going to define. We start by defining the *partie finie* of the function F at the particle 1. For that, we first perform a Laurent-expansion of F around $\boldsymbol{x} = \boldsymbol{y}_1$. When $r_1 \to 0$, we have for all $N \in \mathbb{N}$

$$F(\boldsymbol{x}) = \sum_{p_0 \leq p \leq N} r_1^p \underset{1}{f}_p(\boldsymbol{n}_1) + o(r_1^N) , \tag{6.23}$$

where $r_1 \equiv |\boldsymbol{x} - \boldsymbol{y}_1|$ (and $r_2 \equiv |\boldsymbol{x} - \boldsymbol{y}_2|$) and where $\boldsymbol{n}_1$ is the unit vector $\boldsymbol{n}_1 \equiv \frac{\boldsymbol{x}-\boldsymbol{y}_1}{r_1}$. From (6.23), we first define the *partie finie* of F at the particle 1 as the angular average

$$(F)_1 \equiv \int \frac{\mathrm{d}\Omega_1}{4\pi} \underset{1}{f}_0(\boldsymbol{n}_1) , \tag{6.24}$$

where $\mathrm{d}\Omega_1$ is the solid angle element on the unit sphere centered on $\boldsymbol{y}_1$. Now, we are going to define the *partie finie of the divergent integral* of F. For that, we integrate F on the whole space[1] $\mathbb{R}^3$ except to balls $B_1(s)$ and $B_2(s)$ centered on $\boldsymbol{y}_1$ and $\boldsymbol{y}_2$ with a radius s. Then we add to that integral different terms (cf equation (6.25)) that depend on the partie finie of F at the point $\boldsymbol{y}_1$ and $\boldsymbol{y}_2$ such that the limit $s \to 0$ of the whole sum is finite. Hence the *Hadamard partie finie* of the integral of F is defined as

$$\begin{aligned}\mathrm{Pf}_{s_1,s_2} \int d^3\boldsymbol{x}\, F(\boldsymbol{x}) \quad &\equiv \quad \lim_{s\to 0} \left\{ \int_{\mathbb{R}^3 \backslash B_1(s) \cup B_2(s)} d^3\boldsymbol{x}\, F(\boldsymbol{x}) \right. \\ &\left. + 4\pi \sum_{p+3<0} \frac{s^{p+3}}{p+3} \left(\frac{F}{r_1^p}\right)_1 + 4\pi \ln\left(\frac{s}{s_1}\right) \left(r_1^3 F\right)_1 + 1 \leftrightarrow 2 \right\}. \quad (6.25)\end{aligned}$$

One can check that this quantity is indeed finite. The two constants s_1 and s_2 are arbitrary scales that have been introduced and that reflects some arbitrariness in the choice of the shape of B_1 and B_2. In fact, we could check that changing the shape of these two balls would correspond to a redefinition of s_1 and s_2.

We have to extend the equations (6.23)–(6.25) in the case where F contains logarithmic divergences when $\boldsymbol{x} \to \boldsymbol{y}_1$. For example, if F admits the following Laurent-expansion:

$$F(\boldsymbol{x}) = \sum_{p_0 \le p \le N} r_1^p \left[\underset{1}{f}_p(\boldsymbol{n}_1) + \ln r_1 \underset{1}{\tilde{f}}_p(\boldsymbol{n}_1) \right] + o(r_1^N)\,. \quad (6.26)$$

In that case we still apply the prescription (6.25) with the following value for $(F)_1$:

$$(F)_1 \equiv \int \frac{\mathrm{d}\Omega_1}{4\pi} \left[\underset{1}{f}_0(\boldsymbol{n}_1) + \ln r_1' \underset{1}{\tilde{f}}_0(\boldsymbol{n}_1) \right] , \quad (6.27)$$

where we have introduced a new constant r_1'. Therefore, the final result of (6.22) might depends on the constants s_1, s_2, r_1' and r_2'.

The partie finie (Pf) regularization is a very powerful tool that has been used to deal with UV divergences up to 2PN. Starting at 3PN this technique is not powerful enough and leads to incomplete results. One of the main limitation of this technique is that the equation (6.24) explicitly breaks the Lorentz invariance and has to be amended in order to be compatible with Lorentz invariance [74]. For example, the 3PN equations of motion were first computed using this regularization technique ([72, 73, 74, 75]), and the result obtained contained an ambiguity parameter called λ. The computation of this ambiguity parameter from *first principle* was achieved in [156] by introducing a more powerful regularization technique called *dimensional regularization.*

6.1.3 UV regularization using dimensional regularization

6.1.3.a) General principle

Dimensional regularization is a technique that has been extensively used in quantum field theory for a long time and that has been introduced in the case of post-Newtonian theory in the 2000s. The principle of dimensional regularization is to compute all our quantities in $d+1$

[1] We assume that the integral is convergent when $r \to \infty$ in this section. If it is not the case, then an extra regularization technique to cure infra-red divergences has to be performed as explained in section 6.1.4.

dimensions (instead of 3+1 in classical GR), where d is a complex number. All the computed quantities are therefore finite and well-defined for d belonging to a certain part of the complex plane, and these quantities can be extended by analytical continuation to the whole complex plane $d \in \mathbb{C}$ except for some isolated poles. They are then two possibilities: (i) either we express a physical observable as a function of another observable and no divergence should occur when we take $d \to 3$, (ii) or we express intermediate results (such as the equations of motion) which are gauge-dependent and divergences in $1/\varepsilon$ (where $\varepsilon \equiv d-3$) might occur. In that latter case, we can either keep the $1/\varepsilon$ poles in our intermediate result (knowing that they will cancel out in the final gauge-invariant result) or absorb it through a redefinition of the word-lines of the particles called a *shift*.

6.1.3.b) The Einstein equations in d dimensions

We can derive the Einstein equations in d dimensions by considering the Einstein-Hilbert action in d dimensions with a gauge-fixing term

$$S = \frac{c^3}{16\pi G_N}\int \frac{\mathrm{d}^{d+1}\boldsymbol{x}}{\ell_0^{d-3}}\sqrt{-g}\left[g^{\mu\nu}\left(\Gamma^\rho_{\mu\lambda}\Gamma^\lambda_{\nu\rho} - \Gamma^\rho_{\mu\nu}\Gamma^\lambda_{\rho\lambda}\right) - \frac{1}{2}g_{\mu\nu}\Gamma^\mu\Gamma^\nu\right] + S_m\,, \tag{6.28}$$

where ℓ_0 is an arbitrary constant length-scale that we introduce, and G_N denotes Newton constant in 3 dimensions. We can absorb the factor ℓ_0^{d-3} into Newton constant and define G the Newton constant in d dimensions to be $G \equiv G_N\ell_0^{d-3}$. The matter action in d dimensions is still the usual matter action given by

$$S_m = -\sum_A m_A c^2 \int \mathrm{d}t\sqrt{-(g_{\mu\nu})_A\, v_A^\mu v_A^\nu/c^2}\,, \tag{6.29}$$

In that case, the Einstein equations in harmonic coordinates become [156, 17]:

$$\Box h^{\mu\nu} = \frac{16\pi G}{c^4}|g|T^{\mu\nu} + \Lambda^{\mu\nu}\,, \tag{6.30}$$

where the only differences between (6.7) and (6.30) are (i) G that is now defined as $G = G_N\ell_0^{d-3}$ where G_N is the Newton constant in 3 dimensions and (ii) the expression of $\Lambda^{\mu\nu}$ that in d dimensions reads:

$$\begin{aligned}\Lambda^{\alpha\beta} =& - h^{\mu\nu}\partial^2_{\mu\nu}h^{\alpha\beta} + \partial_\mu h^{\alpha\nu}\partial_\nu h^{\beta\mu} + \frac{1}{2}g^{\alpha\beta}g_{\mu\nu}\partial_\lambda h^{\mu\tau}\partial_\tau h^{\nu\lambda}\\ &- g^{\alpha\mu}g_{\nu\tau}\partial_\lambda h^{\beta\tau}\partial_\mu h^{\nu\lambda} - g^{\beta\mu}g_{\nu\tau}\partial_\lambda h^{\alpha\tau}\partial_\mu h^{\nu\lambda} + g_{\mu\nu}g^{\lambda\tau}\partial_\lambda h^{\alpha\mu}\partial_\tau h^{\beta\nu}\\ &+ \frac{1}{4}(2g^{\alpha\mu}g^{\beta\nu} - g^{\alpha\beta}g^{\mu\nu})\Big(g_{\lambda\tau}g_{\epsilon\pi} - \frac{1}{d-1}g_{\tau\epsilon}g_{\lambda\pi}\Big)\partial_\mu h^{\lambda\pi}\partial_\nu h^{\tau\epsilon}\,.\end{aligned} \tag{6.31}$$

Notice the factor $\frac{1}{d-1}$ which is the only difference between the equation (6.31) and (4.5).

Therefore we need to extend the expression of the metric (6.13) as well as the definition of the potentials (6.14) in d dimensions. The result has been computed in [156]. Defining $\overline{h}^{00ii} \equiv 2\frac{(d-2)\overline{h}^{00}+\overline{h}^{ii}}{d-1}$, it reads

$$\overline{h}^{00ii} = -\frac{4}{c^2}V - \frac{4}{c^4}\left[\frac{d-1}{d-2}V^2 - 2\frac{d-3}{d-2}K\right] \tag{6.32a}$$

$$- \frac{8}{c^6}\left[2\hat{X} + V\hat{W} + \frac{1}{3}\left(\frac{d-1}{d-2}\right)^2 V^3 - 2\frac{d-3}{d-1}V_iV_i - 2\frac{(d-1)(d-3)}{(d-2)^2}KV\right] + \mathcal{O}\left(8\right) ,$$

$$\overline{h}^{0i} = -\frac{4}{c^3}V_i - \frac{4}{c^5}\left(2\hat{R}_i + \frac{d-1}{d-2}VV_i\right) + \mathcal{O}\left(7\right) , \tag{6.32b}$$

$$\overline{h}^{ij} = -\frac{4}{c^4}\left(\hat{W}_{ij} - \frac{1}{2}\delta_{ij}\hat{W}\right) - \frac{16}{c^6}\left(\hat{Z}_{ij} - \frac{1}{2}\delta_{ij}\hat{Z}\right) + \mathcal{O}\left(8\right) . \tag{6.32c}$$

where the potentials in d dimensions are defined by

$$\Box V = -4\pi G\,\sigma\,, \tag{6.33a}$$

$$\Box K = -4\pi G\,\sigma\,V\,, \tag{6.33b}$$

$$\begin{aligned}\Box\hat{X} &= -4\pi G\Big[\frac{V\sigma_{ii}}{d-2} + \frac{2(d-3)}{d-1}\sigma_iV_i + \left(\frac{d-3}{d-2}\right)^2\sigma\left(\frac{V^2}{2}+K\right)\Big] + \hat{W}_{ij}\,\partial^2_{ij}V \\ &\quad + 2V_i\,\partial_t\partial_iV + \frac{d-1}{2(d-2)}V\partial_t^2V + \frac{d(d-1)}{4(d-2)^2}\left(\partial_tV\right)^2 - 2\partial_iV_j\,\partial_jV_i\,,\end{aligned} \tag{6.33c}$$

$$\Box V_i = -4\pi G\,\sigma_i\,, \tag{6.33d}$$

$$\Box\hat{R}_i = -\frac{4\pi G}{d-2}\Big[\frac{5-d}{2}\,V\sigma_i - \frac{d-1}{2}\,V_i\,\sigma\Big] - \frac{d-1}{d-2}\,\partial_kV\partial_iV_k - \frac{d(d-1)}{4(d-2)^2}\,\partial_tV\partial_iV\,, \tag{6.33e}$$

$$\Box\hat{W}_{ij} = -4\pi G\Big(\sigma_{ij} - \delta_{ij}\,\frac{\sigma_{kk}}{d-2}\Big) - \frac{d-1}{2(d-2)}\partial_iV\partial_jV\,, \tag{6.33f}$$

$$\begin{aligned}\Box\hat{Z}_{ij} &= -\frac{4\pi G}{d-2}\,V\Big(\sigma_{ij} - \delta_{ij}\,\frac{\sigma_{kk}}{d-2}\Big) - \frac{d-1}{d-2}\,\partial_tV_{(i}\,\partial_{j)}V + \partial_iV_k\,\partial_jV_k + \partial_kV_i\,\partial_kV_j \\ &\quad - 2\partial_kV_{(i}\,\partial_{j)}V_k - \frac{\delta_{ij}}{d-2}\,\partial_kV_m\left(\partial_kV_m - \partial_mV_k\right) - \frac{d(d-1)}{8(d-2)^3}\,\delta_{ij}\left(\partial_tV\right)^2 \\ &\quad + \frac{(d-1)(d-3)}{2(d-2)^2}\,\partial_{(i}V\partial_{j)}K\,.\end{aligned} \tag{6.33g}$$

For example, in 3 dimensions, at the Newtonian order we have

$$V = \frac{G_Nm_1}{r_1} + \frac{G_Nm_2}{r_2} + \mathcal{O}\left(\frac{1}{c^2}\right) , \tag{6.34}$$

which becomes in d dimensions

$$V^{(d)} = \frac{2(d-2)\tilde{k}}{d-1}\left(\frac{Gm_1}{r_1^{d-2}} + \frac{Gm_2}{r_2^{d-2}}\right) + \mathcal{O}\left(\frac{1}{c^2}\right) , \tag{6.35}$$

where $\tilde{k} \equiv \frac{\Gamma\left(\frac{d-2}{2}\right)}{\pi^{\frac{d-2}{2}}}$ and Γ is the Euler function. The constant $\tilde{k}$ is defined such that $\Delta(\tilde{k}r^{2-d}) = -4\pi\delta^{(d)}(\boldsymbol{x})$ in d dimensions. For the rest of the manuscript, we will use for simplicity the same notation G for the Newton constant in 3 dimensions (G_N) and in d dimensions ($G_N\ell_0^{d-3}$).

6.1.3.c) Difference between dimensional regularization and Hadamard partie finie

In practice, we do not apply dimensional regularization for UV divergences right away. It is in fact easier and clearer to do a first computation in 3 dimensions only, using the

Hadamard partie finie, and then to compute explicitly the difference between the dimensional regularization and the Hadamard partie finie for the UV divergences. We define $\mathcal{D}I$ as the difference between equation (6.22) and its generalization in d dimensions:

$$\mathcal{D}I \equiv I^{(d)} - I\,, \tag{6.36}$$

where

$$I^{(d)} = \int F^{(d)}(x)\frac{\mathrm{d}^d\boldsymbol{x}}{\ell_0^{d-3}}\,. \tag{6.37}$$

where $F^{(d)}$ is the generalization in d dimensions of the function F. To compute (6.36), we start by doing an expansion similar to the Laurent expansion done in (6.23), but in d dimensions

$$F^{(d)}(\boldsymbol{x}) = \sum_{\substack{p_0\leq p\leq N\\ q_0\leq q\leq q_1}} r_1^p \left(\frac{r_1}{\ell_0}\right)^{q\varepsilon} \underset{1}{f}{}_{p,q}^{(\varepsilon)}(\boldsymbol{n}_1) + o(r_1^N)\,. \tag{6.38}$$

At the 4PN order, there is no pole in $1/\varepsilon$ in the integrand $F^{(d)}$ which enters the source of the Fokker action. Therefore $F^{(d)}$ will tend to F when $d\to 3$. This leads to the following equation relating the expansion of $F^{(d=3)}$ and $F^{(d)}$ around $\boldsymbol{y}_1$

$$\sum_{q=q_0}^{q_1} \underset{1}{f}{}_{p,q}^{(\varepsilon=0)}(\boldsymbol{n}_1) = \underset{1}{f}{}_p(\boldsymbol{n}_1)\,. \tag{6.39}$$

As shown in [157], the difference (6.36) only depends on the coefficients $f_{1\,p}$ and $f_{1\,p,q}^{\,(d)}$ that describe the function F around $\boldsymbol{y}_1$ and reads

$$\mathcal{D}I = \frac{\Omega_{2+\varepsilon}}{\varepsilon}\sum_{q=q_0}^{q_1}\left[\frac{1}{q+1} + \varepsilon\ln\left(\frac{s_1}{\ell_0}\right)\right]\langle \underset{1}{f}{}_{-3,q}^{(\varepsilon)}\rangle_{2+\varepsilon} + 1 \leftrightarrow 2 + \mathcal{O}(\varepsilon)\,, \tag{6.40}$$

where the spherical average performed in d dimensions is defined by

$$\langle f\rangle_{d-1} \equiv \int \frac{d\Omega_{d-1}(\boldsymbol{n}_1)}{\Omega_{d-1}}\, f(\boldsymbol{n}_1)\,. \tag{6.41}$$

The volume of the $(d-1)$-dimensional sphere, embedded into d-dimensional space, is given by $\Omega_{d-1} = 2\pi^{\frac{d}{2}}/\Gamma(\frac{d}{2})$; for instance, $\Omega_2 = 4\pi$. Actually, we can see that the Ω_{d-1}'s cancel out between (6.40) and (6.41).

At the end of the day, the constants s_1 and s_2 that were introduced in the Hadamard partie finie regularization, disappear when computing the difference with dimensional regularization using the equations (6.40). In exchange, the result contains $1/\varepsilon$ poles, as well as the length scale constant ℓ_0.

Similarly to what is done in 6.1.2.b), the equations (6.38)–(6.40) have to be adapted in the presence of logarithm divergences. In the case of Hadamard partie finie, the logarithm divergences introduce the constants $\ln r_1'$ and $\ln r_2'$. These constants vanish when we compute the difference with dimensional regularization and are replaced by $\ln\ell_0$ [156]. However, (i) we set $\ell_0 = 1$ for simplicity in the rest of the manuscript (except in the expression of the shift in the appendice B) (ii) the specific shifts we apply systematically replace the $\ln\ell_0$ by $\ln r_1'$ and $\ln r_2'$ for conveniency. Therefore, our final result in d dimensions (after application of the shifts) contains the constants $\ln r_1'$ and $\ln r_2'$ through the quantities $\ln r_0'$ and $\ln r_0''$ defined in the equations (7.10).

6.1.4 Infra-red regularization

6.1.4.a) Infra-red divergences

In order to obtain a post-Newtonian expansion of the Fokker Lagrangian, the instantaneous part of the metric injected in the total action $S = S_g + S_m$ is post-Newtonian expanded. The post-Newtonian expansion of the metric is valid in the near-zone only and diverges when $r \to \infty$. Therefore, when we integrate over the whole space the Lagrangian density expressed with the post-Newtonian metric $\bar{h}^{\mu\nu}$

$$\int \mathrm{d}^3\boldsymbol{x}\; \mathcal{L}_g\left(\bar{h}^{\mu\nu}\right), \tag{6.42}$$

divergences appear because the integrand $\mathcal{L}_g\left(\bar{h}^{\mu\nu}\right)$ blows up for $r \to \infty$. These infra-red (IR) divergences appear only at the 4PN order in the Fokker Lagrangian and we also use regularization techniques to cure them.

6.1.4.b) The Finite Part regularization

Let us focus on the infra-red regularization of the integration of a generic function F. We only want to study the infra-red bound at infinity, so we define

$$I_{\mathcal{R}} = \int_{r>\mathcal{R}} \mathrm{d}^3\boldsymbol{x}\, F(\boldsymbol{x})\,, \tag{6.43}$$

where $\mathcal{R}$ is a sufficiently large radius. Similarly to the Finite Part (FP) regularization introduced in chapter 4, we multiply the function F by a factor $\left(\frac{r}{r_0}\right)^B$ where B is a complex number whose real part is negatively large enough so that the integral

$$\int_{r>\mathcal{R}} \mathrm{d}^3\boldsymbol{x} \left(\frac{r}{r_0}\right)^B F(\boldsymbol{x})\,, \tag{6.44}$$

is well-defined. For functions that admit an expansion at infinity of the type of (6.46), the result can be extended for values of B through all the complex plane except for isolated poles by analytical continuation. We then define the Finite Part regularization by doing a Laurent expansion of the result when $B \to 0$ and taking the Finite Part in B (i.e. the zeroth power of B in this expansion)

$$I_{\mathcal{R}}^{\mathrm{HR}} = \underset{B=0}{\mathrm{FP}} \int_{r>\mathcal{R}} \mathrm{d}^3\boldsymbol{x} \left(\frac{r}{r_0}\right)^B F(\boldsymbol{x})\,. \tag{6.45}$$

It is important to notice that (6.44) is well-defined for $\Re B$ negatively large enough while the regularization used in the MPM algorithm required $\Re B$ to be positively large enough. This is due to the fact that we are regularizing an IR divergence while the MPM algorithm was facing an UV divergence. We are going to provide an explicit expression for (6.45). For that, let us develop F when $r \to \infty$ as

$$F(\boldsymbol{x}) = \sum_{p=-p_0}^{N} \frac{1}{r^p}\, \varphi_p(\boldsymbol{n}) + o\left(\frac{1}{r^N}\right)\,. \tag{6.46}$$

By injecting (6.46) into (6.45) we find that

$$I_{\mathcal{R}}^{\mathrm{HR}} = -\sum_{p\neq 3} \frac{\mathcal{R}^{3-p}}{3-p} \int \mathrm{d}\Omega_2\, \varphi_p(\boldsymbol{n}) - \ln\left(\frac{\mathcal{R}}{r_0}\right) \int \mathrm{d}\Omega_2\, \varphi_3(\boldsymbol{n})\,, \tag{6.47}$$

which is the formula that is used to perform the IR Finite Part regularization. Notice that it depends both on $\mathcal{R}$ and r_0. The dependence on $\mathcal{R}$ disappears when we compute the full integral

$$I = \int \mathrm{d}^3\boldsymbol{x} F(\boldsymbol{x}) = \int_{r\leq\mathcal{R}} \mathrm{d}^3\boldsymbol{x} F(\boldsymbol{x}) + \int_{r\geq\mathcal{R}} \mathrm{d}^3\boldsymbol{x} F(\boldsymbol{x})\,. \tag{6.48}$$

Note that the Fokker Lagrangian, or the equations of motion are not observables but intermediate results, that depend on the choice of gauge, and can depend on gauge constants such as s_1, s_2 or r_0.

6.1.5 Adding the tail effects in 3 dimensions

According to the matching equation we recall that we have (cf equation (5.41))

$$\begin{aligned}\overline{h}^{\mu\nu} = \overline{h}^{\mu\nu}_{\text{part}} &- \frac{4G}{c^4}\sum_{\ell=0}^{+\infty}\frac{(-1)^\ell}{\ell!}\,\partial_L\left\{\frac{\mathcal{F}_L^{\mu\nu}(t-r/c) - \mathcal{F}_L^{\mu\nu}(t+r/c)}{2r}\right\}\\ &- \frac{4G}{c^4}\sum_{\ell=0}^{+\infty}\frac{(-1)^\ell}{\ell!}\,\partial_L\left\{\frac{\mathcal{R}_L^{\mu\nu}(t-r/c) - \mathcal{R}_L^{\mu\nu}(t+r/c)}{2r}\right\}\,,\end{aligned} \tag{6.49}$$

where the term $\overline{h}^{\mu\nu}_{\text{part}}$ corresponds to the metric computed with the potentials in equations (6.32). The terms depending on $\mathcal{F}_L^{\mu\nu}$ correspond to dissipative radiation reaction terms at 2.5PN and 3.5PN. As we are only looking to the conservative part of the dynamics, there is no need to include them here. The last terms depending on $\mathcal{R}_L^{\mu\nu}$ correspond however to the tails back-scattered into the near-zone and contribute to the conservative part of the equations of motion at 4PN. We have therefore to include them in the Fokker Lagrangian. Therefore, we are interested in computing

$$\overline{\mathcal{H}}^{\mu\nu} \equiv -\frac{4G}{c^4}\sum_{\ell=0}^{+\infty}\frac{(-1)^\ell}{\ell!}\,\partial_L\left\{\frac{\mathcal{R}_L^{\mu\nu}(t-r/c) - \mathcal{R}_L^{\mu\nu}(t+r/c)}{2r}\right\}\,, \tag{6.50}$$

with (cf equation (5.33))

$$\mathcal{R}_L^{\mu\nu} = \underset{B}{\mathrm{FP}}\int \mathrm{d}^3\boldsymbol{x}\left(\frac{|\boldsymbol{x}|}{s_0}\right)^B \hat{x}_L \int_1^\infty \gamma_\ell(z)\mathcal{M}(\tau^{\mu\nu})(\boldsymbol{x}, t - z\boldsymbol{x}/c)\,. \tag{6.51}$$

In equation (6.51), we have replaced the r_0 by another constant s_0 because as we are going to see, we do not control the scale at which the tail is back-scattered into the near zone when we do the computation only in 3d. This term is explicitly known for compact binary systems since 1993 [150] and is given at the leading 4PN order by

$$\overline{\mathcal{H}}^{00} = \frac{8G^2M}{15c^{10}}x^i x^j \int_0^{+\infty}\mathrm{d}\tau \ln\left(\frac{c\tau}{2s_0}\right) I_{ij}^{(7)}(t-\tau) + \mathcal{O}\left(\frac{1}{c^{12}}\right)\,, \tag{6.52a}$$

$$\overline{\mathcal{H}}^{0i} = -\frac{8G^2M}{3c^9}x^j \int_0^{+\infty} \mathrm{d}\tau \ln\left(\frac{c\tau}{2s_0}\right) I_{ij}^{(6)}(t-\tau) + \mathcal{O}\left(\frac{1}{c^{11}}\right), \tag{6.52b}$$

$$\overline{\mathcal{H}}^{ij} = \frac{8G^2M}{c^8} \int_0^{+\infty} \mathrm{d}\tau \ln\left(\frac{c\tau}{2s_0}\right) I_{ij}^{(5)}(t-\tau) + \mathcal{O}\left(\frac{1}{c^{10}}\right). \tag{6.52c}$$

By injecting (6.52) into the Fokker Lagrangian and computing its contribution at 4PN in the action we obtain, after discarding total time derivatives

$$S_{\mathrm{F}}^{\mathrm{tail}} = -\frac{G^2M}{5c^8} \int_{-\infty}^{+\infty} \mathrm{d}t\, I_{ij}(t) \int_0^{+\infty} \mathrm{d}\tau \ln\left(\frac{c\tau}{2s_0}\right) \left[I_{ij}^{(7)}(t-\tau) - I_{ij}^{(7)}(t+\tau)\right]. \tag{6.53}$$

6.1.6 A first result in disagreement with self-force computation

In [92], Bernard *et al.* computed the 4PN Fokker Lagrangian using the method described above. This result contains one ambiguity parameter $\alpha = \ln\left(\frac{r_0}{s_0}\right)$, where r_0 is the constant introduced in the Finite Part regularization for the infra-red and s_0 the constant normalizing the logarithm in the tails. This constant was adjusted in order to be in agreement with the energy of circular orbits predicted by self-force computation in the small mass ratio limit ($\nu \to 0$). However, by doing so, they did not recover previous results obtained by Damour, Jaranowski, Schäfer [90]. Moreover, their result was in disagreement with the prediction of self-force computation of the periastron advance, while Damour, Jaranowski, Schäfer's result was in agreement with these predictions.

The discrepancy between Bernard et al. [92] and Damour et al. [90] can be parametrized by only two coefficients called *ambiguities*. If L_1 is the Fokker Lagrangian obtained through the method described above, then the following Lagrangian L_2 is in agreement with the self-force results [93, 154]

$$L_2 = L_1 + G^4 \frac{m m_1^2 m_2^2}{c^8 r_{12}^4}(\delta_1 n_{12} v_{12} + \delta_2 v_{12}^2), \tag{6.54}$$

with

$$\delta_1 = -\frac{2179}{315}, \quad \delta_2 = \frac{192}{35}. \tag{6.55}$$

This discrepancy is imputed to the Finite Part regularization method for the IR which no longer provides a complete result at 4PN. This regularization method breaks the Lorentz invariance of the underlying theory which is a strong hint that it might not work at high post-Newtonian orders. Therefore, it was decided [94] to compute the Fokker Lagrangian using systematically dimensional regularization. In fact, this regularization technique that has been used in particle physics for decades has proven to be extremely powerful in perturbation computations, and does preserve the Lorentz invariance of general relativity.

6.2 The systematic use of dimensional regularization

6.2.1 Infra-red dimensional regularization

6.2.1.a) The method

We are now going to consider dimensional regularization to cure both IR divergences and the UV divergences (as described in 6.1.3).

Denoting $F^{(d)}$ the version of F in d dimensions, we define

$$I_{\mathcal{R}}^{\mathrm{DR}} = \int_{r>\mathcal{R}} \frac{\mathrm{d}^d \boldsymbol{x}}{\ell_0^{d-3}} F^{(d)}(\boldsymbol{x}) \,. \tag{6.56}$$

To compute explicitly (6.56), we first define the expansion of $F^{(d)}$ when $r \to \infty$

$$F^{(d)}(\boldsymbol{x}) = \sum_{p \geqslant -p_0} \sum_{q=-q_0}^{q_1} \frac{1}{r^p} \left(\frac{\ell_0}{r}\right)^{q\varepsilon} \varphi_{p,q}^{(\varepsilon)}(\boldsymbol{n}) \,. \tag{6.57}$$

Similarly to equation (6.39), the fact that $F^{(d)}$ does not have a pole when $d \to 3$ can be translated into the following equation

$$\varphi_p(\boldsymbol{n}) = \sum_{q=-q_0}^{q_1} \varphi_{p,q}^{(\varepsilon=0)}(\boldsymbol{n}) \,. \tag{6.58}$$

Injecting (6.57) into (6.56) we find that

$$I_{\mathcal{R}}^{\mathrm{DR}} = -\sum_{p\neq 3} \frac{\mathcal{R}^{3-p}}{3-p} \int \mathrm{d}\Omega_2 \, \varphi_p(\boldsymbol{n}) + \sum_{q=-q_0}^{q_1} \left[\frac{1}{(q-1)\varepsilon} - \ln\left(\frac{\mathcal{R}}{\ell_0}\right)\right] \int \mathrm{d}\Omega_{2+\varepsilon} \, \varphi_{3,q}^{(\varepsilon)}(\boldsymbol{n}) + \mathcal{O}\left(\varepsilon\right) \,. \tag{6.59}$$

It is interesting to compute the difference between the Finite Part and the dimensional regularization for the IR divergence $\mathcal{D}I_{\mathcal{R}} = I_{\mathcal{R}}^{HR} - I_{\mathcal{R}}^{DR}$. Doing so, we obtain

$$\mathcal{D}I_{\mathcal{R}} = \sum_{q=-q_0}^{q_1} \left[\frac{1}{(q-1)\varepsilon} - \ln\left(\frac{r_0}{\ell_0}\right)\right] \int \mathrm{d}\Omega_{2+\varepsilon} \, \varphi_{3,q}^{(\varepsilon)}(\boldsymbol{n}) + \mathcal{O}\left(\varepsilon\right) \,. \tag{6.60}$$

Note that the pole $1/\varepsilon$ here is an IR pole.

6.2.1.b) The result for the instantaneous terms

Using the equation, (6.60), the difference of the instantaneous part of the Fokker Lagrangians computed with dimensional regularization and Finite Part regularization for the infra-red divergences was computed in [94]. If we apply to this difference the specific shift $\boldsymbol{\chi}$ provided in the appendix B equation (B.7), it reduces to

$$\begin{aligned}\mathcal{D}L_g^{\mathrm{inst}} &= \frac{G^2 m}{5c^8}\left[\frac{1}{\varepsilon} - 2\ln\left(\frac{\sqrt{\bar{q}}\, r_0}{\ell_0}\right)\right]\left(I_{ij}^{(3)}\right)^2 \\ &+ \frac{G^4 m\, m_1^2 m_2^2}{c^8 r_{12}^4}\left(-\frac{2479}{150}(n_{12}v_{12})^2 + \frac{1234}{75}v_{12}^2\right) + \mathcal{O}\left(\varepsilon\right) \,,\end{aligned} \tag{6.61}$$

where we have defined $\bar{q} \equiv 4\pi e^{\gamma_E}$ with γ_E being the Euler constant. Besides, it is crucial that $\left(I_{ij}^{(3)}\right)^2$ is taken in d dimensions, which brings extra ε corrections

$$\begin{aligned}\left(I_{ij}^{(3)}\right)^2 &= \frac{G^3 m_1^2 m_2^2}{r_{12}^4}\left(-\frac{88}{3}(n_{12}v_{12})^2 + 32 v_{12}^2\right)\left[1 - \frac{\varepsilon}{2}\ln\left(\frac{\sqrt{\bar{q}}\, r_{12}}{\ell_0}\right)\right] \\ &+ \varepsilon \frac{G^3 m_1^2 m_2^2}{r_{12}^4}\left(-\frac{836}{9}(n_{12}v_{12})^2 + 96 v_{12}^2\right) + \mathcal{O}\left(\varepsilon^2\right) \,.\end{aligned} \tag{6.62}$$

6.2.2 The tails in d dimensions

The following corresponds to the contribution of this thesis in the results presented in this chapter. For conveniency, we set $\ell_0 = 1$ in this section, and we restore the constant ℓ_0 for the result of the computation.

6.2.2.a) The matching equation in DimReg

The result presented in (6.53) corresponds to a computation in 3 dimensions, using a Finite Part regularization (cf equation (6.51)), which as we have seen is incomplete (presence of ambiguities) at 4PN. Therefore, we are going to show how to derive in dimensional regularization the contribution of the tails to the Fokker Lagrangian. In d dimensions, the retarded propagator $\Box^{-1(d)}_{\text{ret}}$ becomes

$$\Box^{-1(d)}_{\text{ret}}[F] = -\frac{\tilde{k}}{4\pi}\int \mathrm{d}^d\boldsymbol{x}' \int_1^{+\infty} \mathrm{d}z\, \gamma_{\frac{1-d}{2}}(z)\, \frac{F(\boldsymbol{x}', t - z|\boldsymbol{x}-\boldsymbol{x}'|/c)}{|\boldsymbol{x}-\boldsymbol{x}'|^{d-2}}\,, \tag{6.63}$$

where $\tilde{k} = \frac{\Gamma(\frac{d}{2}-1)}{\pi^{\frac{d}{2}-1}}$ (Γ being the Eulerian function) and

$$\gamma_{\frac{1-d}{2}}(z) = \frac{2\sqrt{\pi}}{\Gamma(\frac{3-d}{2})\Gamma(\frac{d}{2}-1)}\left(z^2-1\right)^{\frac{1-d}{2}}\,. \tag{6.64}$$

It turns out that we also need to introduce a new regularization factor r^η in order to have only convergent integrals. This regulator is exactly the same as the $\left(\frac{r}{r_0}\right)^B$ factor introduced in the Finite Part regularization, but now considered in d dimensions. We thus denote it by a different name. But it turns out that, in d dimensions, in contrast to 3 dimensions, no $1/\eta$ pole should normally remain in our final result. Therefore we define

$$\widetilde{\Box^{-1(d)}_{\text{ret}}}[F] \equiv \Box^{-1(d)}_{\text{ret}}[r^\eta F]\,, \tag{6.65}$$

with the prescription that we should take $\eta \to 0$ at the end of the computation (i.e. after having taken $\varepsilon \equiv d-3 \to 0$). This procedure is called the $\eta\varepsilon$-regularization technique.

In order to compute the tails in d dimensions, we need first to derive a new matching equation, similar to equation (5.41), but in d dimensions. The first step is to extend the lemma 1 (i.e. equation (5.32)) to d dimensions. This has been done in [94] (cf equation (3.15) in [94]), and the result is

$$\overline{\widetilde{\Box^{-1(d)}_{\text{ret}}}[\mathcal{M}(\Lambda^{\mu\nu})]} = \widetilde{\Box^{-1(d)}_{\text{ret}}}\left[\overline{\mathcal{M}(\Lambda^{\mu\nu})}\right] + \overline{\mathcal{H}}^{(d)\mu\nu}\,, \tag{6.66}$$

where

$$\overline{\mathcal{H}}^{(d)\mu\nu} = -\frac{\tilde{k}}{4\pi}\sum_{q=0}^{+\infty}\frac{(-1)^q}{q!}\sum_{j=0}^{+\infty}\Delta^{-j}\hat{x}_Q\int_1^{+\infty}\mathrm{d}z\,\gamma_{\frac{1-d}{2}}(z)$$
$$\int \mathrm{d}^d\boldsymbol{x}'\, r'^\eta\, \hat{\partial}'_Q\left[\frac{\mathcal{M}\left(\Lambda^{\mu\nu(2j)}\right)(\mathbf{y}, t - zr')}{r'^{d-2}}\right]_{\mathbf{y}=\boldsymbol{x}'}\,. \tag{6.67}$$

Now, we can see that $\overline{\mathcal{H}}^{(d)\mu\nu}$ plays a role similar of the last term in (5.32). Based on that remark, it can be shown that the matching equation in d dimensions leads to

$$\overline{h}^{\mu\nu} = \frac{16\pi G}{c^4}\,\overline{\Box^{-1}_{\text{ret}}}\left[r^{\eta}\,\overline{\tau}^{\mu\nu}\right] + \overline{\mathcal{H}}^{(d)\mu\nu}\,. \tag{6.68}$$

$\mathcal{H}^{(d)\mu\nu}$ is therefore the generalization in d dimensions of the quantity computed in equations (6.50)–(6.52) and contains the tails that we want to compute.

6.2.2.b) Computing the tails

In order to compute the tails in d dimensions, we have to compute at the lowest 4PN order the equation (6.67). For that, we need to compute through the use of the MPM algorithm, the lowest-order terms in $\Lambda^{\mu\nu}$ contributing in equation (6.67). The part of the first post-Minkowskian metric that depends on the mass multipole moments can be written in d dimensions as

$$h^{00}_{(1)} = -\frac{4G}{c^2}\sum_{\ell=0}^{+\infty}\frac{(-1)^\ell}{\ell!}\,\partial_L \tilde{I}_L\,, \tag{6.69a}$$

$$h^{0i}_{(1)} = \frac{4G}{c^3}\sum_{\ell=1}^{+\infty}\frac{(-1)^\ell}{\ell!}\,\partial_{L-1} \tilde{I}^{(1)}_{iL-1}\,, \tag{6.69b}$$

$$h^{ij}_{(1)} = -\frac{4G}{c^4}\sum_{\ell=2}^{+\infty}\frac{(-1)^\ell}{\ell!}\,\partial_{L-2} \tilde{I}^{(2)}_{ijL-2}\,, \tag{6.69c}$$

where $\tilde{I}_L(t,r)$ is the generalization of $\frac{I(t-r/c)}{r}$ in d dimensions and is defined as

$$\tilde{I}_L(t,r) = \frac{\tilde{k}}{r^{d-2}}\int_1^{+\infty}\mathrm{d}z\,\gamma_{\frac{1-d}{2}}(z)\,I_L(t-zr/c)\,, \tag{6.70}$$

which, in the monopole case, reduces to $\tilde{M}(r) = \tilde{k}Mr^{2-d}$. The lowest order of the source $\Lambda^{\mu\nu}$ is given by its quadratic part $N(h,h)$ that can be deduced in d dimensions directly from (6.31). It reads

$$N^{00}_{M\times I_{kl}} = -h^{00}_M\partial^2_{00}h^{00}_{I_{kl}} - h^{ij}_{I_{kl}}\partial^2_{ij}h^{00}_M - \frac{3(d-2)}{2(d-1)}\partial_i h^{00}_M\partial_i h^{00}_{I_{kl}} + \partial_i h^{00}_M\partial_0 h^{0i}_{I_{kl}}\,, \tag{6.71a}$$

$$\begin{aligned}N^{0i}_{M\times I_{kl}} = {}&-h^{00}_M\partial^2_{00}h^{0i}_{I_{kl}} + \frac{d}{2(d-1)}\partial_i h^{00}_M\partial_0 h^{00}_{I_{kl}} + \partial_j h^{00}_M\partial_0 h^{ij}_{I_{kl}}\\ &+ \partial_j h^{00}_M\left(\partial_i h^{0j}_{I_{kl}} - \partial_j h^{0i}_{I_{kl}}\right)\,,\end{aligned} \tag{6.71b}$$

$$\begin{aligned}N^{ij}_{M\times I_{kl}} = {}&-h^{00}_M\partial^2_{00}h^{ij}_{I_{kl}} + \frac{d-2}{d-1}\partial_{(i}h^{00}_M\partial_{j)}h^{00}_{I_{kl}} - \frac{d-2}{2(d-1)}\delta_{ij}\partial_k h^{00}_M\partial_k h^{00}_{I_{kl}}\\ &- \delta_{ij}\partial_k h^{00}_M\partial_0 h^{0k}_{I_{kl}} + 2\partial_{(i}h^{00}_M\partial_0 h^{j)0}_{I_{kl}}\,.\end{aligned} \tag{6.71c}$$

Therefore we need to inject the $\tilde{I}_{ij}$ and the $\tilde{M}$ part of the metric into (6.71) and inject the result into (6.67).

For the interaction $M \times I_{ij}$, the second post-Minkowskian order of $\Lambda^{\mu\nu}$ is a sum of the form

$$\Lambda^{\mu\nu}_{(2)} = \sum_{k,p,\ell} r^{-k-2\varepsilon}\, \hat{n}_L \int_1^{+\infty} \mathrm{d}y\, y^p\, \gamma_{-1-\frac{\varepsilon}{2}}(y)\, F_L^{\mu\nu}(t - yr/c)\,, \tag{6.72}$$

where the finite sum ranges over integers k, p, as well as the multipolarity ℓ and the functions $F_L^{\mu\nu}$ are made of the products involving M and time derivatives of I_{ij}. Injecting (6.72) into (6.67), we get

$$\overline{\mathcal{H}}^{(d)\mu\nu}(\boldsymbol{x},t) = \sum_{\ell=0}^{+\infty}\sum_{j=0}^{+\infty} \frac{1}{c^{2j}}\, \Delta^{-j}\hat{x}_L\, f_L^{(2j)\mu\nu}(t)\,, \tag{6.73}$$

where, the j-th iterated inverse Poisson operator Δ^{-j} acts on $\hat{x}_L$ as

$$\Delta^{-j}\hat{x}_L = \frac{\Gamma(\ell+\frac{d}{2})}{\Gamma(\ell+j+\frac{d}{2})}\, \frac{r^{2j}\hat{x}_L}{2^{2j}j!}\,, \tag{6.74}$$

and $f_L^{\mu\nu}$ is given as

$$\begin{aligned} f_L^{\mu\nu} = \sum \frac{(-1)^{\ell+k}\, C_\ell^{p,k}}{2\ell+1+\varepsilon}\, &\frac{\Gamma(2\varepsilon-\eta)}{\Gamma(\ell+k-1+2\varepsilon-\eta)} \\ &\times \int_0^{+\infty} \mathrm{d}\tau\, \tau^{-2\varepsilon+\eta}\, F_L^{\mu\nu(\ell+k-1)}(t-\tau)\,. \end{aligned} \tag{6.75}$$

$C_\ell^{p,k}$ are dimensionless coefficients given by

$$\begin{aligned} C_\ell^{p,k} = &\int_1^{+\infty} \mathrm{d}y\, y^p\, \gamma_{-1-\frac{\varepsilon}{2}}(y) \\ &\times \int_1^{+\infty} \mathrm{d}z\, (y+z)^{\ell+k-2+2\varepsilon-\eta}\, \gamma_{-\ell-1-\frac{\varepsilon}{2}}(z)\,, \end{aligned} \tag{6.76}$$

that can be computed in analytic closed form as described in the Appendix D of [94].

If we apply the formulae (6.75)–(6.76) to obtain the leading tail effect in the metric at the 4PN order, we get (with $\overline{\mathcal{H}}^{(d)00ii} = \frac{2}{d-1}[(d-2)\overline{\mathcal{H}}^{(d)00} + \overline{\mathcal{H}}^{(d)ii}]$)

$$\overline{\mathcal{H}}^{(d)00ii} = \frac{8G^2M}{15c^{10}}\, x^{ij} \int_0^{+\infty} \mathrm{d}\tau \left[\ln\left(\frac{c\sqrt{\bar{q}}\,\tau}{2\ell_0}\right) - \frac{1}{2\varepsilon} + \frac{61}{60}\right] I_{ij}^{(7)}(t-\tau) + \mathcal{O}\left(\frac{1}{c^{12}}\right)\,, \tag{6.77a}$$

$$\overline{\mathcal{H}}^{(d)0i} = -\frac{8G^2M}{3c^9}\, x^{j} \int_0^{+\infty} \mathrm{d}\tau \left[\ln\left(\frac{c\sqrt{\bar{q}}\,\tau}{2\ell_0}\right) - \frac{1}{2\varepsilon} + \frac{107}{120}\right] I_{ij}^{(6)}(t-\tau) + \mathcal{O}\left(\frac{1}{c^{11}}\right)\,, \tag{6.77b}$$

$$\overline{\mathcal{H}}^{(d)ij} = \frac{8G^2M}{c^8} \int_0^{+\infty} \mathrm{d}\tau \left[\ln\left(\frac{c\sqrt{\bar{q}}\,\tau}{2\ell_0}\right) - \frac{1}{2\varepsilon} + \frac{4}{5}\right] I_{ij}^{(5)}(t-\tau) + \mathcal{O}\left(\frac{1}{c^{10}}\right)\,. \tag{6.77c}$$

The equations (6.77) are therefore the generalization in d dimensions of the result provided by the equations (6.52). If we inject the tails in d dimensions into the Fokker Lagrangian in d dimensions, their contributions to the action turn out to be

$$S_g^{\mathrm{tail}} = \frac{G^2M}{5c^8} \int_{-\infty}^{+\infty} \mathrm{d}t\, I_{ij}^{(3)}(t) \int_0^{+\infty} \mathrm{d}\tau \left[\ln\left(\frac{c\sqrt{\bar{q}}\,\tau}{2\ell_0}\right) - \frac{1}{2\varepsilon} + \frac{41}{60}\right] \left(I_{ij}^{(4)}(t-\tau) - I_{ij}^{(4)}(t+\tau)\right)\,. \tag{6.78}$$

Therefore, the difference between the tail part of Fokker Lagrangian computed in d dimensions (equation (6.78)) and in 3 dimensions (cf equation (6.53)) is

$$\mathcal{D}L_g^{\text{tail}} = \frac{G^2 m}{5c^8}\left[-\frac{1}{\varepsilon} + \frac{41}{30} + 2\ln\left(\frac{\sqrt{\bar{q}}\, s_0}{\ell_0}\right)\right]\left(I_{ij}^{(3)}\right)^2 . \tag{6.79}$$

In equation (6.79), the pole is a UV pole, and exactly cancels the IR pole in equation (6.61).

6.2.3 Conclusion

The difference between the Fokker Lagrangian obtained using the method described in section 6.1, and the Fokker Lagrangian computed using systematically dimensional regularization is therefore the sum of (6.79) and (6.61). If we add these two contributions, we see that the $1/\varepsilon$ pole disappears non-trivially as well as the $\ln\left(\frac{\sqrt{\bar{q}}\, s_0}{\ell_0}\right)$ terms. The remaining term in the total difference is

$$\mathcal{D}L_g^{\text{total}} = \frac{G^4 m\, m_1^2 m_2^2}{c^8 r_{12}^4}\Big(-\frac{2179}{315}(n_{12}v_{12})^2 + \frac{192}{35}v_{12}^2\Big) , \tag{6.80}$$

which corresponds exactly to the ambiguities introduced in (6.54). Therefore, the work done in [94, 2] shows that the computation of the Fokker Lagrangian using systematically dimensional regularization yields the 4PN equations of motion without any ambiguities from *first principles*. The resulting 4PN Lagrangian is shown in appendix B. Let us emphasize again that this Lagrangian, is today the only derivation from first principles of the 4PN dynamics, that it agrees with the result from Damour-Jaranowski-Schäfer [90], and is in perfect agreement with the predictions of the conserved energy as well as the periastron advance of self-force computation in the small mass ratio limit.

Indeed, in the ADM formalism results obtained by Damour, Jaranowski and Schäfer [90, 91], the full 4PN dynamics is not entirely derived from first principle due to one remaining ambiguity parameter C that needs to be fitted to self-force computation of the energy for circular orbits. This ambiguity is due to the scale entering the logarithm in the tail effect.

While the full 4PN dynamics has not been derived yet using the effective-field-theory (EFT) framework, significant results have been already published within that method. In particular, the effect of the tail on the dynamics has been computed in 2016 by Galley *et al.* [98], and our result (6.78) -and in particular the coefficient 41/60- is in perfect agreement with their own result (cf equation (3.3) in [98]). This is the main reason why we think that the EFT method might be able to computed the 4PN dynamics from *first principles* as well.

7 – Conserved quantities and equations of motion in the center of mass

In this chapter, we are going to study in detail the dynamics generated by the Fokker Lagrangian at the 4^{th} post-Newtonian order derived in the previous chapter and provided in appendix B. In harmonic coordinates, this Lagrangian is manifestly invariant under the Poincaré group transformation. This leads to 10 Noetherian conserved integrals of the motion: the integral of the center of mass associated with the invariance under Lorentz boosts (3 conserved quantities), the conserved angular momentum associated with rotations (3 conserved quantities), the conserved energy associated with the invariance with respect to time (1 conserved quantity), and finally the conserved linear momentum associated with translation invariance (3 conserved quantities).

We first compute explicitly the center of mass at 4PN in order to define the center of mass (CM) frame at 4PN. Once this is done, we systematically work in the CM frame where all the results are significantly simpler. The next steps are to express the acceleration in the CM frame of the compact bodies, and to find a CM Lagrangian, i.e., a Lagrangian whose Euler-Lagrange equations yield the dynamics of the Fokker Lagrangian expressed in the CM frame. We then explicitly compute and provide the CM conserved energy and angular momentum. Finally, we study the dynamics of circular orbits at the 4PN order, as well as the dissipative effects.

The content of this chapter is mainly based on the work published in [3].

7.1 Conserved integrals of the motion

Any physical quantity Q investigated in this chapter is the sum of (i) many *instantaneous* (local-in-time) terms up to the 4PN order, (ii) the non-local conservative tail term arising at the 4PN order, and, in most cases, (iii) (see section 7.2.3) dissipative radiation-reaction terms present at the 2.5PN, 3.5PN, as well as the 4PN orders. Accordingly, we write

$$Q = Q^{\text{inst}} + Q^{\text{tail}} + Q^{\text{diss}} \,. \tag{7.1}$$

Since the long explicit results presented in this chapter concern the instantaneous part of the dynamics, we adopt the convention that any Q^{inst} is directly given by the sequence of its PN coefficients $Q_{n\mathrm{PN}}$:

$$Q^{\mathrm{inst}} = Q_{\mathrm{N}} + \frac{1}{c^2}Q_{1\mathrm{PN}} + \frac{1}{c^4}Q_{2\mathrm{PN}} + \frac{1}{c^6}Q_{3\mathrm{PN}} + \frac{1}{c^8}Q_{4\mathrm{PN}} + \mathcal{O}\left(\frac{1}{c^{10}}\right) . \tag{7.2}$$

Furthermore, as the 4PN coefficient is especially lengthy, we split it into non-linear contributions corresponding to increasing powers of G:

$$Q_{4\mathrm{PN}} = Q^{(0)}_{4\mathrm{PN}} + G\,Q^{(1)}_{4\mathrm{PN}} + G^2Q^{(2)}_{4\mathrm{PN}} + G^3Q^{(3)}_{4\mathrm{PN}} + G^4Q^{(4)}_{4\mathrm{PN}} + G^5Q^{(5)}_{4\mathrm{PN}} . \tag{7.3}$$

7.1.1 The center of mass

To begin with, let us display the CM position $\boldsymbol{G}$ defined as $\boldsymbol{G} = \boldsymbol{P}t + \boldsymbol{Z}$ where $\boldsymbol{P}$ is the conserved linear momentum and $\boldsymbol{Z}$ the conserved CM integral. $\boldsymbol{G}$ satisfies

$$\frac{\mathrm{d}\boldsymbol{G}}{\mathrm{d}t} = \boldsymbol{P} , \tag{7.4}$$

while $\boldsymbol{Z}$ and $\boldsymbol{P}$ are conserved ($\frac{\mathrm{d}\boldsymbol{P}}{\mathrm{d}t} = 0$ and $\frac{\mathrm{d}\boldsymbol{Z}}{\mathrm{d}t} = 0$). The complete results are

$$\boldsymbol{G}_{\mathrm{N}} = m_1\boldsymbol{y}_1 + 1 \leftrightarrow 2 , \tag{7.5a}$$

$$\boldsymbol{G}_{1\mathrm{PN}} = \boldsymbol{y}_1\biggl(- \frac{G m_1 m_2}{2r_{12}} + \frac{m_1 v_1^2}{2}\biggr) + 1 \leftrightarrow 2 , \tag{7.5b}$$

$$\begin{aligned}\boldsymbol{G}_{2\mathrm{PN}} = {}& \boldsymbol{v}_1 G m_1 m_2\biggl(- \frac{7}{4}(n_{12}v_1) - \frac{7}{4}(n_{12}v_2)\biggr) + \boldsymbol{y}_1\biggl(- \frac{5G^2m_1^2m_2}{4r_{12}^2} + \frac{7G^2m_1m_2^2}{4r_{12}^2} \\ & + \frac{3m_1v_1^4}{8} + \frac{Gm_1m_2}{r_{12}}\biggl(- \frac{1}{8}(n_{12}v_1)^2 - \frac{1}{4}(n_{12}v_1)(n_{12}v_2) + \frac{1}{8}(n_{12}v_2)^2 \\ & + \frac{19}{8}v_1^2 - \frac{7}{4}(v_1v_2) - \frac{7}{8}v_2^2\biggr)\biggr) + 1 \leftrightarrow 2 ,\end{aligned} \tag{7.5c}$$

$$\begin{aligned}\boldsymbol{G}_{3\mathrm{PN}} = {}& \boldsymbol{v}_1\biggl(\frac{235G^2m_1^2m_2}{24r_{12}}\Bigl((n_{12}v_1) - (n_{12}v_2)\Bigr) - \frac{235G^2m_1m_2^2}{24r_{12}}\Bigl((n_{12}v_1) - (n_{12}v_2)\Bigr) \\ & + Gm_1m_2\biggl(\frac{5}{12}(n_{12}v_1)^3 + \frac{3}{8}(n_{12}v_1)^2(n_{12}v_2) + \frac{3}{8}(n_{12}v_1)(n_{12}v_2)^2 \\ & + \frac{5}{12}(n_{12}v_2)^3 - \frac{15}{8}(n_{12}v_1)v_1^2 - (n_{12}v_2)v_1^2 + \frac{1}{4}(n_{12}v_1)(v_1v_2) \\ & + \frac{1}{4}(n_{12}v_2)(v_1v_2) - (n_{12}v_1)v_2^2 - \frac{15}{8}(n_{12}v_2)v_2^2\biggr)\biggr) \\ & + \boldsymbol{y}_1\biggl(\frac{5m_1v_1^6}{16} + \frac{Gm_1m_2}{r_{12}}\biggl(\frac{1}{16}(n_{12}v_1)^4 + \frac{1}{8}(n_{12}v_1)^3(n_{12}v_2) + \frac{3}{16}(n_{12}v_1)^2(n_{12}v_2)^2 \\ & + \frac{1}{4}(n_{12}v_1)(n_{12}v_2)^3 - \frac{1}{16}(n_{12}v_2)^4 - \frac{5}{16}(n_{12}v_1)^2v_1^2 - \frac{1}{2}(n_{12}v_1)(n_{12}v_2)v_1^2 \\ & - \frac{11}{8}(n_{12}v_2)^2v_1^2 + \frac{53}{16}v_1^4 + \frac{3}{8}(n_{12}v_1)^2(v_1v_2) + \frac{3}{4}(n_{12}v_1)(n_{12}v_2)(v_1v_2) + \frac{5}{4}(n_{12}v_2)^2(v_1v_2) \\ & - 5v_1^2(v_1v_2) + \frac{17}{8}(v_1v_2)^2 - \frac{1}{4}(n_{12}v_1)^2v_2^2 - \frac{5}{8}(n_{12}v_1)(n_{12}v_2)v_2^2 + \frac{5}{16}(n_{12}v_2)^2v_2^2 \\ & + \frac{31}{16}v_1^2v_2^2 - \frac{15}{8}(v_1v_2)v_2^2 - \frac{11}{16}v_2^4\biggr) + \frac{G^2m_1^2m_2}{r_{12}^2}\biggl(\frac{79}{12}(n_{12}v_1)^2 - \frac{17}{3}(n_{12}v_1)(n_{12}v_2)\end{aligned}$$

$$
\begin{aligned}
&+ \frac{17}{6}(n_{12}v_2)^2 - \frac{175}{24}v_1^2 + \frac{40}{3}(v_1v_2) - \frac{20}{3}v_2^2\bigg) + \frac{G^2m_1m_2^2}{r_{12}^2}\bigg(- \frac{7}{3}(n_{12}v_1)^2 \\
&+ \frac{29}{12}(n_{12}v_1)(n_{12}v_2) + \frac{2}{3}(n_{12}v_2)^2 + \frac{101}{12}v_1^2 - \frac{40}{3}(v_1v_2) + \frac{139}{24}v_2^2\bigg) \\
&- \frac{19G^3m_1^2m_2^2}{8r_{12}^3} + \frac{G^3m_1^3m_2}{r_{12}^3}\bigg(\frac{13721}{1260} - \frac{22}{3}\ln\left(\frac{r_{12}}{r'_1}\right)\bigg) \\
&+ \frac{G^3m_1m_2^3}{r_{12}^3}\bigg(- \frac{14351}{1260} + \frac{22}{3}\ln\left(\frac{r_{12}}{r'_2}\right)\bigg)\bigg) + 1 \leftrightarrow 2\,, \qquad (7.5\text{d})
\end{aligned}
$$

together with

$$
\boldsymbol{G}_{4\mathrm{PN}}^{(0)} = \frac{35}{128}m_1\boldsymbol{y}_1v_1^8 + 1 \leftrightarrow 2\,, \qquad (7.6\text{a})
$$

$$
\begin{aligned}
\boldsymbol{G}_{4\mathrm{PN}}^{(1)} = m_1m_2\boldsymbol{v}_1 \bigg\{&-\frac{13}{64}(n_{12}v_1)^5 - \frac{11}{64}(n_{12}v_1)^4(n_{12}v_2) - \frac{5}{32}(n_{12}v_1)^3(n_{12}v_2)^2 \\
&- \frac{5}{32}(n_{12}v_1)^2(n_{12}v_2)^3 - \frac{11}{64}(n_{12}v_1)(n_{12}v_2)^4 - \frac{13}{64}(n_{12}v_2)^5 + \frac{1}{16}(n_{12}v_1)^3(v_1v_2) \\
&+ \frac{5}{16}(n_{12}v_1)^2(n_{12}v_2)(v_1v_2) + \frac{5}{16}(n_{12}v_1)(n_{12}v_2)^2(v_1v_2) + \frac{1}{16}(n_{12}v_2)^3(v_1v_2) \\
&+ \frac{3}{16}(n_{12}v_1)(v_1v_2)^2 + \frac{3}{16}(n_{12}v_2)(v_1v_2)^2 + \frac{77}{96}(n_{12}v_1)^3v_1^2 + \frac{13}{32}(n_{12}v_1)^2(n_{12}v_2)v_1^2 \\
&+ \frac{7}{32}(n_{12}v_1)(n_{12}v_2)^2v_1^2 + \frac{17}{96}(n_{12}v_2)^3v_1^2 + \frac{3}{16}(n_{12}v_1)(v_1v_2)v_1^2 + \frac{1}{16}(n_{12}v_2)(v_1v_2)v_1^2 \\
&- \frac{123}{64}(n_{12}v_1)v_1^4 - \frac{49}{64}(n_{12}v_2)v_1^4 + \frac{17}{96}(n_{12}v_1)^3v_2^2 + \frac{7}{32}(n_{12}v_1)^2(n_{12}v_2)v_2^2 \\
&+ \frac{13}{32}(n_{12}v_1)(n_{12}v_2)^2v_2^2 + \frac{77}{96}(n_{12}v_2)^3v_2^2 + \frac{1}{16}(n_{12}v_1)(v_1v_2)v_2^2 + \frac{3}{16}(n_{12}v_2)(v_1v_2)v_2^2 \\
&-\frac{33}{32}(n_{12}v_1)v_1^2v_2^2 - \frac{33}{32}(n_{12}v_2)v_1^2v_2^2 - \frac{49}{64}(n_{12}v_1)v_2^4 - \frac{123}{64}(n_{12}v_2)v_2^4\bigg\} \\
+ \frac{m_1m_2\boldsymbol{y}_1}{r_{12}} \bigg\{&-\frac{5}{128}(n_{12}v_1)^6 - \frac{5}{64}(n_{12}v_1)^5(n_{12}v_2) - \frac{15}{128}(n_{12}v_1)^4(n_{12}v_2)^2 \\
&- \frac{5}{32}(n_{12}v_1)^3(n_{12}v_2)^3 - \frac{25}{128}(n_{12}v_1)^2(n_{12}v_2)^4 - \frac{15}{64}(n_{12}v_1)(n_{12}v_2)^5 + \frac{5}{128}(n_{12}v_2)^6 \\
&- \frac{11}{64}(n_{12}v_1)^4(v_1v_2) - \frac{5}{16}(n_{12}v_1)^3(n_{12}v_2)(v_1v_2) - \frac{15}{32}(n_{12}v_1)^2(n_{12}v_2)^2(v_1v_2) \\
&- \frac{11}{16}(n_{12}v_1)(n_{12}v_2)^3(v_1v_2) - \frac{65}{64}(n_{12}v_2)^4(v_1v_2) + \frac{5}{32}(n_{12}v_1)^2(v_1v_2)^2 \\
&+ \frac{5}{16}(n_{12}v_1)(n_{12}v_2)(v_1v_2)^2 - \frac{29}{32}(n_{12}v_2)^2(v_1v_2)^2 + \frac{1}{16}(v_1v_2)^3 + \frac{27}{128}(n_{12}v_1)^4v_1^2 \\
&+ \frac{11}{32}(n_{12}v_1)^3(n_{12}v_2)v_1^2 + \frac{27}{64}(n_{12}v_1)^2(n_{12}v_2)^2v_1^2 + \frac{15}{32}(n_{12}v_1)(n_{12}v_2)^3v_1^2 \\
&+ \frac{137}{128}(n_{12}v_2)^4v_1^2 + \frac{13}{32}(n_{12}v_1)^2(v_1v_2)v_1^2 + \frac{7}{16}(n_{12}v_1)(n_{12}v_2)(v_1v_2)v_1^2 \\
&+ \frac{81}{32}(n_{12}v_2)^2(v_1v_2)v_1^2 + \frac{97}{32}(v_1v_2)^2v_1^2 - \frac{53}{128}(n_{12}v_1)^2v_1^4 - \frac{31}{64}(n_{12}v_1)(n_{12}v_2)v_1^4 \\
&- \frac{225}{128}(n_{12}v_2)^2v_1^4 - \frac{433}{64}(v_1v_2)v_1^4 + \frac{515}{128}v_1^6 + \frac{15}{128}(n_{12}v_1)^4v_2^2 + \frac{9}{32}(n_{12}v_1)^3(n_{12}v_2)v_2^2
\end{aligned}
$$

$$
\begin{aligned}
&+\frac{33}{64}(n_{12}v_1)^2(n_{12}v_2)^2v_2^2+\frac{27}{32}(n_{12}v_1)(n_{12}v_2)^3v_2^2-\frac{27}{128}(n_{12}v_2)^4v_2^2\\
&+\frac{7}{32}(n_{12}v_1)^2(v_1v_2)v_2^2+\frac{13}{16}(n_{12}v_1)(n_{12}v_2)(v_1v_2)v_2^2+\frac{77}{32}(n_{12}v_2)^2(v_1v_2)v_2^2\\
&+\frac{67}{32}(v_1v_2)^2v_2^2-\frac{23}{64}(n_{12}v_1)^2v_1^2v_2^2-\frac{23}{32}(n_{12}v_1)(n_{12}v_2)v_1^2v_2^2-\frac{157}{64}(n_{12}v_2)^2v_1^2v_2^2\\
&-\frac{161}{32}(v_1v_2)v_1^2v_2^2+\frac{381}{128}v_1^4v_2^2-\frac{31}{128}(n_{12}v_1)^2v_2^4-\frac{53}{64}(n_{12}v_1)(n_{12}v_2)v_2^4\\
&+\frac{53}{128}(n_{12}v_2)^2v_2^4-\frac{123}{64}(v_1v_2)v_2^4+\frac{251}{128}v_1^2v_2^4-\frac{75}{128}v_2^6\biggr\}+1\leftrightarrow 2\,,
\end{aligned}
\tag{7.6b}
$$

$$
\begin{aligned}
\boldsymbol{G}^{(2)}_{4\mathrm{PN}}=\boldsymbol{v}_1\biggl\{&\frac{m_1^2m_2}{r_{12}}\biggl[-\frac{3341}{480}(n_{12}v_1)^3+\frac{10223}{480}(n_{12}v_1)^2(n_{12}v_2)-\frac{3781}{160}(n_{12}v_1)(n_{12}v_2)^2\\
&+\frac{4621}{480}(n_{12}v_2)^3-\frac{4529}{240}(n_{12}v_1)(v_1v_2)+\frac{6499}{240}(n_{12}v_2)(v_1v_2)+\frac{9229}{480}(n_{12}v_1)v_1^2\\
&-\frac{8849}{480}(n_{12}v_2)v_1^2+\frac{2293}{160}(n_{12}v_1)v_2^2-\frac{3733}{160}(n_{12}v_2)v_2^2\biggr]+\frac{m_1m_2^2}{r_{12}}\biggl[\frac{4621}{480}(n_{12}v_1)^3\\
&-\frac{3781}{160}(n_{12}v_1)^2(n_{12}v_2)+\frac{10223}{480}(n_{12}v_1)(n_{12}v_2)^2-\frac{3341}{480}(n_{12}v_2)^3\\
&+\frac{6499}{240}(n_{12}v_1)(v_1v_2)-\frac{4529}{240}(n_{12}v_2)(v_1v_2)-\frac{3733}{160}(n_{12}v_1)v_1^2+\frac{2293}{160}(n_{12}v_2)v_1^2\\
&-\frac{8849}{480}(n_{12}v_1)v_2^2+\frac{9229}{480}(n_{12}v_2)v_2^2\biggr]\biggr\}\\
+\boldsymbol{y}_1\biggl\{&\frac{m_1^2m_2}{r_{12}^2}\biggl[-\frac{1693}{960}(n_{12}v_1)^4+\frac{53}{240}(n_{12}v_1)^3(n_{12}v_2)\\
&-\frac{4079}{480}(n_{12}v_1)^2(n_{12}v_2)^2+\frac{1133}{240}(n_{12}v_1)(n_{12}v_2)^3\\
&-\frac{1133}{960}(n_{12}v_2)^4-\frac{509}{60}(n_{12}v_1)^2(v_1v_2)-\frac{127}{60}(n_{12}v_1)(n_{12}v_2)(v_1v_2)\\
&-\frac{179}{60}(n_{12}v_2)^2(v_1v_2)+\frac{109}{80}(v_1v_2)^2+\frac{247}{60}(n_{12}v_1)^2v_1^2+\frac{451}{60}(n_{12}v_1)(n_{12}v_2)v_1^2\\
&+\frac{17}{60}(n_{12}v_2)^2v_1^2+\frac{713}{240}(v_1v_2)v_1^2-\frac{3803}{960}v_1^4+\frac{1709}{120}(n_{12}v_1)^2v_2^2\\
&-\frac{139}{10}(n_{12}v_1)(n_{12}v_2)v_2^2+\frac{139}{20}(n_{12}v_2)^2v_2^2+\frac{3433}{240}(v_1v_2)v_2^2-\frac{2873}{480}v_1^2v_2^2-\frac{2931}{320}v_2^4\biggr]\\
&+\frac{m_1m_2^2}{r_{12}^2}\biggl[\frac{1133}{960}(n_{12}v_1)^4+\frac{1337}{240}(n_{12}v_1)^3(n_{12}v_2)-\frac{7141}{480}(n_{12}v_1)^2(n_{12}v_2)^2\\
&+\frac{2197}{240}(n_{12}v_1)(n_{12}v_2)^3-\frac{4187}{960}(n_{12}v_2)^4+\frac{247}{30}(n_{12}v_1)^2(v_1v_2)\\
&+\frac{37}{60}(n_{12}v_1)(n_{12}v_2)(v_1v_2)+\frac{59}{60}(n_{12}v_2)^2(v_1v_2)+\frac{2091}{80}(v_1v_2)^2-\frac{31}{5}(n_{12}v_1)^2v_1^2\\
&+\frac{2}{5}(n_{12}v_1)(n_{12}v_2)v_1^2-\frac{239}{120}(n_{12}v_2)^2v_1^2-\frac{10153}{240}(v_1v_2)v_1^2+\frac{5631}{320}v_1^4-\frac{83}{15}(n_{12}v_1)^2v_2^2\\
&+\frac{313}{120}(n_{12}v_1)(n_{12}v_2)v_2^2+\frac{241}{120}(n_{12}v_2)^2v_2^2-\frac{7193}{240}(v_1v_2)v_2^2+\frac{9473}{480}v_1^2v_2^2+\frac{9083}{960}v_2^4\biggr]\biggr\}\\
+1\leftrightarrow 2\,,&
\end{aligned}
\tag{7.6c}
$$

$$\begin{aligned}
\boldsymbol{G}^{(3)}_{4\mathrm{PN}} = \boldsymbol{v}_1 \Bigg\{ & \frac{m_1^2 m_2^2}{r_{12}^2}\left[\frac{1099}{144}(n_{12}v_1) - \frac{41}{64}\pi^2(n_{12}v_1) + \frac{1099}{144}(n_{12}v_2) - \frac{41}{64}\pi^2(n_{12}v_2)\right] \\
& + \frac{m_1^3 m_2}{r_{12}^2}\left[-\frac{562}{9}(n_{12}v_1) + 44\ln\left(\frac{r_{12}}{r'_1}\right)(n_{12}v_1) + \frac{14377}{280}(n_{12}v_2) - \frac{110}{3}\ln\left(\frac{r_{12}}{r'_1}\right)(n_{12}v_2)\right] \\
& + \frac{m_1 m_2^3}{r_{12}^2}\left[\frac{14377}{280}(n_{12}v_1) - \frac{110}{3}\ln\left(\frac{r_{12}}{r'_2}\right)(n_{12}v_1) - \frac{562}{9}(n_{12}v_2) + 44\ln\left(\frac{r_{12}}{r'_2}\right)(n_{12}v_2)\right]\Bigg\} \\
+ \boldsymbol{y}_1 \Bigg\{ & \frac{m_1^2 m_2^2}{r_{12}^3}\left[\frac{2059}{96}(n_{12}v_1)^2 - \frac{123}{128}\pi^2(n_{12}v_1)^2 - \frac{3115}{48}(n_{12}v_1)(n_{12}v_2)\right. \\
& + \frac{123}{64}\pi^2(n_{12}v_1)(n_{12}v_2) + \frac{2317}{96}(n_{12}v_2)^2 - \frac{123}{128}\pi^2(n_{12}v_2)^2 + \frac{4429}{144}(v_1v_2) \\
& \left. - \frac{41}{64}\pi^2(v_1v_2) - \frac{1071}{32}v_1^2 + \frac{123}{128}\pi^2 v_1^2 + \frac{439}{288}v_2^2 - \frac{41}{128}\pi^2 v_2^2\right] \\
& + \frac{m_1^3 m_2}{r_{12}^3}\left[-\frac{9921}{2800}(n_{12}v_1)^2 + 22\ln\left(\frac{r_{12}}{r'_1}\right)(n_{12}v_1)^2 - \frac{198097}{4200}(n_{12}v_1)(n_{12}v_2)\right. \\
& - 22\ln\left(\frac{r_{12}}{r'_1}\right)(n_{12}v_1)(n_{12}v_2) + \frac{198097}{8400}(n_{12}v_2)^2 + 11\ln\left(\frac{r_{12}}{r'_1}\right)(n_{12}v_2)^2 - \frac{9875}{1008}(v_1v_2) \\
& \left. + \frac{154}{3}\ln\left(\frac{r_{12}}{r'_1}\right)(v_1v_2) + \frac{160193}{10080}v_1^2 - 33\ln\left(\frac{r_{12}}{r'_1}\right)v_1^2 - \frac{937}{1440}v_2^2 - 22\ln\left(\frac{r_{12}}{r'_1}\right)v_2^2\right] \\
& + \frac{m_1 m_2^3}{r_{12}^3}\left[-\frac{185497}{8400}(n_{12}v_1)^2 - 11\ln\left(\frac{r_{12}}{r'_2}\right)(n_{12}v_1)^2 + \frac{6397}{75}(n_{12}v_1)(n_{12}v_2)\right. \\
& - \frac{59501}{1200}(n_{12}v_2)^2 - \frac{937}{720}(v_1v_2) - 44\ln\left(\frac{r_{12}}{r'_2}\right)(v_1v_2) + \frac{2737}{1440}v_1^2 + 22\ln\left(\frac{r_{12}}{r'_2}\right)v_1^2 \\
& \left. - \frac{12689}{2016}v_2^2 + \frac{77}{3}\ln\left(\frac{r_{12}}{r'_2}\right)v_2^2\right]\Bigg\} + 1 \leftrightarrow 2\,,
\end{aligned} \tag{7.6d}$$

$$\begin{aligned}
\boldsymbol{G}^{(4)}_{4\mathrm{PN}} = \boldsymbol{y}_1 \Bigg\{ & \frac{m_1^4 m_2}{r_{12}^4}\left[-\frac{213929}{3600} + \frac{220}{3}\ln\left(\frac{r_{12}}{r'_1}\right)\right] + \frac{m_1 m_2^4}{r_{12}^4}\left[\frac{215279}{3600} - \frac{220}{3}\ln\left(\frac{r_{12}}{r'_2}\right)\right] \\
& + \frac{m_1^2 m_2^3}{r_{12}^4}\left[\frac{1301639}{12600} - \frac{11}{2}\pi^2 + 16\ln\left(\frac{r_{12}}{r'_1}\right) - \frac{110}{3}\ln\left(\frac{r_{12}}{r'_2}\right)\right] + \frac{m_1^3 m_2^2}{r_{12}^4}\left[-\frac{144347}{1800}\right. \\
& \left. + \frac{11}{2}\pi^2 + \frac{88}{3}\ln\left(\frac{r_{12}}{r'_1}\right) - 16\ln\left(\frac{r_{12}}{r'_2}\right)\right]\Bigg\} + 1 \leftrightarrow 2\,.
\end{aligned} \tag{7.6e}$$

The frame of the CM is defined by $\boldsymbol{G} = 0$, which we solve iteratively for the variable $\boldsymbol{y}_1$ and $\boldsymbol{y}_2$ starting from the Newtonian order, up to the fourth PN order. Doing so, we have to replace several times the accelerations by their values in the CM found at the previous post-Newtonian orders. This standard technique is called *standard order reduction of accelerations*. This gives the individual positions of the particles $\boldsymbol{y}_A$ in the CM frame as

$$\boldsymbol{y}_1 = \Big[X_2 + \nu(X_1 - X_2)P\Big]\boldsymbol{x} + \nu(X_1 - X_2)Q\,\boldsymbol{v}\,, \tag{7.7a}$$

$$\boldsymbol{y}_2 = \Big[-X_1 + \nu(X_1 - X_2)P\Big]\boldsymbol{x} + \nu(X_1 - X_2)Q\,\boldsymbol{v}\,, \tag{7.7b}$$

where $\boldsymbol{x} = \boldsymbol{y}_1 - \boldsymbol{y}_2$ and $\boldsymbol{v} = \mathrm{d}\boldsymbol{x}/\mathrm{d}t$ are the relative separation and velocity and where $X_1 = m_1/(m_1 + m_2)$ and $X_2 = m_2/(m_1 + m_2)$. Besides we define r as $r \equiv |\boldsymbol{x}|$ and $\boldsymbol{n}$ as $\boldsymbol{x} = r\boldsymbol{n}$. It is important not to confuse the variables $\boldsymbol{x}, \boldsymbol{n}, r$ used to denote the relative separation in the CM, with the field variables also note $\boldsymbol{x}, \boldsymbol{n}, r$ described in the figure A.1. As the context always clarifies without ambiguity which variables we are using, we will keep this notation in order to be consistent with the notations used in the literature.

The coefficients P and Q admit the following detailed 4PN expansions:[1]

$$P_{\rm 1PN} = \frac{v^2}{2} - \frac{Gm}{2\,r}\,, \tag{7.8a}$$

$$\begin{aligned} P_{\rm 2PN} &= \frac{3\,v^4}{8} - \frac{3\,\nu\,v^4}{2} \\ &+ \frac{Gm}{r}\left(-\frac{\dot r^2}{8} + \frac{3\,\dot r^2\,\nu}{4} + \frac{19\,v^2}{8} + \frac{3\,\nu\,v^2}{2}\right) \\ &+ \frac{G^2m^2}{r^2}\left(\frac{7}{4} - \frac{\nu}{2}\right)\,, \end{aligned} \tag{7.8b}$$

$$\begin{aligned} P_{\rm 3PN} &= \frac{5\,v^6}{16} - \frac{11\,\nu\,v^6}{4} + 6\,\nu^2\,v^6 \\ &+ \frac{Gm}{r}\left(\frac{\dot r^4}{16} - \frac{5\,\dot r^4\,\nu}{8} + \frac{21\,\dot r^4\,\nu^2}{16} - \frac{5\,\dot r^2\,v^2}{16} + \frac{21\,\dot r^2\,\nu\,v^2}{16}\right. \\ &\qquad \left. - \frac{11\,\dot r^2\,\nu^2\,v^2}{2} + \frac{53\,v^4}{16} - 7\,\nu\,v^4 - \frac{15\,\nu^2\,v^4}{2}\right) \\ &+ \frac{G^2m^2}{r^2}\left(-\frac{7\,\dot r^2}{3} + \frac{73\,\dot r^2\,\nu}{8} + 4\,\dot r^2\,\nu^2 + \frac{101\,v^2}{12} - \frac{33\,\nu\,v^2}{8} + 3\,\nu^2\,v^2\right) \\ &+ \frac{G^3m^3}{r^3}\left(-\frac{14351}{1260} + \frac{\nu}{8} - \frac{\nu^2}{2} + \frac{22}{3}\,\ln\left(\frac{r}{r''_0}\right)\right)\,, \end{aligned} \tag{7.8c}$$

$$P^{(0)}_{\rm 4PN} = \left(\frac{35}{128} - \frac{125}{32}\nu + \frac{145}{8}\nu^2 - \frac{55}{2}\nu^3\right)v^8\,, \tag{7.8d}$$

$$\begin{aligned} P^{(1)}_{\rm 4PN} &= \frac{m}{r}\left(-\frac{5}{128}\dot r^6 + \frac{35}{64}\nu\dot r^6 - \frac{125}{64}\nu^2\dot r^6 + \frac{55}{32}\nu^3\dot r^6 + \frac{27}{128}\dot r^4 v^2 - \frac{115}{64}\nu\dot r^4 v^2 + \frac{517}{64}\nu^2\dot r^4 v^2\right. \\ &- \frac{213}{16}\nu^3\dot r^4 v^2 - \frac{53}{128}\dot r^2 v^4 + \frac{3}{2}\nu\dot r^2 v^4 - \frac{95}{8}\nu^2\dot r^2 v^4 + 36\nu^3\dot r^2 v^4 + \frac{515}{128}v^6 \\ &\left. - \frac{749}{32}\nu v^6 + \frac{91}{4}\nu^2 v^6 + 42\nu^3 v^6\right)\,, \end{aligned} \tag{7.8e}$$

$$\begin{aligned} P^{(2)}_{\rm 4PN} &= \frac{m^2}{r^2}\left(\frac{1133}{960}\dot r^4 - \frac{1007}{48}\nu\dot r^4 + \frac{169}{24}\nu^2\dot r^4 + 9\nu^3\dot r^4 - \frac{31}{5}\dot r^2 v^2 + 26\nu\dot r^2 v^2 - \frac{541}{8}\nu^2\dot r^2 v^2\right. \\ &\left. - \frac{83}{2}\nu^3\dot r^2 v^2 + \frac{5631}{320}v^4 - \frac{139}{4}\nu v^4 + \frac{71}{4}\nu^2 v^4 - \frac{45}{2}\nu^3 v^4\right)\,, \end{aligned} \tag{7.8f}$$

$$P^{(3)}_{\rm 4PN} = \frac{m^3}{r^3}\left(-\frac{185497}{8400}\dot r^2 - \frac{64347}{1120}\nu\dot r^2 - \frac{123}{128}\pi^2\nu\dot r^2 + \frac{495}{16}\nu^2\dot r^2 + \frac{55}{4}\nu^3\dot r^2 + 11\nu\ln\left(\frac{r}{r'_0}\right)\dot r^2\right.$$

[1] For consistency, we also write the dissipative contributions, coming from the dissipative equations of motion. These terms come from using the dissipative part of the equations of motion when performing the standard order reductions of acceleration. We write only those that appear at the 2.5PN order, which turn out to be only of the type $Q_{\rm 2.5PN}$ (thus, we have $P_{\rm 2.5PN} = 0$). We also expect 3.5PN contributions $P_{\rm 3.5PN}$ and $Q_{\rm 3.5PN}$, but we do not need these to control the 3.5PN terms in the CM energy and angular momentum (equations (7.38)–(7.41)), and they have not been computed yet.

$$
\begin{aligned}
& - 11\ln\Big(\frac{r}{r''_0}\Big)\dot{r}^2 + 33\nu\ln\Big(\frac{r}{r''_0}\Big)\dot{r}^2 + \frac{2737}{1440}v^2 - \frac{87181}{3360}\nu v^2 + \frac{123}{128}\pi^2\nu v^2 - \frac{117}{8}\nu^2 v^2 \\
& +5\nu^3 v^2 - 11\nu\ln\Big(\frac{r}{r'_0}\Big)v^2 + 22\ln\Big(\frac{r}{r''_0}\Big)v^2\Big)\,, \qquad (7.8g)
\end{aligned}
$$

$$
\begin{aligned}
P^{(4)}_{4\mathrm{PN}} = {} & \frac{m^4}{r^4}\Big(\frac{215279}{3600} + \frac{22043}{720}\nu - \frac{11}{2}\pi^2\nu - \frac{3}{2}\nu^2 - \frac{1}{2}\nu^3 + 16\ln\Big(\frac{r}{r'_0}\Big) - 60\nu\ln\Big(\frac{r}{r'_0}\Big) \\
& -\frac{268}{3}\ln\Big(\frac{r}{r''_0}\Big) + 120\nu\ln\Big(\frac{r}{r''_0}\Big)\Big)\,, \qquad (7.8h)
\end{aligned}
$$

and

$$Q_{2\mathrm{PN}} = -\frac{7\,G\,m\,\dot{r}}{4}\,, \qquad (7.9a)$$

$$Q_{2.5\mathrm{PN}} = \frac{4\,G\,m\,v^2}{5} - \frac{8\,G^2m^2}{5\,r}\,, \qquad (7.9b)$$

$$
\begin{aligned}
Q_{3\mathrm{PN}} = {} & G\,m\,\dot{r}\left(\frac{5\,\dot{r}^2}{12} - \frac{19\,\dot{r}^2\,\nu}{24} - \frac{15\,v^2}{8} + \frac{21\,\nu\,v^2}{4}\right) \\
& + \frac{G^2m^2\,\dot{r}}{r}\left(-\frac{235}{24} - \frac{21\,\nu}{4}\right)\,, \qquad (7.9c)
\end{aligned}
$$

$$
\begin{aligned}
Q^{(1)}_{4\mathrm{PN}} = {} & m\Big(-\frac{13}{64}\dot{r}^5 + \frac{25}{32}\nu\dot{r}^5 - \frac{17}{32}\nu^2\dot{r}^5 + \frac{77}{96}\dot{r}^3v^2 - \frac{187}{48}\nu\dot{r}^3v^2 + \frac{19}{4}\nu^2\dot{r}^3v^2 - \frac{123}{64}\dot{r}v^4 \\
& +\frac{199}{16}\nu\dot{r}v^4 - 21\nu^2\dot{r}v^4\Big)\,, \qquad (7.9d)
\end{aligned}
$$

$$Q^{(2)}_{4\mathrm{PN}} = \frac{m^2}{r}\Big(\frac{4621}{480}\dot{r}^3 + \frac{113}{24}\nu\dot{r}^3 + \frac{7}{12}\nu^2\dot{r}^3 - \frac{3733}{160}\dot{r}v^2 + \frac{95}{4}\nu\dot{r}v^2 + 28\nu^2\dot{r}v^2\Big)\,, \qquad (7.9e)$$

$$
\begin{aligned}
Q^{(3)}_{4\mathrm{PN}} = {} & \frac{m^3}{r^2}\Big(\frac{14377}{280} + \frac{71509}{5040}\nu - \frac{41}{64}\pi^2\nu - \frac{49}{4}\nu^2 \\
& +\frac{22}{3}\nu\ln\Big(\frac{r}{r'_0}\Big) - \frac{110}{3}\ln\Big(\frac{r}{r''_0}\Big) - \frac{44}{3}\nu\ln\Big(\frac{r}{r''_0}\Big)\Big)\,\dot{r}\,. \qquad (7.9f)
\end{aligned}
$$

We have used the variable $\dot{r}$ defined as $\dot{r} = \boldsymbol{v}\cdot\boldsymbol{n}$. The CM velocities $\boldsymbol{v}_A$ are obtained by differentiating the equations (7.7) with order reduction of accelerations. The formulae (7.8)–(7.9) contain logarithmic terms depending on the gauge constants r'_0 and r''_0 (*i.e.*, not affecting physical results) defined as

$$\ln r'_0 = X_1\ln r'_1 + X_2\ln r'_2\,, \qquad (7.10a)$$

$$\ln r''_0 = \frac{X_1^2\ln r'_1 - X_2^2\ln r'_2}{X_1 - X_2}\,. \qquad (7.10b)$$

We recall that the variables r'_1 and r'_2 were introduced by the Hadamard partie finie UV regularization (cf the equation (6.27)); they are then replaced by $\ln\ell_0$ when we compute the difference between dimensional regularization and the Hadamard partie finie. However, the shifts that we apply (cf the shifts in appendix B) removed the $\ln\ell_0$ and re-introduced the r'_1 and r'_2. This is purely an arbitrary gauge choice that we make, and this has no physical meaning.

Even if the definition of r''_0 is not well defined for $X_1 = X_2$ (i.e. for $m_1 = m_2$), the results are still well-defined as no divergence appears in that case when the results are expressed using the variables r'_1 and r'_2.

7.1.2 Equations of motion in the center of mass frame

Now that the CM frame is defined at 4PN we can present the acceleration in the CM coming from the Fokker Lagrangian. In reality, the computation of the acceleration in the CM frame was done simultaneously to the computation of $\boldsymbol{y}_A$ in the CM frame as this latter computation is done post-Newtonian order by order using systematically standard reduction of accelerations. The final result is of the form

$$\boldsymbol{a} = -\frac{Gm}{r^2}\Big[(1+A)\,\boldsymbol{n} + B\,\boldsymbol{v}\Big]\,, \tag{7.11}$$

where the various PN coefficients are given by

$$\begin{aligned}
A_{1\mathrm{PN}} &= -\frac{3\,\dot{r}^2\,\nu}{2} + v^2 + 3\,\nu\,v^2 - \frac{Gm}{r}\,(4+2\,\nu)\;, && (7.12\mathrm{a})\\
A_{2\mathrm{PN}} &= \frac{15\,\dot{r}^4\,\nu}{8} - \frac{45\,\dot{r}^4\,\nu^2}{8} - \frac{9\,\dot{r}^2\,\nu\,v^2}{2} + 6\,\dot{r}^2\,\nu^2\,v^2 + 3\,\nu\,v^4 - 4\,\nu^2\,v^4\\
&\quad + \frac{Gm}{r}\left(-2\,\dot{r}^2 - 25\,\dot{r}^2\,\nu - 2\,\dot{r}^2\,\nu^2 - \frac{13\,\nu\,v^2}{2} + 2\,\nu^2\,v^2\right)\\
&\quad + \frac{G^2m^2}{r^2}\left(9 + \frac{87\,\nu}{4}\right)\,, && (7.12\mathrm{b})\\
A_{3\mathrm{PN}} &= -\frac{35\,\dot{r}^6\,\nu}{16} + \frac{175\,\dot{r}^6\,\nu^2}{16} - \frac{175\,\dot{r}^6\,\nu^3}{16} + \frac{15\,\dot{r}^4\,\nu\,v^2}{2}\\
&\quad - \frac{135\,\dot{r}^4\,\nu^2\,v^2}{4} + \frac{255\,\dot{r}^4\,\nu^3\,v^2}{8} - \frac{15\,\dot{r}^2\,\nu\,v^4}{2} + \frac{237\,\dot{r}^2\,\nu^2\,v^4}{8}\\
&\quad - \frac{45\,\dot{r}^2\,\nu^3\,v^4}{2} + \frac{11\,\nu\,v^6}{4} - \frac{49\,\nu^2\,v^6}{4} + 13\,\nu^3\,v^6\\
&\quad + \frac{Gm}{r}\left(79\,\dot{r}^4\,\nu - \frac{69\,\dot{r}^4\,\nu^2}{2} - 30\,\dot{r}^4\,\nu^3 - 121\,\dot{r}^2\,\nu\,v^2 + 16\,\dot{r}^2\,\nu^2\,v^2\right.\\
&\qquad\left. + 20\,\dot{r}^2\,\nu^3\,v^2 + \frac{75\,\nu\,v^4}{4} + 8\,\nu^2\,v^4 - 10\,\nu^3\,v^4\right)\\
&\quad + \frac{G^2m^2}{r^2}\left(\dot{r}^2 + \frac{32573\,\dot{r}^2\,\nu}{168} + \frac{11\,\dot{r}^2\,\nu^2}{8} - 7\,\dot{r}^2\,\nu^3 + \frac{615\,\dot{r}^2\,\nu\,\pi^2}{64} - \frac{26987\,\nu\,v^2}{840}\right.\\
&\qquad\left. + \nu^3\,v^2 - \frac{123\,\nu\,\pi^2\,v^2}{64} - 110\,\dot{r}^2\,\nu\,\ln\left(\frac{r}{r'_0}\right) + 22\,\nu\,v^2\,\ln\left(\frac{r}{r'_0}\right)\right)\\
&\quad + \frac{G^3m^3}{r^3}\left(-16 - \frac{437\,\nu}{4} - \frac{71\,\nu^2}{2} + \frac{41\,\nu\,\pi^2}{16}\right)\,, && (7.12\mathrm{c})
\end{aligned}$$

up to 3PN order, together with, for the 4PN terms,

$$\begin{aligned}
A^{(0)}_{4\mathrm{PN}} &= \left(\frac{315}{128}\nu - \frac{2205}{128}\nu^2 + \frac{2205}{64}\nu^3 - \frac{2205}{128}\nu^4\right)\dot{r}^8 + \left(-\frac{175}{16}\nu + \frac{595}{8}\nu^2 - \frac{2415}{16}\nu^3\right.\\
&\quad\left. + \frac{735}{8}\nu^4\right)\dot{r}^6v^2 + \left(\frac{135}{8}\nu - \frac{1875}{16}\nu^2 + \frac{4035}{16}\nu^3 - \frac{1335}{8}\nu^4\right)\dot{r}^4v^4 + \left(-\frac{21}{2}\nu + \frac{1191}{16}\nu^2\right.\\
&\quad\left. - \frac{327}{2}\nu^3 + 99\nu^4\right)\dot{r}^2v^6 + \left(\frac{21}{8}\nu - \frac{175}{8}\nu^2 + 61\nu^3 - 54\nu^4\right)v^8\,, && (7.12\mathrm{d})
\end{aligned}$$

$$A^{(1)}_{4\mathrm{PN}} = \frac{m}{r}\left(\frac{2973}{40}\nu\dot{r}^6 + 407\nu^2\dot{r}^6 + \frac{181}{2}\nu^3\dot{r}^6 - 86\nu^4\dot{r}^6 + \frac{1497}{32}\nu\dot{r}^4v^2 - \frac{1627}{2}\nu^2\dot{r}^4v^2\right.$$
$$- 81\nu^3\dot{r}^4v^2 + 228\nu^4\dot{r}^4v^2 - \frac{2583}{16}\nu\dot{r}^2v^4 + \frac{1009}{2}\nu^2\dot{r}^2v^4 + 47\nu^3\dot{r}^2v^4 - 104\nu^4\dot{r}^2v^4$$
$$\left.+\frac{1067}{32}\nu v^6 - 58\nu^2v^6 - 44\nu^3v^6 + 58\nu^4v^6\right), \tag{7.12e}$$

$$A^{(2)}_{4\mathrm{PN}} = \frac{m^2}{r^2}\left(\frac{2094751}{960}\nu\dot{r}^4 + \frac{45255}{1024}\pi^2\nu\dot{r}^4 + \frac{326101}{96}\nu^2\dot{r}^4 - \frac{4305}{128}\pi^2\nu^2\dot{r}^4 - \frac{1959}{32}\nu^3\dot{r}^4\right.$$
$$- 126\nu^4\dot{r}^4 + 385\nu^2\ln\left(\frac{r}{r'_0}\right)\dot{r}^4 + 385\nu\ln\left(\frac{r}{r''_0}\right)\dot{r}^4 - 1540\nu^2\ln\left(\frac{r}{r''_0}\right)\dot{r}^4 - \frac{1636681}{1120}\nu\dot{r}^2v^2$$
$$- \frac{12585}{512}\pi^2\nu\dot{r}^2v^2 - \frac{255461}{112}\nu^2\dot{r}^2v^2 + \frac{3075}{128}\pi^2\nu^2\dot{r}^2v^2 - \frac{309}{4}\nu^3\dot{r}^2v^2 + 63\nu^4\dot{r}^2v^2$$
$$- 330\nu\ln\left(\frac{r}{r'_0}\right)\dot{r}^2v^2 - 275\nu^2\ln\left(\frac{r}{r'_0}\right)\dot{r}^2v^2 - 275\nu\ln\left(\frac{r}{r''_0}\right)\dot{r}^2v^2 + 1100\nu^2\ln\left(\frac{r}{r''_0}\right)\dot{r}^2v^2$$
$$+ \frac{1096941}{11200}\nu v^4 + \frac{1155}{1024}\pi^2\nu v^4 + \frac{7263}{70}\nu^2v^4 - \frac{123}{64}\pi^2\nu^2v^4 + \frac{145}{2}\nu^3v^4 - 16\nu^4v^4$$
$$\left.+66\nu\ln\left(\frac{r}{r'_0}\right)v^4 + 22\nu^2\ln\left(\frac{r}{r'_0}\right)v^4 + 22\nu\ln\left(\frac{r}{r''_0}\right)v^4 - 88\nu^2\ln\left(\frac{r}{r''_0}\right)v^4\right), \tag{7.12f}$$

$$A^{(3)}_{4\mathrm{PN}} = \frac{m^3}{r^3}\left(-2\dot{r}^2 + \frac{1297943}{8400}\nu\dot{r}^2 - \frac{2969}{16}\pi^2\nu\dot{r}^2 + \frac{1255151}{840}\nu^2\dot{r}^2 + \frac{7095}{32}\pi^2\nu^2\dot{r}^2 - 17\nu^3\dot{r}^2\right.$$
$$- 24\nu^4\dot{r}^2 + 384\ln\left(\frac{r}{r'_0}\right)\dot{r}^2 - 920\nu\ln\left(\frac{r}{r'_0}\right)\dot{r}^2 + 3100\nu^2\ln\left(\frac{r}{r'_0}\right)\dot{r}^2 - 384\ln\left(\frac{r}{r''_0}\right)\dot{r}^2$$
$$+ 3152\nu\ln\left(\frac{r}{r''_0}\right)\dot{r}^2 - 6464\nu^2\ln\left(\frac{r}{r''_0}\right)\dot{r}^2 + \frac{1237279}{25200}\nu v^2 + \frac{3835}{96}\pi^2\nu v^2 - \frac{693947}{2520}\nu^2v^2$$
$$- \frac{229}{8}\pi^2\nu^2v^2 + \frac{19}{2}\nu^3v^2 - 64\ln\left(\frac{r}{r'_0}\right)v^2 + 80\nu\ln\left(\frac{r}{r'_0}\right)v^2 - \frac{1616}{3}\nu^2\ln\left(\frac{r}{r'_0}\right)v^2$$
$$\left.+64\ln\left(\frac{r}{r''_0}\right)v^2 - \frac{1576}{3}\nu\ln\left(\frac{r}{r''_0}\right)v^2 + \frac{3232}{3}\nu^2\ln\left(\frac{r}{r''_0}\right)v^2\right), \tag{7.12g}$$

$$A^{(4)}_{4\mathrm{PN}} = \frac{m^4}{r^4}\left(25 + \frac{6625537}{12600}\nu - \frac{4543}{96}\pi^2\nu + \frac{477763}{720}\nu^2 + \frac{3}{4}\pi^2\nu^2 + 16\ln\left(\frac{r}{r'_0}\right) - 20\nu\ln\left(\frac{r}{r'_0}\right)\right.$$
$$\left.+98\nu^2\ln\left(\frac{r}{r'_0}\right) - 16\ln\left(\frac{r}{r''_0}\right) + \frac{394}{3}\nu\ln\left(\frac{r}{r''_0}\right) - \frac{808}{3}\nu^2\ln\left(\frac{r}{r''_0}\right)\right). \tag{7.12h}$$

Similarly

$$B_{1\mathrm{PN}} = -4\,\dot{r} + 2\,\dot{r}\,\nu\,, \tag{7.13a}$$

$$B_{2\mathrm{PN}} = \frac{9\,\dot{r}^3\,\nu}{2} + 3\,\dot{r}^3\,\nu^2 - \frac{15\,\dot{r}\,\nu\,v^2}{2} - 2\,\dot{r}\,\nu^2\,v^2$$
$$+ \frac{Gm}{r}\left(2\,\dot{r} + \frac{41\,\dot{r}\,\nu}{2} + 4\,\dot{r}\,\nu^2\right), \tag{7.13b}$$

$$B_{3\mathrm{PN}} = -\frac{45\,\dot{r}^5\,\nu}{8} + 15\,\dot{r}^5\,\nu^2 + \frac{15\,\dot{r}^5\,\nu^3}{4} + 12\,\dot{r}^3\,\nu\,v^2 - \frac{111\,\dot{r}^3\,\nu^2\,v^2}{4} - 12\,\dot{r}^3\,\nu^3\,v^2$$
$$- \frac{65\,\dot{r}\,\nu\,v^4}{8} + 19\,\dot{r}\,\nu^2\,v^4 + 6\,\dot{r}\,\nu^3\,v^4 + \frac{Gm}{r}\left(\frac{329\,\dot{r}^3\,\nu}{6} + \frac{59\,\dot{r}^3\,\nu^2}{2} + 18\,\dot{r}^3\,\nu^3\right.$$

$$-15\,\dot{r}\,\nu\,v^2 - 27\,\dot{r}\,\nu^2\,v^2 - 10\,\dot{r}\,\nu^3\,v^2\Big) + \frac{G^2m^2}{r^2}\,\Bigg(-4\,\dot{r} - \frac{18169\,\dot{r}\,\nu}{840}$$

$$+25\,\dot{r}\,\nu^2 + 8\,\dot{r}\,\nu^3 - \frac{123\,\dot{r}\,\nu\,\pi^2}{32} + 44\,\dot{r}\,\nu\,\ln\left(\frac{r}{r'_0}\right)\Bigg)\,, \tag{7.13c}$$

$$B^{(0)}_{4\text{PN}} = \left(\frac{105}{16}\nu - \frac{245}{8}\nu^2 + \frac{385}{16}\nu^3 + \frac{35}{8}\nu^4\right)\dot{r}^7 + \left(-\frac{165}{8}\nu + \frac{1665}{16}\nu^2 - \frac{1725}{16}\nu^3 - \frac{105}{4}\nu^4\right)\dot{r}^5v^2$$
$$+ \left(\frac{45}{2}\nu - \frac{1869}{16}\nu^2 + 129\nu^3 + 54\nu^4\right)\dot{r}^3v^4 + \left(-\frac{157}{16}\nu + 54\nu^2\right.$$
$$\left. - 69\nu^3 - 24\nu^4\right)\dot{r}v^6\,, \tag{7.13d}$$

$$B^{(1)}_{4\text{PN}} = \frac{m}{r}\left(-\frac{54319}{160}\nu\dot{r}^5 - \frac{901}{8}\nu^2\dot{r}^5 + 60\nu^3\dot{r}^5 + 30\nu^4\dot{r}^5 + \frac{25943}{48}\nu\dot{r}^3v^2 + \frac{1199}{12}\nu^2\dot{r}^3v^2\right.$$
$$\left.-\frac{349}{2}\nu^3\dot{r}^3v^2 - 98\nu^4\dot{r}^3v^2 - \frac{5725}{32}\nu\dot{r}v^4 - \frac{389}{8}\nu^2\dot{r}v^4 + 118\nu^3\dot{r}v^4 + 44\nu^4\dot{r}v^4\right)\,, \tag{7.13e}$$

$$B^{(2)}_{4\text{PN}} = \frac{m^2}{r^2}\left(-\frac{9130111}{3360}\nu\dot{r}^3 - \frac{4695}{256}\pi^2\nu\dot{r}^3 - \frac{184613}{112}\nu^2\dot{r}^3 + \frac{1845}{64}\pi^2\nu^2\dot{r}^3 + \frac{209}{2}\nu^3\dot{r}^3 + 74\nu^4\dot{r}^3\right.$$
$$+ 660\nu\ln\left(\frac{r}{r'_0}\right)\dot{r}^3 - 330\nu^2\ln\left(\frac{r}{r'_0}\right)\dot{r}^3 - 220\nu\ln\left(\frac{r}{r''_0}\right)\dot{r}^3 + 880\nu^2\ln\left(\frac{r}{r''_0}\right)\dot{r}^3 + \frac{8692601}{5600}\nu\dot{r}v^2$$
$$+ \frac{1455}{256}\pi^2\nu\dot{r}v^2 + \frac{58557}{70}\nu^2\dot{r}v^2 - \frac{123}{8}\pi^2\nu^2\dot{r}v^2 - 70\nu^3\dot{r}v^2 - 34\nu^4\dot{r}v^2 - 264\nu\ln\left(\frac{r}{r'_0}\right)\dot{r}v^2$$
$$\left.+176\nu^2\ln\left(\frac{r}{r'_0}\right)\dot{r}v^2 + 110\nu\ln\left(\frac{r}{r''_0}\right)\dot{r}v^2 - 440\nu^2\ln\left(\frac{r}{r''_0}\right)\dot{r}v^2\right)\,, \tag{7.13f}$$

$$B^{(3)}_{4\text{PN}} = \frac{m^3}{r^3}\left(2 - \frac{619267}{525}\nu + \frac{791}{16}\pi^2\nu - \frac{28406}{45}\nu^2 - \frac{2201}{32}\pi^2\nu^2 + 66\nu^3 + 16\nu^4 - 128\ln\left(\frac{r}{r'_0}\right)\right.$$
$$+ 600\nu\ln\left(\frac{r}{r'_0}\right) - \frac{3188}{3}\nu^2\ln\left(\frac{r}{r'_0}\right) + 128\ln\left(\frac{r}{r''_0}\right) - \frac{3284}{3}\nu\ln\left(\frac{r}{r''_0}\right)$$
$$\left.+\frac{6992}{3}\nu^2\ln\left(\frac{r}{r''_0}\right)\right)\dot{r}\,. \tag{7.13g}$$

7.1.3 Lagrangian in the center of mass frame

7.1.3.a) The general method

The previous CM equations of motion actually derive from a Lagrangian. This Lagrangian, which is also a generalized one[2], can be constructed as follows. We start from the general-frame Lagrangian, which is a functional of $\boldsymbol{y}_A$, $\boldsymbol{v}_A$ and $\boldsymbol{a}_A$, and admits the CM integral $\boldsymbol{G}[\boldsymbol{y}_A, \boldsymbol{v}_A]$ explicitly given by (7.5)–(7.6). Then, we perform the change of variables $(\boldsymbol{y}_1, \boldsymbol{y}_2) \longrightarrow (\boldsymbol{x}, \boldsymbol{G})$, where we recall that $\boldsymbol{x} = \boldsymbol{y}_1 - \boldsymbol{y}_2$. Since to Newtonian order we have $\boldsymbol{G} = m_1\,\boldsymbol{y}_1 + m_2\,\boldsymbol{y}_2 + \mathcal{O}(c^{-2})$, we find for instance $\boldsymbol{y}_1 = X_2\boldsymbol{x} + \frac{1}{m}\boldsymbol{G} + \mathcal{O}(c^{-2})$ and $\boldsymbol{v}_1 = X_2\boldsymbol{v} + \frac{1}{m}\frac{\mathrm{d}\boldsymbol{G}}{\mathrm{d}t} + \mathcal{O}(c^{-2})$. Proceeding iteratively with the help of (7.5)–(7.6), it is easy to see that the old variables $\boldsymbol{y}_A$ are obtained as functionals of the new variables $(\boldsymbol{x}, \boldsymbol{G})$ and their derivatives up to some high differentiation order depending on the PN order. In the

[2]I.e. it depends also on the acceleration.

process, we do not perform any order reduction of accelerations, so that we get

$$\boldsymbol{y}_A = \boldsymbol{y}_A\big[\boldsymbol{x},\boldsymbol{v},\boldsymbol{a},\cdots;\boldsymbol{G},\tfrac{\mathrm{d}\boldsymbol{G}}{\mathrm{d}t},\tfrac{\mathrm{d}^2\boldsymbol{G}}{\mathrm{d}t^2},\cdots\big]\,. \tag{7.14}$$

Plugging those relations into the original general-frame Lagrangian and performing time derivatives, but still without order reduction of the accelerations, yields an equivalent Lagrangian, which is now "doubly generalized" in terms of the two types of variables, *i.e.*

$$L = L\big[\boldsymbol{x},\boldsymbol{v},\boldsymbol{a},\cdots;\boldsymbol{G},\tfrac{\mathrm{d}\boldsymbol{G}}{\mathrm{d}t},\tfrac{\mathrm{d}^2\boldsymbol{G}}{\mathrm{d}t^2},\cdots\big]\,. \tag{7.15}$$

The ensuing equations of motion read

$$\frac{\delta L}{\delta \boldsymbol{x}} \equiv \frac{\partial L}{\partial \boldsymbol{x}} - \frac{\mathrm{d}}{\mathrm{d}t}\left(\frac{\partial L}{\partial \boldsymbol{v}}\right) + \frac{\mathrm{d}^2}{\mathrm{d}t^2}\left(\frac{\partial L}{\partial \boldsymbol{a}}\right) + \cdots = \boldsymbol{0}\,, \tag{7.16}$$

together with the equation $\frac{\delta L}{\delta \boldsymbol{G}} = 0$, which is necessarily equivalent to the conservation law for the CM integral, hence we have

$$\frac{\delta L}{\delta \boldsymbol{G}} = \boldsymbol{0} \quad\Longleftrightarrow\quad \frac{\mathrm{d}^2\boldsymbol{G}}{\mathrm{d}t^2} = \boldsymbol{0}\,. \tag{7.17}$$

As a result, we can choose $\boldsymbol{G} = 0$ as a solution of these equations. The CM equations of motion are then given by (7.16) in which we pose, everywhere, $\boldsymbol{G} = \boldsymbol{0}$, $\frac{\mathrm{d}\boldsymbol{G}}{\mathrm{d}t} = \boldsymbol{0}$, $\cdots$; these equations are nothing but the CM equations of motion (7.11)–(7.13). Now it is clear, since (7.16) and (7.17) are independent, that those CM equations of motion derive precisely from the Lagrangian (7.15) in which we set, everywhere, $\boldsymbol{G} = \boldsymbol{0}$, $\frac{\mathrm{d}\boldsymbol{G}}{\mathrm{d}t} = \boldsymbol{0}$, $\cdots$, hence the CM Lagrangian is

$$L_{\mathrm{CM}} = L\big[\boldsymbol{x},\boldsymbol{v},\boldsymbol{a},\cdots;\boldsymbol{0},\boldsymbol{0},\cdots\big]\,. \tag{7.18}$$

7.1.3.b) Result

Using the usual notations, the CM Lagrangian is given by $\mathcal{L} = L_{\mathrm{CM}}/\mu$, where

$$\mathcal{L}_{\mathrm{N}} = \frac{v^2}{2} + \frac{Gm}{r}\,, \tag{7.19a}$$

$$\mathcal{L}_{1\mathrm{PN}} = \frac{v^4}{8} - \frac{3\,\nu\,v^4}{8} + \frac{Gm}{r}\left(\frac{\dot{r}^2\,\nu}{2} + \frac{3\,v^2}{2} + \frac{\nu\,v^2}{2}\right) - \frac{G^2m^2}{2\,r^2}\,, \tag{7.19b}$$

$$\begin{aligned}\mathcal{L}_{2\mathrm{PN}} = {}& \frac{v^6}{16} - \frac{7\,\nu\,v^6}{16} + \frac{13\,\nu^2\,v^6}{16} \\ & + \frac{Gm}{r}\left(\frac{3\,\dot{r}^4\,\nu^2}{8} - \frac{\dot{r}^2\,a_n\,\nu\,r}{8} + \frac{\dot{r}^2\,\nu\,v^2}{4} - \frac{5\,\dot{r}^2\,\nu^2\,v^2}{4} + \frac{7\,a_n\,\nu\,r\,v^2}{8}\right. \\ & \qquad \left. + \frac{7\,v^4}{8} - \frac{5\,\nu\,v^4}{4} - \frac{9\,\nu^2\,v^4}{8} - \frac{7\,\dot{r}\,\nu\,r\,a_v}{4}\right) \\ & + \frac{G^2m^2}{r^2}\left(\frac{\dot{r}^2}{2} + \frac{41\,\dot{r}^2\,\nu}{8} + \frac{3\,\dot{r}^2\,\nu^2}{2} + \frac{7\,v^2}{4} - \frac{27\,\nu\,v^2}{8} + \frac{\nu^2\,v^2}{2}\right) \\ & + \frac{G^3m^3}{r^3}\left(\frac{1}{2} + \frac{15\,\nu}{4}\right)\,, \end{aligned} \tag{7.19c}$$

$$
\begin{aligned}
\mathcal{L}_{3\mathrm{PN}} = {} & \frac{5\,v^8}{128} - \frac{59\,\nu\,v^8}{128} + \frac{119\,\nu^2\,v^8}{64} - \frac{323\,\nu^3\,v^8}{128} \\
& + \frac{Gm}{r}\left(\frac{5\,\dot r^6\,\nu^3}{16} + \frac{\dot r^4\,a_n\,\nu\,r}{16} - \frac{5\,\dot r^4\,a_n\,\nu^2\,r}{16} - \frac{3\,\dot r^4\,\nu\,v^2}{16}\right. \\
& \quad + \frac{7\,\dot r^4\,\nu^2\,v^2}{4} - \frac{33\,\dot r^4\,\nu^3\,v^2}{16} - \frac{3\,\dot r^2\,a_n\,\nu\,r\,v^2}{16} - \frac{\dot r^2\,a_n\,\nu^2\,r\,v^2}{16} \\
& \quad + \frac{5\,\dot r^2\,\nu\,v^4}{8} - 3\,\dot r^2\,\nu^2\,v^4 + \frac{75\,\dot r^2\,\nu^3\,v^4}{16} + \frac{7\,a_n\,\nu\,r\,v^4}{8} \\
& \quad - \frac{7\,a_n\,\nu^2\,r\,v^4}{2} + \frac{11\,v^6}{16} - \frac{55\,\nu\,v^6}{16} + \frac{5\,\nu^2\,v^6}{2} \\
& \quad + \frac{65\,\nu^3\,v^6}{16} + \frac{5\,\dot r^3\,\nu\,r\,a_v}{12} - \frac{13\,\dot r^3\,\nu^2\,r\,a_v}{8} \\
& \quad \left. - \frac{37\,\dot r\,\nu\,r\,v^2\,a_v}{8} + \frac{35\,\dot r\,\nu^2\,r\,v^2\,a_v}{4}\right) \\
& + \frac{G^2m^2}{r^2}\left(-\frac{109\,\dot r^4\,\nu}{144} - \frac{259\,\dot r^4\,\nu^2}{36} + 2\,\dot r^4\,\nu^3 - \frac{17\,\dot r^2\,a_n\,\nu\,r}{6}\right. \\
& \quad + \frac{97\,\dot r^2\,a_n\,\nu^2\,r}{12} + \frac{\dot r^2\,v^2}{4} - \frac{41\,\dot r^2\,\nu\,v^2}{6} - \frac{2287\,\dot r^2\,\nu^2\,v^2}{48} \\
& \quad - \frac{27\,\dot r^2\,\nu^3\,v^2}{4} + \frac{203\,a_n\,\nu\,r\,v^2}{12} + \frac{149\,a_n\,\nu^2\,r\,v^2}{6} \\
& \quad + \frac{45\,v^4}{16} + \frac{53\,\nu\,v^4}{24} + \frac{617\,\nu^2\,v^4}{24} - \frac{9\,\nu^3\,v^4}{4} \\
& \quad \left. - \frac{235\,\dot r\,\nu\,r\,a_v}{24} + \frac{235\,\dot r\,\nu^2\,r\,a_v}{6}\right) \\
& + \frac{G^3m^3}{r^3}\left(\frac{3\,\dot r^2}{2} - \frac{12041\,\dot r^2\,\nu}{420} + \frac{37\,\dot r^2\,\nu^2}{4} + \frac{7\,\dot r^2\,\nu^3}{2} - \frac{123\,\dot r^2\,\nu\,\pi^2}{64}\right. \\
& \quad + \frac{5\,v^2}{4} + \frac{387\,\nu\,v^2}{70} - \frac{7\,\nu^2\,v^2}{4} + \frac{\nu^3\,v^2}{2} + \frac{41\,\nu\,\pi^2\,v^2}{64} \\
& \quad \left. + 22\,\dot r^2\,\nu\,\ln\left(\frac{r}{r_0'}\right) - \frac{22\,\nu\,v^2}{3}\ln\left(\frac{r}{r_0'}\right)\right) \\
& + \frac{G^4m^4}{r^4}\left(-\frac{3}{8} - \frac{18469\,\nu}{840} + \frac{22\,\nu}{3}\ln\left(\frac{r}{r_0'}\right)\right), \qquad (7.19\mathrm{d})
\end{aligned}
$$

$$
\mathcal{L}^{(0)}_{4\mathrm{PN}} = \frac{7}{256}v^{10} - \frac{121}{256}\nu v^{10} + \frac{785}{256}\nu^2 v^{10} - \frac{1127}{128}\nu^3 v^{10} + \frac{2415}{256}\nu^4 v^{10}, \qquad (7.19\mathrm{e})
$$

$$
\begin{aligned}
\mathcal{L}^{(1)}_{4\mathrm{PN}} = \frac{m}{r}\Bigg(& \frac{23}{20}\nu^2 a_v r\dot r^5 - \frac{5}{128}\nu\dot r^8 + \frac{35}{128}\nu^2\dot r^8 - \frac{35}{64}\nu^3\dot r^8 + \frac{35}{128}\nu^4\dot r^8 + \frac{7}{4}\nu a_v r\dot r^3 v^2 \\
& + \frac{361}{24}\nu^3 a_v r\dot r^3 v^2 + \frac{19}{32}\nu a_n r\dot r^4 v^2 + \frac{85}{32}\nu^3 a_n r\dot r^4 v^2 - \frac{5}{16}\nu\dot r^6 v^2 - \frac{31}{16}\nu^2\dot r^6 v^2 \\
& + \frac{45}{32}\nu^3\dot r^6 v^2 - \frac{85}{32}\nu^4\dot r^6 v^2 + \frac{341}{4}\nu^2 a_v r\dot r v^4 + \frac{245}{32}\nu^2 a_n r\dot r^2 v^4 - \frac{17}{64}\nu\dot r^4 v^4 - \frac{11}{8}\nu^2\dot r^4 v^4 \\
& - \frac{193}{16}\nu^3\dot r^4 v^4 + \frac{693}{64}\nu^4\dot r^4 v^4 + \frac{217}{96}\nu a_n r v^6 + \frac{2261}{96}\nu^3 a_n r v^6 - \frac{11}{48}\nu\dot r^2 v^6 - \frac{29}{4}\nu^2\dot r^2 v^6
\end{aligned}
$$

$$+\frac{1021}{96}\nu^3\dot{r}^2v^6-\frac{665}{32}\nu^4\dot{r}^2v^6+\frac{75}{128}v^8-\frac{1595}{384}\nu v^8+\frac{2917}{128}\nu^2v^8+\frac{493}{192}\nu^3v^8$$
$$-\frac{2261}{128}\nu^4v^8\Bigg)\,, \tag{7.19f}$$

$$\mathcal{L}^{(2)}_{4\text{PN}}=\frac{m^2}{r^2}\Bigg(\frac{5407}{288}\nu a_v r\dot{r}^3-\frac{5531}{3200}\nu\dot{r}^6-\frac{487}{40}\nu^2\dot{r}^6+\frac{13}{5}\nu^3\dot{r}^6+\frac{3}{2}\nu^4\dot{r}^6+\frac{11497}{48}\nu^2a_v r\dot{r}v^2$$
$$+\frac{469}{4}\nu^3a_v r\dot{r}v^2+\frac{517}{48}\nu^2a_n r\dot{r}^2v^2-\frac{61183}{5760}\nu\dot{r}^4v^2+\frac{3079}{96}\nu^2\dot{r}^4v^2-\frac{161}{8}\nu^3\dot{r}^4v^2$$
$$-\frac{27}{2}\nu^4\dot{r}^4v^2+\frac{14627}{384}\nu a_n rv^4+\frac{3}{16}\dot{r}^2v^4-\frac{12091}{640}\nu\dot{r}^2v^4-\frac{22045}{192}\nu^2\dot{r}^2v^4+\frac{255}{64}\nu^3\dot{r}^2v^4$$
$$+\frac{569}{16}\nu^4\dot{r}^2v^4+\frac{115}{32}v^6+\frac{593}{120}\nu v^6+\frac{9467}{192}\nu^2v^6+\frac{599}{64}\nu^3v^6+\frac{195}{16}\nu^4v^6\Bigg)\,, \tag{7.19g}$$

$$\mathcal{L}^{(3)}_{4\text{PN}}=\frac{m^3}{r^3}\Bigg(\frac{4937}{1260}\nu^2a_v r\dot{r}-\frac{41}{32}\pi^2\nu^2a_v r\dot{r}+\frac{44}{3}\nu^2a_v r\ln\left(\frac{r}{r'_0}\right)\dot{r}+\frac{22}{3}\nu a_v r\ln\left(\frac{r}{r''_0}\right)\dot{r}-\frac{246373}{2240}\nu\dot{r}^4$$
$$-\frac{2155}{1024}\pi^2\nu\dot{r}^4-\frac{210733}{2016}\nu^2\dot{r}^4+\frac{205}{128}\pi^2\nu^2\dot{r}^4+\frac{367}{32}\nu^3\dot{r}^4+\frac{29}{4}\nu^4\dot{r}^4-\frac{55}{3}\nu^2\ln\left(\frac{r}{r'_0}\right)\dot{r}^4$$
$$-\frac{55}{3}\nu\ln\left(\frac{r}{r''_0}\right)\dot{r}^4+\frac{220}{3}\nu^2\ln\left(\frac{r}{r''_0}\right)\dot{r}^4+\frac{229319}{6300}\nu a_n rv^2-\frac{21}{32}\pi^2\nu a_n rv^2+\frac{49}{4}\nu^3a_n rv^2$$
$$+44\nu a_n r\ln\left(\frac{r}{r'_0}\right)v^2+\frac{44}{3}\nu^2a_n r\ln\left(\frac{r}{r''_0}\right)v^2+\frac{7}{4}\dot{r}^2v^2+\frac{516319}{4200}\nu\dot{r}^2v^2+\frac{447}{512}\pi^2\nu\dot{r}^2v^2$$
$$+\frac{53099}{560}\nu^2\dot{r}^2v^2+\frac{123}{64}\pi^2\nu^2\dot{r}^2v^2-\frac{1003}{16}\nu^3\dot{r}^2v^2-\frac{47}{2}\nu^4\dot{r}^2v^2-55\nu\ln\left(\frac{r}{r'_0}\right)\dot{r}^2v^2$$
$$-22\nu^2\ln\left(\frac{r}{r'_0}\right)\dot{r}^2v^2+11\nu\ln\left(\frac{r}{r''_0}\right)\dot{r}^2v^2-88\nu^2\ln\left(\frac{r}{r''_0}\right)\dot{r}^2v^2+\frac{91}{16}v^4-\frac{166703}{20160}\nu v^4$$
$$+\frac{133}{1024}\pi^2\nu v^4+\frac{10601}{3360}\nu^2v^4-\frac{123}{128}\pi^2\nu^2v^4+\frac{567}{32}\nu^3v^4-\frac{15}{4}\nu^4v^4+\frac{55}{3}\nu\ln\left(\frac{r}{r'_0}\right)v^4$$
$$+11\nu^2\ln\left(\frac{r}{r'_0}\right)v^4+\frac{44}{3}\nu^2\ln\left(\frac{r}{r''_0}\right)v^4\Bigg)\,, \tag{7.19h}$$

$$\mathcal{L}^{(4)}_{4\text{PN}}=\frac{m^4}{r^4}\Bigg(\frac{9}{4}\dot{r}^2-\frac{245971}{4200}\nu\dot{r}^2+\frac{2771}{96}\pi^2\nu\dot{r}^2-\frac{8089}{140}\nu^2\dot{r}^2-44\pi^2\nu^2\dot{r}^2+\frac{185}{8}\nu^3\dot{r}^2+\frac{15}{2}\nu^4\dot{r}^2$$
$$-64\ln\left(\frac{r}{r'_0}\right)\dot{r}^2+\frac{482}{3}\nu\ln\left(\frac{r}{r'_0}\right)\dot{r}^2-436\nu^2\ln\left(\frac{r}{r'_0}\right)\dot{r}^2+64\ln\left(\frac{r}{r''_0}\right)\dot{r}^2-\frac{1499}{3}\nu\ln\left(\frac{r}{r''_0}\right)\dot{r}^2$$
$$+\frac{2924}{3}\nu^2\ln\left(\frac{r}{r''_0}\right)\dot{r}^2+\frac{15}{16}v^2+\frac{2039993}{50400}\nu v^2-\frac{191}{32}\pi^2\nu v^2-\frac{52907}{1008}\nu^2v^2+11\pi^2\nu^2v^2$$
$$-\frac{1}{8}\nu^3v^2+\frac{1}{2}\nu^4v^2+16\ln\left(\frac{r}{r'_0}\right)v^2-\frac{71}{3}\nu\ln\left(\frac{r}{r'_0}\right)v^2+\frac{349}{3}\nu^2\ln\left(\frac{r}{r'_0}\right)v^2-16\ln\left(\frac{r}{r''_0}\right)v^2$$
$$+124\nu\ln\left(\frac{r}{r''_0}\right)v^2-240\nu^2\ln\left(\frac{r}{r''_0}\right)v^2\Bigg)\,, \tag{7.19i}$$

$$\mathcal{L}^{(5)}_{4\text{PN}}=\frac{m^5}{r^5}\Bigg(\frac{3}{8}+\frac{1697177}{25200}\nu+\frac{105}{32}\pi^2\nu+\frac{55111}{720}\nu^2-11\pi^2\nu^2-16\ln\left(\frac{r}{r'_0}\right)+\frac{82}{3}\nu\ln\left(\frac{r}{r'_0}\right)$$
$$-120\nu^2\ln\left(\frac{r}{r'_0}\right)+16\ln\left(\frac{r}{r''_0}\right)-124\nu\ln\left(\frac{r}{r''_0}\right)+240\nu^2\ln\left(\frac{r}{r''_0}\right)\Bigg)\,. \tag{7.19j}$$

The CM Lagrangian in harmonic coordinates still depends on accelerations starting at 2PN order, through $a_n=\boldsymbol{a}\cdot\boldsymbol{n}$ and $a_v=\boldsymbol{a}\cdot\boldsymbol{v}$, as well as logarithms of r/r'_0 and r/r''_0 (cf (7.10) for a definition of r_0' and r_0'').

7.1.4 Energy and angular momentum in the center of mass frame

Now that the CM position is defined at 4PN, we can compute the conserved energy and the conserved angular momentum at this order in the CM frame. The following quantities can be computed in two ways: we can take the CM Lagrangian defined in the previous section and compute them using Noether's theorem, or we can compute them from the Fokker Lagrangian presented in appendix B, and then apply the CM transformation (7.7) to the result. We used these two methods and explicitly checked that they provided the same answers, which is also a nice way to test our computations. We recall that we only provide here the conserved quantity of the instantaneous part of the dynamic. The tail contribution to these quantities are detailed in 7.2.

7.1.4.a) Energy

The reduced CM energy is defined by $\mathcal{E} = E/\mu$ where μ is the reduced mass $\mu \equiv (m_1 m_2)/(m_1 + m_2)$. It reads

$$\mathcal{E}_{\mathrm{N}} = \frac{v^2}{2} - \frac{Gm}{r}\,, \tag{7.20a}$$

$$\mathcal{E}_{1\mathrm{PN}} = \frac{3\,v^4}{8} - \frac{9\,\nu\,v^4}{8} + \frac{Gm}{r}\left(\frac{\dot{r}^2\,\nu}{2} + \frac{3\,v^2}{2} + \frac{\nu\,v^2}{2}\right) + \frac{G^2m^2}{2r^2}\,, \tag{7.20b}$$

$$\begin{aligned}\mathcal{E}_{2\mathrm{PN}} = {} & \frac{5\,v^6}{16} - \frac{35\,\nu\,v^6}{16} + \frac{65\,\nu^2\,v^6}{16} \\ & + \frac{Gm}{r}\left(-\frac{3\,\dot{r}^4\,\nu}{8} + \frac{9\,\dot{r}^4\,\nu^2}{8} + \frac{\dot{r}^2\,\nu\,v^2}{4} - \frac{15\,\dot{r}^2\,\nu^2\,v^2}{4} + \frac{21\,v^4}{8} - \frac{23\,\nu\,v^4}{8} - \frac{27\,\nu^2\,v^4}{8}\right) \\ & + \frac{G^2m^2}{r^2}\left(\frac{\dot{r}^2}{2} + \frac{69\,\dot{r}^2\,\nu}{8} + \frac{3\,\dot{r}^2\,\nu^2}{2} + \frac{7\,v^2}{4} - \frac{55\,\nu\,v^2}{8} + \frac{\nu^2\,v^2}{2}\right) \\ & + \frac{G^3m^3}{r^3}\left(-\frac{1}{2} - \frac{15\,\nu}{4}\right)\,,\end{aligned} \tag{7.20c}$$

$$\begin{aligned}\mathcal{E}_{3\mathrm{PN}} = {} & \frac{35\,v^8}{128} - \frac{413\,\nu\,v^8}{128} + \frac{833\,\nu^2\,v^8}{64} - \frac{2261\,\nu^3\,v^8}{128} \\ & + \frac{Gm}{r}\biggl(\frac{5\,\dot{r}^6\,\nu}{16} - \frac{25\,\dot{r}^6\,\nu^2}{16} + \frac{25\,\dot{r}^6\,\nu^3}{16} - \frac{9\,\dot{r}^4\,\nu\,v^2}{16} + \frac{21\,\dot{r}^4\,\nu^2\,v^2}{4} \\ & \quad - \frac{165\,\dot{r}^4\,\nu^3\,v^2}{16} - \frac{21\,\dot{r}^2\,\nu\,v^4}{16} - \frac{75\,\dot{r}^2\,\nu^2\,v^4}{16} + \frac{375\,\dot{r}^2\,\nu^3\,v^4}{16} \\ & \quad + \frac{55\,v^6}{16} - \frac{215\,\nu\,v^6}{16} + \frac{29\,\nu^2\,v^6}{4} + \frac{325\,\nu^3\,v^6}{16}\biggr) \\ & + \frac{G^2m^2}{r^2}\biggl(-\frac{731\,\dot{r}^4\,\nu}{48} + \frac{41\,\dot{r}^4\,\nu^2}{4} + 6\,\dot{r}^4\,\nu^3 + \frac{3\,\dot{r}^2\,v^2}{4} + \frac{31\,\dot{r}^2\,\nu\,v^2}{2} \\ & \quad - \frac{815\,\dot{r}^2\,\nu^2\,v^2}{16} - \frac{81\,\dot{r}^2\,\nu^3\,v^2}{4} + \frac{135\,v^4}{16} - \frac{97\,\nu\,v^4}{8} + \frac{203\,\nu^2\,v^4}{8} - \frac{27\,\nu^3\,v^4}{4}\biggr)\end{aligned}$$

$$+\frac{G^3m^3}{r^3}\left(\frac{3\,\dot{r}^2}{2}+\frac{803\,\dot{r}^2\,\nu}{840}+\frac{51\,\dot{r}^2\,\nu^2}{4}+\frac{7\,\dot{r}^2\,\nu^3}{2}-\frac{123\,\dot{r}^2\,\nu\,\pi^2}{64}+\frac{5\,v^2}{4}\right.$$
$$-\frac{6747\,\nu\,v^2}{280}-\frac{21\,\nu^2\,v^2}{4}+\frac{\nu^3\,v^2}{2}+\frac{41\,\nu\,\pi^2\,v^2}{64}$$
$$\left.+22\,\dot{r}^2\,\nu\,\ln\left(\frac{r}{r_0'}\right)-\frac{22\,\nu\,v^2}{3}\,\ln\left(\frac{r}{r_0'}\right)\right)$$
$$+\frac{G^4m^4}{r^4}\left(\frac{3}{8}+\frac{18469\,\nu}{840}-\frac{22\,\nu}{3}\,\ln\left(\frac{r}{r_0'}\right)\right)\,, \tag{7.20d}$$

$$\mathcal{E}^{(0)}_{4\mathrm{PN}}=\left(\frac{63}{256}-\frac{1089}{256}\nu+\frac{7065}{256}\nu^2-\frac{10143}{128}\nu^3+\frac{21735}{256}\nu^4\right)v^{10}\,, \tag{7.20e}$$

$$\mathcal{E}^{(1)}_{4\mathrm{PN}}=\frac{m}{r}\left(-\frac{35}{128}\nu\dot{r}^8+\frac{245}{128}\nu^2\dot{r}^8-\frac{245}{64}\nu^3\dot{r}^8+\frac{245}{128}\nu^4\dot{r}^8+\frac{25}{32}\nu\dot{r}^6v^2-\frac{125}{16}\nu^2\dot{r}^6v^2\right.$$
$$+\frac{185}{8}\nu^3\dot{r}^6v^2-\frac{595}{32}\nu^4\dot{r}^6v^2+\frac{27}{64}\nu\dot{r}^4v^4+\frac{243}{32}\nu^2\dot{r}^4v^4-\frac{1683}{32}\nu^3\dot{r}^4v^4+\frac{4851}{64}\nu^4\dot{r}^4v^4$$
$$-\frac{147}{32}\nu\dot{r}^2v^6+\frac{369}{32}\nu^2\dot{r}^2v^6+\frac{423}{8}\nu^3\dot{r}^2v^6-\frac{4655}{32}\nu^4\dot{r}^2v^6+\frac{525}{128}v^8-\frac{4011}{128}\nu v^8$$
$$\left.+\frac{9507}{128}\nu^2v^8-\frac{357}{64}\nu^3v^8-\frac{15827}{128}\nu^4v^8\right)\,, \tag{7.20f}$$

$$\mathcal{E}^{(2)}_{4\mathrm{PN}}=\frac{m^2}{r^2}\left(-\frac{4771}{640}\nu\dot{r}^6-\frac{461}{8}\nu^2\dot{r}^6-\frac{17}{2}\nu^3\dot{r}^6+\frac{15}{2}\nu^4\dot{r}^6+\frac{5347}{384}\nu\dot{r}^4v^2+\frac{19465}{96}\nu^2\dot{r}^4v^2\right.$$
$$-\frac{439}{8}\nu^3\dot{r}^4v^2-\frac{135}{2}\nu^4\dot{r}^4v^2+\frac{15}{16}\dot{r}^2v^4-\frac{5893}{128}\nu\dot{r}^2v^4-\frac{12995}{64}\nu^2\dot{r}^2v^4+\frac{18511}{64}\nu^3\dot{r}^2v^4$$
$$\left.+\frac{2845}{16}\nu^4\dot{r}^2v^4+\frac{575}{32}v^6-\frac{4489}{128}\nu v^6+\frac{5129}{64}\nu^2v^6-\frac{8289}{64}\nu^3v^6+\frac{975}{16}\nu^4v^6\right)\,, \tag{7.20g}$$

$$\mathcal{E}^{(3)}_{4\mathrm{PN}}=\frac{m^3}{r^3}\left(-\frac{2599207}{6720}\nu\dot{r}^4-\frac{6465}{1024}\pi^2\nu\dot{r}^4-\frac{103205}{224}\nu^2\dot{r}^4+\frac{615}{128}\pi^2\nu^2\dot{r}^4+\frac{69}{32}\nu^3\dot{r}^4+\frac{87}{4}\nu^4\dot{r}^4\right.$$
$$-55\nu^2\ln\left(\frac{r}{r_0'}\right)\dot{r}^4-55\nu\ln\left(\frac{r}{r_0''}\right)\dot{r}^4+220\nu^2\ln\left(\frac{r}{r_0''}\right)\dot{r}^4+\frac{21}{4}\dot{r}^2v^2+\frac{1086923}{1680}\nu\dot{r}^2v^2$$
$$+\frac{333}{512}\pi^2\nu\dot{r}^2v^2+\frac{206013}{560}\nu^2\dot{r}^2v^2+\frac{123}{64}\pi^2\nu^2\dot{r}^2v^2-\frac{2437}{16}\nu^3\dot{r}^2v^2-\frac{141}{2}\nu^4\dot{r}^2v^2$$
$$-33\nu\ln\left(\frac{r}{r_0'}\right)\dot{r}^2v^2-22\nu^2\ln\left(\frac{r}{r_0'}\right)\dot{r}^2v^2+55\nu\ln\left(\frac{r}{r_0''}\right)\dot{r}^2v^2-220\nu^2\ln\left(\frac{r}{r_0''}\right)\dot{r}^2v^2+\frac{273}{16}v^4$$
$$-\frac{22649399}{100800}\nu v^4+\frac{1071}{1024}\pi^2\nu v^4+\frac{521063}{10080}\nu^2v^4-\frac{205}{128}\pi^2\nu^2v^4+\frac{2373}{32}\nu^3v^4-\frac{45}{4}\nu^4v^4$$
$$\left.+11\nu\ln\left(\frac{r}{r_0'}\right)v^4+\frac{55}{3}\nu^2\ln\left(\frac{r}{r_0'}\right)v^4-\frac{22}{3}\nu\ln\left(\frac{r}{r_0''}\right)v^4+\frac{88}{3}\nu^2\ln\left(\frac{r}{r_0''}\right)v^4\right)\,, \tag{7.20h}$$

$$\mathcal{E}^{(4)}_{4\mathrm{PN}}=\frac{m^4}{r^4}\left(\frac{9}{4}\dot{r}^2-\frac{1622437}{12600}\nu\dot{r}^2+\frac{2645}{96}\pi^2\nu\dot{r}^2-\frac{289351}{2520}\nu^2\dot{r}^2-\frac{1367}{32}\pi^2\nu^2\dot{r}^2+\frac{213}{8}\nu^3\dot{r}^2\right.$$
$$+\frac{15}{2}\nu^4\dot{r}^2-64\ln\left(\frac{r}{r_0'}\right)\dot{r}^2+\frac{746}{3}\nu\ln\left(\frac{r}{r_0'}\right)\dot{r}^2-\frac{1352}{3}\nu^2\ln\left(\frac{r}{r_0'}\right)\dot{r}^2+64\ln\left(\frac{r}{r_0''}\right)\dot{r}^2$$
$$-507\nu\ln\left(\frac{r}{r_0''}\right)\dot{r}^2+1004\nu^2\ln\left(\frac{r}{r_0''}\right)\dot{r}^2+\frac{15}{16}v^2+\frac{1859363}{16800}\nu v^2-\frac{149}{32}\pi^2\nu v^2$$
$$+\frac{22963}{5040}\nu^2v^2+\frac{311}{32}\pi^2\nu^2v^2-\frac{29}{8}\nu^3v^2+\frac{1}{2}\nu^4v^2+16\ln\left(\frac{r}{r_0'}\right)v^2-\frac{335}{3}\nu\ln\left(\frac{r}{r_0'}\right)v^2$$

$$+131\nu^2 \ln\left(\frac{r}{r'_0}\right)v^2 - 16\ln\left(\frac{r}{r''_0}\right)v^2 + \frac{394}{3}\nu\ln\left(\frac{r}{r''_0}\right)v^2 - \frac{808}{3}\nu^2\ln\left(\frac{r}{r''_0}\right)v^2\Big)\,, \tag{7.20i}$$

$$\mathcal{E}^{(5)}_{4\mathrm{PN}} = \frac{m^5}{r^5}\Big(-\frac{3}{8} - \frac{1697177}{25200}\nu - \frac{105}{32}\pi^2\nu - \frac{55111}{720}\nu^2 + 11\pi^2\nu^2 + 16\ln\left(\frac{r}{r'_0}\right) - \frac{82}{3}\nu\ln\left(\frac{r}{r'_0}\right)$$
$$+120\nu^2\ln\left(\frac{r}{r'_0}\right) - 16\ln\left(\frac{r}{r''_0}\right) + 124\nu\ln\left(\frac{r}{r''_0}\right) - 240\nu^2\ln\left(\frac{r}{r''_0}\right)\Big)\,, \tag{7.20j}$$

7.1.4.b) Angular momentum

The reduced CM angular momentum is defined by $\mathcal{J} = J/J_\mathrm{N}$, which is the Euclidean norm $J = |\boldsymbol{J}|$ rescaled by that of the Newtonian angular momentum $\boldsymbol{J}_\mathrm{N} = \mu\,\boldsymbol{x}\times\boldsymbol{v}$. We have

$$\mathcal{J}_\mathrm{N} = 1\,, \tag{7.21a}$$

$$\mathcal{J}_{1\mathrm{PN}} = (1-3\,\nu)\,\frac{v^2}{2} + \frac{Gm}{r}\,(3+\nu)\,, \tag{7.21b}$$

$$\mathcal{J}_{2\mathrm{PN}} = \frac{3\,v^4}{8} - \frac{21\,\nu\,v^4}{8} + \frac{39\,\nu^2\,v^4}{8}$$
$$+\frac{Gm}{r}\left(-\dot{r}^2\,\nu - \frac{5\,\dot{r}^2\,\nu^2}{2} + \frac{7\,v^2}{2} - 5\,\nu\,v^2 - \frac{9\,\nu^2\,v^2}{2}\right)$$
$$+\frac{G^2m^2}{r^2}\left(\frac{7}{2} - \frac{41\,\nu}{4} + \nu^2\right)\,, \tag{7.21c}$$

$$\mathcal{J}_{3\mathrm{PN}} = \frac{5\,v^6}{16} - \frac{59\,\nu\,v^6}{16} + \frac{119\,\nu^2\,v^6}{8} - \frac{323\,\nu^3\,v^6}{16}$$
$$+\frac{Gm}{r}\left(\frac{3\,\dot{r}^4\,\nu}{4} - \frac{3\,\dot{r}^4\,\nu^2}{4} - \frac{33\,\dot{r}^4\,\nu^3}{8} - 3\,\dot{r}^2\,\nu\,v^2 + \frac{7\,\dot{r}^2\,\nu^2\,v^2}{4}\right.$$
$$\left.+\frac{75\,\dot{r}^2\,\nu^3\,v^2}{4} + \frac{33\,v^4}{8} - \frac{71\,\nu\,v^4}{4} + \frac{53\,\nu^2\,v^4}{4} + \frac{195\,\nu^3\,v^4}{8}\right)$$
$$+\frac{G^2m^2}{r^2}\left(\frac{\dot{r}^2}{2} - \frac{287\,\dot{r}^2\,\nu}{24} - \frac{317\,\dot{r}^2\,\nu^2}{8} - \frac{27\,\dot{r}^2\,\nu^3}{2} + \frac{45\,v^2}{4}\right.$$
$$\left.-\frac{161\,\nu\,v^2}{6} + \frac{105\,\nu^2\,v^2}{4} - 9\,\nu^3\,v^2\right)$$
$$+\frac{G^3m^3}{r^3}\left(\frac{5}{2} - \frac{5199\,\nu}{280} - 7\,\nu^2 + \nu^3 + \frac{41\,\nu\,\pi^2}{32} - \frac{44\,\nu}{3}\ln\left(\frac{r}{r'_0}\right)\right)\,, \tag{7.21d}$$

$$\mathcal{J}^{(0)}_{4\mathrm{PN}} = \left(\frac{35}{128} - \frac{605}{128}\nu + \frac{3925}{128}\nu^2 - \frac{5635}{64}\nu^3 + \frac{12075}{128}\nu^4\right)v^8\,, \tag{7.21e}$$

$$\mathcal{J}^{(1)}_{4\mathrm{PN}} = \frac{m}{r}\Big(-\frac{5}{8}\nu\dot{r}^6 + \frac{15}{8}\nu^2\dot{r}^6 + \frac{45}{16}\nu^3\dot{r}^6 - \frac{85}{16}\nu^4\dot{r}^6 + 3\nu\dot{r}^4v^2 - \frac{45}{4}\nu^2\dot{r}^4v^2 - \frac{135}{16}\nu^3\dot{r}^4v^2$$
$$+\frac{693}{16}\nu^4\dot{r}^4v^2 - \frac{53}{8}\nu\dot{r}^2v^4 + \frac{423}{16}\nu^2\dot{r}^2v^4 + \frac{299}{16}\nu^3\dot{r}^2v^4 - \frac{1995}{16}\nu^4\dot{r}^2v^4 + \frac{75}{16}v^6$$
$$-\frac{151}{4}\nu v^6 + \frac{1553}{16}\nu^2v^6 - \frac{425}{16}\nu^3v^6 - \frac{2261}{16}\nu^4v^6\Big)\,, \tag{7.21f}$$

$$\mathcal{J}^{(2)}_{4\mathrm{PN}} = \frac{m^2}{r^2}\Big(\frac{14773}{320}\nu\dot{r}^4 + \frac{3235}{48}\nu^2\dot{r}^4 - \frac{155}{4}\nu^3\dot{r}^4 - 27\nu^4\dot{r}^4 + \frac{3}{4}\dot{r}^2v^2 - \frac{5551}{60}\nu\dot{r}^2v^2$$

$$
\begin{aligned}
&- \frac{256}{3}\nu^2\dot{r}^2v^2 + \frac{4459}{16}\nu^3\dot{r}^2v^2 + \frac{569}{4}\nu^4\dot{r}^2v^2 + \frac{345}{16}v^4 - \frac{65491}{960}\nu v^4 + \frac{12427}{96}\nu^2 v^4 \\
&- \frac{3845}{32}\nu^3 v^4 + \frac{585}{8}\nu^4 v^4\bigg) \,, \qquad (7.21g)
\end{aligned}
$$

$$
\begin{aligned}
\mathcal{J}^{(3)}_{4\mathrm{PN}} = \frac{m^3}{r^3}\bigg(&\frac{7}{2}\dot{r}^2 + \frac{7775977}{16800}\nu\dot{r}^2 + \frac{447}{256}\pi^2\nu\dot{r}^2 + \frac{121449}{560}\nu^2\dot{r}^2 - \frac{1025}{8}\nu^3\dot{r}^2 - 47\nu^4\dot{r}^2 \\
&- 110\nu\ln\left(\frac{r}{r_0'}\right)\dot{r}^2 + 44\nu\ln\left(\frac{r}{r_0''}\right)\dot{r}^2 - 176\nu^2\ln\left(\frac{r}{r_0''}\right)\dot{r}^2 + \frac{91}{4}v^2 - \frac{13576009}{50400}\nu v^2 \\
&+ \frac{469}{256}\pi^2\nu v^2 + \frac{276433}{5040}\nu^2 v^2 - \frac{41}{16}\pi^2\nu^2 v^2 + \frac{637}{8}\nu^3 v^2 - 15\nu^4 v^2 - \frac{44}{3}\nu\ln\left(\frac{r}{r_0'}\right)v^2 \\
&+ \frac{88}{3}\nu^2\ln\left(\frac{r}{r_0'}\right)v^2 - \frac{22}{3}\nu\ln\left(\frac{r}{r_0''}\right)v^2 + \frac{88}{3}\nu^2\ln\left(\frac{r}{r_0''}\right)v^2\bigg) \,, \qquad (7.21h)
\end{aligned}
$$

$$
\begin{aligned}
\mathcal{J}^{(4)}_{4\mathrm{PN}} = \frac{m^4}{r^4}\bigg(&\frac{15}{8} + \frac{3809041}{25200}\nu - \frac{85}{8}\pi^2\nu - \frac{20131}{420}\nu^2 + \frac{663}{32}\pi^2\nu^2 - \frac{15}{4}\nu^3 + \nu^4 + 32\ln\left(\frac{r}{r_0'}\right) \\
&- \frac{406}{3}\nu\ln\left(\frac{r}{r_0'}\right) + \frac{742}{3}\nu^2\ln\left(\frac{r}{r_0'}\right) - 32\ln\left(\frac{r}{r_0''}\right) + \frac{766}{3}\nu\ln\left(\frac{r}{r_0''}\right) \\
&- \frac{1528}{3}\nu^2\ln\left(\frac{r}{r_0''}\right)\bigg) \,. \qquad (7.21i)
\end{aligned}
$$

7.2 Circular orbit and dissipative effects

7.2.1 Effects of the tails

All the quantities provided so far did not take the non-local part of the action into account. The main reasons why we did so are that (i) there is no analytical closed form to express the acceleration and the contribution to the conserved quantities due to the tails unless we specify it for circular orbits, (ii) it turns out that even for generic orbits, the tails do not contribute to the conserved CM, therefore there was no need to take it into account to reduce all the quantities in the CM frame.

The non-local part of the Fokker Lagrangian is

$$
\begin{aligned}
L^{\mathrm{tail}} &= \frac{G^2M}{5c^8}\, I^{(3)}_{ij}(t) \underset{2r_{12}/c}{\mathrm{Pf}} \int_{-\infty}^{+\infty} \frac{\mathrm{d}t'}{|t-t'|} I^{(3)}_{ij}(t') \\
&= \frac{G^2M}{5c^8}\, I^{(3)}_{ij}(t) \int_0^{+\infty} \mathrm{d}\tau\, \ln\left(\frac{c\tau}{2r_{12}}\right)\left[I^{(4)}_{ij}(t-\tau) - I^{(4)}_{ij}(t+\tau)\right] \,. \qquad (7.22)
\end{aligned}
$$

The contribution of (7.22) to the acceleration in the CM is

$$
\begin{aligned}
a^{i\,\mathrm{tail}} = &- \frac{4G^2M}{5c^8}x^j \underset{2r_{12}/c}{\mathrm{Pf}} \int_{-\infty}^{+\infty} \frac{\mathrm{d}t'}{|t-t'|} I^{(6)}_{ij}(t') \\
&+ \frac{8G^2M}{5c^8}x^j\left[\left(I^{(3)}_{ij}\ln r\right)^{(3)} - I^{(6)}_{ij}\ln r\right] - \frac{2G^2}{5c^8\nu}\frac{n^i}{r}\left(I^{(3)}_{jk}\right)^2 \,. \qquad (7.23)
\end{aligned}
$$

Because of the non-locality of the (7.22), the contribution of the tails to the conserved energy and conserved angular momentum is rather complex to derive. A proper derivation of these quantities have been done in [93]. In the case of circular orbit, this derivation leads to analytically-closed results that we will simply provide in the following section. For the remaining of this chapter, all the presented quantities consistently include the tail effect.

7.2.2 Circular orbit

Now that we have the dynamics in the CM frame, we are in the position to reduce all the relevant quantities to the case of circular orbits. The conservative part of the relative acceleration is then given by the purely radial acceleration $\boldsymbol{a} = -\omega^2 \boldsymbol{x}$, the physical content of which is entirely encoded into the relation between the orbital frequency ω and the orbital separation r.

The tails contribution to ω ($\boldsymbol{a}^{\text{tail}} = -\omega^2_{\text{tail}}\, \boldsymbol{x}$) is [94, 3]

$$\omega^2_{\text{tail}} = \frac{128}{5}\frac{Gm}{r^3}\gamma^4\nu\Big[\ln(16\gamma) + 2\gamma_{\text{E}} + \frac{1}{2}\Big]\,, \tag{7.24}$$

where we have used the PN parameter γ defined as $\gamma \equiv \frac{GM}{rc^2}$; we recall that γ_{E} is Euler's constant.

The instantaneous contributions are computed by a straightforward reduction of the equations of motion (7.12)–(7.13) to circular orbits, with $\dot{r} = 0$ and $v^2 = r^2\omega^2$ (since we neglect the dissipative terms). Adding the tail contribution (7.24), we get

$$\begin{aligned}
\omega^2 = \frac{Gm}{r^3}\Bigg\{& 1 + (-3+\nu)\gamma + \left(6 + \frac{41}{4}\nu + \nu^2\right)\gamma^2 \\
&+ \left(-10 + \left[-\frac{75707}{840} + \frac{41}{64}\pi^2 + 22\ln\left(\frac{r}{r'_0}\right)\right]\nu + \frac{19}{2}\nu^2 + \nu^3\right)\gamma^3 + \Bigg(15 + 48\ln\left(\frac{r'_0}{r''_0}\right) \\
&+\nu\left[\frac{19644217}{33600} + \frac{163}{1024}\pi^2 + \frac{256}{5}\gamma_E + \frac{128}{5}\ln(16\gamma) + 82\ln\left(\frac{r}{r'_0}\right) - 372\ln\left(\frac{r}{r''_0}\right)\right] \\
&+\nu^2\left[\frac{44329}{336} - \frac{1907}{64}\pi^2 - \frac{992}{3}\ln\left(\frac{r}{r'_0}\right) + 720\ln\left(\frac{r}{r''_0}\right)\right] + \frac{51}{4}\nu^3 + \nu^4\Bigg)\gamma^4\Bigg\}\,.
\end{aligned} \tag{7.25}$$

This is a gauge dependent result, as the separation r refers to harmonic coordinates. It also depends on the gauge constants r'_0 and r''_0 defined in (7.10). Inverting (7.25), we express $\gamma = \frac{Gm}{rc^2}$ as a function of the orbital frequency ω or, rather, of the PN parameter $x \equiv (\frac{Gm\omega}{c^3})^{2/3}$ (cf equation (4.127))

$$\begin{aligned}
\gamma = x\Bigg\{& 1 + x\left(1 - \frac{1}{3}\nu\right) + x^2\left(1 - \frac{65}{12}\nu\right) \\
&+ x^3\left(1 + \nu\left[-\frac{2203}{2520} - \frac{41}{192}\pi^2 - \frac{22}{3}\ln\left(\frac{Gm}{c^2 r'_0}\right) + \frac{22}{3}\ln(x)\right] + \frac{229}{36}\nu^2 + \frac{\nu^3}{81}\right) \\
&+ x^4\Bigg(1 + 16\ln\left(\frac{Gm}{c^2 r'_0}\right) - 16\ln\left(\frac{Gm}{c^2 r''_0}\right) - \frac{1261}{324}\nu^3 + \frac{\nu^4}{243} \\
&\quad + \nu\left[-\frac{2067859}{33600} - \frac{256}{15}\gamma_E - \frac{5411}{3072}\pi^2 - 86\ln\left(\frac{Gm}{c^2 r'_0}\right)\right. \\
&\quad\quad \left. +124\ln\left(\frac{Gm}{c^2 r''_0}\right) - \frac{256}{15}\ln 4 - \frac{698}{15}\ln(x)\right]
\end{aligned}$$

$$+\nu^2\left[\frac{153613}{15120}+\frac{6049}{576}\pi^2+\frac{1168}{9}\ln\left(\frac{Gm}{c^2r_0'}\right)-240\ln\left(\frac{Gm}{c^2r_0''}\right)+\frac{992}{9}\ln(x)\right]\bigg)\bigg\}. \quad (7.26)$$

Let us deal next with the conserved energy as a function of the separation r. All the instantaneous terms in the CM frame are presented in (7.20). We just need to reduce it for circular orbits and add the contribution of the tails [94]. This leads to

$$\begin{aligned}E = -\frac{\mu c^2\gamma}{2}\bigg\{&1+\left(-\frac{7}{4}+\frac{1}{4}\nu\right)\gamma+\left(-\frac{7}{8}+\frac{49}{8}\nu+\frac{1}{8}\nu^2\right)\gamma^2+\bigg(-\frac{235}{64}\\&+\left[\frac{46031}{2240}-\frac{123}{64}\pi^2+\frac{22}{3}\ln\left(\frac{r}{r_0'}\right)\right]\nu+\frac{27}{32}\nu^2+\frac{5}{64}\nu^3\bigg)\gamma^3+\bigg(-\frac{649}{128}+16\ln\left(\frac{r_0'}{r_0''}\right)\\&+\nu\left[-\frac{3357833}{28800}+\frac{384}{5}\gamma_E+\frac{192}{5}\ln(16\gamma)+\frac{14935}{1024}\pi^2+31\ln\left(\frac{r}{r_0'}\right)-124\ln\left(\frac{r}{r_0''}\right)\right]\\&+\nu^2\left[\frac{83959}{8064}-\frac{957}{128}\pi^2-\frac{349}{3}\ln\left(\frac{r}{r_0'}\right)+240\ln\left(\frac{r}{r_0''}\right)\right]+\frac{69}{64}\nu^3+\frac{7}{128}\nu^4\bigg)\gamma^4\bigg\}. \quad (7.27)\end{aligned}$$

This result is not yet the invariant we are looking for, as it still depends on the constant r_0' and r_0''. However, these constants are canceled when we replace γ by the frequency-related gauge-invariant parameter x, using (7.26). Finally, we arrive at

$$\begin{aligned}E = -\frac{\mu c^2 x}{2}\bigg\{&1+\left(-\frac{3}{4}-\frac{\nu}{12}\right)x+\left(-\frac{27}{8}+\frac{19}{8}\nu-\frac{\nu^2}{24}\right)x^2\\&+\left(-\frac{675}{64}+\left[\frac{34445}{576}-\frac{205}{96}\pi^2\right]\nu-\frac{155}{96}\nu^2-\frac{35}{5184}\nu^3\right)x^3\\&+\bigg(-\frac{3969}{128}+\left[-\frac{123671}{5760}+\frac{9037}{1536}\pi^2+\frac{896}{15}\gamma_\mathrm{E}+\frac{448}{15}\ln(16x)\right]\nu\\&\quad+\left[-\frac{498449}{3456}+\frac{3157}{576}\pi^2\right]\nu^2+\frac{301}{1728}\nu^3+\frac{77}{31104}\nu^4\bigg)x^4\bigg\}. \quad (7.28)\end{aligned}$$

Equation (7.28) includes the tail contribution which reads

$$\tilde{E}^{\mathrm{tail}} = -\frac{224}{15}\mu c^2\nu x^5\left[\ln(16x)+2\gamma_\mathrm{E}+\frac{2}{7}\right]. \quad (7.29)$$

The 4PN angular momentum for circular orbits can be found either by a direct calculation, or from the *thermodynamic* relation $\frac{\mathrm{d}E}{\mathrm{d}\omega}=\omega\,\frac{\mathrm{d}J}{\mathrm{d}\omega}$, which is a particular case of the first law of compact binary mechanics; this law has been derived up to the 4PN order, taking into account the non locality associated with the tail effect [158]. We get

$$\begin{aligned}J = \frac{G\,\mu\,m}{c\,x^{1/2}}\bigg\{&1+\left(\frac{3}{2}+\frac{\nu}{6}\right)x+\left(\frac{27}{8}-\frac{19}{8}\nu+\frac{\nu^2}{24}\right)x^2\\&+\left(\frac{135}{16}+\left[-\frac{6889}{144}+\frac{41}{24}\pi^2\right]\nu+\frac{31}{24}\nu^2+\frac{7}{1296}\nu^3\right)x^3\\&+\bigg(\frac{2835}{128}+\left[\frac{98869}{5760}-\frac{6455}{1536}\pi^2-\frac{128}{3}\gamma_\mathrm{E}-\frac{64}{3}\ln(16x)\right]\nu\\&\quad+\left[\frac{356035}{3456}-\frac{2255}{576}\pi^2\right]\nu^2-\frac{215}{1728}\nu^3-\frac{55}{31104}\nu^4\bigg)x^4\bigg\}, \quad (7.30)\end{aligned}$$

with the tail contribution therein[3]

$$\tilde{J}^{\rm tail} = -\frac{64}{3}\frac{G\,\mu^2\,x^{7/2}}{c}\left[\ln\left(16x\right)+2\gamma_{\rm E}+\frac{1}{5}\right]. \tag{7.31}$$

7.2.3 Dissipative effects

So far, we have only considered the conservative part of the equations of motion, that are derived through the use of the Fokker Lagrangian. However, due to the emission of gravitational waves, dissipative effects should be included in the equations of motion. A first kind of dissipative terms are instantaneous and arise at the 2.5PN and the 3.5PN orders. They are well-known ([82, 83, 62, 159, 160, 80]) and are given here in the CM frame, with the notation of (7.11)–(7.13)

$$\begin{aligned}
A_{2.5\rm PN} &= \frac{8G\,m\,\nu}{5r}\dot{r}\left[-\frac{17}{3}\frac{Gm}{r}-3v^2\right], &(7.32a)\\
B_{2.5\rm PN} &= \frac{8G\,m\,\nu}{5r}\left[3\frac{Gm}{r}+v^2\right], &(7.32b)\\
A_{3.5\rm PN} &= \frac{Gm\nu}{r}\dot{r}\left[\frac{G^2m^2}{r^2}\left(\frac{3956}{35}+\frac{184}{5}\nu\right)+\frac{Gm\,v^2}{r}\left(\frac{692}{35}-\frac{724}{15}\nu\right)\right.\\
&\quad +v^4\left(\frac{366}{35}+12\nu\right)+\frac{Gm\,\dot{r}^2}{r}\left(\frac{294}{5}+\frac{376}{5}\nu\right)\\
&\quad \left.-v^2\dot{r}^2\left(114+12\nu\right)+112\dot{r}^4\right], &(7.32c)\\
B_{3.5\rm PN} &= \frac{Gm\nu}{r}\left[\frac{G^2m^2}{r^2}\left(-\frac{1060}{21}-\frac{104}{5}\nu\right)+\frac{Gmv^2}{r}\left(\frac{164}{21}+\frac{148}{5}\nu\right)\right.\\
&\quad +v^4\left(-\frac{626}{35}-\frac{12}{5}\nu\right)+\frac{Gm\dot{r}^2}{r}\left(-\frac{82}{3}-\frac{848}{15}\nu\right)\\
&\quad \left.+v^2\dot{r}^2\left(\frac{678}{5}+\frac{12}{5}\nu\right)-120\dot{r}^4\right]. &(7.32d)
\end{aligned}$$

The second kind of dissipative terms is the dissipative contribution of the tails that occurs at the (formally even) 4PN order. The conservative tail acceleration was obtained in (7.23). It contains the tail integral

$$\underset{2r_{12}/c}{\rm Pf}\int_{-\infty}^{+\infty}\frac{{\rm d}t'}{|t-t'|}I^{(6)}_{ij}(t') = \int_0^{+\infty}{\rm d}\tau\ln\left(\frac{c\tau}{2r_{12}}\right)\left[I^{(7)}_{ij}(t-\tau)-I^{(7)}_{ij}(t+\tau)\right], \tag{7.33}$$

which only corresponds to the conservative part of the tail effect. Indeed, we recognize a "time-symmetric" decomposition, which is conservative in the sense that the corresponding acceleration is purely radial in the case of circular orbits, as we have seen in (7.24). The dissipative part is given by the corresponding *time-antisymmetric* combination, hence the dissipative tail acceleration is

$$a^{i\,\rm tail}_{1\,\rm diss} = -\frac{4G^2M}{5c^8}\,y_1^j\int_0^{+\infty}{\rm d}\tau\ln\left(\frac{\tau}{2P}\right)\left[I^{(7)}_{ij}(t-\tau)+I^{(7)}_{ij}(t+\tau)\right]. \tag{7.34}$$

[3]Notice that the tail contributions (7.29) and (7.31) satisfy separately the first law: $\frac{{\rm d}\tilde{E}^{\rm tail}}{{\rm d}\omega}=\omega\,\frac{{\rm d}\tilde{J}^{\rm tail}}{{\rm d}\omega}$.

In this expression, P denotes an arbitrary scale, but it is easy to check that this scale cancels out from the two terms of (7.34) so that we can choose $P = r_{12}/c$. Thus, the complete tail part of the acceleration is the sum of (7.23) and (7.34). It reads

$$\begin{aligned} a_1^{i\,\text{tail}} &= -\frac{8G^2M}{5c^8}\,y_1^j\int_0^{+\infty}\mathrm{d}\tau\ln\left(\frac{c\tau}{2r_{12}}\right)I_{ij}^{(7)}(t-\tau)\\ &+\frac{8G^2M}{5c^8}y_1^j\left[\left(I_{ij}^{(3)}\ln r_{12}\right)^{(3)}-I_{ij}^{(6)}\ln r_{12}\right]-\frac{2G^2M}{5m_1c^8}\frac{n_{12}^i}{r_{12}}\left(I_{jk}^{(3)}\right)^2. \end{aligned} \tag{7.35}$$

The non-local tail term agrees with the result found from first-principle derivations of the near zone metric in [161, 150, 162]. In the case of (quasi-)circular orbits, the 4PN equations of motion, including the 2.5PN, 3.5PN and 4PN radiation reaction effects, become

$$\boldsymbol{a} = -\omega^2\boldsymbol{x} - \frac{32}{5}\frac{G^3m^3\nu}{c^5r^4}\left[1+\left(-\frac{743}{336}-\frac{11}{4}\nu\right)\gamma+4\pi\gamma^{3/2}\right]\boldsymbol{v}\,. \tag{7.36}$$

The orbital frequency as a function of the separation r, with all conservative terms, has been obtained in (7.25). In the above equation, we witness the contribution of the radiation reaction 4PN tail effect with coefficient 4π.

With the radiation reaction terms added to the conservative acceleration, the energy and angular momentum are no longer conserved. Their time derivatives are now equal to (minus) the corresponding fluxes in gravitational waves. In order to recover the familiar expressions for those fluxes,[4] we have to transfer certain terms in the form of total time derivatives from the right-hand side of the balance equations to the left-hand side. This implies that the energy and angular momentum also acquire certain radiation-reaction contributions. The balance equations read

$$\frac{\mathrm{d}E}{\mathrm{d}t} = -F\,,\quad \frac{\mathrm{d}\boldsymbol{J}}{\mathrm{d}t} = -\boldsymbol{M}\,, \tag{7.37}$$

with purely dissipative energy and angular momentum fluxes F and $\boldsymbol{M}$ in the right-hand side. The conservative parts of the CM energy $\mathcal{E} = E/\mu$ and angular momentum $\mathcal{J} = J/J_N$ have already been provided in (7.20) and (7.21). We now present the 2.5PN and 3.5PN dissipative contributions to the balance equation for the energy [82, 83, 62, 159, 160, 80]

$$\mathcal{E}_{2.5\text{PN}} = \frac{8G^2m^2\,\nu}{5r^2}\dot{r}v^2\,, \tag{7.38a}$$

$$\begin{aligned} \mathcal{E}_{3.5\text{PN}} = -\frac{8G^2m^2\,\nu}{5r^2}\dot{r}\Bigg[&\left(\frac{271}{28}+6\nu\right)v^4+\left(-\frac{77}{4}-\frac{3}{2}\nu\right)v^2\dot{r}^2+\left(\frac{79}{14}-\frac{92}{7}\nu\right)v^2\frac{Gm}{r}\\ &+10\dot{r}^4+\left(\frac{5}{42}+\frac{242}{21}\nu\right)\dot{r}^2\frac{Gm}{r}+\left(-\frac{4}{21}+\frac{16}{21}\nu\right)\left(\frac{Gm}{r}\right)^2\Bigg]\,, \end{aligned} \tag{7.38b}$$

together with the corresponding terms in the flux (with $\mathcal{F} = F/\mu$)

$$\mathcal{F}_{2.5\text{PN}} = \frac{8G^3m^3\,\nu}{5r^4}\left(4v^2-\frac{11}{3}\dot{r}^2\right)\,, \tag{7.39a}$$

[4] *I.e.*, the familiar Einstein quadrupole formula at leading order, and its extension, at next-to-leading orders, built from an irreducible STF decomposition of the mass and current (radiative type) multipole moments (see for example (68) in [17]).

$$\mathcal{F}_{3.5\mathrm{PN}} = \frac{8G^3m^3\,\nu}{5r^4}\biggl[\left(\frac{785}{84}-\frac{71}{7}\nu\right)v^4 + \left(-\frac{680}{21}+\frac{40}{21}\nu\right)v^2\frac{Gm}{r} + \left(-\frac{1487}{42}+\frac{232}{7}\nu\right)v^2\dot{r}^2 + \left(\frac{734}{21}-\frac{10}{7}\nu\right)\dot{r}^2\frac{Gm}{r} + \left(\frac{687}{28}-\frac{155}{7}\nu\right)\dot{r}^4 + \left(\frac{4}{21}-\frac{16}{21}\nu\right)\left(\frac{Gm}{r}\right)^2\biggr]. \tag{7.39b}$$

As we said, this expression is nothing but the standard *irreducible* expression for the flux reduced to the case of binary motion in the CM frame. For the angular momentum, we have

$$\mathcal{J}_{2.5\mathrm{PN}} = -\frac{8G^2m^2\,\nu}{5r^2}\dot{r}\,, \tag{7.40a}$$

$$\mathcal{J}_{3.5\mathrm{PN}} = -\frac{8G^2\,m^2\,\nu}{5r^2}\dot{r}\biggl[\left(\frac{40}{3}-\frac{11}{21}\nu\right)v^2 + \left(-\frac{439}{28}+\frac{18}{7}\nu\right)\dot{r}^2 + \left(-\frac{17}{21}-\frac{169}{21}\nu\right)\left(\frac{Gm}{r}\right)\biggr], \tag{7.40b}$$

while the flux contributions are (with $\mathcal{M} = M/J_\mathrm{N}$ and $J_\mathrm{N} = \mu|\boldsymbol{x}\times\boldsymbol{v}|$)

$$\mathcal{M}_{2.5\mathrm{PN}} = \frac{8G^2m^2\,\nu}{5r^3}\left(2v^2+2\frac{Gm}{r}-3\dot{r}^2\right), \tag{7.41a}$$

$$\mathcal{M}_{3.5\mathrm{PN}} = \frac{8G^2m^2\,\nu}{5r^3}\biggl[\left(\frac{307}{84}-\frac{137}{21}\nu\right)v^4 + \left(-\frac{58}{21}-\frac{95}{21}\nu\right)v^2\frac{Gm}{r} + \left(-\frac{37}{7}+\frac{277}{14}\nu\right)v^2\dot{r}^2 + \left(\frac{62}{7}+\frac{197}{42}\nu\right)\dot{r}^2\frac{Gm}{r} + \left(\frac{95}{28}-\frac{90}{7}\nu\right)\dot{r}^4 + \left(-\frac{745}{42}+\frac{\nu}{21}\right)\left(\frac{Gm}{r}\right)^2\biggr]. \tag{7.41b}$$

We must still include the dissipative 4PN tail contributions to both fluxes. From the expression of the corresponding acceleration in (7.34), we readily compute the corresponding terms in the right-hand sides of the balance equations (7.37) as

$$F^\mathrm{tail}_\mathrm{diss} = \frac{2G^2M}{5c^8}\,I^{(1)}_{ij}(t)\int_0^{+\infty}\mathrm{d}\tau\,\ln\left(\frac{c\tau}{2r_{12}}\right)\left[I^{(7)}_{ij}(t-\tau)+I^{(7)}_{ij}(t+\tau)\right], \tag{7.42a}$$

$$M^{i\,\mathrm{tail}}_\mathrm{diss} = \frac{4G^2M}{5c^8}\,\epsilon_{ijk}\,I_{jl}(t)\int_0^{+\infty}\mathrm{d}\tau\,\ln\left(\frac{c\tau}{2r_{12}}\right)\left[I^{(7)}_{kl}(t-\tau)+I^{(7)}_{kl}(t+\tau)\right]. \tag{7.42b}$$

8 – Computing the source mass quadrupole moment at 4PN

In chapter 4, we expressed the far-zone metric as a function of unspecified source multipole moments. Using the matching equation, we found an explicit expression for them in chapter 5. The computations of these multipole moments are crucial within the Blanchet-Damour-Iyer formalism, but they are quite involved and cumbersome. In order to obtain the 4.5PN phase of the gravitational waves (and in particular in order to obtain the gravitational wave flux at the 4PN order), the mass quadrupole moment at the fourth post-Newtonian order as well as the current quadrupole moment at the third post-Newtonian order have to be computed.

In this chapter, we detail the computation of the mass quadrupole moment at 4PN and we present a preliminary result of this computation in section 8.4.

8.1 Expression of the mass quadrupole as a function of the potentials

8.1.1 General introduction

In order to compute the mass quadrupole at the 4^{th} post-Newtonian order, we start from the equation (5.50) obtained at the end of the chapter 5

$$\begin{aligned}
\mathrm{I}_L(u) = \underset{B}{\mathrm{FP}} \int \mathrm{d}^3\boldsymbol{x} \left(\frac{|\boldsymbol{x}|}{r_0}\right)^B \int_{-1}^{1} \mathrm{d}z \Big\{ &\delta_\ell \hat{x}_L \Sigma - \frac{4(2\ell+1)}{c^2(\ell+1)(2\ell+3)} \delta_{\ell+1} \hat{x}_{iL} \Sigma_i^{(1)} \\
&+ \frac{2(2\ell+1)}{c^4(\ell+1)(\ell+2)(2\ell+5)} \delta_{\ell+2} \hat{x}_{ijL} \Sigma_{ij}^{(2)} \Big\} (u + zr/c, \boldsymbol{x}) \,, \qquad (8.1)
\end{aligned}$$

where

$$\Sigma = \frac{\overline{\tau}^{00} + \overline{\tau}^{ii}}{c^2} \,, \qquad (8.2\text{a})$$

$$\Sigma_i = \frac{\overline{\tau}^{0i}}{c} \,, \qquad (8.2\text{b})$$

$$\Sigma_{ij} = \overline{\tau}^{ij} \,, \qquad (8.2\text{c})$$

and where we recall that $\delta_\ell(z) = \frac{(2\ell+1)!!}{2^{(\ell+1)}\ell!}(1-z^2)^\ell$. The functions Σ, Σ_i and Σ_{ij} are to be evaluated at the spatial point $\boldsymbol{x}$ and at time $u + zr/c$. As we are computing a post-Newtonian expansion of I_L, the integral over dz can be evaluated as an asymptotic series in power of $1/c$ using the following properties of the functions $\delta_\ell(z)$

$$\int_{-1}^{1} \mathrm{d}z\delta_\ell(z)\Sigma(u+z|\boldsymbol{x}|/c,\boldsymbol{x}) = \sum_{k=0}^{\infty} \alpha_{k,\ell} \left(\frac{|\boldsymbol{x}|}{c}\frac{\partial}{\partial u}\right)^{2k} \Sigma(u,\boldsymbol{x})\,, \tag{8.3}$$

where

$$\alpha_{k,\ell} \equiv \frac{(2\ell+1)!!}{(2k)!!(2\ell+2k+1)!!}\,. \tag{8.4}$$

Therefore, $I_L(u)$ is an integral over the space with the volume element $\mathrm{d}^3\boldsymbol{x}$ of post-Newtonian quantities depending on the energy-impulsion pseudo-tensor $\overline{\tau}^{\mu\nu}$ where

$$\tau^{\alpha\beta} = |g|T^{\alpha\beta} + \frac{c^4}{16\pi G}\Lambda^{\alpha\beta}(h^{\mu\nu})\,. \tag{8.5}$$

We recall that $T^{\mu\nu}$ is the energy-impulsion tensor of the matter present in the spacetime while $\Lambda^{\alpha\beta}(h^{\mu\nu})$ corresponds to the stress energy associated with the gravitational field. In the case of a compact binary system we use the usual point-particle energy-impulsion tensor for the matter. This energy-impulsion tensor can be derived from the point-particle action S_m defined in (6.4)

$$T^{\mu\nu} = \frac{2}{\sqrt{-g}}\frac{\delta S_m}{\delta g_{\mu\nu}}\,. \tag{8.6}$$

This yields

$$T^{00} = \mu_1\delta^{(3)}(\boldsymbol{x}-\boldsymbol{y_1}) + \mu_2\delta^{(3)}(\boldsymbol{x}-\boldsymbol{y_2})\,, \tag{8.7a}$$
$$T^{0i} = \mu_1 v_1^i\delta^{(3)}(\boldsymbol{x}-\boldsymbol{y_1}) + \mu_2 v_2^i\delta^{(3)}(\boldsymbol{x}-\boldsymbol{y_2})\,, \tag{8.7b}$$
$$T^{ij} = \mu_1 v_1^i v_1^j\delta^{(3)}(\boldsymbol{x}-\boldsymbol{y_1}) + \mu_2 v_1^i v_2^j\delta^{(3)}(\boldsymbol{x}-\boldsymbol{y_2})\,, \tag{8.7c}$$

where

$$\mu_1 = m_1 c\frac{1}{\sqrt{-(g_{\mu\nu})_1 v_1^\mu v_1^\nu}}\frac{1}{\sqrt{-(g)_1}}\,, \tag{8.8a}$$
$$\tilde{\mu}_1 = \left(1+\frac{v_{1i}v_{1i}}{c^2}\right)\mu_1\,. \tag{8.8b}$$

Hence if we inject (8.8) into (8.7), and then into (8.5), the mass quadrupole can be expressed at 4PN as a function of the metric $h^{\mu\nu}$. Then, we need to parametrize the metric with some potentials as done in the chapter 6. Finally, the integrals with respect to $\boldsymbol{x}$ have to be performed. These integrals lead to both IR divergences (when $r\to\infty$) as well as UV divergences (when $\boldsymbol{x}\to\boldsymbol{y}_1$ or $\boldsymbol{x}\to\boldsymbol{y}_2$).

The infra-red divergences are cured using the Finite-Part regularization. The choice of this regularization is a direct consequence of the matching equation leading to (8.1). However, as we will discuss in the section 8.4, more work is required to understand the problem of the IR divergence in the 4PN mass quadrupole moment.

Concerning the UV divergences (due to the point-particle approximation), they can be cured using Hadamard partie finie regularization up to the second post-Newtonian order.

This technique no longer works at the third post-Newtonian order and dimensional regularization has to be systematically used at the third and the fourth post-Newtonian orders.

All of these regularization techniques have been explained in section 6.1.2 and 6.1.4 in the case of the integral defining the Fokker Lagrangian. The way we use them in the case of the source multipole moments is exactly similar. In particular, a first computation using the Hadamard partie finie for the UV divergences is done, and then the difference between dimensional regularization and Hadamard partie finie for those divergences is computed and added to the first result.

8.1.2 Generalization in d dimensions

The use of dimensional regularization requires to extend to d dimensions the formulae (8.1) and (8.3). This has been done in [135] and reads

$$
\begin{aligned}
I_L(t) \;=\; \frac{d-1}{2(d-2)} \underset{B}{\mathrm{FP}} \int \frac{\mathrm{d}^d\mathbf{y}}{\ell_0^{d-3}} \left(\frac{|\mathbf{y}|}{r_0}\right)^B \Big\{ & \widehat{y}_L\, \overline{\Sigma}_{[\ell]}(\mathbf{y},t) \\
& - \frac{4(d+2\ell-2)}{c^2(d+\ell-2)(d+2\ell)}\, \widehat{y}_{iL}\, \dot{\overline{\Sigma}}_{i[\ell+1]}(\mathbf{y},t) \\
& + \frac{2(d+2\ell-2)}{c^4(d+\ell-1)(d+\ell-2)(d+2\ell+2)}\, \widehat{y}_{ijL}\, \ddot{\overline{\Sigma}}_{ij[\ell+2]}(\mathbf{y},t) \\
& - \frac{4(d-3)(d+2\ell-2)}{c^2(d-1)(d+\ell-2)(d+2\ell)}\, B\, \widehat{y}_{iL} \frac{y_j}{|\mathbf{y}|^2} \overline{\Sigma}_{ij[\ell+1]}(\mathbf{y},t) \Big\} \,,
\end{aligned} \tag{8.9}
$$

where (8.3) becomes in d dimensions

$$
\begin{aligned}
\overline{\Sigma}_{[\ell]}(\mathbf{y},t) &= \int_{-1}^{1} dz\, \delta_\ell^{(\varepsilon)}(z)\, \overline{\Sigma}(\mathbf{y}, t+z|\mathbf{y}|/c) \\
&= \sum_{k=0}^{+\infty} \alpha_\ell^k \left(\frac{|\mathbf{y}|}{c}\frac{\partial}{\partial t}\right)^{2k} \overline{\Sigma}(\mathbf{y},t)\,.
\end{aligned} \tag{8.10}
$$

The numerical coefficients α_ℓ^k are given by

$$
\alpha_\ell^k = \frac{1}{(2k)!!(2\ell+d)(2\ell+d+2)\cdots(2\ell+d+2k-2)}\,. \tag{8.11}
$$

8.1.3 Metric in d dimensions

In the computation of the Fokker Lagrangian, the *n+2 method* told us at which post-Newtonian order we have to expand the metric. In the case of the mass quadrupole, such a method does not exist, and $h^{\mu\nu}$ has to be systematically expanded in such a way that we get all the term up to $1/c^8$ in (8.9). A careful study of the structure of this equation shows that we need the metric at the order $(h^{00}, h^{0i}, h^{ij}) \sim (\mathcal{O}(c^{-8}), \mathcal{O}(c^{-7}), \mathcal{O}(c^{-8}))$. This metric can be parametrized as [157]

$$
h^{00} = -\frac{1}{c^2}\frac{2(-1+d)V}{-2+d} + \frac{1}{c^4}\left[\frac{4(-3+d)(-1+d)K}{(-2+d)^2} - \frac{2(-1+d)^2V^2}{(-2+d)^2} - 2\hat{W}\right]
$$

$$
\begin{aligned}
&+\frac{1}{c^6}\left[-\frac{4(-1+d)^3V^3}{3(-2+d)^3}+\frac{8(-3+d)V_aV_a}{-2+d}+V(\frac{8(-3+d)(-1+d)^2K}{(-2+d)^3}\right.\\
&\left.-\frac{4(-1+d)\hat{W}}{-2+d})-\frac{8(-1+d)\hat{X}}{-2+d}-8\hat{Z}\right]\\
&+\frac{1}{c^8}\left[\frac{2d\hat{W}_{ab}\hat{W}_{ab}}{-2+d}-\frac{2(-3+d)^2(-1+d)(-4+3d)K^2}{(-2+d)^4}+\frac{32\hat{M}}{-2+d}-\frac{32(-1+d)\hat{T}}{-2+d}\right.\\
&-\frac{2(-1+d)^4V^4}{3(-2+d)^4}+\frac{16(-4+d)\hat{R}_aV_a}{-2+d}+\frac{8(-3+d)(-1+d)K\hat{W}}{(-2+d)^2}-2\hat{W}^2\\
&+\frac{8(-3+d)(-1+d)^3KV^2}{(-2+d)^4}-\frac{4(-1+d)^2\hat{W}V^2}{(-2+d)^2}+\frac{16(-3+d)(-1+d)VV_aV_a}{(-2+d)^2}\\
&\left.-\frac{4(-1+d)(-4+3d)\hat{X}V}{(-2+d)^2}-\frac{16(-1+d)\hat{Z}V}{-2+d}\right],
\end{aligned}\tag{8.12a}
$$

$$
\begin{aligned}
h^{0i}=&\frac{4}{c^3}V_i+\frac{1}{c^5}\left[8\hat{R}_i+\frac{4(-1+d)V_iV}{-2+d}\right]\\
&+\frac{1}{c^7}\left[16\hat{Y}_i-\frac{8(-3+d)(-1+d)V_iK}{(-2+d)^2}+\frac{8(-1+d)\hat{R}_iV}{-2+d}+\frac{4(-1+d)^2V_iV^2}{(-2+d)^2}\right.\\
&\left.-8\hat{W}_{ia}V_a+8V_i\hat{W}\right],
\end{aligned}\tag{8.12b}
$$

$$
\begin{aligned}
h^{ij}=&\frac{1}{c^4}\left[-4\hat{W}_{ij}+2\delta_{ij}\hat{W}\right]+\frac{1}{c^6}\left[-16\hat{Z}_{ij}+8\delta_{ij}\hat{Z}\right]\\
&+\frac{1}{c^8}\left[-32\hat{M}_{ij}-16V_i\hat{R}_j-16\hat{R}_iV_j-8\hat{W}_{ij}\hat{W}+8\hat{W}_{ia}\hat{W}_{ja}\right.\\
&\left.+\delta_{ij}\left\{-\frac{2(-3+d)^2(-1+d)K^2}{(-2+d)^3}+16\hat{R}_aV_a+2\hat{W}^2-2\hat{W}_{ab}\hat{W}_{ab}-\frac{4(-1+d)V\hat{X}}{-2+d}\right\}\right],
\end{aligned}\tag{8.12c}
$$

where most of the potentials have already been defined in 6.1.3. The new potentials appearing in (8.12) at the 4PN order are denoted $\hat{T}$, $\hat{M}_{ij}$ and $\hat{Y}_i$. They obey the flat space-time wave equations

$$
\begin{aligned}
\Box\hat{Y}_i=&-4\pi G\Big[-\frac{1}{2}\left(\frac{d-1}{d-2}\right)\sigma\hat{R}_i-\frac{(5-d)(d-1)}{4(d-2)^2}\sigma VV_i+\frac{1}{2}\sigma_a\hat{W}_{ia}+\frac{1}{2}\sigma_{ia}V_a\\
&\qquad+\frac{1}{2(d-2)}\sigma_{aa}V_i-\frac{d-3}{(d-2)^2}\sigma_i\left(V^2+\frac{5-d}{2}K\right)\Big]\\
&+\hat{W}_{ab}\,\partial_{ab}V_i-\frac{1}{2}\left(\frac{d-1}{d-2}\right)\partial_t\hat{W}_{ia}\,\partial_aV+\partial_i\hat{W}_{ab}\,\partial_aV_b-\partial_a\hat{W}_{ib}\,\partial_bV_a\\
&-\frac{d-1}{d-2}\,\partial_aV\partial_i\hat{R}_a-\frac{d(d-1)}{4(d-2)^2}\,V_a\,\partial_iV\partial_aV-\frac{d(d-1)^2}{8(d-2)^3}\,V\partial_tV\partial_iV\\
&-\frac{1}{2}\left(\frac{d-1}{d-2}\right)^2V\partial_aV\partial_aV_i+\frac{1}{2}\left(\frac{d-1}{d-2}\right)V\partial_t^2V_i+2V_a\,\partial_a\partial_tV_i\\
&+\frac{(d-1)(d-3)}{(d-2)^2}\,\partial_aK\partial_iV_a+\frac{d(d-1)(d-3)}{4(d-2)^3}\left(\partial_tV\partial_iK+\partial_iV\partial_tK\right),
\end{aligned}\tag{8.13}
$$

$$
\begin{aligned}
\Box\hat{T} = -4\pi G\Big[&\frac{1}{2(d-1)}\,\sigma_{ab}\hat{W}_{ab} + \frac{5-d}{4(d-2)^2}\,V^2\sigma_{aa} + \frac{1}{d-2}\,\sigma V_a V_a - \frac{1}{2}\left(\frac{d-3}{d-2}\right)\sigma\hat{X} \\
&- \frac{1}{12}\left(\frac{d-3}{d-2}\right)^3\sigma V^3 - \frac{1}{2}\left(\frac{d-3}{d-2}\right)^3\sigma V K + \frac{(5-d)(d-3)}{2(d-1)(d-2)}\,\sigma_a V_a V \\
&+ \frac{d-3}{d-1}\,\sigma_a\hat{R}_a - \frac{d-3}{2(d-2)^2}\,\sigma_{aa}K\Big] + \hat{Z}_{ab}\,\partial_{ab}V + \hat{R}_a\,\partial_t\partial_a V \\
&- 2\partial_a V_b\,\partial_b\hat{R}_a - \partial_a V_b\,\partial_t\hat{W}_{ab} + \frac{1}{2}\left(\frac{d-1}{d-2}\right)V V_a\,\partial_t\partial_a V + \frac{d-1}{d-2}\,V_a\,\partial_b V_a\,\partial_b V \\
&+ \frac{d(d-1)}{4(d-2)^2}\,V_a\,\partial_t V\,\partial_a V + \frac{1}{8}\left(\frac{d-1}{d-2}\right)^2 V^2\partial_t^2 V + \frac{d(d-1)^2}{8(d-2)^3}\,V\,(\partial_t V)^2 \\
&- \frac{1}{2}\,(\partial_t V_a)^2 - \frac{(d-1)(d-3)}{4(d-2)^2}\,V\partial_t^2 K - \frac{d(d-1)(d-3)}{4(d-2)^3}\,\partial_t V\,\partial_t K \\
&- \frac{(d-1)(d-3)}{4(d-2)^2}\,K\partial_t^2 V - \frac{d-3}{d-2}\,V_a\,\partial_t\partial_a K - \frac{1}{2}\left(\frac{d-3}{d-2}\right)\hat{W}_{ab}\,\partial_{ab}K\,, \qquad (8.14)
\end{aligned}
$$

$$
\begin{aligned}
\Box\hat{M}_{ij} = -4\pi G\Bigg[&-\frac{(-3+d)\sigma_{ij}K}{(-2+d)^2} - \frac{1}{2}\sigma_i\hat{R}_j + \frac{\sigma_{ij}V^2}{(-2+d)^2} - \frac{(5-d)\sigma_i V V_j}{4(-2+d)} + \frac{1}{4}\sigma_{ia}\hat{W}_{ja} \\
&- \frac{(-3+d)^2(-1+d)\delta_{ij}KV\sigma}{4(-2+d)^3} - \frac{(-3+d)^2(-1+d)\delta_{ij}V^3\sigma}{16(-2+d)^3} - \frac{(-1+d)\delta_{ij}V_aV_a\sigma}{4(-2+d)} \\
&+ \frac{(-1+d)V_iV_j\sigma}{2(-2+d)} - \frac{(-1+d)\delta_{ij}\hat{X}\sigma}{8(-2+d)} + \frac{1}{2}\delta_{ij}\hat{R}_a\sigma_a - \frac{(-4+d)\delta_{ij}VV_a\sigma_a}{2(-2+d)} - \frac{1}{2}\hat{R}_i\sigma_j \\
&- \frac{(5-d)V_iV\sigma_j}{4(-2+d)} - \frac{(-1+d)\delta_{ij}V^2\sigma_{aa}}{8(-2+d)^2} - \frac{\delta_{ij}\hat{W}\sigma_{aa}}{4(4-2d)} + \frac{1}{4}\hat{W}_{ia}\sigma_{ja} - \frac{1}{8}\delta_{ij}\hat{W}_{ab}\sigma_{ab}\Bigg] \\
&- \frac{1}{4}\delta_{ij}\partial_b\hat{W}_{ae}\partial_e\hat{W}_{ab} + \frac{(-1+d)\partial_t^2\hat{W}_{ij}V}{4(-2+d)} + \partial_t\partial_a\hat{W}_{ij}V_a - \frac{1}{4}\delta_{ij}\partial_b\partial_a\hat{W}\hat{W}_{ab} \\
&- \frac{(d-1)\delta_{ij}V\hat{W}_{ab}\partial_a\partial_b V}{8(d-2)} + \frac{1}{2}\partial_b\partial_a\hat{W}_{ij}\hat{W}_{ab} - \frac{(-1+d)\partial_i V\partial_t\hat{R}_j}{2(-2+d)} + \frac{(-1+d)\partial_i VV_j\partial_t V}{8(-2+d)} \\
&- \frac{d(3-4d+d^2)\delta_{ij}\partial_t K\partial_t V}{8(-2+d)^3} + \frac{(-1+d)^2 d\delta_{ij}V(\partial_t V)^2}{32(-2+d)^3} - \partial_t V_i\partial_t V_j \\
&+ \frac{(3-4d+d^2)\partial_i K\partial_t V_j}{2(-2+d)^2} - \frac{(-1+d)^2\partial_i VV\partial_t V_j}{4(-2+d)^2} - \frac{1}{2}\partial_a V_i\partial_t\hat{W}_{ja} + \frac{1}{2}\partial_i V_a\partial_t\hat{W}_{ja} \\
&- \frac{(-1+d)\delta_{ij}VV_a\partial_t\partial_a V}{4(-2+d)} - \frac{1}{2}\delta_{ij}V_a\partial_t\partial_a\hat{W} - \frac{(-1+d)^2\delta_{ij}V^2\partial_t^2 V}{16(-2+d)^2} \\
&- \frac{(-1+d)\delta_{ij}V\partial_t^2\hat{W}}{8(-2+d)} - \frac{(-1+d)\delta_{ij}V_a\partial_t V\partial_a V}{8(-2+d)} - \partial_i\hat{R}_a\partial_a V_j \\
&- \frac{(-1+d)\partial_i VV_a\partial_a V_j}{2(-2+d)} - \frac{1}{2}\partial_b\hat{W}_{ia}\partial_a\hat{W}_{jb} - \frac{(3-4d+d^2)\delta_{ij}\partial_t V_a\partial_a K}{2(-2+d)^2} - \partial_i V_a\partial_a\hat{R}_j \\
&+ \frac{(-1+d)\partial_a V_iV_j\partial_a V}{2(-2+d)} + \frac{(-1+d)\partial_i V\hat{W}_{ja}\partial_a V}{8(-2+d)} + \frac{(-1+d)\delta_{ij}\partial_t\hat{R}_a\partial_a V}{2(-2+d)} \\
&+ \frac{(-1+d)^2\delta_{ij}V\partial_t V_a\partial_a V}{4(-2+d)^2} + \frac{(-1+d)V_i\partial_a V_j\partial_a V}{2(-2+d)} - \frac{1}{2}\partial_t\hat{W}_{ia}\partial_a V_j + \delta_{ij}\partial_a V_b\partial_b\hat{R}_a
\end{aligned}
$$

$$
\begin{aligned}
&- \frac{(-1+d)\delta_{ij}\hat{W}_{ab}\partial_a V\partial_b V}{16(-2+d)} - \frac{1}{2}\delta_{ij}\partial_t\hat{W}_{ab}\partial_b V_a + \frac{(-1+d)\delta_{ij}V\partial_a V_b\partial_b V_a}{4(-2+d)} \\
&+ \frac{1}{2}\partial_i\hat{W}_{ab}\partial_b\hat{W}_{ja} + \frac{(3-4d+d^2)\partial_t V_i\partial_j K}{2(-2+d)^2} - \frac{(-3+d)^2(-1+d)\partial_i K\partial_j K}{4(-2+d)^3} \\
&- \partial_a V_i\partial_j\hat{R}_a + \partial_i V_a\partial_j\hat{R}_a - \frac{(-1+d)\partial_t\hat{R}_i\partial_j V}{2(-2+d)} - \frac{(-1+d)\partial_i\hat{X}\partial_j V}{4(-2+d)} \\
&- \frac{(-1+d)^2\partial_t V_i V\partial_j V}{4(-2+d)^2} - \frac{(-1+d)\partial_a V_i V_a\partial_j V}{2(-2+d)} + \frac{(-1+d)V_i\partial_t V\partial_j V}{8(-2+d)} \\
&+ \frac{(-1+d)\hat{W}_{ia}\partial_a V\partial_j V}{8(-2+d)} - \partial_a\hat{R}_i\partial_j V_a + \partial_i\hat{R}_a\partial_j V_a + \frac{1}{2}\partial_t\hat{W}_{ia}\partial_j V_a + \frac{1}{2}\partial_b\hat{W}_{ia}\partial_j\hat{W}_{ab} \\
&- \frac{1}{4}\partial_i\hat{W}_{ab}\partial_j\hat{W}_{ab} - \frac{(-1+d)\partial_i V\partial_j\hat{X}}{4(-2+d)}\,. \qquad (8.15)
\end{aligned}
$$

8.1.4 Simplification of the result

The expression of the mass quadrupole moment as a function of the potentials is given in the appendix C. This result has been obtained by inserting (8.12) into (8.5) and then into (8.9). Then, different crucial simplifications have to be done. In fact, we do not know explicitly all the potentials entering the metric (either in 3 or d dimensions), and we are going to perform different operations in order to transform their contributions into computable forms.

8.1.4.a) Integration by part

The first technique to simplify the expression of the source mass quadrupole is to integrate by part some terms. For example, we systematically perform the substitution

$$\partial_a V\partial_a V \mapsto \frac{1}{2}\Delta V^2 - V\Delta V\,. \qquad (8.16)$$

In (8.16), we can further simplify the right-hand side using

$$
\begin{aligned}
\Delta V &= \Box V + \frac{1}{c^2}\frac{\partial^2}{\partial t^2}V \\
&= -4\pi G\sigma + \frac{1}{c^2}\frac{\partial^2}{\partial t^2}V\,, \qquad (8.17)
\end{aligned}
$$

where we have used the definition of V in (8.17). Thus, a complicated integral of the form $\int \mathrm{d}^3\boldsymbol{x}\ \hat{x}_L\partial_a V\partial_a V$ is transformed into two simpler terms: a compact term $\int \mathrm{d}^3\boldsymbol{x}\ \hat{x}_L\sigma$ and a surface term $\int \mathrm{d}^3\boldsymbol{x}\ \hat{x}_L\Delta V^2$. These two terms are much easier to integrate as we will see in section 8.2.1 and 8.2.3. This kind of integration by part is done as much as possible for the different potentials (and not only for V), generating so-called *Laplacian surface terms.*

8.1.4.b) Super-potential

The main technique we use to explicitly compute all the terms at 4PN is called the method of super-potentials. Some of the terms are of the form $\tilde{V}\tilde{P}$ where $\tilde{V}$ is one of the following potentials: $\{\partial_i V, \partial_{ij}V, \partial_t^2 V, \partial_t\partial_i V, \partial_j V_i\}$, and $\tilde{P}$ represents a complicated potential whose explicit expression is not known (for example $\hat{M}_{ij}$ obeying the equation (8.15)). In order to compute these terms we define the super potential $\Psi_L^{\tilde{V}}$ such that

$$\Delta\Psi_L^{\tilde{V}} \equiv \hat{x}_L \tilde{V} \,. \tag{8.18}$$

Then we perform the following integration by part

$$\begin{aligned}\int \frac{\mathrm{d}^d\boldsymbol{x}}{\ell_0^{d-3}} \hat{x}_L \tilde{V} \tilde{P} &= \int \frac{\mathrm{d}^d\boldsymbol{x}}{\ell_0^{d-3}} \Delta\Psi_L^{\tilde{V}} \tilde{P} \\ &= \int \frac{\mathrm{d}^d\boldsymbol{x}}{\ell_0^{d-3}} \Delta\tilde{P}\Psi_L^{\tilde{V}} + \int \frac{\mathrm{d}^d\boldsymbol{x}}{\ell_0^{d-3}} \partial_a \left(-\Psi_L^{\tilde{V}}\partial^a\tilde{P} + \tilde{P}\partial^a\Psi_L^{\tilde{V}}\right) .\end{aligned} \tag{8.19}$$

We can now substitute $\Delta\tilde{P} \mapsto \Box\tilde{P} + \frac{1}{c^2}\frac{\partial^2}{\partial t^2}\tilde{P}$ and replace $\Box\tilde{P}$ by its source which is made of simpler potentials. The term $-\frac{1}{c^2}\frac{\partial^2}{\partial t^2}\tilde{P}$ will be of higher post-Newtonian order which will reduce the post-Newtonian order at which $\tilde{P}$ has to be computed. The last term of (8.19) is called a *divergence term* and is also a surface term relatively easy to integrate (cf section 8.2.3).

Once these two techniques have been applied, we obtain the result presented in the appendix C. The following two sections provide all the material needed to compute the terms of the mass quadrupole presented in the appendix C. In particular, we see in section 8.2 the formulae required to integrate the different types of term, while the section 8.3 focuses on listing and computing explicitly the different potentials entering the source of these terms.

8.2 Integrating the different terms

In this section, we explain how to integrate in practice the different types of term of the source mass quadrupole.

8.2.1 Integrating the compact support terms

Some of the integrals that we have to perform to compute the mass quadrupole are *compact terms* and their integrations are actually relatively straightforward. Their integrands are proportional to one of the following three quantities

$$\sigma = \tilde{\mu}_1\delta^{(d)}(\boldsymbol{x}-\boldsymbol{y}_1) + \tilde{\mu}_2\delta^{(d)}(\boldsymbol{x}-\boldsymbol{y}_2)\,, \tag{8.20a}$$

$$\sigma_i = \mu_1 v_1^i \delta^{(d)}(\boldsymbol{x}-\boldsymbol{y}_1) + \mu_2 v_2^i \delta^{(d)}(\boldsymbol{x}-\boldsymbol{y}_2)\,, \tag{8.20b}$$

$$\sigma_{ij} = \mu_1 v_1^i v_1^j \delta^{(d)}(\boldsymbol{x}-\boldsymbol{y}_1) + \mu_2 v_2^i v_2^j \delta^{(d)}(\boldsymbol{x}-\boldsymbol{y}_2)\,, \tag{8.20c}$$

where we recall the definitions of μ_A and $\tilde{\mu}_A$ in the equations (8.22) below. The Dirac functions in $\boldsymbol{y}_1$ and $\boldsymbol{y}_2$ are due to the presence of the two point-particles. We recall that

$$\int \mathrm{d}^d\boldsymbol{x}\; \delta^{(d)}(\boldsymbol{x}-\boldsymbol{y}_1)F = (F)_1 \,, \tag{8.21}$$

where $(F)_1$ is the value of F at the point $\boldsymbol{x} = \boldsymbol{y}_1$ in d dimensions. In fact, as F can diverge when $\boldsymbol{x} \to \boldsymbol{y}_1$, we need to use dimensional regularization to cure the UV divergence that might occur.

8.2.2 μ_1 and $\tilde{\mu}_1$

The expressions of μ_1 and $\tilde{\mu}_1$ in 3 dimensions (equations (8.8)) can be extended in d dimensions

$$\mu_1 = m_1 c \frac{1}{\sqrt{-(g_{\mu\nu})_1 v_1^\mu v_1^\nu}} \frac{1}{\sqrt{-(g)_1}}\,, \tag{8.22a}$$

$$\tilde{\mu}_1 = \frac{2}{d-1}\left(d-2+\frac{v_{1i}v_{1i}}{c^2}\right)\mu_1\,, \tag{8.22b}$$

where g is the determinant of the metric, where $(g)_1$ and $(g_{\mu\nu})_1$ are evaluated at $\boldsymbol{x} = \boldsymbol{y}_1$, and where $v_1^0 = c$. For the mass quadrupole at 4PN, the 3PN expression of μ_1 as well as the 4PN expression of $\tilde{\mu}_1$ are required. They are given in terms of the potentials as

$$\begin{aligned}
\frac{\mu_1}{m_1} &= 1 + \frac{1}{c^2}\left[\frac{1}{2}\boldsymbol{v}_1^2 + \frac{(-4+d)V}{-2+d}\right] \\
&+ \frac{1}{c^4}\left[-4v_1^iV_i - \frac{2(-4+d)(-3+d)K}{(-2+d)^2} + \frac{3}{8}\boldsymbol{v}_1^4 + \frac{3}{2}\boldsymbol{v}_1^2V + \frac{(-4+d)^2V^2}{2(-2+d)^2} - 2\hat{W}\right] \\
&+ \frac{1}{c^6}\left[-8\hat{R}^iv_{1i} + \frac{4(-4+d)V_iV^i}{-2+d} - \frac{3(-3+d)\boldsymbol{v}_1^2K}{-2+d} + 2\hat{W}_{ij}v_1^iv_1^j + \frac{5}{16}\boldsymbol{v}_1^6\right. \\
&- \frac{4(-5+2d)v_1^iV_iV}{-2+d} - \frac{2(-4+d)^2(-3+d)KV}{(-2+d)^3} + \frac{3(-8+5d)\boldsymbol{v}_1^4V}{8(-2+d)} \\
&+ \frac{9}{4}\boldsymbol{v}_1^2V^2 + \frac{(-4+d)^3V^3}{6(-2+d)^3} - 6\boldsymbol{v}_1^2v_1^jV_j - \boldsymbol{v}_1^2\hat{W} - \frac{2(-4+d)V\hat{W}}{-2+d} \\
&\left.+\frac{4(-4+d)\hat{X}}{-2+d} - 8\hat{Z}\right]\,,
\end{aligned} \tag{8.23a}$$

$$\begin{aligned}
\frac{(d-1)\tilde{\mu}_1}{2m_1} &= (d-2) + \frac{1}{c^2}\left[\frac{1}{2}d\boldsymbol{v}_1^2 + (-4+d)V\right] \\
&+ \frac{1}{c^4}\left[-4(-2+d)v_1^iV_i - \frac{2(-4+d)(-3+d)K}{-2+d} + \frac{1}{8}(-2+3d)\boldsymbol{v}_1^4\right. \\
&\left.+\frac{(4-10d+3d^2)\boldsymbol{v}_1^2V}{2(-2+d)} + \frac{(-4+d)^2V^2}{2(-2+d)} - 2(-2+d)\hat{W}\right] \\
&+ \frac{1}{c^6}\left[-8(-2+d)\hat{R}^iv_{1i} + 4(-4+d)V_iV^i - \frac{(-3+d)(4-10d+3d^2)\boldsymbol{v}_1^2K}{(-2+d)^2}\right. \\
&+ 2(-2+d)\hat{W}_{ij}v_1^iv_1^j + \frac{1}{16}(-4+5d)\boldsymbol{v}_1^6 - 4(-5+2d)v_1^iV_iV \\
&- \frac{2(-4+d)^2(-3+d)KV}{(-2+d)^2} + \frac{3}{8}(-4+5d)\boldsymbol{v}_1^4V \\
&+ \frac{(-40+92d-52d^2+9d^3)\boldsymbol{v}_1^2V^2}{4(-2+d)^2} + \frac{(-4+d)^3V^3}{6(-2+d)^2} - 2(-4+3d)\boldsymbol{v}_1^2v_1^jV_j \\
&\left.- d\boldsymbol{v}_1^2\hat{W} - 2(-4+d)V\hat{W} + 4(-4+d)\hat{X} - 8(-2+d)\hat{Z}\right] \\
&+ \frac{1}{c^8}\left[-32\hat{R}^iV_i + 2d\hat{W}_{ij}^2 - 16(-2+d)v_1^i\hat{Y}_i + \frac{8(-3+d)(-5+2d)v_1^iV_iK}{-2+d}\right.
\end{aligned}$$

$$
\begin{aligned}
&+\frac{2(-3+d)^2(16-9d+2d^2)K^2}{(-2+d)^3}+32\hat{M}+16(-4+d)\hat{T}+8(-2+d)\hat{Z}_{ij}v_1^iv_1^j\\
&-4(-4+3d)\hat{R}^iv_{1i}\boldsymbol{v}_1^2-\frac{3(-3+d)(-4+5d)K\boldsymbol{v}_1^4}{4(-2+d)}+\frac{5}{128}(-6+7d)\boldsymbol{v}_1^4\\
&-8(-5+2d)\hat{R}^iv_{1i}V+\frac{4(-4+d)^2V_iV^iV}{-2+d}\\
&-\frac{(-3+d)(-40+92d-52d^2+9d^3)\boldsymbol{v}_1^2KV}{(-2+d)^3}+6(-2+d)\hat{W}_{ij}v_1^iv_1^jV\\
&+\frac{(52-90d+35d^2)\boldsymbol{v}_1^6V}{16(-2+d)}-\frac{2(26-22d+5d^2)v_1^iV_iV^2}{-2+d}\\
&-\frac{(-4+d)^3(-3+d)KV^2}{(-2+d)^3}+\frac{3(40-68d+25d^2)\boldsymbol{v}_1^4V^2}{16(-2+d)}\\
&+\frac{(304-768d+624d^2-214d^3+27d^4)\boldsymbol{v}_1^2V^3}{12(-2+d)^3}+\frac{(-4+d)^4V^4}{24(-2+d)^3}-\frac{3}{2}(-6+5d)\boldsymbol{v}_1^4v_1^aV_a\\
&+16(-2+d)v_1^iv_1^jV_iV_j-\frac{2(32-41d+12d^2)\boldsymbol{v}_1^2v_1^jVV_j}{-2+d}\\
&-8(-2+d)v_1^i\hat{W}_{ij}V^j+\frac{2(4-10d+3d^2)\boldsymbol{v}_1^2V_jV^j}{-2+d}+8(-2+d)v_1^iV_i\hat{W}\\
&+\frac{4(-4+d)(-3+d)K\hat{W}}{-2+d}-\frac{1}{4}(-2+3d)\boldsymbol{v}_1^4\hat{W}-\frac{(4-10d+3d^2)\boldsymbol{v}_1^2V\hat{W}}{-2+d}\\
&-\frac{(-4+d)^2V^2\hat{W}}{-2+d}+2(-2+d)\hat{W}^2+(-4+3d)\boldsymbol{v}_1^2v_1^iv_1^j\hat{W}_{ij}\\
&+\frac{2(4-10d+3d^2)\boldsymbol{v}_1^2\hat{X}}{-2+d}+\frac{4(16-9d+2d^2)V\hat{X}}{-2+d}-4d\boldsymbol{v}_1^2\hat{Z}-8(-4+d)V\hat{Z}\Bigg]\,,
\end{aligned}
\tag{8.23b}
$$

where all the potentials are evaluated at the point $\boldsymbol{x}=\boldsymbol{y}_1$.

8.2.3 Integrating the surface terms

Following the notation of [163], let us consider the following *Laplacian term*

$$
\mathcal{J}_L \equiv \underset{B}{\mathrm{FP}} \int \mathrm{d}^3\boldsymbol{x} \left(\frac{|\boldsymbol{x}|}{r_0}\right)^B \hat{x}_L \Delta G\,. \tag{8.24}
$$

We can integrate by part (8.24):

$$
\begin{aligned}
\mathcal{J}_L =& \underset{B}{\mathrm{FP}} \int \mathrm{d}^3\boldsymbol{x} \Delta\left[\left(\frac{|\boldsymbol{x}|}{r_0}\right)^B \hat{x}_L\right] G\\
&+\underset{B}{\mathrm{FP}} \int \mathrm{d}^3\boldsymbol{x}\ \partial_a\left[-G\partial_a\left\{\left(\frac{|\boldsymbol{x}|}{r_0}\right)^B \hat{x}_L\right\}+\left(\frac{|\boldsymbol{x}|}{r_0}\right)^B \hat{x}_L\partial_a G\right]\,.
\end{aligned}
\tag{8.25}
$$

The second term in the right-hand side of (8.25) is a surface integral and is zero when $\Re B$ is negatively large enough. Therefore, by analytical continuation, this term is exactly zero. In order to compute $\mathcal{J}_L$, we are going to apply the Laplacian operator (we recall that $\Delta\hat{x}_L = 0$)

$$\begin{aligned}\mathcal{J}_L &= \underset{B}{\mathrm{FP}}\, B(B+2\ell+1)\int \mathrm{d}^3\boldsymbol{x}\left(\frac{|\boldsymbol{x}|}{r_0}\right)^{B-2}\frac{1}{r_0^2}\hat{x}_L G\\ &= \underset{B}{\mathrm{FP}}\, B(B+2\ell+1)\int_{r<\mathcal{R}} \mathrm{d}^3\boldsymbol{x}\left(\frac{|\boldsymbol{x}|}{r_0}\right)^{B-2}\frac{1}{r_0^2}\hat{x}_L G\\ &\quad+ \underset{B}{\mathrm{FP}}\, B(B+2\ell+1)\int_{r\geq\mathcal{R}} \mathrm{d}^3\boldsymbol{x}\left(\frac{|\boldsymbol{x}|}{r_0}\right)^{B-2}\frac{1}{r_0^2}\hat{x}_L G\,. \end{aligned} \tag{8.26}$$

The first term of (8.26) is actually zero. Indeed, the matching equation is originally done for smooth matter distribution, and therefore the metric is normally smooth everywhere in the near zone. As G is a potential built from the metric, it is also smooth in that region, and because of the B pre-factor in (8.26), this term is zero by the Finite-Part procedure. In practice, the point-particle approximation leads to divergences when $\boldsymbol{x}\to\boldsymbol{y}_1$ or $\boldsymbol{x}\to\boldsymbol{y}_2$, but these UV divergences are killed by the dimensional regularization, and the Finite Part plays no role in it. Let us focus on the second term of (8.26). Because of the B in the pre-factor of this term, we need to look at the $1/B$ pole in the integral. This pole can only come from radial integrals of the form $\int \mathrm{d}r r^{B-1} = r^B/B$. Because $\mathrm{d}^3\boldsymbol{x} = r^2\mathrm{d}r\mathrm{d}\Omega$ and $\hat{x}_L\sim r^\ell$ when $r\to\infty$ we need to look for the $r^{-\ell-1}$ term in the asymptotic expansion of G when $r\to\infty$. Hence, if we define $X_\ell(\boldsymbol{n})$ to be that coefficient, i.e.,

$$G = \cdots + \frac{X_\ell(\boldsymbol{n})}{r^{\ell+1}} + \mathcal{O}\left(r^{-\ell-2}\right)\,, \tag{8.27}$$

we obtain

$$\begin{aligned}\mathcal{J}_L &= \underset{B}{\mathrm{FP}}\, B(B+2\ell+1) r_0^{-B}\int_{\mathcal{R}}^{\infty}\mathrm{d}r r^{B-1}\int \mathrm{d}\Omega\hat{n}_L X_\ell(\boldsymbol{n})\\ &= -(2\ell+1)\int \mathrm{d}\Omega\hat{n}_L X_\ell(\boldsymbol{n})\,. \end{aligned} \tag{8.28}$$

We see that the final result does not depend on $\mathcal{R}$ nor on r_0. It is simply an angular integral involving the $1/r^{\ell+1}$ coefficient of G. Therefore, there is no need to know G everywhere but just its asymptotical expansion, which is much easier as we are going to see in section 8.3.7.

The other surface integrals occurring are the *divergence terms*. They come from the use of the superpotentials and are of the form

$$\mathcal{K} \equiv \underset{B}{\mathrm{FP}}\int \mathrm{d}^3\boldsymbol{x}\left(\frac{|\boldsymbol{x}|}{r_0}\right)^{B}\partial_a H_a\,. \tag{8.29}$$

A similar reasoning as before shows that the Finite Part procedure yields

$$\mathcal{K} = \int \mathrm{d}\Omega n_a Y_a(\boldsymbol{n})\,, \tag{8.30}$$

where $Y_a(\boldsymbol{n})$ is the $1/r^2$ coefficient of the asymptotic expansion of H_a when $r\to\infty$:

$$H_a = \cdots + \frac{Y_a(\boldsymbol{n})}{r^2} + \mathcal{O}\left(r^{-3}\right)\,, \tag{8.31}$$

8.2.4 Integrating the non-compact terms

The rest of the integrals are *non-compact terms*, i.e., terms whose sources have non compact support, and are the most difficult terms to compute. Such terms are of the form $\int \mathrm{d}^3\boldsymbol{x}\tilde{V}$ where $\tilde{V}$ represents a generic product of potentials and of derivatives of potentials.

8.2.4.a) Volume integral

The first task, which is the longest computational task, is to compute this integral using the Finite Part regularization for the IR divergences as well as the Hadamard partie finie regularization for the UV ones. This is systematically done using a routine developed mainly by G. Faye in *Mathematica* using the *xAct* library [164]. It has been used for different projects (such as the Fokker Lagrangian project and the computation of the multipole moments at lower order), and has been heavily tested.

8.2.4.b) Dimensional regularization difference

Once this is done, the difference between dimensional regularization and Hadamard partie finie needs to be computed as usual. For that, we proceed as explained in section 6.1.3. The only information required is the expansion of $\tilde{V}$ in d dimensions in a neighborhood of $\boldsymbol{y}_1$ and $\boldsymbol{y}_2$, in order to apply equation (6.40).

8.2.4.c) Distributional derivative and the Gel'Fand-Shilov formula

Finally, we need to take care of the compact terms generated by the distributional derivatives appearing in the non-compact terms. Let us consider the following example

$$T = \int \mathrm{d}^3\boldsymbol{x} V \partial_{ij} V\,, \tag{8.32}$$

and compute the distributional derivative part of this term at the newtonian order. As $V = G\frac{m_1}{r_1} + G\frac{m_2}{r_2}$ we have

$$\partial_{ij} V = -\frac{4}{3} G\pi\delta_{ij}\left[m_1\delta(\boldsymbol{y}_1) + m_2\delta(\boldsymbol{y}_2)\right]\,. \tag{8.33}$$

Hence, the Dirac functions generate compact terms and the contribution of the distributional derivatives to T is

$$T_{\text{distr.der.}} = -\frac{4}{3} G\pi\delta_{ij}\left[m_1(V)_1 + m_2(V)_2\right]\,. \tag{8.34}$$

More generally, the distributional derivative of a function f is computed using the Gel'Fand-Shilov equation [108]:

$$\partial_{ij} f = \partial^{\text{ord}}_{ij} f + D_i\left[\partial^{\text{ord}}_j f\right] + \partial^{\text{ord}}_i D_j\left[f\right]\,, \tag{8.35}$$

where ∂^{ord}_i is the ordinary derivative and D the distributional derivative operator. If f is a positively homogenous function of degree $-\lambda$ where $\lambda \in \mathbb{N}$ with $\lambda \geq 2$, i.e. if for all $a > 0,\ f(a\boldsymbol{x}) = a^{-\lambda} f(\boldsymbol{x})$ then

$$D_i\left[f\right] = \frac{(-1)^k}{k!}\partial_{i_1\ldots i_k}\left[\delta(\boldsymbol{x})\right]\int_\Sigma f(r,\Omega) x^{i_1}\ldots x^{i_k}\mathrm{d}S_i\,, \tag{8.36}$$

where $k = \lambda - 2$. The integral is over a sphere Σ of radius r and centered on $r = 0$, where $\mathrm{d}S_i = n_i r^2 \mathrm{d}\Omega$.

For most of the potentials, the equation (8.36) is used for $f \sim n^L/r^m$. In that case, the operator D_i is given by [108]

$$D_i\left(\frac{n^L}{r^m}\right) = 4\pi \frac{(-1)^m 2^m (\ell+1)! \left(\frac{l+m-1}{2}\right)!}{(l+m)!} \sum_{p=p_0}^{m/2} \frac{\Delta^{p-1}\partial_{(M-2P}\delta_{iL+2P-M)}\delta^3(\boldsymbol{x})}{2^{2p}(p-1)!(m-2p)!\left(\frac{l+1-m}{2}+p\right)!}\,. \tag{8.37}$$

8.3 Computing the potentials

8.3.1 Summary of the potentials required

Based on the computational methods explained above and the list of terms composing the mass quadrupole provided in the appendix C, we can list all the potentials required to compute the mass quadrupole at 4PN. These potentials can be required either everywhere when they enter non-compact integrals, or only at $\boldsymbol{x} = \boldsymbol{y}_1$ when they enter compact terms. Besides, we need them in d dimensions in a neighborhood of $\boldsymbol{y}_1$ when they enter non-compact integrals in order to implement the UV dimensional regularization. Finally, in order to compute surface terms, we need to know their explicit expressions when $r \to \infty$ in 3 dimensions.

The table 8.1 summarized the different potentials required for this computation.

8.3.2 Computing the potentials in 3 dimensions

8.3.2.a) Compact source potentials

The first potentials to compute are the so-called *compact source potentials*, i.e. V, V_i and K. In fact the d'Alembertian of these potentials are proportional to σ, σ_i or σ_{ij}. Their sources are a combination of products of a function of time (including μ_1 and $\tilde{\mu}_1$ for example) multiplied by a Dirac function (either $\delta^{(3)}(\boldsymbol{x}-\boldsymbol{y}_1)$ or $\delta^{(3)}(\boldsymbol{x}-\boldsymbol{y}_2)$). It is therefore quite straightforward to compute them using the following

$$\Delta^{-1}\delta^{(3)}(\boldsymbol{x}-\boldsymbol{y}_1) = -\frac{1}{4\pi} r_1^{-1}\,, \tag{8.38a}$$

$$\Delta^{-1} r_1^a = \frac{r_1^{a+2}}{(a+2)(a+3)}, \quad \text{for } a \notin \{-2,-3\}\,. \tag{8.38b}$$

8.3.2.b) $\partial V \partial V$ terms: the case of $\hat{W}_{ij}$ at 0PN

The source of $\hat{W}_{ij}$ contains both compact terms and so-called $\partial V \partial V$ terms:

$$\Box \hat{W}_{ij} = -4\pi G\Big(\sigma_{ij} - \delta_{ij}\,\sigma_{kk}\Big) - \partial_i V \partial_j V\,. \tag{8.39}$$

The source $-4\pi G\Big(\sigma_{ij} - \delta_{ij}\,\sigma_{kk}\Big)$ is easily integrated as explained in (8.3.2.a)). Now, at 0PN, we have

$$V = \frac{Gm_1}{r_1} + \frac{Gm_2}{r_2}\,. \tag{8.40}$$

Potentials	3 dimensions	d dimensions near $\boldsymbol{y}_1$	$\boldsymbol{y}_1$	$r \to \infty$
V	2PN	2PN	3PN	3PN
V_i	2PN	2PN	2PN	2PN
$\Psi_{ij}^{\partial_a\partial_b V}$	2PN	2PN	2PN	2PN
$\Psi_{ij}^{\partial_a V_b}$	1PN	1PN	1PN	1PN
$\Psi_{ij}^{\partial_t\partial_a V}$	1PN	1PN	1PN	1PN
$\Psi_{ijk}^{\partial_a V}$	1PN	1PN	1PN	1PN
$\hat{W}_{ij}$	1PN	1PN	1PN	2PN
$\hat{W}$	1PN	1PN	1PN	2PN
$\hat{Z}_{ij}$	0PN	0PN	0PN	1PN
$\hat{Z}$	0PN	0PN	0PN	1PN
$\hat{R}_i$	0PN	0PN	1PN	1PN
$\hat{Y}_i$	$\times$	$\times$	0PN	0PN
$\hat{X}$	0PN	0PN	1PN	1PN
$\hat{M}_{ij}$	$\times$	$\times$	$\times$	0PN
$\hat{M}$	$\times$	$\times$	0PN	0PN
$\hat{T}$	$\times$	$\times$	0PN	0PN

Table 8.1: List of the post-Newtonian order required for the different potentials in order to get the 4PN mass quadrupole. The *3 dimensions* column corresponds to the potentials computed in 3 dimensions for all $\boldsymbol{x} \in \mathbb{R}^3$. The *d dimensions* column to the potentials computed in d dimensions around $\boldsymbol{y}_1$ (and $\boldsymbol{y}_2$). The next column is the value of the potentials at the point $\boldsymbol{y}_1$ (and therefore $\boldsymbol{y}_2$), and the last column at spatial infinity. In addition to these potentials, $\tilde{\mu}$ is required at 4PN and μ at 3PN.

Hence

$$\partial_i V \partial_j V = G^2 m_1^2 \left[\partial_i \frac{1}{r_1} \partial_j \frac{1}{r_1}\right] + G^2 m_1 m_2 \left[\partial_i \frac{1}{r_1} \partial_j \frac{1}{r_2}\right] + 1 \leftrightarrow 2 \,. \tag{8.41}$$

The term proportional to m_1^2 is called a self-term and can be computed using the fact that $\partial_i \frac{1}{r_1} \partial_j \frac{1}{r_1} = \frac{n_{1i} n_{1j}}{r_1^4}$. In fact, terms depending only on $\boldsymbol{n}_1$ and r_1, can be easily integrated using the following [74]:

$$r_1^a \hat{n}_{1L} = \Delta \left\{ \frac{r_1^{a+2} \hat{n}_{1L}}{(a-\ell+2)(a+\ell+3)} \right\} \text{ for } a \in \mathbb{C} \backslash \{\ell-2, -\ell-3\} \,, \tag{8.42a}$$

$$r_1^{\ell-2} \hat{n}_{1L} = \Delta \left\{ \frac{1}{2\ell+1} \left[\ln\left(\frac{r_1}{r_0}\right) - \frac{1}{2\ell+1} \right] r_1^{\ell} \hat{n}_{1L} \right\} , \tag{8.42b}$$

$$r_1^{-\ell-3} \hat{n}_{1L} = \Delta \left\{ -\frac{1}{2\ell+1} \left[\ln\left(\frac{r_1}{r_0}\right) + \frac{1}{2\ell+1} \right] \frac{\hat{n}_{1L}}{r_1^{\ell+1}} \right\} . \tag{8.42c}$$

The constant normalizing the logarithm terms can be taken arbitrary here, as it will be fixed by the matching procedure of the potentials as explained in section 8.3.3.

The term proportional to $m_1 m_2$ is called a cross-term, or an interaction term. It represents the non-linear interaction between the Newtonian fields generated by m_1 and m_2. To integrate it, we are going to use the fact that $\partial_i \frac{1}{r_1} = -\partial_{1i} \frac{1}{r_1}$ where ∂_{1i} represents the space derivative with respect to y_1^i. Hence we obtain

$$\begin{aligned}\partial_i \frac{1}{r_1} \partial_j \frac{1}{r_2} &= \partial_{1i} \frac{1}{r_1} \partial_{2j} \frac{1}{r_2} \\ &= \partial_{1i}\partial_{2j} \left[\frac{1}{r_1}\frac{1}{r_2}\right] .\end{aligned} \tag{8.43}$$

We have been able to factorize the derivatives as r_1 does not depend on $\boldsymbol{y}_2$ and r_2 does not depend on $\boldsymbol{y}_1$. Now, we have

$$\begin{aligned}\Delta^{-1}\partial_{1i}\partial_{2j} \left[\frac{1}{r_1}\frac{1}{r_2}\right] &= \partial_{1i}\partial_{2j} \left[\Delta^{-1}\frac{1}{r_1}\frac{1}{r_2}\right] \\ &= \partial_{1i}\partial_{2j} g \,,\end{aligned} \tag{8.44}$$

where g is such that $\Delta g = \frac{1}{r_1 r_2}$. Such a function g has been known for a long time and is given by

$$g = \ln(r_1 + r_2 + r_{12}) \,. \tag{8.45}$$

Adding up all these computational techniques, we are able to compute $\hat{W}_{ij}$ at 0PN in 3 dimensions. Computing $\hat{W}_{ij}$ at 1PN, as well as computing more complicated potentials such as $\hat{Z}_{ij}$ at Newtonian order, relies on the same kind of tricks. In particular, it relies on the functions f^{12} and f satisfying $\Delta f^{12} = \frac{r_1}{r_2}$ and $\Delta f = 2g$ respectively. These are given by [74]

$$f = \frac{1}{3} r_1 r_2 \boldsymbol{n}_1 \cdot \boldsymbol{n}_2 \left(g - \frac{1}{3}\right) + \frac{1}{6}(r_1 r_{12} + r_2 r_{12} - r_1 r_2) \,, \tag{8.46a}$$

$$f^{12} = \frac{1}{3} r_1 r_{12} \boldsymbol{n}_1 \cdot \boldsymbol{n}_{12} \left(g - \frac{1}{3}\right) + \frac{1}{6}(r_2 r_{12} + r_1 r_2 - r_1 r_{12}) \,. \tag{8.46b}$$

Similarly, a solution of $\Delta h = 2f$ has been recently computed and is given by[1]:

$$\begin{aligned}h = \frac{1}{720}\Big[&-11 g r_{12}^4 - 11 r_1 r_{12}^2 r_2 - 34 g r_1^2 r_2^2 + 11(r_1 r_{12}^3 + r_{12}^3 r_2) - 11(r_1^2 r_{12} r_2 + r_1 r_{12} r_2^2) \\ &+ \left(-\frac{46}{9} + 22 g\right)(r_1^2 r_{12}^2 + r_{12}^2 r_2^2) + 11(r_1^3 r_2 + r_1 r_2^3) + 5(-r_1^3 r_{12} - r_{12} r_2^3) \\ &+ \left(\frac{104}{15} - 11 g\right)(r_1^4 + r_2^4)\Big] + \frac{1}{3} f r_1 r_2 \boldsymbol{n}_1 \cdot \boldsymbol{n}_2 \,.\end{aligned} \tag{8.47}$$

8.3.3 Performing correctly the matching

The metric $h^{\mu\nu}$ that is parametrized by the potentials $V, V_i, \ldots$ is the instantaneous part of the metric in the near-zone satisfying the matching equation (5.42)[2]. This means that when a potential P satisfies the equation $\Box P = S$ then P should be computed as

$$P = \widetilde{\Box^{-1}_{\text{ret}}} S = \mathop{\text{FP}}_{B} \Box^{-1}_{\text{ret}} \left[\left(\frac{r}{r_0}\right)^B S\right] . \tag{8.48}$$

[1] Private communication from A. Bohé, L. Bernard and L. Blanchet.
[2] Indeed, the potentials do not include the tail effects by definition.

In practice, in order to compute P, we use the different functions f, g, $\Delta^{-1} r_1^a \hat{n}_{1L}$ defined in section 8.3.2; however we are not making sure that we are following the right prescription, i.e., that we are using the operator $\widetilde{\Box^{-1}_{\text{ret}}}$. Said otherwise, there might be an extra homogeneous solution that we could add to our potentials P. The first step that we can do to solve that issue is to define g_{match} and f_{match} in such a way that

$$\widetilde{\Delta^{-1}} g_{\text{match}} = \frac{1}{r_1 r_2}\,, \tag{8.49a}$$

$$\widetilde{\Delta^{-1}} f_{\text{match}} = \frac{r_1}{r_2}\,. \tag{8.49b}$$

Such a procedure has been studied in [74] where the value of g_{match} and f_{match} are provided.

However, we can proceed in a much more systematic way which ensures us to find automatically the proper homogeneous solution. Let us assume that we have found a solution P_{part} such that $\Box P_{\text{part}} = S$. We need to compute the homogeneous solution $H \equiv P - P_{\text{part}}$ to be added to P_{part}. As H is equal to its multipolar expansion, we have

$$H = \mathcal{M}(H) = \mathcal{M}(P) - \mathcal{M}(P_{\text{part}})\,. \tag{8.50}$$

The only unknown in (8.50) is $\mathcal{M}(P) = \mathcal{M}(\widetilde{\Box^{-1}_{\text{ret}}} S)$. Looking at the equation (5.40), we see that if we formally replace $h^{\mu\nu}$ by P and $\Lambda^{\mu\nu}$ by S, we would obtain an explicit expression for $\mathcal{M}(\widetilde{\Box^{-1}_{\text{ret}}} S)$. Using techniques similar to the techniques used to derive (5.40), we can show that

$$\begin{aligned}\mathcal{M}(P) = &\sum_{\ell\geq 0} \frac{(-1)^\ell}{\ell!} \partial_L \left[\frac{1}{r} \mathcal{M}^L_S(t - r/c)\right] \\ &+ \sum_{k\geq 0} \frac{(-1)^k}{k!} \left(\frac{\partial}{c\partial t}\right)^k \underset{B}{\text{FP}} \int \frac{\mathrm{d}^3 \boldsymbol{x}'}{(-4\pi)} \left(\frac{|\boldsymbol{x}'|}{r_0}\right)^B |\boldsymbol{x} - \boldsymbol{x}'|^{k-1} \mathcal{M}(S)(\boldsymbol{x}', t)\,,\end{aligned} \tag{8.51}$$

where

$$\mathcal{M}^L_S(u) = -\frac{1}{4\pi} \underset{B}{\text{FP}} \int \mathrm{d}^3 \boldsymbol{x}' \left(\frac{|\boldsymbol{x}'|}{r_0}\right)^B x'_L S(\boldsymbol{x}', u)\,. \tag{8.52}$$

For a potential computed at a given post-Newtonian order, the equation (8.51) usually reduces to few terms, and while the matching procedure seems to be cumbersome at first sight, its implementation is rather straightforward.

8.3.4 Known formulae in d dimensions

The computation of potentials in d dimensions is closely similar to the computation done in 3 dimensions. The compact parts of the sources of the potentials can be integrated using the extension to d dimensions of (8.38), i.e.,

$$\Delta^{-1} \delta^{(d)}(\boldsymbol{x} - \boldsymbol{y}_1) = -\frac{1}{4\pi} \tilde{k}\, r_1^{2-d}\,, \tag{8.53a}$$

$$\Delta^{-1} r_1^\alpha = \frac{r_1^{\alpha+2}}{(\alpha+2)(\alpha+d)}\,, \tag{8.53b}$$

where $\tilde{k} = \Gamma(\frac{d-2}{2})/\pi^{\frac{d-2}{2}}$.

The self-term in d dimensions are integrated using the extension of equation (8.42)

$$\Delta^{-1}\hat{n}_{1L}r_1^{\alpha} = \frac{\hat{n}_{1L}r_1^{\alpha+2}}{(\alpha-\ell+2)(\alpha+\ell+d)}\,. \tag{8.54}$$

The generalization of g in d dimensions is known, but its expression is rather cumbersome and quite inconvenient if one wants to use it to compute potentials in d dimensions in the full space-time. However, the development of g in d dimensions around $\boldsymbol{y}_1$, which is also known [156], is quite handy. Therefore, while some potentials cannot be easily computed for all $\boldsymbol{x} \in \mathbb{R}^d$, we can compute them around $\boldsymbol{y}_1$ and $\boldsymbol{y}_2$, which is what we need for the UV dimensional regularization.

8.3.5 Superpotentials

In order to obtain the result presented in appendix C, we have extensively used superpotentials Ψ_L^{ϕ}, i.e., potentials such that

$$\Delta\Psi_L^{\phi} = \hat{x}_L\phi\,. \tag{8.55}$$

The computation of such super-potentials was done in [165], using the following equation

$$\Psi_L^{\phi} = \sum_{k=0}^{\ell}\frac{(-2)^k\ell!}{(l-k)!}x_{<L-K}\partial_{K>}\phi_{2k+2}\,, \tag{8.56}$$

where have defined the functions ϕ_k by $\phi_0 = \phi$ and $\Delta\phi_{2k+2} = \phi_{2k}$. The equation (8.56) have been derived in 3 dimensions in [165] but all the proofs work as well in d dimensions and no extra factor needs to be added.

For example, let us find a general formula for Ψ_L^V assuming that V is defined by[3]

$$\begin{aligned} V &= I^{-1}\big(-4\pi G[\tilde{\mu}_1\delta(\boldsymbol{y_1}) + \tilde{\mu}_2\delta(\boldsymbol{y_2})]\big) \\ &= -4\pi G\sum_{k\geq 0}\Delta^{-k-1}\left(\frac{\partial}{c\partial t}\right)^{2k}[\tilde{\mu}_1\delta(\boldsymbol{y_1}) + \tilde{\mu}_2\delta(\boldsymbol{y_2})] \\ &= \sum_{k\geq 0}\left(\frac{\partial}{c\partial t}\right)^{2k}U_{2k}\,, \end{aligned} \tag{8.57}$$

where $U_{2k} = \Delta^{-1-k}\big(-4\pi G[\tilde{\mu}_1\delta(\boldsymbol{y_1}) + \tilde{\mu}_2\delta(\boldsymbol{y_2})]\big)$. It is quite straightforward to compute the functions U_{2k} using the appendix of [156]:

$$U_{2k} = \frac{G\tilde{k}}{(2k)!!(2k+2-d)(2k-1)\dots(6-d)(4-d)}\left(\tilde{\mu}_1 r_1^{2k+2-d} + \tilde{\mu}_2 r_2^{2k+2-1}\right)\,. \tag{8.58}$$

Now, for $\phi = V$, the function ϕ_{2k} are given by

$$\phi_{2k} = U_{2k} + \frac{\partial^2}{c^2\partial t^2}U_{2k+2} + \dots = \sum_{j\geq 0}\left(\frac{\partial^2}{c^2\partial t^2}\right)^{2j}U_{2k+2j}\,. \tag{8.59}$$

[3]In reality, V is defined using $\Box_{\text{ret}}^{-1}$ instead of I^{-1}. But this does not impact our computation here, as the difference is made of *odd* dissipative terms.

By inserting (8.59) into (8.56) we can obtain at each post-Newtonian order an explicit expression for the superpotential Ψ^V_L. To compute $\Psi^{\partial^k_t \partial_L V}_L$, i.e., the superpotential associated with $\partial^k_t \partial_L V$, we proceed similarly as all the space derivatives and time derivatives commute. Thus, we just have to substitute ϕ_{2k} in (8.56) by $\partial^k_t \partial_L \phi_{2k}$.

All these equations enable us to compute $\Psi^{\partial_a \partial_b V}_{ij}$, $\Psi^{\partial_t \partial_a V}_{ij}$ and $\Psi^{\partial_a V}_{ijk}$. The computation of $\Psi^{\partial_a V_a}_{ij}$ is done in a similar way as the source of V_i is also compact.

8.3.6 Potentials at the locations of the point particles

For the integrals with compact support entering the source mass quadrupole, only the values of the potentials in $\boldsymbol{x} = \boldsymbol{y}_1$ and $\boldsymbol{x} = \boldsymbol{y}_2$ are required. When the potentials are known in d dimensions around $\boldsymbol{y}_1$, we can directly deduce their values in $\boldsymbol{x} = \boldsymbol{y}_1$. This is however not the case for some of the most difficult potentials. In particular, we have to use another way to compute $\hat{Y}_i$, $\hat{M}_{ij}$ and $\hat{T}$ at $\boldsymbol{x} = \boldsymbol{y}_1$ in d dimensions.

Let S be the source of a potential P that we want to compute at $\boldsymbol{x} = \boldsymbol{y}_1$ at Newtonian order. At 0PN, we have $\Delta P = S$ and the problem amounts to computing $(\Delta^{-1}S)_1$. We assume that we can compute S in 3 dimensions for all $\boldsymbol{x}$, and in d dimensions around $\boldsymbol{y}_1$ and that we known the following decomposition for the source in 3 dimensions

$$S(\boldsymbol{x}) = \sum_{p_0 \leq p \leq N} r_1^p \underset{1}{s}_p(\boldsymbol{n}_1) + o(r_1^N)\,, \tag{8.60}$$

as well as the similar decomposition in d dimensions

$$S^{(d)}(\boldsymbol{x}) = \sum_{\substack{p_0 \leq p \leq N \\ q_0 \leq q \leq q_1}} r_1^p \left(\frac{r_1}{\ell_0}\right)^{q\varepsilon} \underset{1}{s}{}^{(\varepsilon)}_{p,q}(\boldsymbol{n}_1) + o(r_1^N)\,. \tag{8.61}$$

As usual, we will proceed in two steps. First of all, let us compute $(\Delta^{-1}S)_1$ in 3 dimensions using Hadamard partie finie. In [75], has been shown that

$$(P)_1 = -\frac{1}{4\pi}\mathrm{Pf}_{s_1,s_2}\int \frac{\mathrm{d}^3\boldsymbol{x}}{r_1} S(\boldsymbol{x}) + \left[\ln\left(\frac{r'_1}{s_1}\right) - 1\right] < \underset{1}{s}_{-2}(\boldsymbol{n}_1) >\,, \tag{8.62}$$

where

$$< \underset{1}{s}_{-2} > \equiv \frac{1}{4\pi}\int \mathrm{d}\Omega_1(\boldsymbol{n}_1)\, \underset{1}{s}_{-2}(\boldsymbol{n}_1)\,. \tag{8.63}$$

Then, the difference between dimensional regularization and Hadamard partie finie is given by [156]

$$\begin{aligned}\mathcal{D}(P)_1 = &-\frac{1}{\varepsilon(1+\varepsilon)} \sum_{q_0 \leq q \leq q_1} \left(\frac{1}{q} + \varepsilon\left[\ln\left(\frac{r'_1}{\ell_0}\right) - 1\right]\right) < \underset{1}{s}{}^{(\varepsilon)}_{-2,q}(\boldsymbol{n}_1) > \\ &- \frac{1}{\varepsilon(1+\varepsilon)} \sum_{q_0 \leq q \leq q_1} \left(\frac{1}{q+1} + \varepsilon \ln\left(\frac{s_2}{\ell_0}\right)\right) \sum_{\ell \geq 0} \frac{(-1)^\ell}{\ell!} \partial_L \left(\frac{1}{r_{12}^{1+\varepsilon}}\right) < n_2^L \underset{2}{s}{}^{(\varepsilon)}_{-\ell-3,q}(\boldsymbol{n}_1) > \\ &+ \mathcal{O}(\varepsilon)\,.\end{aligned} \tag{8.64}$$

The values of $\hat{M}_{ij}$, $\hat{M}$, $\hat{Y}_i$ and $\hat{T}$ at $\boldsymbol{x} = \boldsymbol{y}_1$ are computed using (8.62)–(8.64).

8.3.7 Potentials at infinity

Finally, the value of some potentials are required at $r \to \infty$ in order to compute the surface terms. For the potentials that are already known in 3 dimensions for all $\boldsymbol{x} \in \mathbb{R}^3$, we just perform their expansions when $r \to \infty$. However, other potentials are not known, namely $\hat{W}_{ij}$ at 2PN, $\hat{Z}_{ij}$ at 1PN, $\hat{X}$ at 1PN, and $\hat{T}$, $\hat{Y}_i$ as well as $\hat{M}_{ij}$ at 0PN. For those potentials, we proceed differently.

Let us assume that we want to compute the asymptotic value of a potential P satisfying $\Box P = S$. The first step is to develop S when $r \to \infty$:

$$S_{r\to\infty} = \sum_{p \geq -p_0} \sum_{\ell} S^{\ell,p}(\boldsymbol{y}_1, \boldsymbol{v}_1, \boldsymbol{y}_2, \boldsymbol{v}_2) \hat{n}_L r^p + o(r^{-p_0}) \,. \tag{8.65}$$

Then we can compute P by:

$$P = \Delta^{-1} S + \frac{1}{c^2} \frac{\partial^2}{\partial t^2} \Delta^{-2} S + \frac{1}{c^4} \frac{\partial^4}{\partial t^4} \Delta^{-3} S + \dots \,, \tag{8.66}$$

To apply (8.66) we need the following formulae that are similar to equations (8.42):

$$r^a \hat{n}_L = \Delta \left\{ \frac{r^{a+2} \hat{n}_L}{(a-l+2)(a+l+3)} \right\} \text{ for } a \in \mathbb{C} \backslash \{\ell - 2, -\ell - 3\} \,, \tag{8.67a}$$

$$r^{\ell-2} \hat{n}_L = \Delta \left\{ \frac{1}{2\ell+1} \left[\ln\left(\frac{r}{r_0}\right) - \frac{1}{2\ell+1} \right] r^\ell \hat{n}_L \right\} \,, \tag{8.67b}$$

$$r^{-\ell-3} \hat{n}_L = \Delta \left\{ -\frac{1}{2\ell+1} \left[\ln\left(\frac{r}{r_0}\right) + \frac{1}{2\ell+1} \right] \frac{\hat{n}_L}{r^{\ell+1}} \right\} \,. \tag{8.67c}$$

Besides, for $\hat{X}$ at 1PN and $\hat{W}_{ij}$ at 2PN, we need to integrate terms proportional to $\log\left(\frac{r}{r_0}\right) r^a \hat{n}_L$. For that, we use the same method as what was done in equation (4.96) and say that

$$\widetilde{\Delta}^{-1} \log\left(\frac{r}{r_0}\right) r^a \hat{n}_L = \underset{B}{\mathrm{FP}} \frac{\mathrm{d}}{\mathrm{d}B} \Delta^{-1} \frac{r^{a+B}}{r_0^B} \hat{n}_L \,, \tag{8.68}$$

which can be easily integrated using equation (8.67a).

8.4 Results

8.4.1 A preliminary result

We have applied the method described in this chapter to compute the source mass quadrupole moment at the 4PN order, using dimensional regularization to cure the UV divergences and the Finite Part regularization to cure the IR divergences. The final result contains around 75000 terms.

8.4.1.a) Applying a shift

As for the Fokker Lagrangian computation, we first used Hadamard partie finie to cure the UV divergences, and obtain a first result depending on $\ln s_1$ and $\ln s_2$. Then we computed the difference between the Hadamard partie finie regularization and the dimensional regularization for the UV divergences, and obtained a new result free of $\ln s_1$ and $\ln s_2$ but containing poles in $1/\varepsilon$.

Let us recall that these poles should cancel out when expressing physical observables such as the energy flux or the phase of the system, but can still be present in intermediate results such as the equations of motion or the source multipole moments. However, in that case, it is convenient to remove them by applying a common shift to all our intermediate quantities. Indeed, at the 3PN order, the same shift was applied to the equations of motion and to the source mass quadrupole, and was able to remove all the UV poles.

At the 4PN, the situation is a bit more complicated. The shift that we applied to the Fokker Lagrangian in order to obtain the result presented in the appendix B, and from which we derived all the conserved quantities in chapter 7 is composed of three terms: (i) the shift $\boldsymbol{\xi}$ published in [92] and given in the appendix B by equation (B.4). This shift removes all the UV $1/\varepsilon$ poles in the Fokker Lagrangian; (ii) the shift $\boldsymbol{\chi}$ (equation (B.7)) that was applied in [94] and removes all the IR $1/\varepsilon$ poles of the Fokker Lagrangian; (iii) and finally the shift $\boldsymbol{\eta}$ (equation (B.9)) published in [3] that does not contain any pole and was used for conveniency.

As we have not used dimensional regularization to cure the IR divergence of the mass quadrupole moment (this is left to future work), we cannot apply the shift $\boldsymbol{\chi}$ to our result, but we can still check whether the shift $\boldsymbol{\xi}$ removes the UV $1/\varepsilon$ poles.

We have therefore applied the shift $\boldsymbol{\xi}$ to the mass quadrupole and all the UV $1/\varepsilon$ poles (as well as the constants γ_E) cancelled out. This constitutes a major achievement and confirms our understanding of the connection between the source multipole moments and the equations of motions within the Blanchet-Damour-Iyer formalism. Besides it corroborates our result, by robustly checking our UV dimensional regularization computations.

8.4.1.b) Expressing the result in the center of mass frame for circular orbits

The next steps is to reduce our result into the center of mass (CM) frame for circular orbits. It turns out that we only need the 3PN order CM coordinate, and the 3PN circular equations of motion to express the source mass quadrupole moment at the 4PN order in the CM frame for circular orbits. Therefore, even if our result does not use dimensional regularization to cure the IR divergence, we can still consistently express it in the CM for circular orbits — as the 3PN dynamics can be derived using the Finite Part regularization for the IR, and as the shift $\boldsymbol{\chi}$ only starts at the 4PN order. The result is then much more compact and is given below in 8.4.1.c).

8.4.1.c) Result

The UV-shifted mass quadrupole (with dimensional regularization for the UV and Finite Part regularization for the IR) in the CM frame for circular orbits at the 4PN order reads:

$$\mathrm{I}_{ij} = \delta I_{ij} + \mu \left(A\, x_{\langle ij\rangle} + B\, \frac{r^2}{c^2} v_{\langle ij\rangle} + \frac{48}{7}\, \frac{G^2 m^2 \nu}{c^5 r}\, C\, x_{\langle i}v_{j\rangle} \right) + \mathcal{O}\left(\frac{1}{c^9}\right) , \tag{8.69}$$

with

$$A = 1 + \gamma \left(-\frac{1}{42} - \frac{13}{14}\nu \right) + \gamma^2 \left(-\frac{461}{1512} - \frac{18395}{1512}\nu - \frac{241}{1512}\nu^2 \right)$$

$$
\begin{aligned}
&+\gamma^3\left(\frac{395899}{13200}-\frac{428}{105}\ln\left(\frac{r}{r_0}\right)+\left[\frac{3304319}{166320}-\frac{44}{3}\ln\left(\frac{r}{r'_0}\right)\right]\nu+\frac{162539}{16632}\nu^2+\frac{2351}{33264}\nu^3\right)\\
&+\gamma^4\left(-\frac{590993023429}{12713500800}+\frac{31886}{2205}\ln\left(\frac{r}{r_0}\right)+32\ln\left(\frac{r''_0}{r'_0}\right)+\left[-\frac{213814424807}{4237833600}-\frac{2783}{1792}\pi^2\right.\right.\\
&\left.-\frac{35491}{735}\ln\left(\frac{r}{r_0}\right)-\frac{7129}{63}\ln\left(\frac{r}{r'_0}\right)+248\ln\left(\frac{r}{r''_0}\right)\right]\nu\\
&+\left[\frac{29248139281}{121080960}+\frac{44909}{2688}\pi^2+\frac{319}{7}\ln\left(\frac{r}{r_0}\right)+\frac{5183}{21}\ln\left(\frac{r}{r'_0}\right)-480\ln\left(\frac{r}{r''_0}\right)\right]\nu^2\\
&\left.-\frac{3318635713}{25945920}\nu^3+\frac{18836039}{1572480}\nu^4\right)\,,
\end{aligned}
\tag{8.70a}
$$

$$
\begin{aligned}
B=&\frac{11}{21}-\frac{11}{7}\nu+\gamma\left(\frac{1607}{378}-\frac{1681}{378}\nu+\frac{229}{378}\nu^2\right)\\
&+\gamma^2\left(-\frac{357761}{19800}+\frac{428}{105}\ln\left(\frac{r}{r_0}\right)-\frac{92339}{5544}\nu+\frac{35759}{924}\nu^2+\frac{457}{5544}\nu^3\right)\\
&+\gamma^3\left(\frac{3883914647}{1589187600}+\left[-\frac{1293127977}{176576400}+\frac{143}{192}\pi^2-\frac{1714}{49}\ln\left(\frac{r}{r_0}\right)-\frac{968}{63}\ln\left(\frac{r}{r'_0}\right)\right]\nu\right.\\
&\left.+\left[\frac{688171447}{15135120}-\frac{41}{24}\pi^2+\frac{968}{21}\ln\left(\frac{r}{r'_0}\right)\right]\nu^2-\frac{3128539}{81081}\nu^3-\frac{3053}{432432}\nu^4\right)\,,
\end{aligned}
\tag{8.70b}
$$

$$
C=1+\gamma\left(-\frac{256}{135}-\frac{1532}{405}\nu\right)\,. \tag{8.70c}
$$

We recall that γ is a 1PN parameter defined as $\gamma\equiv\frac{Gm}{rc^2}$, r_0 is the constant introduced by the Finite Part regularization, and r'_0 and r''_0 depends on r'_1 and r'_2 and are defined by the equations (7.10). The equations (8.69)–(8.70) extend to the 4PN order the expression of the mass source quadrupole moment that was known at the 3.5PN order [140, 45, 128].

δI_{ij} represents some surface terms whose computations are still being performed and we expect to have them within few weeks[4]. In fact, the sources of some integrals contain up to few millions terms, and their integrations require huge amount of computational power. The terms in δI_{ij} do not contain UV poles as they are only surface terms. Therefore, our conclusion regarding the fact that the shift $\boldsymbol{\xi}$ removes all the UV poles will of course be still valid once δI_{ij} is fully computed.

8.4.2 Checks and perspectives

The equations (8.69)–(8.70) constitute a preliminary result of the source mass quadrupole at the 4PN order done in this thesis. However, the fact that the UV $1/\varepsilon$ poles disappear after the application of the shift $\boldsymbol{\xi}$, is an excellent check of the dimensional regularization procedure for the UV divergences.

[4] Using the notation of the appendix C, δI_{ij} is the 4PN coefficient in the sum of $\{-\frac{(-1+d)\hat{W}^{bi}\partial_a\Psi^{\partial_{bi}V}_{ij}}{2(-2+d)}\}$ from $\mathrm{MQSISD}_{2\mathrm{PN}}$, $\{-\frac{(-1+d)^2V\hat{X}}{(-2+d)^2}\}$ from $\mathrm{MQSISL}_{3\mathrm{PN}}$, $\{\frac{2(-1+d)\Psi^{\partial_t\partial_bV}_{ij}\partial_a\hat{R}_b}{-2+d}, \frac{2(-1+d)\Psi^{\partial_{bi}V}_{ij}\partial_a\hat{Z}_{bi}}{-2+d}, \frac{2(-1+d)\hat{Z}^{bi}\partial_a\Psi^{\partial_{bi}V}_{ij}}{-2+d}, \frac{4(-1+d)\Psi^{\partial_bV_i}_{ij}\partial_b\partial_a\hat{R}_i}{-2+d}, \frac{4(-1+d)\partial_a\Psi^{\partial_iV_b}_{ij}\partial^i\hat{R}^b}{-2+d}\}$ from $\mathrm{MQSISD}_{3\mathrm{PN}}$, $\{\frac{4(-1+d)\hat{M}^a{}_aV}{(-2+d)^2}\}$ from $\mathrm{MQSISL}_{4\mathrm{PN}}$, $\{-\frac{4(-1+d)M^{bi}\partial_a\Psi^{\partial_{bi}V}_{ij}}{-2+d}\}$ from $\mathrm{MQSISD}_{4\mathrm{PN}}$, $\{\frac{(-1+d)^2(2+d)\hat{R}_aV}{(-2+d)^2d(4+d)}\}$ from $\mathrm{MQVISL}_{3\mathrm{PN}}$ and $\{\frac{2(-1+d)^2(2+d)\Psi^{\partial_bV}_{iji}\partial_i\partial_a\hat{R}_b}{(-2+d)^2d(4+d)}, \frac{2(-1+d)^2(2+d)\partial_a\Psi^{\partial_bV}_{iji}\partial^i\hat{R}^b}{(-2+d)^2d(4+d)}\}$ from $\mathrm{MQVISD}_{3\mathrm{PN}}$.

Different checks are currently being performed on our result, especially regarding the integration of the surface sources, and regarding our implementation of distributional derivatives; (8.69)–(8.70) are just preliminary results and have not been published yet.

The next steps, which is left to future work, is therefore to implement the dimensional regularization to cure the IR divergences, and to apply the IR shift $\boldsymbol{\chi}$ [94], and to check whether the IR poles vanish as well. This requires however, a better understanding of the matching procedure in d dimensions, in order to extend the formula (8.1) in full dimensional regularization.

Once this is done, we can use the source mass quadrupole moment to express observable quantities, such as the energy flux, that depends on $\frac{\mathrm{d}^3 I_{ij}}{\mathrm{d}t^2}\frac{\mathrm{d}^3 I_{ij}}{\mathrm{d}t^2}$. We expect all the remaining constants (i.e. r_0, r_0' and r_0'') to disappear in the final result.

Conclusion

We have explained in chapters 1 and 2, how post-Newtonian theory plays a major role in the development of banks of templates, and how the accuracy of these templates directly impacts our ability to detect gravitational waves and to analyze the data collected by gravitational-wave detectors. This framework is therefore crucial to study general relativity and produce great science in the new field of gravitational wave astrophysics.

The projects carried out during this thesis were motivated by the goal to get the 4.5PN phase of gravitational waves for spinless compact binary systems in circular orbits, using the Blanchet-Damour-Iyer formalism. We performed computations in the different components of this framework and obtained new results in each of them: the multipolar-post-Minkowskian algorithm studying the radiative field, the equations of motion and the conserved quantities associated with the dynamics, and finally the computation of the source multipole moments. Besides, we saw how a matching equation relates all these projects together by matching the near-zone and the far-zone expansions of the metric.

In our journey to the 4.5PN phase, we made in this thesis significant progress. In the radiative field, the third-order tail effect at 4.5PN is fully determined. Hence, for circular orbits, we were able to compute the full 4.5PN coefficient in the energy flux. The last ambiguity parameter of the 4PN dynamics has been computed from first principles using the Fokker Lagrangian and the systematic use of the dimensional regularization. Besides, all the conserved quantities of the dynamics at 4PN are now explicitly computed. Finally, we computed all the potentials required to get the 4PN source mass quadrupole and obtained a preliminary result of this quadrupole based on the Finite Part regularization to treat the IR divergences. This latter result still needs to be checked by an independent computation. Besides, it appears now that dimensional regularization will also be required to cure the IR divergences of the 4PN mass quadrupole.This study will be the topic of further work.

Perspective

While the achievements done during this thesis get us closer to the 4.5PN phase of the signal, there are still few computations left to perform. The three main remaining tasks are:

1. The implementation of the dimensional regularization to cure the IR divergences of the mass quadrupole. Once this is done, we can check that the shift $\boldsymbol{\chi}$ removes the $1/\varepsilon$ IR poles.

2. The computation of the source current quadrupole J_{ij} at 3PN. This computation should also rely on dimensional regularization for the ultra-violet divergences but should be

however rather straightforward as we believe that most of the technical difficulties have been solved while computing the 4PN source mass quadrupole.

3. The computation of the 4PN coefficient in the flux. This coefficient requires both the 4PN mass quadrupole moments and the 3PN current quadrupole moments (as well as other multipole moments at lower PN orders which are already known). Besides, the leading order effect of the tails entering the flux at 1.5PN, should have a 2.5PN relative contribution due to the past dynamics of the binary. This contribution therefore modifies the 4PN coefficient in the flux.

While these three remaining tasks can be rather long and fastidious, we have now tackled and understood most of their technical difficulties (either in this thesis, or in previous work), and it would be reasonable to think that the 4.5PN phase and 4PN waveform will be obtained soon.

A – Conventions and notations

This appendix summarizes the conventions and the notations used within this thesis.

A.1 Indices and summation convention

In all this thesis, the metric $g_{\mu\nu}$ has a signature $+2$ and the Minkowski metric is given by $\eta_{\mu\nu} = \mathrm{diag}(-,+,+,+)$. Greek indices $(\alpha, \beta, \dots \mu, \nu, \dots)$ are space-time indices and take their values in $\{0,1,2,3\}$, while latin indices $(a, b, \dots, i, j, \dots)$ are space indices and take their values in $\{1,2,3\}$.

$g^{\mu\nu}$ is defined as the inverse of $g_{\mu\nu}$, i.e. $g^{\mu\rho}g_{\rho\nu} = \delta^{\mu}_{\nu}$. We raise and lower the indices of all the tensors appearing in this manuscript using the Minkowski metric $\eta_{\mu\nu}$(except for $g_{\mu\nu}$, $R^{\alpha}_{\beta\mu\nu}$ $R_{\mu\nu}$). Therefore, when summing over space indices using the Einstein convention, we might omit to raise one of the summed indices: $T_{ii} \equiv T^{i}_{i} = T_{ij}\eta^{ij}$.

In chapters 1 and 2, $h_{\mu\nu}$ is defined as $h_{\mu\nu} \equiv g_{\mu\nu} - \eta_{\mu\nu}$. In chapters 4 to 8, we define $h^{\mu\nu}$ as $h^{\mu\nu} \equiv \sqrt{-g}g^{\mu\nu} - \eta^{\mu\nu}$. Notice that in the harmonic coordinates, these two quantities correspond at linear order.

A.2 The Einstein equations

The Riemann tensor is defined as:

$$R^{\lambda}{}_{\rho\mu\nu} = \partial_{\mu}\Gamma^{\lambda}_{\rho\nu} - \partial_{\nu}\Gamma^{\lambda}_{\mu\rho} + \Gamma^{\epsilon}_{\rho\nu}\Gamma^{\lambda}_{\epsilon\mu} - \Gamma^{\epsilon}_{\mu\rho}\Gamma^{\lambda}_{\epsilon\nu} \,. \tag{A.1}$$

The Ricci tensor as well as the curvature scalar are defined as:

$$R_{\mu\nu} = R^{\lambda}_{\mu\lambda\nu} \,, R = R_{\mu\nu}g^{\mu\nu} \,. \tag{A.2}$$

We consider the Einstein equations without cosmological constant:

$$R_{\mu\nu} - \frac{1}{2}g_{\mu\nu}R = \frac{8\pi G}{c^4}T_{\mu\nu} \,. \tag{A.3}$$

A.3 Multiple indices

We often use the notation L to describe ℓ space indices: $L \equiv i_1 i_2 \dots i_\ell$ with $i_k \in \{1,2,3\}$. Similarly, $L-1$ represents $\ell-1$ space indices and so on. For example:

$$\partial_L I_L \equiv \partial_{i_1}\partial_{i_2} \dots \partial_{i_\ell} I_{i_1 i_2 \dots i_\ell} \,, \tag{A.4a}$$

$$\partial_{iL-1} I_{L-1} \equiv \partial_i \partial_{i_1}\partial_{i_2} \dots \partial_{i_{\ell-1}} I_{i_1 i_2 \dots i_{\ell-1}} \,. \tag{A.4b}$$

A.4 Geometrical variables

The figure A.1 lists the different variables used in this thesis to describe a compact binary systems. Quantities in bold ($\boldsymbol{y}_1$, $\boldsymbol{n}$ etc.) represent vectors.

In chapter 7, some results are expressed in the center of mass frame. In that frame, we usually denotes r_{12} as r and $\boldsymbol{n}_{12}$ as $\boldsymbol{n}$. While this notation is in conflict with the notation used for the field point $\boldsymbol{x} = r\boldsymbol{n}$, the context always removes any ambiguity in the notation.

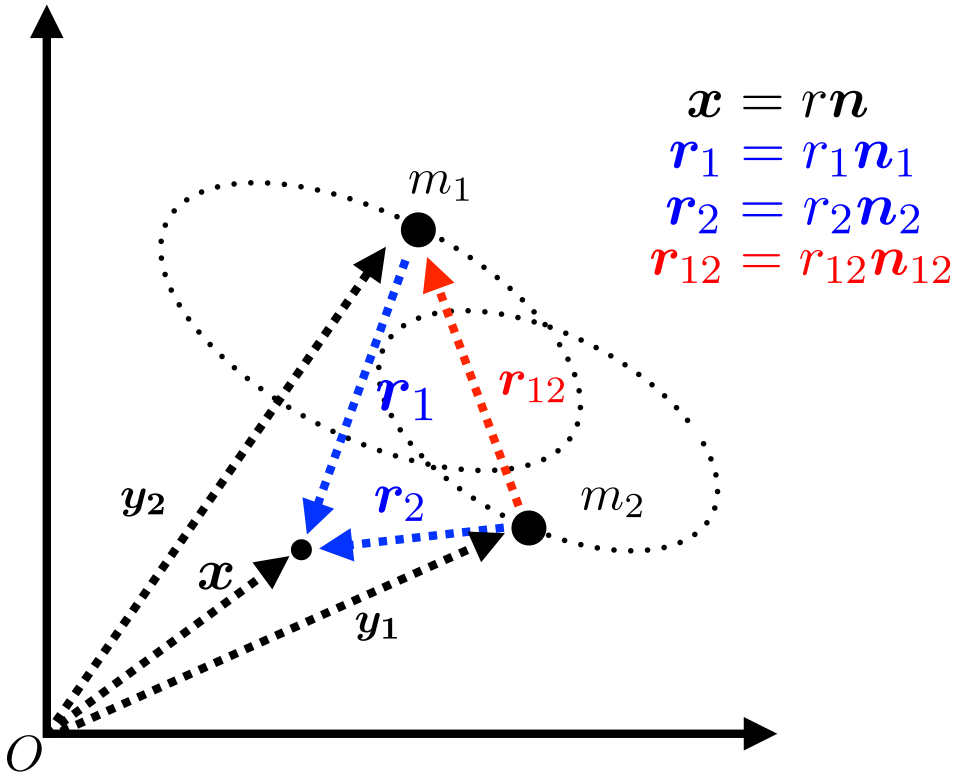

Figure A.1

B – 4PN Fokker Lagrangian

This appendix provides the 4PN Fokker Lagrangian which constitutes the final result of chapter 6. This Lagrangian was computed in [92, 93] with the last ambiguities being fully determined in [94, 2]. This result corresponds to the computation explained in chapter 6, modulo a shift given in section B.2

B.1 The Fokker Lagrangian

$$L_{\mathrm{N}} = \frac{Gm_1m_2}{2r_{12}} + \frac{m_1v_1^2}{2} + 1 \leftrightarrow 2\,, \tag{B.1a}$$

$$\begin{aligned}L_{1\mathrm{PN}} = &-\frac{G^2m_1^2m_2}{2r_{12}^2} + \frac{m_1v_1^4}{8}\\ &+ \frac{Gm_1m_2}{r_{12}}\left(-\frac{1}{4}(n_{12}v_1)(n_{12}v_2) + \frac{3}{2}v_1^2 - \frac{7}{4}(v_1v_2)\right) + 1 \leftrightarrow 2\,,\end{aligned} \tag{B.1b}$$

$$\begin{aligned}L_{2\mathrm{PN}} = &\frac{G^3m_1^3m_2}{2r_{12}^3} + \frac{19G^3m_1^2m_2^2}{8r_{12}^3}\\ &+ \frac{G^2m_1^2m_2}{r_{12}^2}\left(\frac{7}{2}(n_{12}v_1)^2 - \frac{7}{2}(n_{12}v_1)(n_{12}v_2) + \frac{1}{2}(n_{12}v_2)^2 + \frac{1}{4}v_1^2 - \frac{7}{4}(v_1v_2) + \frac{7}{4}v_2^2\right)\\ &+ \frac{Gm_1m_2}{r_{12}}\Big(\frac{3}{16}(n_{12}v_1)^2(n_{12}v_2)^2 - \frac{7}{8}(n_{12}v_2)^2v_1^2 + \frac{7}{8}v_1^4 + \frac{3}{4}(n_{12}v_1)(n_{12}v_2)(v_1v_2)\\ &\quad - 2v_1^2(v_1v_2) + \frac{1}{8}(v_1v_2)^2 + \frac{15}{16}v_1^2v_2^2\Big) + \frac{m_1v_1^6}{16}\\ &+ Gm_1m_2\left(-\frac{7}{4}(a_1v_2)(n_{12}v_2) - \frac{1}{8}(n_{12}a_1)(n_{12}v_2)^2 + \frac{7}{8}(n_{12}a_1)v_2^2\right) + 1 \leftrightarrow 2\,,\end{aligned} \tag{B.1c}$$

$$\begin{aligned}L_{3\mathrm{PN}} = &\frac{G^2m_1^2m_2}{r_{12}^2}\Big(\frac{13}{18}(n_{12}v_1)^4 + \frac{83}{18}(n_{12}v_1)^3(n_{12}v_2) - \frac{35}{6}(n_{12}v_1)^2(n_{12}v_2)^2 - \frac{245}{24}(n_{12}v_1)^2v_1^2\\ &\quad + \frac{179}{12}(n_{12}v_1)(n_{12}v_2)v_1^2 - \frac{235}{24}(n_{12}v_2)^2v_1^2 + \frac{373}{48}v_1^4 + \frac{529}{24}(n_{12}v_1)^2(v_1v_2)\\ &\quad - \frac{97}{6}(n_{12}v_1)(n_{12}v_2)(v_1v_2) - \frac{719}{24}v_1^2(v_1v_2) + \frac{463}{24}(v_1v_2)^2 - \frac{7}{24}(n_{12}v_1)^2v_2^2\\ &\quad - \frac{1}{2}(n_{12}v_1)(n_{12}v_2)v_2^2 + \frac{1}{4}(n_{12}v_2)^2v_2^2 + \frac{463}{48}v_1^2v_2^2 - \frac{19}{2}(v_1v_2)v_2^2 + \frac{45}{16}v_2^4\Big)\\ &+ Gm_1m_2\Big(\frac{3}{8}(a_1v_2)(n_{12}v_1)(n_{12}v_2)^2 + \frac{5}{12}(a_1v_2)(n_{12}v_2)^3 + \frac{1}{8}(n_{12}a_1)(n_{12}v_1)(n_{12}v_2)^3\end{aligned}$$

$$
\begin{aligned}
&+\frac{1}{16}(n_{12}a_1)(n_{12}v_2)^4+\frac{11}{4}(a_1v_1)(n_{12}v_2)v_1^2-(a_1v_2)(n_{12}v_2)v_1^2\\
&-2(a_1v_1)(n_{12}v_2)(v_1v_2)+\frac{1}{4}(a_1v_2)(n_{12}v_2)(v_1v_2)\\
&+\frac{3}{8}(n_{12}a_1)(n_{12}v_2)^2(v_1v_2)-\frac{5}{8}(n_{12}a_1)(n_{12}v_1)^2v_2^2+\frac{15}{8}(a_1v_1)(n_{12}v_2)v_2^2\\
&-\frac{15}{8}(a_1v_2)(n_{12}v_2)v_2^2-\frac{1}{2}(n_{12}a_1)(n_{12}v_1)(n_{12}v_2)v_2^2\\
&-\frac{5}{16}(n_{12}a_1)(n_{12}v_2)^2v_2^2\Big)+\frac{5m_1v_1^8}{128}\\
+\,&\frac{G^2m_1^2m_2}{r_{12}}\Big(-\frac{235}{24}(a_2v_1)(n_{12}v_1)-\frac{29}{24}(n_{12}a_2)(n_{12}v_1)^2-\frac{235}{24}(a_1v_2)(n_{12}v_2)\\
&-\frac{17}{6}(n_{12}a_1)(n_{12}v_2)^2+\frac{185}{16}(n_{12}a_1)v_1^2-\frac{235}{48}(n_{12}a_2)v_1^2\\
&-\frac{185}{8}(n_{12}a_1)(v_1v_2)+\frac{20}{3}(n_{12}a_1)v_2^2\Big)\\
+\,&\frac{Gm_1m_2}{r_{12}}\Big(-\frac{5}{32}(n_{12}v_1)^3(n_{12}v_2)^3+\frac{1}{8}(n_{12}v_1)(n_{12}v_2)^3v_1^2+\frac{5}{8}(n_{12}v_2)^4v_1^2\\
&-\frac{11}{16}(n_{12}v_1)(n_{12}v_2)v_1^4+\frac{1}{4}(n_{12}v_2)^2v_1^4+\frac{11}{16}v_1^6\\
&-\frac{15}{32}(n_{12}v_1)^2(n_{12}v_2)^2(v_1v_2)+(n_{12}v_1)(n_{12}v_2)v_1^2(v_1v_2)\\
&+\frac{3}{8}(n_{12}v_2)^2v_1^2(v_1v_2)-\frac{13}{16}v_1^4(v_1v_2)+\frac{5}{16}(n_{12}v_1)(n_{12}v_2)(v_1v_2)^2\\
&+\frac{1}{16}(v_1v_2)^3-\frac{5}{8}(n_{12}v_1)^2v_1^2v_2^2-\frac{23}{32}(n_{12}v_1)(n_{12}v_2)v_1^2v_2^2+\frac{1}{16}v_1^4v_2^2\\
&-\frac{1}{32}v_1^2(v_1v_2)v_2^2\Big)\\
-\,&\frac{3G^4m_1^4m_2}{8r_{12}^4}+\frac{G^4m_1^3m_2^2}{r_{12}^4}\left(-\frac{9707}{420}+\frac{22}{3}\ln\left(\frac{r_{12}}{r'_1}\right)\right)\\
+\,&\frac{G^3m_1^2m_2^2}{r_{12}^3}\Big(\frac{383}{24}(n_{12}v_1)^2-\frac{889}{48}(n_{12}v_1)(n_{12}v_2)\\
&-\frac{123}{64}(n_{12}v_1)(n_{12}v_{12})\pi^2-\frac{305}{72}v_1^2+\frac{41}{64}\pi^2(v_1v_{12})+\frac{439}{144}(v_1v_2)\Big)\\
+\,&\frac{G^3m_1^3m_2}{r_{12}^3}\Big(-\frac{8243}{210}(n_{12}v_1)^2+\frac{15541}{420}(n_{12}v_1)(n_{12}v_2)+\frac{3}{2}(n_{12}v_2)^2+\frac{15611}{1260}v_1^2\\
&-\frac{17501}{1260}(v_1v_2)+\frac{5}{4}v_2^2+22(n_{12}v_1)(n_{12}v_{12})\ln\left(\frac{r_{12}}{r'_1}\right)\\
&-\frac{22}{3}(v_1v_{12})\ln\left(\frac{r_{12}}{r'_1}\right)\Big)+1\leftrightarrow 2\,.
\end{aligned}
\tag{B.1d}
$$

The following 4PN part of the harmonic-coordinates Lagrangian, is expressed using the convention defined by equation (7.3).

$$
L^{(0)}_{\rm 4PN}=\frac{7}{256}m_1v_1^{10}+1\leftrightarrow 2\,,
\tag{B.2a}
$$

$$
\begin{aligned}
L^{(1)}_{4\mathrm{PN}} = m_1 m_2 \Bigg(& \frac{13}{64}(a_2v_1)(n_{12}v_1)^5 + \frac{5}{128}(a_2n_{12})(n_{12}v_1)^6 - \frac{13}{64}(n_{12}v_1)^5(a_2v_2) \\
& + \frac{11}{64}(a_2v_1)(n_{12}v_1)^4(n_{12}v_2) + \frac{5}{64}(a_2n_{12})(n_{12}v_1)^5(n_{12}v_2) \\
& + \frac{5}{32}(a_2v_1)(n_{12}v_1)^3(n_{12}v_2)^2 - \frac{5}{32}(a_1n_{12})(n_{12}v_1)^3(n_{12}v_2)^3 \\
& - \frac{1}{16}(a_2v_1)(n_{12}v_1)^3(v_1v_2) + \frac{11}{64}(a_2n_{12})(n_{12}v_1)^4(v_1v_2) \\
& + \frac{5}{16}(a_2n_{12})(n_{12}v_1)^3(n_{12}v_2)(v_1v_2) + \frac{5}{16}(n_{12}v_1)^2(a_1v_2)(n_{12}v_2)(v_1v_2) \\
& - \frac{3}{16}(a_2v_1)(n_{12}v_1)(v_1v_2)^2 + \frac{1}{16}(a_1v_1)(n_{12}v_2)(v_1v_2)^2 \\
& + \frac{5}{16}(a_1n_{12})(n_{12}v_1)(n_{12}v_2)(v_1v_2)^2 - \frac{77}{96}(a_2v_1)(n_{12}v_1)^3v_1^2 - \frac{27}{128}(a_2n_{12})(n_{12}v_1)^4v_1^2 \\
& + \frac{77}{96}(n_{12}v_1)^3(a_2v_2)v_1^2 - \frac{13}{32}(a_2v_1)(n_{12}v_1)^2(n_{12}v_2)v_1^2 - \frac{11}{32}(a_2n_{12})(n_{12}v_1)^3(n_{12}v_2)v_1^2 \\
& - \frac{7}{32}(a_2v_1)(n_{12}v_1)(n_{12}v_2)^2v_1^2 - \frac{27}{64}(a_2n_{12})(n_{12}v_1)^2(n_{12}v_2)^2v_1^2 - \frac{19}{32}(a_1v_1)(n_{12}v_2)^3v_1^2 \\
& - \frac{3}{16}(a_2v_1)(n_{12}v_1)(v_1v_2)v_1^2 - \frac{13}{32}(a_2n_{12})(n_{12}v_1)^2(v_1v_2)v_1^2 \\
& + \frac{33}{16}(n_{12}v_1)(a_2v_2)(v_1v_2)v_1^2 - \frac{7}{16}(a_2n_{12})(n_{12}v_1)(n_{12}v_2)(v_1v_2)v_1^2 \\
& + \frac{1}{16}(a_1v_2)(n_{12}v_2)(v_1v_2)v_1^2 + \frac{123}{64}(a_2v_1)(n_{12}v_1)v_1^4 + \frac{53}{128}(a_2n_{12})(n_{12}v_1)^2v_1^4 \\
& - \frac{123}{64}(n_{12}v_1)(a_2v_2)v_1^4 + \frac{49}{64}(a_2v_1)(n_{12}v_2)v_1^4 + \frac{31}{64}(a_2n_{12})(n_{12}v_1)(n_{12}v_2)v_1^4 \\
& + \frac{49}{64}(a_2n_{12})(v_1v_2)v_1^4 - \frac{75}{128}(a_2n_{12})v_1^6 + \frac{17}{96}(n_{12}v_1)^3(a_1v_2)v_2^2 \\
& - \frac{23}{32}(a_1v_1)(n_{12}v_1)^2(n_{12}v_2)v_2^2 + \frac{15}{32}(a_1n_{12})(n_{12}v_1)^3(n_{12}v_2)v_2^2 \\
& + \frac{17}{32}(a_1n_{12})(n_{12}v_1)^2(v_1v_2)v_2^2 + \frac{33}{32}(a_2v_1)(n_{12}v_1)v_1^2v_2^2 + \frac{93}{32}(a_1v_1)(n_{12}v_2)v_1^2v_2^2 \\
& - \frac{23}{32}(a_1n_{12})(n_{12}v_1)(n_{12}v_2)v_1^2v_2^2\Bigg) \\
+ \frac{m_1m_2}{r_{12}} \Bigg(& \frac{35}{128}(n_{12}v_1)^5(n_{12}v_2)^3 - \frac{35}{256}(n_{12}v_1)^4(n_{12}v_2)^4 \\
& - \frac{15}{128}(n_{12}v_1)^4(n_{12}v_2)^2(v_1v_2) + \frac{15}{32}(n_{12}v_1)^3(n_{12}v_2)^3(v_1v_2) \\
& - \frac{15}{32}(n_{12}v_1)^3(n_{12}v_2)(v_1v_2)^2 + \frac{5}{32}(n_{12}v_1)^2(v_1v_2)^3 - \frac{3}{16}(n_{12}v_1)(n_{12}v_2)(v_1v_2)^3 \\
& + \frac{1}{32}(v_1v_2)^4 - \frac{5}{32}(n_{12}v_1)^3(n_{12}v_2)^3v_1^2 - \frac{5}{16}(n_{12}v_1)(n_{12}v_2)^3(v_1v_2)v_1^2 \\
& + \frac{9}{32}(n_{12}v_1)(n_{12}v_2)(v_1v_2)^2v_1^2 - \frac{15}{32}(n_{12}v_2)^2(v_1v_2)^2v_1^2 + \frac{1}{32}(v_1v_2)^3v_1^2 \\
& + \frac{57}{128}(n_{12}v_1)(n_{12}v_2)^3v_1^4 - \frac{15}{128}(n_{12}v_2)^4v_1^4 + \frac{39}{128}(n_{12}v_2)^2(v_1v_2)v_1^4 + \frac{3}{4}(v_1v_2)^2v_1^4 \\
& - \frac{11}{32}(n_{12}v_2)^2v_1^6 - \frac{5}{4}(v_1v_2)v_1^6 + \frac{75}{128}v_1^8 - \frac{75}{128}(n_{12}v_1)^5(n_{12}v_2)v_2^2
\end{aligned}
$$

$$
\begin{aligned}
& - \frac{53}{128}(n_{12}v_1)^4(v_1v_2)v_2^2 + \frac{99}{64}(n_{12}v_1)^3(n_{12}v_2)v_1^2v_2^2 - \frac{21}{64}(n_{12}v_1)^2(n_{12}v_2)^2v_1^2v_2^2 \\
& + \frac{11}{64}(n_{12}v_1)^2(v_1v_2)v_1^2v_2^2 + \frac{35}{32}(n_{12}v_1)(n_{12}v_2)(v_1v_2)v_1^2v_2^2 - \frac{1}{32}(v_1v_2)^2v_1^2v_2^2 \\
& - \frac{185}{128}(n_{12}v_1)(n_{12}v_2)v_1^4v_2^2 + \frac{23}{64}(n_{12}v_2)^2v_1^4v_2^2 - \frac{99}{128}(v_1v_2)v_1^4v_2^2 + \frac{5}{8}v_1^6v_2^2 \\
& + \frac{3}{256}v_1^4v_2^4\Big) + 1 \leftrightarrow 2 \,, \qquad \text{(B.2b)}
\end{aligned}
$$

$$
\begin{aligned}
L^{(2)}_{\rm 4PN} = & \frac{m_1^2m_2}{r_{12}}\Big(\frac{2099}{288}(a_1v_1)(n_{12}v_1)^3 + \frac{3341}{480}(a_2v_1)(n_{12}v_1)^3 + \frac{59}{180}(n_{12}v_1)^3(a_2v_2) \\
& + \frac{2197}{240}(a_1n_{12})(n_{12}v_1)^3(n_{12}v_2) + \frac{6661}{720}(a_2n_{12})(n_{12}v_1)^3(n_{12}v_2) \\
& + \frac{10223}{480}(n_{12}v_1)^2(a_1v_2)(n_{12}v_2) + \frac{3059}{96}(a_1v_1)(n_{12}v_1)(n_{12}v_2)^2 \\
& - \frac{3781}{160}(n_{12}v_1)(a_1v_2)(n_{12}v_2)^2 + \frac{1337}{240}(a_1n_{12})(n_{12}v_1)(n_{12}v_2)^3 + \frac{4621}{480}(a_1v_2)(n_{12}v_2)^3 \\
& + \frac{1133}{960}(a_1n_{12})(n_{12}v_2)^4 + \frac{3613}{48}(a_1v_1)(n_{12}v_1)(v_1v_2) + \frac{4529}{240}(a_2v_1)(n_{12}v_1)(v_1v_2) \\
& + \frac{2099}{96}(a_1n_{12})(n_{12}v_1)^2(v_1v_2) - \frac{23}{60}(a_1n_{12})(n_{12}v_1)(n_{12}v_2)(v_1v_2) \\
& + \frac{6499}{240}(a_1v_2)(n_{12}v_2)(v_1v_2) + \frac{247}{30}(a_1n_{12})(n_{12}v_2)^2(v_1v_2) + \frac{2503}{96}(a_1n_{12})(v_1v_2)^2 \\
& + \frac{7193}{240}(a_2v_1)(n_{12}v_1)v_1^2 + \frac{3021}{320}(a_2n_{12})(n_{12}v_1)^2v_1^2 + \frac{4723}{96}(n_{12}v_1)(a_1v_2)v_1^2 \\
& + \frac{3679}{480}(n_{12}v_1)(a_2v_2)v_1^2 + \frac{13549}{480}(a_1v_1)(n_{12}v_2)v_1^2 + \frac{8849}{480}(a_2v_1)(n_{12}v_2)v_1^2 \\
& + \frac{2063}{96}(a_1n_{12})(n_{12}v_1)(n_{12}v_2)v_1^2 + \frac{166}{15}(a_2n_{12})(n_{12}v_1)(n_{12}v_2)v_1^2 \\
& + \frac{4621}{320}(a_2n_{12})(n_{12}v_2)^2v_1^2 + \frac{8849}{480}(a_2n_{12})(v_1v_2)v_1^2 + \frac{6943}{384}(a_1n_{12})v_1^4 \\
& + \frac{2293}{160}(n_{12}v_1)(a_1v_2)v_2^2 + \frac{3733}{160}(a_1v_1)(n_{12}v_2)v_2^2 + \frac{7}{5}(a_1n_{12})(n_{12}v_1)(n_{12}v_2)v_2^2 \\
& - \frac{3733}{160}(a_1v_2)(n_{12}v_2)v_2^2 - \frac{139}{20}(a_1n_{12})(n_{12}v_2)^2v_2^2 - \frac{5593}{240}(a_1n_{12})(v_1v_2)v_2^2 \\
& + \frac{3613}{192}(a_1n_{12})v_1^2v_2^2 + \frac{2931}{320}(a_1n_{12})v_2^4\Big) \\
& + \frac{m_1^2m_2}{r_{12}^2}\Big(-\frac{4027}{800}(n_{12}v_1)^6 + \frac{3227}{800}(n_{12}v_1)^5(n_{12}v_2) - \frac{6301}{240}(n_{12}v_1)^4(n_{12}v_2)^2 \\
& + \frac{6661}{240}(n_{12}v_1)^3(n_{12}v_2)^3 - \frac{2221}{64}(n_{12}v_1)^4(v_1v_2) + \frac{25267}{720}(n_{12}v_1)^3(n_{12}v_2)(v_1v_2) \\
& - \frac{6661}{480}(n_{12}v_1)^2(n_{12}v_2)^2(v_1v_2) - \frac{23401}{480}(n_{12}v_1)^2(v_1v_2)^2 \\
& + \frac{4529}{240}(n_{12}v_1)(n_{12}v_2)(v_1v_2)^2 - \frac{8369}{480}(v_1v_2)^3 + \frac{17393}{2880}(n_{12}v_1)^4v_1^2 \\
& - \frac{26237}{720}(n_{12}v_1)^3(n_{12}v_2)v_1^2 + \frac{4561}{160}(n_{12}v_1)^2(n_{12}v_2)^2v_1^2 + \frac{691}{240}(n_{12}v_1)(n_{12}v_2)^3v_1^2 \\
& + \frac{4621}{240}(n_{12}v_2)^4v_1^2 - \frac{14987}{960}(n_{12}v_1)^2(v_1v_2)v_1^2 + \frac{2601}{160}(n_{12}v_1)(n_{12}v_2)(v_1v_2)v_1^2
\end{aligned}
$$

$$
\begin{aligned}
&+\frac{14649}{320}(n_{12}v_2)^2(v_1v_2)v_1^2+\frac{97}{5}(v_1v_2)^2v_1^2-\frac{4879}{320}(n_{12}v_1)^2v_1^4\\
&+\frac{5399}{192}(n_{12}v_1)(n_{12}v_2)v_1^4+\frac{83}{15}(n_{12}v_2)^2v_1^4+\frac{749}{128}(v_1v_2)v_1^4+\frac{20389}{1920}v_1^6\\
&+\frac{107}{180}(n_{12}v_1)^4v_2^2-\frac{1823}{240}(n_{12}v_1)^3(n_{12}v_2)v_2^2-\frac{1}{2}(n_{12}v_1)^2(n_{12}v_2)^2v_2^2\\
&+\frac{1021}{120}(n_{12}v_1)^2(v_1v_2)v_2^2+\frac{1}{2}(n_{12}v_1)(n_{12}v_2)(v_1v_2)v_2^2+\frac{67}{4}(v_1v_2)^2v_2^2\\
&-\frac{21709}{960}(n_{12}v_1)^2v_1^2v_2^2-\frac{1873}{480}(n_{12}v_1)(n_{12}v_2)v_1^2v_2^2-\frac{4621}{320}(n_{12}v_2)^2v_1^2v_2^2\\
&-\frac{42017}{960}(v_1v_2)v_1^2v_2^2+\frac{11119}{960}v_1^4v_2^2-\frac{21}{8}(n_{12}v_1)^2v_2^4-\frac{3}{8}(n_{12}v_1)(n_{12}v_2)v_2^4\\
&+\frac{3}{16}(n_{12}v_2)^2v_2^4-\frac{105}{8}(v_1v_2)v_2^4+\frac{105}{16}v_1^2v_2^4+\frac{115}{32}v_2^6\Bigg)+1\leftrightarrow 2\,,
\end{aligned}
\tag{B.2c}
$$

$$
\begin{aligned}
L^{(3)}_{4\mathrm{PN}}=&\frac{m_1^2m_2^2}{r_{12}^2}\Bigg(-\frac{1099}{144}(a_2v_1)(n_{12}v_1)+\frac{41}{64}\pi^2(a_2v_1)(n_{12}v_1)+\frac{2005}{96}(a_2n_{12})(n_{12}v_1)^2\\
&-\frac{123}{128}\pi^2(a_2n_{12})(n_{12}v_1)^2+\frac{225233}{1800}(a_1v_1)(n_{12}v_2)-\frac{43}{64}\pi^2(a_1v_1)(n_{12}v_2)\\
&-\frac{477941}{3600}(a_1n_{12})(v_1v_2)+\frac{21}{16}\pi^2(a_1n_{12})(v_1v_2)+\frac{477941}{7200}(a_1n_{12})v_1^2\\
&-\frac{21}{32}\pi^2(a_1n_{12})v_1^2\Bigg)\\
+&\frac{m_1^2m_2^2}{r_{12}^3}\Bigg(-\frac{173617}{2880}(n_{12}v_1)^4-\frac{2155}{1024}\pi^2(n_{12}v_1)^4\\
&+\frac{173587}{720}(n_{12}v_1)^3(n_{12}v_2)+\frac{2155}{256}\pi^2(n_{12}v_1)^3(n_{12}v_2)-\frac{85871}{480}(n_{12}v_1)^2(n_{12}v_2)^2\\
&-\frac{6465}{1024}\pi^2(n_{12}v_1)^2(n_{12}v_2)^2+\frac{5651}{300}(n_{12}v_1)^2(v_1v_2)-\frac{939}{256}\pi^2(n_{12}v_1)^2(v_1v_2)\\
&-\frac{6851}{300}(n_{12}v_1)(n_{12}v_2)(v_1v_2)+\frac{939}{256}\pi^2(n_{12}v_1)(n_{12}v_2)(v_1v_2)+\frac{49139}{720}(v_1v_2)^2\\
&-\frac{195}{512}\pi^2(v_1v_2)^2-\frac{3677}{1200}(n_{12}v_1)^2v_1^2+\frac{447}{512}\pi^2(n_{12}v_1)^2v_1^2-\frac{222679}{1200}(n_{12}v_1)(n_{12}v_2)v_1^2\\
&-\frac{189}{256}\pi^2(n_{12}v_1)(n_{12}v_2)v_1^2+\frac{153079}{800}(n_{12}v_2)^2v_1^2-\frac{69}{512}\pi^2(n_{12}v_2)^2v_1^2\\
&-\frac{61733}{900}(v_1v_2)v_1^2-\frac{55}{256}\pi^2(v_1v_2)v_1^2+\frac{10337}{320}v_1^4+\frac{133}{1024}\pi^2v_1^4-\frac{116123}{3600}v_1^2v_2^2\\
&+\frac{477}{1024}\pi^2v_1^2v_2^2\Bigg)\\
+&\frac{m_1^3m_2}{r_{12}^2}\Bigg(\frac{44023}{720}(a_1v_1)(n_{12}v_1)+\frac{562}{9}(a_2v_1)(n_{12}v_1)\\
&+44\ln\left(\frac{r_{12}}{r'_1}\right)(n_{12}v_1)(a_1v_2)-44\ln\left(\frac{r_{12}}{r'_1}\right)(n_{12}v_1)(a_2v_2)+\frac{110}{3}\ln\left(\frac{r_{12}}{r'_1}\right)(a_1v_1)(n_{12}v_2)\\
&+\frac{6397}{75}(a_1n_{12})(n_{12}v_1)(n_{12}v_2)+\frac{198097}{4200}(a_2n_{12})(n_{12}v_1)(n_{12}v_2)\\
&+22\ln\left(\frac{r_{12}}{r'_1}\right)(a_2n_{12})(n_{12}v_1)(n_{12}v_2)+\frac{14377}{280}(a_1v_2)(n_{12}v_2)
\end{aligned}
$$

$$
\begin{aligned}
&- \frac{110}{3} \ln\left(\frac{r_{12}}{r'_1}\right)(a_1 v_2)(n_{12} v_2) + \frac{44023}{720}(a_1 n_{12})(v_1 v_2) - 44 \ln\left(\frac{r_{12}}{r'_1}\right)(a_1 n_{12})(v_1 v_2) \\
&+44 \ln\left(\frac{r_{12}}{r'_1}\right)(a_1 n_{12}) v_1^2 + \frac{14377}{560}(a_2 n_{12}) v_1^2 + \frac{937}{1440}(a_1 n_{12}) v_2^2\bigg) \\
&+ \frac{m_1^3 m_2}{r_{12}^3}\bigg(-\frac{30313}{360}(n_{12}v_1)^4 + \frac{64001}{720}(n_{12}v_1)^3(n_{12}v_2) - \frac{185917}{1680}(n_{12}v_1)^2(n_{12}v_2)^2 \\
&- 55\ln\left(\frac{r_{12}}{r'_1}\right)(n_{12}v_1)^2(n_{12}v_2)^2 + \frac{179617}{1680}(n_{12}v_1)(n_{12}v_2)^3 + 55\ln\left(\frac{r_{12}}{r'_1}\right)(n_{12}v_1)(n_{12}v_2)^3 \\
&- \frac{94667}{400}(n_{12}v_1)^2(v_1v_2) + \frac{338099}{1400}(n_{12}v_1)(n_{12}v_2)(v_1v_2) \\
&+ 22\ln\left(\frac{r_{12}}{r'_1}\right)(n_{12}v_1)(n_{12}v_2)(v_1v_2) - \frac{214897}{8400}(n_{12}v_2)^2(v_1v_2) \\
&- 11\ln\left(\frac{r_{12}}{r'_1}\right)(n_{12}v_2)^2(v_1v_2) - \frac{737}{18}(v_1v_2)^2 + \frac{903589}{16800}(n_{12}v_1)^2 v_1^2 \\
&- 55\ln\left(\frac{r_{12}}{r'_1}\right)(n_{12}v_1)^2 v_1^2 - \frac{96287}{1120}(n_{12}v_1)(n_{12}v_2)v_1^2 + 55\ln\left(\frac{r_{12}}{r'_1}\right)(n_{12}v_1)(n_{12}v_2)v_1^2 \\
&+ \frac{426731}{4200}(n_{12}v_2)^2 v_1^2 + 11\ln\left(\frac{r_{12}}{r'_1}\right)(n_{12}v_2)^2 v_1^2 + \frac{202687}{3360}(v_1v_2)v_1^2 \\
&- \frac{55}{3}\ln\left(\frac{r_{12}}{r'_1}\right)(v_1v_2)v_1^2 + \frac{22769}{2016}v_1^4 + \frac{55}{3}\ln\left(\frac{r_{12}}{r'_1}\right)v_1^4 - \frac{177}{8}(n_{12}v_1)^2 v_2^2 \\
&+ 66\ln\left(\frac{r_{12}}{r'_1}\right)(n_{12}v_1)^2 v_2^2 - \frac{120397}{4200}(n_{12}v_1)(n_{12}v_2)v_2^2 - 88\ln\left(\frac{r_{12}}{r'_1}\right)(n_{12}v_1)(n_{12}v_2)v_2^2 \\
&+ \frac{7}{4}(n_{12}v_2)^2 v_2^2 - \frac{43}{2}(v_1v_2)v_2^2 + 22\ln\left(\frac{r_{12}}{r'_1}\right)(v_1v_2)v_2^2 - \frac{8357}{560}v_1^2 v_2^2 - 22\ln\left(\frac{r_{12}}{r'_1}\right)v_1^2 v_2^2 \\
&+\frac{91}{16}v_2^4\bigg) + 1 \leftrightarrow 2\,, \qquad \text{(B.2d)}
\end{aligned}
$$

$$
\begin{aligned}
L^{(4)}_{\rm 4PN} = \frac{m_1^4 m_2}{r_{12}^4}&\bigg(\frac{282629}{900}(n_{12}v_1)^2 - \frac{880}{3}\ln\left(\frac{r_{12}}{r'_1}\right)(n_{12}v_1)^2 - \frac{283979}{900}(n_{12}v_1)(n_{12}v_2) \\
&+ \frac{880}{3}\ln\left(\frac{r_{12}}{r'_1}\right)(n_{12}v_1)(n_{12}v_2) + \frac{9}{4}(n_{12}v_2)^2 + \frac{208529}{3600}(v_1v_2) - \frac{220}{3}\ln\left(\frac{r_{12}}{r'_1}\right)(v_1v_2) \\
&-\frac{211229}{3600}v_1^2 + \frac{220}{3}\ln\left(\frac{r_{12}}{r'_1}\right)v_1^2 + \frac{15}{16}v_2^2\bigg) \\
+ \frac{m_1^3 m_2^2}{r_{12}^4}&\bigg(-\frac{1268557}{50400}(n_{12}v_1)^2 + \frac{659}{96}\pi^2(n_{12}v_1)^2 \\
&- \frac{286}{3}\ln\left(\frac{r_{12}}{r'_1}\right)(n_{12}v_1)^2 + \frac{11530469}{25200}(n_{12}v_1)(n_{12}v_2) \\
&- \frac{1715}{48}\pi^2(n_{12}v_1)(n_{12}v_2) + 44\ln\left(\frac{r_{12}}{r'_1}\right)(n_{12}v_1)(n_{12}v_2) + 64\ln\left(\frac{r_{12}}{r'_2}\right)(n_{12}v_1)(n_{12}v_2) \\
&- \frac{2233689}{5600}(n_{12}v_2)^2 + \frac{2771}{96}\pi^2(n_{12}v_2)^2 + \frac{110}{3}\ln\left(\frac{r_{12}}{r'_1}\right)(n_{12}v_2)^2 - 64\ln\left(\frac{r_{12}}{r'_2}\right)(n_{12}v_2)^2 \\
&- \frac{959797}{8400}(v_1v_2) + \frac{103}{16}\pi^2(v_1v_2) - \frac{154}{3}\ln\left(\frac{r_{12}}{r'_1}\right)(v_1v_2) - 16\ln\left(\frac{r_{12}}{r'_2}\right)(v_1v_2)
\end{aligned}
$$

$$+\frac{858533}{50400}v_1^2-\frac{15}{32}\pi^2v_1^2+\frac{121}{3}\ln\left(\frac{r_{12}}{r'_1}\right)v_1^2+\frac{5482669}{50400}v_2^2-\frac{191}{32}\pi^2v_2^2+\frac{22}{3}\ln\left(\frac{r_{12}}{r'_1}\right)v_2^2$$
$$+16\ln\left(\frac{r_{12}}{r'_2}\right)v_2^2\bigg)+1\leftrightarrow 2\,, \tag{B.2e}$$
$$L^{(5)}_{4\text{PN}}=\frac{3}{8}\frac{m_1^5m_2}{r_{12}^5}+\frac{m_1^3m_2^3}{r_{12}^5}\left(\frac{597771}{5600}-\frac{71}{32}\pi^2-\frac{110}{3}\ln\left(\frac{r_{12}}{r'_1}\right)\right)$$
$$+\frac{m_1^4m_2^2}{r_{12}^5}\left(\frac{1734977}{25200}+\frac{105}{32}\pi^2-\frac{242}{3}\ln\left(\frac{r_{12}}{r'_1}\right)-16\ln\left(\frac{r_{12}}{r'_2}\right)\right)+1\leftrightarrow 2\,. \tag{B.2f}$$

Besides all previous instantaneous terms, there is also the following non-local tail[1]:

$$\begin{aligned}L^{\text{tail}}&=\frac{G^2M}{5c^8}\,I^{(3)}_{ij}(t)\underset{2r_{12}/c}{\text{Pf}}\int_{-\infty}^{+\infty}\frac{\mathrm{d}t'}{|t-t'|}I^{(3)}_{ij}(t')\\&=\frac{G^2M}{5c^8}\,I^{(3)}_{ij}(t)\int_0^{+\infty}\mathrm{d}\tau\,\ln\left(\frac{c\tau}{2r_{12}}\right)\left[I^{(4)}_{ij}(t-\tau)-I^{(4)}_{ij}(t+\tau)\right]\,.\end{aligned} \tag{B.3}$$

B.2 Shifts applied

The Lagrangian shown above corresponds to the final result of the computation of chapter 6, modulo a shift of the trajectory. For clarity, we decompose this shift into 3 pieces.

A first shift $\boldsymbol{\xi}$ used in [92], leading to the Lagrangian provided in [93, 94] is given by the equations (B.4)–(B.6). The poles $1/\varepsilon$ in this shift correspond to UV divergences.

A second shift $\boldsymbol{\chi}$ used in [94] (but not published therein), is provided by the equations (B.7)- (B.8). This shift is used to remove the $1/\varepsilon$ poles due to IR divergences.

Finally, the last shift $\boldsymbol{\eta}$ was published in [3] and is provided by the equations (B.9) - (B.10). This shift does not contain any $1/\varepsilon$ pole and were applied for convenience.

B.2.1 Shift ξ

$$\boldsymbol{\xi}_1=\frac{11}{3}\frac{G^2\,m_1^2}{c^6}\left[\frac{1}{\varepsilon}-2\ln\left(\frac{\overline{q}^{1/2}r'_1}{\ell_0}\right)-\frac{327}{1540}\right]\boldsymbol{a}^{(d)}_{1,\text{N}}+\frac{1}{c^8}\boldsymbol{\xi}_{1,\,4\text{PN}}\,, \tag{B.4}$$

where $\boldsymbol{a}^{(d)}_{1,\text{N}}$ represents the Newtonian acceleration of 1 in d dimensions and $\overline{q}=4\pi e^{\gamma_\text{E}}$ and where

$$\xi^i_{1,\,4\text{PN}}=\frac{1}{\varepsilon}\xi^{i\,(-1)}_{1,\,4\text{PN}}+\xi^{(0,n_{12})}_{1,\,4\text{PN}}n^i_{12}+\xi^{(0,v_1)}_{1,\,4\text{PN}}v^i_1+\xi^{(0,v_{12})}_{1,\,4\text{PN}}v^i_{12}\,, \tag{B.5}$$

with $v^i_{12}=v^i_1-v^i_2$ and

$$\begin{aligned}\xi^{i\,(-1)}_{1,\,4\text{PN}}&=\frac{G^3m_1^2m_2v^i_{12}}{r_{12}^2}(11(n_{12}v_{12})+\frac{11}{3}(n_{12}v_1))+n^i_{12}(\frac{G^4}{r_{12}^3}(\frac{55}{3}m_1^3m_2+\frac{22}{3}m_1^2m_2^2+4m_1m_2^3)\\&+\frac{G^3m_1^2m_2}{r_{12}^2}(\frac{11}{2}(n_{12}v_{12})^2-11(n_{12}v_{12})(n_{12}v_1)+\frac{11}{2}(n_{12}v_1)^2-\frac{22}{3}v_{12}^2))\,,\end{aligned} \tag{B.6a}$$

$$\xi^{(0,n_{12})}_{1,\,4\text{PN}}=G^3m_1m_2^2\Big\{\frac{1}{r_{12}^2}\Big[(-\frac{2539}{560}+\frac{72}{5}\ln(\frac{r_{12}}{r_0}))(n_{12}v_{12})^2$$

[1] For simplicity, we have used r_{12} to normalize the logarithm entering the non-local term in this form of the Lagrangian.

$$
\begin{aligned}
&+ (\frac{18759}{280} + \frac{96}{5}\ln(\frac{r_{12}}{r_0}))(n_{12}v_{12})(n_{12}v_1) + (-\frac{6253}{140} - \frac{64}{5}\ln(\frac{r_{12}}{r_0}))(v_{12}v_1) \\
&+ (\frac{5783}{840} - \frac{32}{5}\ln(\frac{r_{12}}{r_0}))v_{12}^2\Big] + \frac{1}{r_{12}^3}\Big[(\frac{519}{35} + 48\ln(\frac{r_{12}}{r_0}))(n_{12}v_{12})^2(n_{12}y_1) \\
&+ (-\frac{289}{35} - \frac{144}{5}\ln(\frac{r_{12}}{r_0}))(n_{12}v_{12})(v_{12}y_1) + (-\frac{171}{35} - \frac{48}{5}\ln(\frac{r_{12}}{r_0}))(n_{12}y_1)v_{12}^2\Big]\Big\} \\
&+ G^3 m_1^2 m_2\Big\{\frac{1}{r_{12}^2}\Big[(-\frac{2761}{168} - \frac{33}{2}\ln(\frac{\bar{q}^{1/2}r_1'}{\ell_0}) - \frac{11}{2}\ln(\frac{r_{12}}{r_1'}))(n_{12}v_{12})^2 \\
&+ (\frac{41299}{840} + 33\ln(\frac{\bar{q}^{1/2}r_1'}{\ell_0}) + \frac{96}{5}\ln(\frac{r_{12}}{r_0}) + 11\ln(\frac{r_{12}}{r_1'}))(n_{12}v_{12})(n_{12}v_1) \\
&+ (\frac{7489}{840} - \frac{33}{2}\ln(\frac{\bar{q}^{1/2}r_1'}{\ell_0}) - \frac{11}{2}\ln(\frac{r_{12}}{r_1'}))(n_{12}v_1)^2 + (-\frac{6253}{140} - \frac{64}{5}\ln(\frac{r_{12}}{r_0}))(v_{12}v_1) \\
&+ (\frac{3103}{168} + 22\ln(\frac{\bar{q}^{1/2}r_1'}{\ell_0}) + \frac{16}{5}\ln(\frac{r_{12}}{r_0}))v_{12}^2\Big] + \frac{1}{r_{12}^3}\Big[(\frac{519}{35} + 48\ln(\frac{r_{12}}{r_0}))(n_{12}v_{12})^2(n_{12}y_1) \\
&+ (-\frac{289}{35} - \frac{144}{5}\ln(\frac{r_{12}}{r_0}))(n_{12}v_{12})(v_{12}y_1) + (-\frac{171}{35} - \frac{48}{5}\ln(\frac{r_{12}}{r_0}))(n_{12}y_1)v_{12}^2\Big]\Big\} \\
&+ G^4 m_1^2 m_2^2\Big[\frac{1}{r_{12}^3}(-\frac{811}{210} - \frac{88}{3}\ln(\frac{\bar{q}^{1/2}r_1'}{\ell_0}) - \frac{16}{5}\ln(\frac{r_{12}}{r_0})) \\
&+ \frac{1}{r_{12}^4}(-\frac{114}{35} - \frac{32}{5}\ln(\frac{r_{12}}{r_0}))(n_{12}y_1)\Big] \\
&+ G^4 m_1^3 m_2\Big[\frac{1}{r_{12}^3}(-\frac{811}{105} - \frac{220}{3}\ln(\frac{\bar{q}^{1/2}r_1'}{\ell_0}) - \frac{32}{5}\ln(\frac{r_{12}}{r_0})) \\
&+ \frac{1}{r_{12}^4}(-\frac{57}{35} - \frac{16}{5}\ln(\frac{r_{12}}{r_0}))(n_{12}y_1)\Big] + G^4 m_1 m_2^3\Big[\frac{1}{r_{12}^3}(\frac{811}{210} - 16\ln(\frac{\bar{q}^{1/2}r_1'}{\ell_0}) \\
&+ \frac{16}{5}\ln(\frac{r_{12}}{r_0})) + \frac{1}{r_{12}^4}(-\frac{57}{35} - \frac{16}{5}\ln(\frac{r_{12}}{r_0}))(n_{12}y_1)\Big]\,, \qquad \text{(B.6b)}
\end{aligned}
$$

$$
\xi^{(0,v_1)}_{1,\,4\mathrm{PN}} = G^3\Big[\frac{m_1^2 m_2}{r_{12}^2}(\frac{839}{2520} + \frac{32}{15}\ln(\frac{r_{12}}{r_0}))(n_{12}v_{12}) + \frac{m_1 m_2^2}{r_{12}^2}(\frac{839}{2520} + \frac{32}{15}\ln(\frac{r_{12}}{r_0}))(n_{12}v_{12})\Big]\,, \qquad \text{(B.6c)}
$$

$$
\begin{aligned}
\xi^{(0,v_{12})}_{1,\,4\mathrm{PN}} &= G^3 m_1 m_2^2\Big\{\frac{1}{r_{12}^2}\Big[(\frac{2041}{336} - 8\ln(\frac{r_{12}}{r_0}))(n_{12}v_{12}) + (-\frac{6253}{140} - \frac{64}{5}\ln(\frac{r_{12}}{r_0}))(n_{12}v_1)\Big] \\
&+ \frac{1}{r_{12}^3}\Big[(-\frac{289}{35} - \frac{144}{5}\ln(\frac{r_{12}}{r_0}))(n_{12}v_{12})(n_{12}y_1) + (\frac{228}{35} + \frac{64}{5}\ln(\frac{r_{12}}{r_0}))(v_{12}y_1)\Big]\Big\} \\
&+ G^3 m_1^2 m_2\Big\{\frac{1}{r_{12}^2}\Big[(\frac{23113}{1680} - 33\ln(\frac{\bar{q}^{1/2}r_1'}{\ell_0}) + \frac{11}{3}\ln(\frac{r_{12}}{r_1'}))(n_{12}v_{12}) \\
&+ (-\frac{1398}{35} - 11\ln(\frac{\bar{q}^{1/2}r_1'}{\ell_0}) - \frac{64}{5}\ln(\frac{r_{12}}{r_0}) - \frac{11}{3}\ln(\frac{r_{12}}{r_1'}))(n_{12}v_1)\Big] \\
&+ \frac{1}{r_{12}^3}\Big[(-\frac{289}{35} - \frac{144}{5}\ln(\frac{r_{12}}{r_0}))(n_{12}v_{12})(n_{12}y_1) + (\frac{228}{35} + \frac{64}{5}\ln(\frac{r_{12}}{r_0}))(v_{12}y_1)\Big]\Big\}\,. \qquad \text{(B.6d)}
\end{aligned}
$$

B.2.2 Shift χ

$$\chi_1^i = \frac{G^3}{c^8}\left[\frac{1}{\varepsilon}\chi_1^{i\,(3)\varepsilon} + \chi^{(3)\boldsymbol{n_{12}}} n_{12}^i + \chi^{(3)\boldsymbol{y_1}} y_1^i + \chi^{(3)\boldsymbol{v_1}} v_1^i + \chi^{(3)\boldsymbol{v_2}} v_2^i\right] + \frac{G^4}{c^8}\left[\frac{1}{\varepsilon}\chi_1^{i\,(4)\varepsilon} + \chi^{(4)\boldsymbol{n_{12}}} n_{12}^i + \chi^{(4)\boldsymbol{y_1}} y_1^i\right]. \tag{B.7}$$

By defining for convenience Γ as $\Gamma \equiv \frac{\bar{q}r_0^2}{\ell_0^2}$, we have

$$\begin{aligned}
\chi_1^{i\,(3)\varepsilon} = n_{12}^i \Bigg\{ & m_1^2 m_2 \Bigg[-\frac{24(n_{12}v_2)^2(n_{12}y_1)}{r_{12}^3} + (n_{12}v_1)^2\left(-\frac{48}{5r_{12}^2} - \frac{24(n_{12}y_1)}{r_{12}^3}\right) + (v_1v_2)\left(-\frac{16}{5r_{12}^2}\right.\\
& \left. - \frac{48(n_{12}y_1)}{5r_{12}^3}\right) + (v_2v_2)\left(-\frac{8}{5r_{12}^2} + \frac{24(n_{12}y_1)}{5r_{12}^3}\right) + (v_1v_1)\left(\frac{24}{5r_{12}^2} + \frac{24(n_{12}y_1)}{5r_{12}^3}\right)\\
& + (n_{12}v_1)\left((n_{12}v_2)\left[\frac{48}{5r_{12}^2} + \frac{48(n_{12}y_1)}{r_{12}^3}\right] + \frac{72(v_1y_1)}{5r_{12}^3} - \frac{72(v_2y_1)}{5r_{12}^3}\right)\\
& + (n_{12}v_2)\left(-\frac{72(v_1y_1)}{5r_{12}^3} + \frac{72(v_2y_1)}{5r_{12}^3}\right)\Bigg] + m_1 m_2^2 \Bigg[(n_{12}v_1)^2\left(-\frac{84}{5r_{12}^2} - \frac{24(n_{12}y_1)}{r_{12}^3}\right)\\
& + (n_{12}v_2)^2\left(-\frac{36}{5r_{12}^2} - \frac{24(n_{12}y_1)}{r_{12}^3}\right) + (v_1v_2)\left(-\frac{64}{5r_{12}^2} - \frac{48(n_{12}y_1)}{5r_{12}^3}\right) + (v_2v_2)\left(\frac{16}{5r_{12}^2}\right.\\
& \left. + \frac{24(n_{12}y_1)}{5r_{12}^3}\right) + (v_1v_1)\left(\frac{48}{5r_{12}^2} + \frac{24(n_{12}y_1)}{5r_{12}^3}\right) + (n_{12}v_1)\left((n_{12}v_2)\left[\frac{24}{r_{12}^2} + \frac{48(n_{12}y_1)}{r_{12}^3}\right]\right.\\
& \left. + \frac{72(v_1y_1)}{5r_{12}^3} - \frac{72(v_2y_1)}{5r_{12}^3}\right) + (n_{12}v_2)\left(-\frac{72(v_1y_1)}{5r_{12}^3} + \frac{72(v_2y_1)}{5r_{12}^3}\right)\Bigg]\Bigg\}\\
& + v_1^i \Bigg\{ m_1^2 m_2 \Bigg[(n_{12}v_2)\left(\frac{16}{15r_{12}^2} - \frac{72(n_{12}y_1)}{5r_{12}^3}\right) + (n_{12}v_1)\left(\frac{16}{3r_{12}^2} + \frac{72(n_{12}y_1)}{5r_{12}^3}\right) - \frac{32(v_1y_1)}{5r_{12}^3}\\
& + \frac{32(v_2y_1)}{5r_{12}^3}\Bigg] + m_1 m_2^2 \Bigg[(n_{12}v_2)\left(-\frac{44}{15r_{12}^2} - \frac{72(n_{12}y_1)}{5r_{12}^3}\right) + (n_{12}v_1)\left(\frac{28}{3r_{12}^2} + \frac{72(n_{12}y_1)}{5r_{12}^3}\right)\\
& - \frac{32(v_1y_1)}{5r_{12}^3} + \frac{32(v_2y_1)}{5r_{12}^3}\Bigg]\Bigg\} + v_1^i \Bigg\{ m_1^2 m_2 \Bigg[\frac{72(n_{12}v_2)(n_{12}y_1)}{5r_{12}^3} + (n_{12}v_1)\left(-\frac{32}{5r_{12}^2}\right.\\
& \left. - \frac{72(n_{12}y_1)}{5r_{12}^3}\right) + \frac{32(v_1y_1)}{5r_{12}^3} - \frac{32(v_2y_1)}{5r_{12}^3}\Bigg] + m_1 m_2^2 \Bigg[(n_{12}v_1)\left(-\frac{52}{5r_{12}^2} - \frac{72(n_{12}y_1)}{5r_{12}^3}\right)\\
& + (n_{12}v_2)\left(\frac{4}{r_{12}^2} + \frac{72(n_{12}y_1)}{5r_{12}^3}\right) + \frac{32(v_1y_1)}{5r_{12}^3} - \frac{32(v_2y_1)}{5r_{12}^3}\Bigg]\Bigg\} + y_1^i \Bigg\{ m_1^2 m_2 \Bigg[-\frac{8(n_{12}v_1)^2}{5r_{12}^3}\\
& + \frac{8(v_1v_1)}{15r_{12}^3} + \frac{16(n_{12}v_1)(n_{12}v_2)}{5r_{12}^3} - \frac{8(n_{12}v_2)^2}{5r_{12}^3} - \frac{16(v_1v_2)}{15r_{12}^3} + \frac{8(v_2v_2)}{15r_{12}^3}\Bigg]\\
& + m_1 m_2^2 \Bigg[-\frac{8(n_{12}v_1)^2}{5r_{12}^3} + \frac{8(v_1v_1)}{15r_{12}^3} + \frac{16(n_{12}v_1)(n_{12}v_2)}{5r_{12}^3} - \frac{8(n_{12}v_2)^2}{5r_{12}^3} - \frac{16(v_1v_2)}{15r_{12}^3}\\
& + \frac{8(v_2v_2)}{15r_{12}^3}\Bigg]\Bigg\}\,,
\end{aligned} \tag{B.8a}$$

$$\chi^{(3)\boldsymbol{n_{12}}} = m_1 m_2^2 \Bigg\{(v_1v_1)\Bigg[\frac{2096}{175r_{12}^2} - \frac{72\ln\Gamma}{5r_{12}^2} - \frac{48\ln(\frac{r_{12}}{r_0})}{5r_{12}^2} + \Bigg(-\frac{223}{50r_{12}^3} - \frac{36\ln\Gamma}{5r_{12}^3}$$

$$
\begin{aligned}
&-\frac{24\ln(\frac{r_{12}}{r_0})}{5r_{12}^3}\Bigg)(n_{12}y_1)\Bigg]+(v_2v_2)\Bigg[-\frac{2533}{140r_{12}^2}-\frac{24\ln\Gamma}{5r_{12}^2}-\frac{16\ln(\frac{r_{12}}{r_0})}{5r_{12}^2}\\
&+\Bigg(-\frac{223}{50r_{12}^3}-\frac{36\ln\Gamma}{5r_{12}^3}-\frac{24\ln(\frac{r_{12}}{r_0})}{5r_{12}^3}\Bigg)(n_{12}y_1)\Bigg]+(v_1v_2)\Bigg[\frac{4281}{700r_{12}^2}\\
&+\frac{96\ln\Gamma}{5r_{12}^2}+\frac{64\ln(\frac{r_{12}}{r_0})}{5r_{12}^2}+\Bigg(\frac{223}{25r_{12}^3}+\frac{72\ln\Gamma}{5r_{12}^3}+\frac{48\ln(\frac{r_{12}}{r_0})}{5r_{12}^3}\Bigg)(n_{12}y_1)\Bigg]\\
&+(n_{12}v_2)^2\Bigg[\frac{11477}{350r_{12}^2}+\frac{54\ln\Gamma}{5r_{12}^2}+\frac{36\ln(\frac{r_{12}}{r_0})}{5r_{12}^2}+\Bigg(\frac{35}{2r_{12}^3}+\frac{36\ln\Gamma}{r_{12}^3}\\
&+\frac{24\ln(\frac{r_{12}}{r_0})}{r_{12}^3}\Bigg)(n_{12}y_1)\Bigg]+(n_{12}v_1)^2\Bigg[-\frac{21719}{1400r_{12}^2}+\frac{126\ln\Gamma}{5r_{12}^2}+\frac{84\ln(\frac{r_{12}}{r_0})}{5r_{12}^2}\\
&+\Bigg(\frac{35}{2r_{12}^3}+\frac{36\ln\Gamma}{r_{12}^3}+\frac{24\ln(\frac{r_{12}}{r_0})}{r_{12}^3}\Bigg)(n_{12}y_1)\Bigg]+(n_{12}v_2)\Bigg[\Bigg(\frac{669}{50r_{12}^3}\\
&+\frac{108\ln\Gamma}{5r_{12}^3}+\frac{72\ln(\frac{r_{12}}{r_0})}{5r_{12}^3}\Bigg)(v_1y_1)+\Bigg(-\frac{669}{50r_{12}^3}-\frac{108\ln\Gamma}{5r_{12}^3}\\
&-\frac{72\ln(\frac{r_{12}}{r_0})}{5r_{12}^3}\Bigg)(v_2y_1)\Bigg]+(n_{12}v_1)\Bigg[(n_{12}v_2)\Bigg(-\frac{24189}{1400r_{12}^2}-\frac{36\ln\Gamma}{r_{12}^2}-\frac{24\ln(\frac{r_{12}}{r_0})}{r_{12}^2}\\
&+[-\frac{35}{r_{12}^3}-\frac{72\ln\Gamma}{r_{12}^3}-\frac{48\ln(\frac{r_{12}}{r_0})}{r_{12}^3}](n_{12}y_1)\Bigg)+\Bigg(-\frac{669}{50r_{12}^3}-\frac{108\ln\Gamma}{5r_{12}^3}\\
&-\frac{72\ln(\frac{r_{12}}{r_0})}{5r_{12}^3}\Bigg)(v_1y_1)+\Bigg(\frac{669}{50r_{12}^3}+\frac{108\ln\Gamma}{5r_{12}^3}+\frac{72\ln(\frac{r_{12}}{r_0})}{5r_{12}^3}\Bigg)(v_2y_1)\Bigg]\Bigg\}\\
&+m_1^2m_2\Bigg\{(v_1v_1)\Bigg[-\frac{58769}{2100r_{12}^2}-\frac{36\ln\Gamma}{5r_{12}^2}-\frac{24\ln(\frac{r_{12}}{r_0})}{5r_{12}^2}+\Bigg(-\frac{223}{50r_{12}^3}\\
&-\frac{36\ln\Gamma}{5r_{12}^3}-\frac{24\ln(\frac{r_{12}}{r_0})}{5r_{12}^3}\Bigg)(n_{12}y_1)\Bigg]+(v_2v_2)\Bigg[-\frac{30479}{525r_{12}^2}+\frac{12\ln\Gamma}{5r_{12}^2}\\
&+\frac{8\ln(\frac{r_{12}}{r_0})}{5r_{12}^2}+\Bigg(-\frac{223}{50r_{12}^3}-\frac{36\ln\Gamma}{5r_{12}^3}-\frac{24\ln(\frac{r_{12}}{r_0})}{5r_{12}^3}\Bigg)(n_{12}y_1)\Bigg]+(v_1v_2)\Bigg[\frac{36137}{420r_{12}^2}\\
&+\frac{24\ln\Gamma}{5r_{12}^2}+\frac{16\ln(\frac{r_{12}}{r_0})}{5r_{12}^2}+\Bigg(\frac{223}{25r_{12}^3}+\frac{72\ln\Gamma}{5r_{12}^3}+\frac{48\ln(\frac{r_{12}}{r_0})}{5r_{12}^3}\Bigg)(n_{12}y_1)\Bigg]\\
&+(n_{12}v_2)^2\Bigg[\frac{18137}{200r_{12}^2}+\Bigg(\frac{35}{2r_{12}^3}+\frac{36\ln\Gamma}{r_{12}^3}+\frac{24\ln(\frac{r_{12}}{r_0})}{r_{12}^3}\Bigg)(n_{12}y_1)\Bigg]\\
&+(n_{12}v_1)^2\Bigg[\frac{2119}{50r_{12}^2}+\frac{72\ln\Gamma}{5r_{12}^2}+\frac{48\ln(\frac{r_{12}}{r_0})}{5r_{12}^2}+\Bigg(\frac{35}{2r_{12}^3}+\frac{36\ln\Gamma}{r_{12}^3}\\
&+\frac{24\ln(\frac{r_{12}}{r_0})}{r_{12}^3}\Bigg)(n_{12}y_1)\Bigg]+(n_{12}v_2)\Bigg[\Bigg(\frac{669}{50r_{12}^3}+\frac{108\ln\Gamma}{5r_{12}^3}+\frac{72\ln(\frac{r_{12}}{r_0})}{5r_{12}^3}\Bigg)(v_1y_1)\\
&+\Bigg(-\frac{669}{50r_{12}^3}-\frac{108\ln\Gamma}{5r_{12}^3}-\frac{72\ln(\frac{r_{12}}{r_0})}{5r_{12}^3}\Bigg)(v_2y_1)\Bigg]+(n_{12}v_1)\Bigg[(n_{12}v_2)\Bigg(-\frac{26613}{200r_{12}^2}
\end{aligned}
$$

$$
\begin{aligned}
& -\frac{72\ln\Gamma}{5r_{12}^2} - \frac{48\ln(\frac{r_{12}}{r_0})}{5r_{12}^2} + [-\frac{35}{r_{12}^3} - \frac{72\ln\Gamma}{r_{12}^3} - \frac{48\ln(\frac{r_{12}}{r_0})}{r_{12}^3}](n_{12}y_1)\Bigg) \\
& + \left(-\frac{669}{50r_{12}^3} - \frac{108\ln\Gamma}{5r_{12}^3} - \frac{72\ln(\frac{r_{12}}{r_0})}{5r_{12}^3}\right)(v_1y_1) + \left(\frac{669}{50r_{12}^3} + \frac{108\ln\Gamma}{5r_{12}^3}\right. \\
& \left. + \frac{72\ln(\frac{r_{12}}{r_0})}{5r_{12}^3}\right)(v_2y_1)\Bigg]\Bigg\}\,, \qquad \text{(B.8b)}
\end{aligned}
$$

$$
\begin{aligned}
\chi^{(3)\boldsymbol{v}_1} = {} & m_1^2 m_2\Bigg\{(n_{12}v_1)\Bigg[-\frac{769}{24r_{12}^2} - \frac{8\ln\Gamma}{r_{12}^2} - \frac{16\ln(\frac{r_{12}}{r_0})}{3r_{12}^2} + \Bigg(-\frac{669}{50r_{12}^3} \\
& - \frac{108\ln\Gamma}{5r_{12}^3} - \frac{72\ln(\frac{r_{12}}{r_0})}{5r_{12}^3}\Bigg)(n_{12}y_1)\Bigg] + (n_{12}v_2)\Bigg[\frac{37267}{600r_{12}^2} - \frac{8\ln\Gamma}{5r_{12}^2} \\
& - \frac{16\ln(\frac{r_{12}}{r_0})}{15r_{12}^2} + \left(\frac{669}{50r_{12}^3} + \frac{108\ln\Gamma}{5r_{12}^3} + \frac{72\ln(\frac{r_{12}}{r_0})}{5r_{12}^3}\right)(n_{12}y_1)\Bigg] + \Bigg[\frac{202}{25r_{12}^3} \\
& + \frac{48\ln\Gamma}{5r_{12}^3} + \frac{32\ln(\frac{r_{12}}{r_0})}{5r_{12}^3}\Bigg](v_1y_1) + \Bigg[-\frac{202}{25r_{12}^3} - \frac{48\ln\Gamma}{5r_{12}^3} \\
& - \frac{32\ln(\frac{r_{12}}{r_0})}{5r_{12}^3}\Bigg](v_2y_1)\Bigg\} + m_1 m_2^2\Bigg\{(n_{12}v_1)\Bigg[-\frac{561}{35r_{12}^2} - \frac{14\ln\Gamma}{r_{12}^2} - \frac{28\ln(\frac{r_{12}}{r_0})}{3r_{12}^2} \\
& + \left(-\frac{669}{50r_{12}^3} - \frac{108\ln\Gamma}{5r_{12}^3} - \frac{72\ln(\frac{r_{12}}{r_0})}{5r_{12}^3}\right)(n_{12}y_1)\Bigg] + (n_{12}v_2)\Bigg[\frac{32269}{700r_{12}^2} \\
& + \frac{22\ln\Gamma}{5r_{12}^2} + \frac{44\ln(\frac{r_{12}}{r_0})}{15r_{12}^2} + \left(\frac{669}{50r_{12}^3} + \frac{108\ln\Gamma}{5r_{12}^3} + \frac{72\ln(\frac{r_{12}}{r_0})}{5r_{12}^3}\right)(n_{12}y_1)\Bigg] \\
& + \left[\frac{202}{25r_{12}^3} + \frac{48\ln\Gamma}{5r_{12}^3} + \frac{32\ln(\frac{r_{12}}{r_0})}{5r_{12}^3}\right](v_1y_1) + \Bigg[-\frac{202}{25r_{12}^3} - \frac{48\ln\Gamma}{5r_{12}^3} \\
& - \frac{32\ln(\frac{r_{12}}{r_0})}{5r_{12}^3}\Bigg](v_2y_1)\Bigg\}\,, \qquad \text{(B.8c)}
\end{aligned}
$$

$$
\begin{aligned}
\chi^{(3)\boldsymbol{v}_2} = {} & m_1^2 m_2\Bigg\{(n_{12}v_2)\Bigg[-\frac{1969}{30r_{12}^2} + \left(-\frac{669}{50r_{12}^3} - \frac{108\ln\Gamma}{5r_{12}^3} - \frac{72\ln(\frac{r_{12}}{r_0})}{5r_{12}^3}\right)(n_{12}y_1)\Bigg] \\
& + (n_{12}v_1)\Bigg[\frac{10669}{300r_{12}^2} + \frac{48\ln\Gamma}{5r_{12}^2} + \frac{32\ln(\frac{r_{12}}{r_0})}{5r_{12}^2} + \Bigg(\frac{669}{50r_{12}^3} + \frac{108\ln\Gamma}{5r_{12}^3} \\
& + \frac{72\ln(\frac{r_{12}}{r_0})}{5r_{12}^3}\Bigg)(n_{12}y_1)\Bigg] + \left[-\frac{202}{25r_{12}^3} - \frac{48\ln\Gamma}{5r_{12}^3} - \frac{32\ln(\frac{r_{12}}{r_0})}{5r_{12}^3}\right](v_1y_1) + \Bigg[\frac{202}{25r_{12}^3} \\
& + \frac{48\ln\Gamma}{5r_{12}^3} + \frac{32\ln(\frac{r_{12}}{r_0})}{5r_{12}^3}\Bigg](v_2y_1)\Bigg\} + m_1 m_2^2\Bigg\{(n_{12}v_2)\Bigg[-\frac{41681}{840r_{12}^2} \\
& - \frac{6\ln\Gamma}{r_{12}^2} - \frac{4\ln(\frac{r_{12}}{r_0})}{r_{12}^2} + \left(-\frac{669}{50r_{12}^3} - \frac{108\ln\Gamma}{5r_{12}^3} - \frac{72\ln(\frac{r_{12}}{r_0})}{5r_{12}^3}\right)(n_{12}y_1)\Bigg] \\
& + (n_{12}v_1)\Bigg[\frac{82111}{4200r_{12}^2} + \frac{78\ln\Gamma}{5r_{12}^2} + \frac{52\ln(\frac{r_{12}}{r_0})}{5r_{12}^2} + \Bigg(\frac{669}{50r_{12}^3} + \frac{108\ln\Gamma}{5r_{12}^3}
\end{aligned}
$$

$$+\frac{72\ln(\frac{r_{12}}{r_0})}{5r_{12}^3}\Bigg)(n_{12}y_1)\Bigg]+\Bigg[-\frac{202}{25r_{12}^3}-\frac{48\ln\Gamma}{5r_{12}^3}-\frac{32\ln(\frac{r_{12}}{r_0})}{5r_{12}^3}\Bigg](v_1y_1)+\Bigg[\frac{202}{25r_{12}^3}$$
$$+\frac{48\ln\Gamma}{5r_{12}^3}+\frac{32\ln(\frac{r_{12}}{r_0})}{5r_{12}^3}\Bigg](v_2y_1)\Bigg\}\,, \tag{B.8d}$$

$$\chi^{(3)\boldsymbol{y}_1} = m_1^2m_2\Bigg\{\Bigg[\frac{359}{75r_{12}^3}+\frac{12\ln\Gamma}{5r_{12}^3}+\frac{8\ln(\frac{r_{12}}{r_0})}{5r_{12}^3}\Bigg](n_{12}v_1)^2+\Bigg[-\frac{133}{75r_{12}^3}-\frac{4\ln\Gamma}{5r_{12}^3}$$
$$-\frac{8\ln(\frac{r_{12}}{r_0})}{15r_{12}^3}\Bigg](v_1v_1)+\Bigg[-\frac{718}{75r_{12}^3}-\frac{24\ln\Gamma}{5r_{12}^3}-\frac{16\ln(\frac{r_{12}}{r_0})}{5r_{12}^3}\Bigg](n_{12}v_1)(n_{12}v_2)$$
$$+\Bigg[\frac{359}{75r_{12}^3}+\frac{12\ln\Gamma}{5r_{12}^3}+\frac{8\ln(\frac{r_{12}}{r_0})}{5r_{12}^3}\Bigg](n_{12}v_2)^2+\Bigg[\frac{266}{75r_{12}^3}+\frac{8\ln\Gamma}{5r_{12}^3}$$
$$+\frac{16\ln(\frac{r_{12}}{r_0})}{15r_{12}^3}\Bigg](v_1v_2)+\Bigg[-\frac{133}{75r_{12}^3}-\frac{4\ln\Gamma}{5r_{12}^3}-\frac{8\ln(\frac{r_{12}}{r_0})}{15r_{12}^3}\Bigg](v_2v_2)\Bigg\}$$
$$+m_1m_2^2\Bigg\{\Bigg[\frac{359}{75r_{12}^3}+\frac{12\ln\Gamma}{5r_{12}^3}+\frac{8\ln(\frac{r_{12}}{r_0})}{5r_{12}^3}\Bigg](n_{12}v_1)^2+\Bigg[-\frac{133}{75r_{12}^3}$$
$$-\frac{4\ln\Gamma}{5r_{12}^3}-\frac{8\ln(\frac{r_{12}}{r_0})}{15r_{12}^3}\Bigg](v_1v_1)+\Bigg[-\frac{718}{75r_{12}^3}-\frac{24\ln\Gamma}{5r_{12}^3}$$
$$-\frac{16\ln(\frac{r_{12}}{r_0})}{5r_{12}^3}\Bigg](n_{12}v_1)(n_{12}v_2)+\Bigg[\frac{359}{75r_{12}^3}+\frac{12\ln\Gamma}{5r_{12}^3}+\frac{8\ln(\frac{r_{12}}{r_0})}{5r_{12}^3}\Bigg](n_{12}v_2)^2$$
$$+\Bigg[\frac{266}{75r_{12}^3}+\frac{8\ln\Gamma}{5r_{12}^3}+\frac{16\ln(\frac{r_{12}}{r_0})}{15r_{12}^3}\Bigg](v_1v_2)+\Bigg[-\frac{133}{75r_{12}^3}-\frac{4\ln\Gamma}{5r_{12}^3}$$
$$-\frac{8\ln(\frac{r_{12}}{r_0})}{15r_{12}^3}\Bigg](v_2v_2)\Bigg\}\,, \tag{B.8e}$$

$$\chi^{i(4)\varepsilon} = \frac{16m_1^3m_2n_{12}^i}{5r_{12}^3}+\frac{8m_1^2m_2^2n_{12}^i}{5r_{12}^3}-\frac{8m_1m_2^3n_{12}^i}{5r_{12}^3}+\frac{8m_1^3m_2n_{12}^i(n_{12}y_1)}{5r_{12}^4}+\frac{16m_1^2m_2^2n_{12}^i(n_{12}y_1)}{5r_{12}^4}$$
$$+\frac{8m_1m_2^3n_{12}^i(n_{12}y_1)}{5r_{12}^4}-\frac{8m_1^3m_2y_1^i}{15r_{12}^4}-\frac{16m_1^2m_2^2y_1^i}{15r_{12}^4}-\frac{8m_1m_2^3y_1^i}{15r_{12}^4}\,, \tag{B.8f}$$

$$\chi^{(4)\boldsymbol{n}_{12}} = m_1^2m_2^2\Bigg\{-\frac{613}{350r_{12}^3}-\frac{16\ln\Gamma}{5r_{12}^3}-\frac{16\ln(\frac{r_{12}}{r_0})}{5r_{12}^3}+\Bigg[-\frac{61}{25r_{12}^4}-\frac{32\ln\Gamma}{5r_{12}^4}$$
$$-\frac{32\ln(\frac{r_{12}}{r_0})}{5r_{12}^4}\Bigg](n_{12}y_1)\Bigg\}+m_1^3m_2\Bigg\{-\frac{8861}{2100r_{12}^3}-\frac{32\ln\Gamma}{5r_{12}^3}-\frac{32\ln(\frac{r_{12}}{r_0})}{5r_{12}^3}$$
$$+\Bigg[-\frac{61}{50r_{12}^4}-\frac{16\ln\Gamma}{5r_{12}^4}-\frac{16\ln(\frac{r_{12}}{r_0})}{5r_{12}^4}\Bigg](n_{12}y_1)\Bigg\}+m_1m_2^3\Bigg\{\frac{5183}{2100r_{12}^3}$$
$$+\frac{16\ln\Gamma}{5r_{12}^3}+\frac{16\ln(\frac{r_{12}}{r_0})}{5r_{12}^3}+\Bigg[-\frac{61}{50r_{12}^4}-\frac{16\ln\Gamma}{5r_{12}^4}-\frac{16\ln(\frac{r_{12}}{r_0})}{5r_{12}^4}\Bigg](n_{12}y_1)\Bigg\}\,, \tag{B.8g}$$

$$\chi^{(4)\boldsymbol{y}_1} = m_1^3m_2\Bigg\{\frac{73}{75r_{12}^4}+\frac{16\ln\Gamma}{15r_{12}^4}+\frac{16\ln(\frac{r_{12}}{r_0})}{15r_{12}^4}\Bigg\}+m_1m_2^3\Bigg\{\frac{73}{75r_{12}^4}+\frac{16\ln\Gamma}{15r_{12}^4}$$

$$+\frac{16\ln(\frac{r_{12}}{r_0})}{15r_{12}^4}\Bigg\} + m_1^2m_2^2\left\{\frac{146}{75r_{12}^4} + \frac{32\ln\Gamma}{15r_{12}^4} + \frac{32\ln(\frac{r_{12}}{r_0})}{15r_{12}^4}\right\}. \tag{B.8h}$$

B.2.3 Shift η

The last shift $\boldsymbol{\eta}_1$ starts at 4PN and is only made of G^3 and G^4 terms

$$\boldsymbol{\eta}_1 = \frac{G^3}{c^8}\boldsymbol{\eta}^{(3)}_{1\,4\mathrm{PN}} + \frac{G^4}{c^8}\boldsymbol{\eta}^{(4)}_{1\,4\mathrm{PN}}\,. \tag{B.9}$$

with

$$\boldsymbol{\eta}^{(3)}_{1\,4\mathrm{PN}} = \frac{\boldsymbol{v}_{12}}{r_{12}^2}\Big(\frac{769}{24}m_1^2m_2(n_{12}v_{12}) + \frac{561}{35}m_1m_2^2(n_{12}v_{12})\Big) + \frac{\boldsymbol{n}_{12}}{r_{12}^2}\Big[m_1m_2^2\Big(\frac{21719}{1400}(n_{12}v_{12})^2 - \frac{2096}{175}v_{12}^2\Big)$$
$$+ m_1^2m_2\Big(-\frac{2119}{50}(n_{12}v_{12})^2 + \frac{58769}{2100}v_{12}^2\Big)\Big]\,, \tag{B.10a}$$

$$\boldsymbol{\eta}^{(4)}_{1\,4\mathrm{PN}} = \Big(\frac{8861}{2100}m_1^3m_2 + \frac{613}{350}m_1^2m_2^2 - \frac{5183}{2100}m_1m_2^3\Big)\frac{\boldsymbol{n}_{12}}{r_{12}^3}\,. \tag{B.10b}$$

C – The mass quadrupole as a function of the potentials

We recall that in d dimensions, the mass quadrupole is given by the following (cf section 8.1.2):

$$
\begin{aligned}
I_L(t) \quad = \quad & \frac{d-1}{2(d-2)} \mathop{\mathrm{FP}}_{B} \int \frac{\mathrm{d}^d \mathbf{y}}{\ell_0^{d-3}} |\tilde{\mathbf{y}}|^B \Big\{ \widehat{y}_L \, \overline{\Sigma}_{[\ell]}(\mathbf{y},t) \\
& - \frac{4(d+2\ell-2)}{c^2(d+\ell-2)(d+2\ell)} \widehat{y}_{iL} \, \dot{\overline{\Sigma}}_{i[\ell+1]}(\mathbf{y},t) \\
& + \frac{2(d+2\ell-2)}{c^4(d+\ell-1)(d+\ell-2)(d+2\ell+2)} \widehat{y}_{ijL} \, \ddot{\overline{\Sigma}}_{ij[\ell+2]}(\mathbf{y},t) \\
& - \frac{4(d-3)(d+2\ell-2)}{c^2(d-1)(d+\ell-2)(d+2\ell)} B \, \widehat{y}_{iL} \frac{y_j}{|\mathbf{y}|^2} \overline{\Sigma}_{ij[\ell+1]}(\mathbf{y},t) \Big\} \, .
\end{aligned}
\tag{C.1}
$$

The last term of (C.1) does not contribute in because of the B and the $d-3$ factors. The first three terms of (C.1) are noted respectively MQS, MQV and MQT (MQ standing for mass quadrupole and S,V,T for scalar vector and tensor).

As

$$
\overline{\Sigma}_{[\ell]}(\mathbf{y},t) = \sum_{k=0}^{+\infty} \alpha_\ell^k \left(\frac{|\mathbf{y}|}{c} \frac{\partial}{\partial t} \right)^{2k} \overline{\Sigma}(\mathbf{y},t) \, , \tag{C.2}
$$

(where the numerical coefficients α_ℓ^k are given by (8.11)), each term MQS, MQV and MQT corresponds to a finite sum at 4PN indexed by k in (C.2). This sum has 5 elements ($k \in \{0,1,2,3,4\}$) for MQS noted MQSI, MQSII, MQSIV and MQSV, 4 elements for MQV noted MQVI, MQVII, MQVIII and MQVIV and 3 elements for MQT noted MTI, MQTII and MQTIII. Each of these terms contains non-compact terms corresponding to the suffix NC (such as MQSINC), compact terms (suffix C) and surface terms (suffix SL for surface Laplacian terms and SD for surface divergence terms). Hence we have

$$
I_{ij} = \frac{1}{G\pi} (\mathrm{MQS} + \mathrm{MQV} + \mathrm{MQT}) \, , \tag{C.3}
$$

where

$$
\mathrm{MQS} = \mathop{\mathrm{FP}}_{B} \int \mathrm{d}^3 \boldsymbol{x} \, (\mathrm{MQSINC} + G\pi \mathrm{MQSIC} + \hat{x}_{ij} \Delta \mathrm{MQSISD} + \partial_a \mathrm{MQSISL})
$$

$$
\begin{aligned}
&+\frac{\mathrm{d}^2}{\mathrm{d}t^2}\,\mathop{\mathrm{FP}}_{B}\int \mathrm{d}^3\boldsymbol{x}\,(\mathrm{MQSIINC}+G\pi\mathrm{MQSIIC})\\
&+\frac{\mathrm{d}^4}{\mathrm{d}t^4}\,\mathop{\mathrm{FP}}_{B}\int \mathrm{d}^3\boldsymbol{x}\,(\mathrm{MQSIIINC}+G\pi\mathrm{MQSIIIC})\\
&+\frac{\mathrm{d}^6}{\mathrm{d}t^6}\,\mathop{\mathrm{FP}}_{B}\int \mathrm{d}^3\boldsymbol{x}\,(\mathrm{MQSIVNC}+G\pi\mathrm{MQSIVC})\\
&+\frac{\mathrm{d}^8}{\mathrm{d}t^8}\,\mathop{\mathrm{FP}}_{B}\int \mathrm{d}^3\boldsymbol{x}\,(G\pi\mathrm{MQSVC})\ , \qquad \text{(C.4)}
\end{aligned}
$$

$$
\begin{aligned}
\mathrm{MQV} = {} &\frac{\mathrm{d}}{\mathrm{d}t}\,\mathop{\mathrm{FP}}_{B}\int \mathrm{d}^3\boldsymbol{x}\,(\mathrm{MQVINC}+G\pi\mathrm{MQVIC}+\hat{x}_{ija}\Delta\mathrm{MQVISD}+\partial_a\mathrm{MQVISL})\\
&+\frac{\mathrm{d}^3}{\mathrm{d}t^3}\,\mathop{\mathrm{FP}}_{B}\int \mathrm{d}^3\boldsymbol{x}\,(\mathrm{MQVIINC}+G\pi\mathrm{MQVIIC})\\
&+\frac{\mathrm{d}^5}{\mathrm{d}t^5}\,\mathop{\mathrm{FP}}_{B}\int \mathrm{d}^3\boldsymbol{x}\,(\mathrm{MQVIIINC}+G\pi\mathrm{MQVIIIC})\\
&+\frac{\mathrm{d}^7}{\mathrm{d}t^7}\,\mathop{\mathrm{FP}}_{B}\int \mathrm{d}^3\boldsymbol{x}\,(+G\pi\mathrm{MQVIVC})\ , \qquad \text{(C.5)}
\end{aligned}
$$

$$
\begin{aligned}
\mathrm{MQT} = {} &\frac{\mathrm{d}}{\mathrm{d}t^2}\,\mathop{\mathrm{FP}}_{B}\int \mathrm{d}^3\boldsymbol{x}\,(\mathrm{MQTINC}+G\pi\mathrm{MQTIC})\\
&+\frac{\mathrm{d}^4}{\mathrm{d}t^4}\,\mathop{\mathrm{FP}}_{B}\int \mathrm{d}^3\boldsymbol{x}\,(\mathrm{MQTIINC}+G\pi\mathrm{MQTIIC})\\
&+\frac{\mathrm{d}^6}{\mathrm{d}t^6}\,\mathop{\mathrm{FP}}_{B}\int \mathrm{d}^3\boldsymbol{x}\,(\mathrm{MQTIIINC}+G\pi\mathrm{MQTIIIC})\ . \qquad \text{(C.6)}
\end{aligned}
$$

The list of all these coefficients are provided below. We use the notation $\mathrm{MQSINC} = \mathrm{MQSINC}_{0\mathrm{PN}} + \mathrm{MQSINC}_{1\mathrm{PN}}/c^2 + \mathrm{MQSINC}_{2\mathrm{PN}}/c^4 + \mathrm{MQSINC}_{3\mathrm{PN}}/c^6 + \mathrm{MQSINC}_{4\mathrm{PN}}/c^8$. We do not write the terms that are equal to 0.

MQSI non-compact terms

$$
\begin{aligned}
\mathrm{MQSINC}_{2\mathrm{PN}} = {} &\frac{(-4+d)(-1+d)^2\hat{x}_{ij}(\partial_t V)^2}{8(-2+d)^3} - \frac{(-1+d)V^a\hat{x}_{ij}\partial_t\partial_a V}{-2+d} + \frac{(-1+d)^2\Psi_{ij}^{\partial_{ab}V}\partial^a V\partial^b V}{4(-2+d)^2}\\
&+\frac{(-1+d)\hat{x}_{ij}\partial_a V_b\partial^b V^a}{-2+d}.
\end{aligned}
$$

$$
\begin{aligned}
&\mathrm{MQSINC}_{3\mathrm{PN}} =\\
&-\frac{(-4+d)(-3+d)(-1+d)^2\hat{x}_{ij}\partial_t K\partial_t V}{2(-2+d)^4} + \frac{(-4+d)(-1+d)^3 V\hat{x}_{ij}(\partial_t V)^2}{4(-2+d)^4} + \frac{(-1+d)^2 d\Psi_{ij}^{\partial_{aa}V}(\partial_t V)^2}{4(-2+d)^4}\\
&+\frac{2\hat{x}_{ij}\partial_t V_a\partial_t V^a}{-2+d} + \frac{(-1+d)\hat{x}_{ij}\partial_t V\partial_t\hat{W}}{2(-2+d)} + \frac{2(-3+d)(-1+d)V^a\hat{x}_{ij}\partial_t\partial_a K}{(-2+d)^2} - \frac{(-1+d)^2 V V^a\hat{x}_{ij}\partial_t\partial_a V}{(-2+d)^2}\\
&+\frac{(-1+d)\hat{W}\hat{x}_{ij}\partial_t^2 V}{4(-2+d)} - \frac{(-3+d)V^a\hat{x}_{ij}\partial_t^2 V_a}{-2+d} + \frac{(-1+d)V\hat{x}_{ij}\partial_t^2\hat{W}}{4(-2+d)} - \frac{(-1+d)\Psi_{ij}^{\partial_{ab}V}\partial_t^2\hat{W}_{ab}}{2(-2+d)}\\
&-\frac{(-1+d)^2 dV^a\hat{x}_{ij}\partial_t V\partial_a V}{2(-2+d)^3} + \frac{(-1+d)^2 d\Psi_{ij}^{\partial t\partial_a V}\partial_t V\partial_a V}{2(-2+d)^3} + \frac{2(-1+d)^2\Psi_{ij}^{\partial_{ab}V}\partial_t V^b\partial^a V}{(-2+d)^2} - \frac{(-1+d)^2 d\Psi_{ij}^{\partial_a V_b}\partial_t\partial_a V\partial_b V}{(-2+d)^3}\\
&+\frac{(-3+d)(-1+d)\hat{W}^{ab}\hat{x}_{ij}\partial_b\partial_a K}{(-2+d)^2} - \frac{(-1+d)^2 d\Psi_{ij}^{\partial_a V_b}\partial_t V\partial_b\partial_a V}{(-2+d)^3} + \frac{2(-1+d)^2\Psi_{ij}^{\partial t\partial_a V}\partial_a V_b\partial^b V}{(-2+d)^2}
\end{aligned}
$$

$$
-\frac{(-3+d)(-1+d)^2\Psi_{ij}^{\partial_{ab}V}\partial^a K\partial^b V}{(-2+d)^3}-\frac{2(-1+d)^2V^a\hat{x}_{ij}\partial_b V_a\partial^b V}{(-2+d)^2}+\frac{2(-1+d)\hat{x}_{ij}\partial_t\hat{W}_{ab}\partial^b V^a}{-2+d}
-\frac{2(-1+d)\Psi_{ij}^{\partial_{ii}V}\partial_a V_b\partial^b V^a}{(-2+d)^2}+\frac{2(-1+d)\Psi_{ij}^{\partial_{ii}V}\partial_b V_a\partial^b V^a}{(-2+d)^2}-\frac{2(-1+d)\Psi_{ij}^{\partial_{ai}V}\partial_b V^i\partial^b V^a}{-2+d}-\frac{4(-1+d)^2\Psi_{ij}^{\partial_a V_b}\partial_b V^i\partial_i\partial_a V}{(-2+d)^2}
-\frac{4(-1+d)^2\Psi_{ij}^{\partial_a V_b}\partial_b\partial_a V_i\partial^i V}{(-2+d)^2}-\frac{2(-1+d)\Psi_{ij}^{\partial_{bi}V}\partial^b V^a\partial^i V_a}{-2+d}+\frac{4(-1+d)\Psi_{ij}^{\partial_{ai}V}\partial^b V^a\partial^i V_b}{-2+d}.
$$

$\mathrm{MQSINC}_{4\mathrm{PN}} =$

$$
\frac{(-4+d)(-3+d)^2(-1+d)^2\hat{x}_{ij}(\partial_t K)^2}{2(-2+d)^5}-\frac{(-4+d)(-3+d)(-1+d)^3V\hat{x}_{ij}\partial_t K\partial_t V}{(-2+d)^5}+\frac{(-3+d)(-1+d)^2d\Psi_{ij}^{\partial_{aa}V}\partial_t K\partial_t V}{2(-2+d)^4}
-\frac{(-4+d)(-3+d)(-1+d)^3K\hat{x}_{ij}(\partial_t V)^2}{2(-2+d)^5}+\frac{(-1+d)^3V^2\hat{x}_{ij}(\partial_t V)^2}{4(-2+d)^3}+\frac{(-1+d)^2\hat{W}\hat{x}_{ij}(\partial_t V)^2}{2(-2+d)^2}-\frac{(-1+d)^3dV\Psi_{ij}^{\partial_{aa}V}(\partial_t V)^2}{8(-2+d)^4}
+\frac{8\hat{x}_{ij}\partial_t\hat{R}^a\partial_t V_a}{-2+d}-\frac{2(-1+d)(8-5d+d^2)V^a\hat{x}_{ij}\partial_t V\partial_t V_a}{(-2+d)^3}+\frac{4(-1+d)V\hat{x}_{ij}\partial_t V_a\partial_t V^a}{(-2+d)^2}+\frac{4(-1+d)\Psi_{ij}^{\partial_{ab}V}\partial_t V^a\partial_t V^b}{-2+d}
-\frac{(-3+d)(-1+d)\hat{x}_{ij}\partial_t K\partial_t\hat{W}}{(-2+d)^2}+\frac{(-1+d)^2V\hat{x}_{ij}\partial_t V\partial_t\hat{W}}{(-2+d)^2}+\frac{\hat{x}_{ij}(\partial_t\hat{W})^2}{2(-2+d)}+\frac{(-3+d)\hat{x}_{ij}\partial_t\hat{W}_{ab}\partial_t\hat{W}^{ab}}{2(-2+d)}
+\frac{(-4+d)(-1+d)^2\hat{x}_{ij}\partial_t V\partial_t\hat{X}}{(-2+d)^3}+\frac{2(-1+d)\hat{x}_{ij}\partial_t V\partial_t\hat{W}}{-2+d}+\frac{4(-3+d)(-1+d)\hat{R}^a\hat{x}_{ij}\partial_t\partial_a K}{(-2+d)^2}
+\frac{2(-3+d)(-1+d)^2VV^a\hat{x}_{ij}\partial_t\partial_a K}{(-2+d)^3}-\frac{2(-1+d)^2\hat{R}^aV\hat{x}_{ij}\partial_t\partial_a V}{(-2+d)^2}+\frac{2(-3+d)(-1+d)^2KV^a\hat{x}_{ij}\partial_t\partial_a V}{(-2+d)^3}
-\frac{(-1+d)^2(-3+2d)V^2V^a\hat{x}_{ij}\partial_t\partial_a V}{(-2+d)^3}+\frac{(-1+d)^2VV^a\Psi_{ij}^{\partial_{bb}V}\partial_t\partial_a V}{(-2+d)^2}-\frac{8(-1+d)V^a\Psi_{ij}^{\partial t\partial_b V}\partial_t\partial_a V_b}{-2+d}+\frac{2(-1+d)V^a\Psi_{ij}^{\partial_{bb}V}\partial_t\partial_a\hat{W}}{-2+d}
-\frac{4(-1+d)V^a\Psi_{ij}^{\partial_{bi}V}\partial_t\partial_a\hat{W}_{bi}}{-2+d}-\frac{4(-1+d)V^a\hat{x}_{ij}\partial_t\partial_a\hat{X}}{-2+d}+\frac{16(-1+d)V^a\Psi_{ij}^{\partial_b V_i}\partial_t\partial_b\partial_a V_i}{-2+d}+\frac{2(-1+d)V^a\hat{W}_{ab}\hat{x}_{ij}\partial_t\partial^b V}{-2+d}
-\frac{(-3+d)(-1+d)\hat{W}\hat{x}_{ij}\partial_t^2K}{2(-2+d)^2}-\frac{2(-3+d)V^a\hat{x}_{ij}\partial_t^2\hat{R}_a}{-2+d}-\frac{2(-1+d)\Psi_{ij}^{\partial t\partial_a V}\partial_t^2\hat{R}_a}{-2+d}-\frac{(-1+d)^3V^3\hat{x}_{ij}\partial_t^2V}{4(-2+d)^3}
+\frac{(-1+d)^2V\hat{W}\hat{x}_{ij}\partial_t^2V}{2(-2+d)^2}+\frac{(-1+d)\hat{x}_{ij}\hat{W}\partial_t^2V}{-2+d}+\frac{(-1+d)^3V^2\Psi_{ij}^{\partial_{aa}V}\partial_t^2V}{4(-2+d)^3}-\frac{2(-3+d)\hat{R}^a\hat{x}_{ij}\partial_t^2V_a}{-2+d}
-\frac{2(-3+d)(-1+d)VV^a\hat{x}_{ij}\partial_t^2V_a}{(-2+d)^2}-\frac{2(-1+d)^2V\Psi_{ij}^{\partial t\partial_a V}\partial_t^2V_a}{(-2+d)^2}-\frac{(-3+d)(-1+d)K\hat{x}_{ij}\partial_t^2\hat{W}}{2(-2+d)^2}+\frac{(-1+d)^2V^2\hat{x}_{ij}\partial_t^2\hat{W}}{4(-2+d)^2}
+\frac{\hat{W}\hat{x}_{ij}\partial_t^2\hat{W}}{2(-2+d)}+\frac{(-1+d)^2V\Psi_{ij}^{\partial_{aa}V}\partial_t^2\hat{W}}{2(-2+d)^2}-\frac{\hat{W}^{ab}\hat{x}_{ij}\partial_t^2\hat{W}_{ab}}{-2+d}-\frac{(-1+d)^2V\Psi_{ij}^{\partial_{ab}V}\partial_t^2\hat{W}_{ab}}{(-2+d)^2}
+\frac{(-1+d)V\hat{x}_{ij}\partial_t^2\hat{W}}{-2+d}-\frac{2(-1+d)\Psi_{ij}^{\partial_{ab}V}\partial_t^2\hat{Z}_{ab}}{-2+d}+\frac{4(-1+d)\Psi_{ij}^{\partial_a V_b}\partial_t^2\partial_a\hat{R}_b}{-2+d}+\frac{4(-1+d)^2V\Psi_{ij}^{\partial_a V_b}\partial_t^2\partial_a V_b}{(-2+d)^2}
+\frac{(-3+d)(-1+d)^2dV^a\hat{x}_{ij}\partial_t V\partial_a K}{(-2+d)^4}-\frac{(-3+d)(-1+d)^2d\Psi_{ij}^{\partial t\partial_a V}\partial_t V\partial_a K}{(-2+d)^4}+\frac{(-3+d)(-1+d)^2dV^a\hat{x}_{ij}\partial_t K\partial_a V}{(-2+d)^4}
-\frac{(-3+d)(-1+d)^2d\Psi_{ij}^{\partial t\partial_a V}\partial_t K\partial_a V}{(-2+d)^4}-\frac{(-1+d)^2d\hat{R}^a\hat{x}_{ij}\partial_t V\partial_a V}{(-2+d)^3}-\frac{(-1+d)^2d(-5+2d)VV^a\hat{x}_{ij}\partial_t V\partial_a V}{2(-2+d)^4}
+\frac{(-1+d)^2V^a\Psi_{ij}^{\partial_{bb}V}\partial_t V\partial_a V}{2(-2+d)^2}+\frac{(-1+d)^3dV\Psi_{ij}^{\partial t\partial_a V}\partial_t V\partial_a V}{2(-2+d)^4}+\frac{4(-1+d)^2\Psi_{ij}^{\partial_a V_b}\partial_t^2V_b\partial_a V}{(-2+d)^2}
+\frac{16(-1+d)\Psi_{ij}^{\partial_a V_b}\partial_t\partial_i V_b\partial_a V^i}{-2+d}+\frac{2(-3+d)(-1+d)^2\Psi_{ij}^{\partial_{bb}V}\partial_t V_a\partial^a K}{(-2+d)^3}-\frac{4(-3+d)(-1+d)^2\Psi_{ij}^{\partial_{ab}V}\partial_t V^b\partial^a K}{(-2+d)^3}
-\frac{(-3+d)^2(-1+d)^2(-4+3d)V\hat{x}_{ij}\partial_a K\partial^a K}{2(-2+d)^5}-\frac{(-3+d)^2(-1+d)^2(-4+3d)K\hat{x}_{ij}\partial_a V\partial^a K}{(-2+d)^5}
+\frac{2(-3+d)(-1+d)^2\hat{W}\hat{x}_{ij}\partial_a V\partial^a K}{(-2+d)^3}+\frac{2(-3+d)(-1+d)^2V\hat{x}_{ij}\partial_a\hat{W}\partial^a K}{(-2+d)^3}-\frac{2(-1+d)^2\Psi_{ij}^{\partial_{bb}V}\partial_t\hat{R}_a\partial^a V}{(-2+d)^2}
$$

$$
\begin{aligned}
&+\frac{4(-1+d)^2\Psi_{ij}^{\partial_{ab}V}\partial_t\hat{R}^b\partial^aV}{(-2+d)^2}+\frac{(-1+d)^3V^2\hat{x}_{ij}\partial_tV_a\partial^aV}{(-2+d)^3}-\frac{(-1+d)^3V\Psi_{ij}^{\partial_{bb}V}\partial_tV_a\partial^aV}{(-2+d)^3}\\
&+\frac{2(-1+d)^3V\Psi_{ij}^{\partial_{ab}V}\partial_tV^b\partial^aV}{(-2+d)^3}-\frac{(-1+d)^2\hat{X}\hat{x}_{ij}\partial_aV\partial^aV}{(-2+d)^2}-\frac{2(-1+d)^2\hat{x}_{ij}\hat{W}\partial_aV\partial^aV}{(-2+d)^2}+\frac{2(-3+d)(-1+d)^2K\hat{x}_{ij}\partial_a\hat{W}\partial^aV}{(-2+d)^3}\\
&+\frac{(-1+d)d\hat{W}^{bi}\hat{x}_{ij}\partial_a\hat{W}_{bi}\partial^aV}{(-2+d)^2}-\frac{2(-1+d)^2V\hat{x}_{ij}\partial_a\hat{X}\partial^aV}{(-2+d)^2}-\frac{4(-1+d)^2V\hat{x}_{ij}\partial_a\hat{W}\partial^aV}{(-2+d)^2}\\
&+\frac{2(-3+d)(-1+d)^2d\Psi_{ij}^{\partial_aV_b}\partial_t\partial_aV\partial_bK}{(-2+d)^4}+\frac{2(-3+d)(-1+d)^2d\Psi_{ij}^{\partial_aV_b}\partial_t\partial_aK\partial_bV}{(-2+d)^4}-\frac{(-1+d)^3dV\Psi_{ij}^{\partial_aV_b}\partial_t\partial_aV\partial_bV}{(-2+d)^4}\\
&+\frac{4(-1+d)^2\Psi_{ij}^{\partial t\partial_aV}\partial_a\hat{R}^b\partial_bV}{(-2+d)^2}-\frac{(-1+d)^2V^aV^b\hat{x}_{ij}\partial_aV\partial_bV}{(-2+d)^3}+\frac{(-1+d)^2dV^a\Psi_{ij}^{\partial t\partial_bV}\partial_aV\partial_bV}{(-2+d)^3}-\frac{(-1+d)^3d\Psi_{ij}^{\partial_aV_b}\partial_tV\partial_aV\partial_bV}{(-2+d)^4}\\
&+\frac{(-1+d)\Psi_{ij}^{\partial_{ab}V}\partial_a\hat{W}^{ij}\partial_b\hat{W}_{ij}}{-2+d}+\frac{4(-3+d)(-1+d)\hat{x}_{ij}\hat{Z}^{ab}\partial_b\partial_aK}{(-2+d)^2}+\frac{2(-3+d)(-1+d)^2d\Psi_{ij}^{\partial_aV_b}\partial_tV\partial_b\partial_aK}{(-2+d)^4}\\
&-\frac{4(-1+d)\hat{R}^aV^b\hat{x}_{ij}\partial_b\partial_aV}{-2+d}-\frac{(-1+d)^2V^2\hat{W}^{ab}\hat{x}_{ij}\partial_b\partial_aV}{2(-2+d)^2}+\frac{(-1+d)^2V\hat{W}^{ab}\Psi_{ij}^{\partial_{ii}V}\partial_b\partial_aV}{2(-2+d)^2}\\
&+\frac{2(-3+d)(-1+d)^2d\Psi_{ij}^{\partial_aV_b}\partial_tK\partial_b\partial_aV}{(-2+d)^4}-\frac{(-1+d)^3dV\Psi_{ij}^{\partial_aV_b}\partial_tV\partial_b\partial_aV}{(-2+d)^4}+\frac{(-1+d)\hat{W}^{ab}\Psi_{ij}^{\partial_{ii}V}\partial_b\partial_a\hat{W}}{-2+d}\\
&-\frac{2(-1+d)\hat{W}^{ab}\Psi_{ij}^{\partial_{ij}V}\partial_b\partial_a\hat{W}_{ij}}{-2+d}-\frac{2(-1+d)\hat{W}^{ab}\hat{x}_{ij}\partial_b\partial_a\hat{X}}{-2+d}-\frac{4(-3+d)(-1+d)^2\Psi_{ij}^{\partial t\partial_aV}\partial_aV_b\partial^bK}{(-2+d)^3}\\
&+\frac{(-3+d)^2(-1+d)^2\Psi_{ij}^{\partial_{ab}V}\partial^aK\partial^bK}{(-2+d)^4}-\frac{12(-1+d)V^a\hat{x}_{ij}\partial_bV\partial^b\hat{R}_a}{(-2+d)^2}+\frac{4(-1+d)\hat{x}_{ij}\partial_t\hat{W}_{ab}\partial^b\hat{R}^a}{-2+d}\\
&+\frac{4(-1+d)\hat{x}_{ij}\partial_a\hat{R}_b\partial^b\hat{R}^a}{-2+d}-\frac{4(-1+d)\Psi_{ij}^{\partial_{ii}V}\partial_aV_b\partial^b\hat{R}^a}{-2+d}+\frac{8(-1+d)\Psi_{ij}^{\partial_{bi}V}\partial_aV^i\partial^b\hat{R}^a}{-2+d}\\
&+\frac{4(-4+d)(-1+d)V\hat{x}_{ij}\partial_bV_a\partial^b\hat{R}^a}{(-2+d)^2}-\frac{(-1+d)^2V^a\Psi_{ij}^{\partial_{ab}V}\partial_tV\partial^bV}{(-2+d)^2}+\frac{2(-1+d)^2\Psi_{ij}^{\partial t\partial_aV}\partial_t\hat{W}_{ab}\partial^bV}{(-2+d)^2}\\
&+\frac{6(-1+d)^2VV^a\hat{x}_{ij}\partial_aV_b\partial^bV}{(-2+d)^3}+\frac{4(-1+d)^2V^a\Psi_{ij}^{\partial_{bi}V}\partial_aV^i\partial^bV}{(-2+d)^2}-\frac{(-1+d)^2dV\hat{W}_{ab}\hat{x}_{ij}\partial^aV\partial^bV}{4(-2+d)^3}\\
&-\frac{(-1+d)^2\hat{W}_a{}^i\Psi_{ij}^{\partial_{bi}V}\partial^aV\partial^bV}{(-2+d)^2}+\frac{(-1+d)^2\hat{W}_{ab}\Psi_{ij}^{\partial_{ii}V}\partial^aV\partial^bV}{4(-2+d)^2}-\frac{(-3+d)(-1+d)V_aV^a\hat{x}_{ij}\partial_bV\partial^bV}{2(-2+d)^2}\\
&-\frac{12(-1+d)\hat{R}^a\hat{x}_{ij}\partial_bV_a\partial^bV}{(-2+d)^2}+\frac{2(-1+d)^3V\Psi_{ij}^{\partial t\partial_aV}\partial_bV_a\partial^bV}{(-2+d)^3}-\frac{4(-1+d)^2V^a\Psi_{ij}^{\partial_{ai}V}\partial_bV^i\partial^bV}{(-2+d)^2}\\
&-\frac{8(-1+d)V^a\hat{x}_{ij}\partial_tV_b\partial^bV_a}{-2+d}+\frac{4(-3+d)V^a\hat{x}_{ij}\partial_b\hat{W}\partial^bV_a}{-2+d}+\frac{2(-1+d)^2V\hat{x}_{ij}\partial_t\hat{W}_{ab}\partial^bV^a}{(-2+d)^2}\\
&+\frac{2(-1+d)\Psi_{ij}^{\partial_{ii}V}\partial_t\hat{W}_{ab}\partial^bV^a}{-2+d}-\frac{4(-1+d)\Psi_{ij}^{\partial_{bi}V}\partial_t\hat{W}_{ai}\partial^bV^a}{-2+d}+\frac{4(-1+d)\Psi_{ij}^{\partial_{ai}V}\partial_t\hat{W}_{bi}\partial^bV^a}{-2+d}\\
&+\frac{8(-1+d)\hat{x}_{ij}\partial_t\hat{Z}_{ab}\partial^bV^a}{-2+d}+\frac{(-1+d)^2(-7+3d)V^2\hat{x}_{ij}\partial_aV_b\partial^bV^a}{(-2+d)^3}-\frac{(-1+d)^2V\Psi_{ij}^{\partial_{ii}V}\partial_aV_b\partial^bV^a}{(-2+d)^2}\\
&-\frac{2(-3+d)(-1+d)^2K\hat{x}_{ij}\partial_bV_a\partial^bV^a}{(-2+d)^3}-\frac{(-4+d)(-1+d)^2V^2\hat{x}_{ij}\partial_bV_a\partial^bV^a}{(-2+d)^3}+\frac{2(-3+d)\hat{W}\hat{x}_{ij}\partial_bV_a\partial^bV^a}{-2+d}\\
&+\frac{2(-1+d)^2\Psi_{ij}^{\partial_{ab}V}\partial^aV\partial^b\hat{X}}{(-2+d)^2}-\frac{2(-1+d)^2dV^a\Psi_{ij}^{\partial_bV_i}\partial_b\partial_aV\partial_iV}{(-2+d)^3}+\frac{8(-3+d)(-1+d)^2\Psi_{ij}^{\partial_aV_b}\partial_bV^i\partial_i\partial_aK}{(-2+d)^3}\\
&-\frac{8(-1+d)^2\Psi_{ij}^{\partial_aV_b}\partial_b\hat{R}^i\partial_i\partial_aV}{(-2+d)^2}+\frac{(-1+d)\hat{W}_a{}^i\hat{W}^{ab}\hat{x}_{ij}\partial_i\partial_bV}{-2+d}-\frac{2(-1+d)^2dV^a\Psi_{ij}^{\partial_bV_i}\partial_aV\partial_i\partial_bV}{(-2+d)^3}\\
&-\frac{4(-1+d)\hat{W}^{bi}\Psi_{ij}^{\partial t\partial_aV}\partial_i\partial_bV_a}{-2+d}+\frac{8(-3+d)(-1+d)^2\Psi_{ij}^{\partial_aV_b}\partial_b\partial_aV_i\partial^iK}{(-2+d)^3}-\frac{4(-1+d)^2\Psi_{ij}^{\partial_aV_b}\partial_t\partial_a\hat{W}_{bi}\partial^iV}{(-2+d)^2}\\
&-\frac{2(-1+d)^2d\Psi_{ij}^{\partial_aV_b}\partial_aV_i\partial_bV\partial^iV}{(-2+d)^3}-\frac{8(-1+d)^2\Psi_{ij}^{\partial_aV_b}\partial_b\partial_a\hat{R}_i\partial^iV}{(-2+d)^2}-\frac{4(-1+d)^3\Psi_{ij}^{\partial_aV_b}\partial_aV\partial_iV_b\partial^iV}{(-2+d)^3}
\end{aligned}
$$

$$
\begin{aligned}
&- \frac{4(-1+d)^3 V \Psi_{ij}^{\partial_a V_b} \partial_i \partial_a V_b \partial^i V}{(-2+d)^3} - \frac{8(-1+d)\Psi_{ij}^{\partial_{bi} V} \partial^b \hat{R}^a \partial^i V_a}{-2+d} + \frac{8(-1+d)\Psi_{ij}^{\partial_{ai} V} \partial^b \hat{R}^a \partial^i V_b}{-2+d} \\
&- \frac{4(-1+d)\hat{W}_{ai}\hat{x}_{ij}\partial^b V^a \partial^i V_b}{-2+d} - \frac{4(-1+d)^3 V \Psi_{ij}^{\partial_a V_b} \partial_i \partial_a V \partial^i V_b}{(-2+d)^3} + \frac{4(-1+d)V^a \hat{x}_{ij} \partial_a \hat{W}_{bi} \partial^i V^b}{-2+d} \\
&- \frac{4(-1+d)\Psi_{ij}^{\partial t \partial_a V} \partial_a \hat{W}_{bi} \partial^i V^b}{-2+d} + \frac{4(-1+d)\Psi_{ij}^{\partial t \partial_a V} \partial_b \hat{W}_{ai} \partial^i V^b}{-2+d} - \frac{4(-1+d)V^a \hat{x}_{ij} \partial_i \hat{W}_{ab} \partial^i V^b}{-2+d} \\
&+ \frac{(-1+d)dV\hat{x}_{ij}\partial_i \hat{W}_{ab}\partial^i \hat{W}^{ab}}{2(-2+d)^2} - \frac{4(-1+d)^2 \Psi_{ij}^{\partial_a V_b} \partial_t \hat{W}_{bi} \partial^i \partial_a V}{(-2+d)^2} + \frac{8(-1+d)\hat{W}^{ij}\Psi_{ij}^{\partial_a V_b} \partial_j \partial_i \partial_a V_b}{-2+d} \\
&+ \frac{8(-1+d)\Psi_{ij}^{\partial_a V_b} \partial_b \partial_a \hat{W}_{ij} \partial^j V^i}{-2+d} - \frac{8(-1+d)\Psi_{ij}^{\partial_a V_b} \partial_i \partial_a \hat{W}_{bj} \partial^j V^i}{-2+d} - \frac{4(-1+d)\Psi_{ij}^{\partial_{ab} V} \partial_b \hat{W}_{ij} \partial^j \hat{W}_a{}^i}{-2+d} \\
&+ \frac{2(-1+d)\Psi_{ij}^{\partial_{ab} V} \partial_i \hat{W}_{bj} \partial^j \hat{W}_a{}^i}{-2+d} + \frac{(-1+d)\Psi_{ij}^{\partial_{aa} V} \partial_i \hat{W}_{bj} \partial^j \hat{W}^{bi}}{-2+d} + \frac{8(-1+d)\Psi_{ij}^{\partial_a V_b} \partial_b \hat{W}_{ij} \partial^j \partial_a V^i}{-2+d} \\
&- \frac{8(-1+d)\Psi_{ij}^{\partial_a V_b} \partial_i \hat{W}_{bj} \partial^j \partial_a V^i}{-2+d} + \frac{8(-1+d)\Psi_{ij}^{\partial_a V_b} \partial_a \hat{W}_{ij} \partial^j \partial^i V_b}{-2+d}.
\end{aligned}
$$

MQSI compact terms

$$
\mathrm{MQSIC}_{0\mathrm{PN}} = \frac{(-1+d)\hat{x}_{ij}\sigma}{2(-2+d)}.
$$

$$
\mathrm{MQSIC}_{1\mathrm{PN}} = -\frac{(-3+d)(-1+d)V\hat{x}_{ij}\sigma}{(-2+d)^2}.
$$

$$
\begin{aligned}
\mathrm{MQSIC}_{2\mathrm{PN}} = {} & \frac{(-3+d)^2(-1+d)V^2\hat{x}_{ij}\sigma}{(-2+d)^3} + \frac{4(-3+d)V^a\hat{x}_{ij}\sigma_a}{-2+d} + \frac{2(-1+d)V\hat{x}_{ij}\sigma^a{}_a}{(-2+d)^2} \\
& + \frac{2(-1+d)\sigma^{ab}\Psi_{ij}^{\partial_{ab} V}}{-2+d} - \frac{2(-1+d)\sigma^a{}_a \Psi_{ij}^{\partial_{bb} V}}{(-2+d)^2}.
\end{aligned}
$$

$$
\begin{aligned}
&\mathrm{MQSIC}_{3\mathrm{PN}} = \\
&- \frac{2(-3+d)^3(-1+d)V^3\hat{x}_{ij}\sigma}{3(-2+d)^4} + \frac{8(-1+d)V_aV^a\hat{x}_{ij}\sigma}{(-2+d)^2} - \frac{4(-3+d)(-1+d)\hat{X}\hat{x}_{ij}\sigma}{(-2+d)^2} \\
&+ \frac{8(-3+d)\hat{R}^a\hat{x}_{ij}\sigma_a}{-2+d} - \frac{4(-5+d)(-3+d)VV^a\hat{x}_{ij}\sigma_a}{(-2+d)^2} + \frac{4\hat{W}^{ab}\hat{x}_{ij}\sigma_{ab}}{-2+d} \\
&- \frac{2(-5+d)(-1+d)V^2\hat{x}_{ij}\sigma^a{}_a}{(-2+d)^3} + \frac{8(-1+d)V\sigma^{ab}\Psi_{ij}^{\partial_{ab} V}}{(-2+d)^2} - \frac{8(-1+d)V\sigma^a{}_a\Psi_{ij}^{\partial_{bb} V}}{(-2+d)^3} \\
&- \frac{4(-1+d)^2V^a\sigma\Psi_{ij}^{\partial t \partial_a V}}{(-2+d)^2} - \frac{4(-5+d)(-1+d)V\sigma^a\Psi_{ij}^{\partial t \partial_a V}}{(-2+d)^2} + \frac{8(-1+d)^2\sigma\Psi_{ij}^{\partial_a V_b}\partial_a V_b}{(-2+d)^2} \\
&+ \frac{8(-5+d)(-1+d)V\Psi_{ij}^{\partial_a V_b}\partial_a\sigma_b}{(-2+d)^2} + \frac{8(-5+d)(-1+d)\sigma^a\Psi LdjVi^b{}_a\partial_b V}{(-2+d)^2} + \frac{8(-1+d)^2V^a\Psi LdjVi^b{}_a\partial_b\sigma}{(-2+d)^2}.
\end{aligned}
$$

$$
\begin{aligned}
&\mathrm{MQSIC}_{4\mathrm{PN}} = \\
&- \frac{16(-1+d)M^a{}_a\hat{x}_{ij}\sigma}{(-2+d)^2} - \frac{16(-3+d)(-1+d)\hat{T}\hat{x}_{ij}\sigma}{(-2+d)^2} + \frac{(-3+d)(-1+d)(-43+55d-23d^2+3d^3)V^4\hat{x}_{ij}\sigma}{3(-2+d)^5} \\
&- \frac{8(-8+d)(-1+d)\hat{R}^aV_a\hat{x}_{ij}\sigma}{(-2+d)^2} + \frac{4(-1+d)(19-13d+2d^2)VV_aV^a\hat{x}_{ij}\sigma}{(-2+d)^3} - \frac{4(-3+d)(-1+d)^2V^2\hat{W}^a{}_a\hat{x}_{ij}\sigma}{(-2+d)^3}
\end{aligned}
$$

$$
\begin{aligned}
&-\frac{(-1+d)(2+d)\hat{W}_{ab}\hat{W}^{ab}\hat{x}_{ij}\sigma}{(-2+d)^2}+\frac{4(-3+d)(-1+d)(-7+3d)V\hat{X}\hat{x}_{ij}\sigma}{(-2+d)^3}+\frac{8(-1+d)^2V\hat{x}_{ij}\hat{Z}^a{}_a\sigma}{(-2+d)^2}\\
&-\frac{8(19-13d+2d^2)\hat{R}^aV\hat{x}_{ij}\sigma_a}{(-2+d)^2}+\frac{4(-65+71d-25d^2+3d^3)V^2V^a\hat{x}_{ij}\sigma_a}{(-2+d)^3}-\frac{8(-3+d)V^a\hat{W}^b{}_b\hat{x}_{ij}\sigma_a}{-2+d}\\
&+\frac{16(-3+d)\hat{x}_{ij}\hat{Y}^a\sigma_a}{-2+d}+\frac{8(-3+d)V^a\hat{W}_{ab}\hat{x}_{ij}\sigma^b}{-2+d}+\frac{8(-3+d)V^aV^b\hat{x}_{ij}\sigma_{ab}}{-2+d}\\
&-\frac{2(-8-d+d^2)V\hat{W}^{ab}\hat{x}_{ij}\sigma_{ab}}{(-2+d)^2}+\frac{16\hat{x}_{ij}\hat{Z}^{ab}\sigma_{ab}}{-2+d}+\frac{2(-1+d)(56-37d+5d^2)V^3\hat{x}_{ij}\sigma^a{}_a}{3(-2+d)^4}\\
&+\frac{8(-1+d)\hat{X}\hat{x}_{ij}\sigma^a{}_a}{(-2+d)^2}+\frac{8(-3+d)V_aV^a\hat{x}_{ij}\sigma^b{}_b}{(-2+d)^2}+\frac{2(-1+d)dV\hat{W}^a{}_a\hat{x}_{ij}\sigma^b{}_b}{(-2+d)^3}\\
&+\frac{8(-1+d)^2V^aV^b\sigma\Psi_{ij}^{\partial_{ab}V}}{(-2+d)^2}-\frac{16(-1+d)\hat{R}^a\sigma^b\Psi_{ij}^{\partial_{ab}V}}{-2+d}+\frac{8(-5+d)(-1+d)VV^a\sigma^b\Psi_{ij}^{\partial_{ab}V}}{(-2+d)^2}\\
&+\frac{16(-1+d)V^2\sigma^{ab}\Psi_{ij}^{\partial_{ab}V}}{(-2+d)^3}-\frac{(-3+d)^2(-1+d)^2V^3\sigma\Psi_{ij}^{\partial_{aa}V}}{(-2+d)^4}-\frac{2(-1+d)^2\hat{X}\sigma\Psi_{ij}^{\partial_{aa}V}}{(-2+d)^2}\\
&+\frac{8(-1+d)\hat{W}^{ab}\sigma_a{}^i\Psi_{ij}^{\partial_{bi}V}}{-2+d}-\frac{4(-1+d)^2V_aV^a\sigma\Psi_{ij}^{\partial_{bb}V}}{(-2+d)^2}+\frac{8(-1+d)\hat{R}^a\sigma_a\Psi_{ij}^{\partial_{bb}V}}{-2+d}\\
&-\frac{8(-4+d)(-1+d)VV^a\sigma_a\Psi_{ij}^{\partial_{bb}V}}{(-2+d)^2}-\frac{2(-1+d)^2V^2\sigma^a{}_a\Psi_{ij}^{\partial_{bb}V}}{(-2+d)^3}-\frac{2(-1+d)\hat{W}^{ab}\sigma_{ab}\Psi_{ij}^{\partial_{ii}V}}{-2+d}\\
&+\frac{2(-1+d)\hat{W}^a{}_a\sigma^b{}_b\Psi_{ij}^{\partial_{ii}V}}{(-2+d)^2}-\frac{8(-1+d)^2\hat{R}^a\sigma\Psi_{ij}^{\partial t\partial_aV}}{(-2+d)^2}+\frac{4(-5+d)(-1+d)^2VV^a\sigma\Psi_{ij}^{\partial t\partial_aV}}{(-2+d)^3}\\
&-\frac{16(-3+d)(-1+d)V^2\sigma^a\Psi_{ij}^{\partial t\partial_aV}}{(-2+d)^3}+\frac{8(-1+d)V^a\sigma^b{}_b\Psi_{ij}^{\partial t\partial_aV}}{(-2+d)^2}+\frac{8(-1+d)\hat{W}_{ab}\sigma^a\Psi_{ij}^{\partial t\partial_bV}}{-2+d}\\
&+\frac{8(-1+d)V^a\sigma_{ab}\Psi_{ij}^{\partial t\partial_bV}}{-2+d}+\frac{16(-1+d)^2\sigma\Psi_{ij}^{\partial_aV_b}\partial_a\hat{R}_b}{(-2+d)^2}-\frac{8(-5+d)(-1+d)^2V\sigma\Psi_{ij}^{\partial_aV_b}\partial_aV_b}{(-2+d)^3}\\
&-\frac{16(-1+d)\sigma^i{}_i\Psi_{ij}^{\partial_aV_b}\partial_aV_b}{(-2+d)^2}-\frac{16(-1+d)\sigma_{bi}\Psi_{ij}^{\partial_aV_b}\partial_aV^i}{-2+d}+\frac{32(-3+d)(-1+d)V^2\Psi_{ij}^{\partial_aV_b}\partial_a\sigma_b}{(-2+d)^3}\\
&-\frac{16(-1+d)\hat{W}_{bi}\Psi_{ij}^{\partial_aV_b}\partial_a\sigma^i}{-2+d}-\frac{8(-5+d)(-1+d)^2V^a\sigma\Psi LdjVi^b{}_a\partial_bV}{(-2+d)^3}+\frac{64(-3+d)(-1+d)V\sigma^a\Psi LdjVi^b{}_a\partial_bV}{(-2+d)^3}\\
&-\frac{16(-1+d)\sigma^a\Psi_{ij}^{\partial_bV_i}\partial_b\hat{W}_{ai}}{-2+d}+\frac{16(-1+d)^2\hat{R}^a\Psi LdjVi^b{}_a\partial_b\sigma}{(-2+d)^2}-\frac{8(-5+d)(-1+d)^2VV^a\Psi LdjVi^b{}_a\partial_b\sigma}{(-2+d)^3}\\
&-\frac{16(-1+d)V^a\Psi_{ij}^{\partial_bV_i}\partial_b\sigma_{ai}}{-2+d}-\frac{16(-1+d)V^a\Psi LdjVi^b{}_a\partial_b\sigma^i{}_i}{(-2+d)^2}.
\end{aligned}
$$

MQSI surface terms

$$
\mathrm{MQSISL}_{1\mathrm{PN}}=-\frac{(-1+d)^2V^2}{8(-2+d)^2}.
$$

$$
\mathrm{MQSISL}_{2\mathrm{PN}}=\frac{(-3+d)(-1+d)^2KV}{2(-2+d)^3}-\frac{(-1+d)^3V^3}{12(-2+d)^3}+\frac{(-3+d)V_aV^a}{2(-2+d)}-\frac{(-1+d)V\hat{W}^a{}_a}{4(-2+d)}.
$$

$$
\begin{aligned}
\mathrm{MQSISL}_{3\mathrm{PN}}=&-\frac{(-3+d)^2(-1+d)^2K^2}{2(-2+d)^4}+\frac{(-3+d)(-1+d)^3KV^2}{2(-2+d)^4}-\frac{(-1+d)^4V^4}{24(-2+d)^4}\\
&+\frac{2(-3+d)\hat{R}^aV_a}{-2+d}+\frac{(-3+d)(-1+d)VV_aV^a}{(-2+d)^2}+\frac{(-3+d)(-1+d)K\hat{W}^a{}_a}{2(-2+d)^2}\\
&-\frac{(-1+d)^2V^2\hat{W}^a{}_a}{4(-2+d)^2}+\frac{\hat{W}_{ab}\hat{W}^{ab}}{2(-2+d)}-\frac{\hat{W}^a{}_a\hat{W}^b{}_b}{4(-2+d)}-\frac{(-1+d)^2V\hat{X}}{(-2+d)^2}
\end{aligned}
$$

$$- \frac{(-1+d)V\hat{Z}^a{}_a}{-2+d}.$$

$$\begin{aligned}
\mathrm{MQSISL}_{4\mathrm{PN}} = {} & \frac{2(-3+d)\hat{R}_a\hat{R}^a}{-2+d} + \frac{4(-1+d)\hat{M}^a{}_aV}{(-2+d)^2} - \frac{4(-1+d)^2\hat{T}V}{(-2+d)^2} \\
& + \frac{(-3+d)(-1+d)^3(-2+3d)KV^3}{12(-2+d)^5} - \frac{(-1+d)^5V^5}{60(-2+d)^5} \\
& - \frac{(-5+d)(-3+d)(-1+d)KV_aV^a}{(-2+d)^3} + \frac{3(-3+d)(-1+d)^2V^2V_aV^a}{2(-2+d)^3} \\
& - \frac{(-1+d)^3V^3\hat{W}^a{}_a}{6(-2+d)^3} + \frac{(1-d)V\hat{W}^a{}_a\hat{W}^b{}_b}{4(-2+d)} + \frac{2(-3+d)(-1+d)^2K\hat{X}}{(-2+d)^3} \\
& - \frac{(-1+d)\hat{W}^a{}_a\hat{X}}{-2+d} + \frac{4(-3+d)V^a\hat{Y}_a}{-2+d} + \frac{4\hat{W}^{ab}\hat{Z}_{ab}}{-2+d} + \frac{2(-3+d)(-1+d)K\hat{Z}^a{}_a}{(-2+d)^2} \\
& - \frac{2\hat{W}^a{}_a\hat{Z}^b{}_b}{-2+d}.
\end{aligned}$$

$$\mathrm{MQSISD}_{2\mathrm{PN}} = \frac{(-1+d)\Psi_{ij}^{\partial_{bi}V}\partial_a\hat{W}_{bi}}{2(-2+d)} - \frac{(-1+d)\hat{W}^{bi}\partial_a\Psi_{ij}^{\partial_{bi}V}}{2(-2+d)}.$$

$$\begin{aligned}
\mathrm{MQSISD}_{3\mathrm{PN}} = {} & \frac{2(-1+d)\Psi_{ij}^{\partial t\partial_bV}\partial_a\hat{R}_b}{-2+d} + \frac{2(-1+d)\Psi_{ij}^{\partial_{bi}V}\partial_a\hat{Z}_{bi}}{-2+d} - \frac{2(-1+d)\hat{Z}^{bi}\partial_a\Psi_{ij}^{\partial_{bi}V}}{-2+d} \\
& - \frac{2(-1+d)\hat{R}^b\partial_a\Psi_{ij}^{\partial t\partial_bV}}{-2+d} - \frac{4(-1+d)\Psi_{ij}^{\partial_bV_i}\partial_b\partial_a\hat{R}_i}{-2+d} + \frac{4(-1+d)\partial_a\Psi_{ij}^{\partial_iV_b}\partial^i\hat{R}^b}{-2+d}.
\end{aligned}$$

$$\begin{aligned}
\mathrm{MQSISD}_{4\mathrm{PN}} = {} & \frac{4(-1+d)\Psi_{ij}^{\partial_{bi}V}\partial_aM_{bi}}{-2+d} + \frac{4(-1+d)\Psi_{ij}^{\partial t\partial_bV}\partial_a\hat{Y}_b}{-2+d} - \frac{4(-1+d)M^{bi}\partial_a\Psi_{ij}^{\partial_{bi}V}}{-2+d} \\
& - \frac{4(-1+d)\hat{Y}^b\partial_a\Psi_{ij}^{\partial t\partial_bV}}{-2+d} - \frac{8(-1+d)\Psi_{ij}^{\partial_bV_i}\partial_b\partial_a\hat{Y}_i}{-2+d} + \frac{8(-1+d)\partial_a\Psi_{ij}^{\partial_iV_b}\partial^i\hat{Y}^b}{-2+d}.
\end{aligned}$$

MQSII non-compact terms

$$\mathrm{MQSIINC}_{2\mathrm{PN}} = -\frac{(-1+d)^2r^2\hat{x}_{ij}\partial_aV\partial^aV}{8(-2+d)^2(4+d)}.$$

$$\begin{aligned}
\mathrm{MQSIINC}_{3\mathrm{PN}} = {} & \frac{(-4+d)(-1+d)^2r^2\hat{x}_{ij}(\partial_tV)^2}{16(-2+d)^3(4+d)} - \frac{(-1+d)r^2V^a\hat{x}_{ij}\partial_t\partial_aV}{2(-2+d)(4+d)} - \frac{(-1+d)^2r^2V\hat{x}_{ij}\partial_t^2V}{8(-2+d)^2(4+d)} \\
& + \frac{(-3+d)(-1+d)^2r^2\hat{x}_{ij}\partial_aV\partial^aK}{2(-2+d)^3(4+d)} - \frac{(-1+d)^2(-2+3d)r^2V\hat{x}_{ij}\partial_aV\partial^aV}{16(-2+d)^3(4+d)} \\
& - \frac{(-1+d)r^2\hat{x}_{ij}\partial_a\hat{W}^b{}_b\partial^aV}{4(-2+d)(4+d)} - \frac{(-1+d)r^2\hat{W}^{ab}\hat{x}_{ij}\partial_b\partial_aV}{4(-2+d)(4+d)} + \frac{(-1+d)r^2\hat{x}_{ij}\partial_aV_b\partial^bV^a}{2(-2+d)(4+d)} \\
& + \frac{(-3+d)r^2\hat{x}_{ij}\partial_bV_a\partial^bV^a}{2(-2+d)(4+d)}.
\end{aligned}$$

$\mathrm{MQSIINC}_{4\mathrm{PN}} =$

$$
\begin{aligned}
&- \frac{(-4+d)(-3+d)(-1+d)^2 r^2 \hat{x}_{ij} \partial_t K \partial_t V}{4(-2+d)^4(4+d)} + \frac{(-1+d)^2(8-8d+d^2) r^2 V \hat{x}_{ij} (\partial_t V)^2}{16(-2+d)^4(4+d)} + \frac{r^2 \hat{x}_{ij} \partial_t V_a \partial_t V^a}{(-2+d)(4+d)} \\
&+ \frac{(-1+d) r^2 \hat{x}_{ij} \partial_t V \partial_t \hat{W}^a{}_a}{4(-2+d)(4+d)} + \frac{(-3+d)(-1+d) r^2 V^a \hat{x}_{ij} \partial_t \partial_a K}{(-2+d)^2(4+d)} - \frac{(-1+d) r^2 \hat{R}^a \hat{x}_{ij} \partial_t \partial_a V}{(-2+d)(4+d)} \\
&- \frac{3(-1+d)^2 r^2 V V^a \hat{x}_{ij} \partial_t \partial_a V}{2(-2+d)^2(4+d)} + \frac{(-3+d)(-1+d)^2 r^2 V \hat{x}_{ij} \partial_t^2 K}{4(-2+d)^3(4+d)} + \frac{(-3+d)(-1+d)^2 K r^2 \hat{x}_{ij} \partial_t^2 V}{4(-2+d)^3(4+d)} \\
&- \frac{3(-1+d)^3 r^2 V^2 \hat{x}_{ij} \partial_t^2 V}{8(-2+d)^3(4+d)} - \frac{(-1+d) d r^2 V^a \hat{x}_{ij} \partial_t V \partial_a V}{2(-2+d)^2(4+d)} - \frac{(-3+d)^2(-1+d)^2 r^2 \hat{x}_{ij} \partial_a K \partial^a K}{2(-2+d)^4(4+d)} \\
&+ \frac{(-3+d)(-1+d)^2(-2+3d) r^2 V \hat{x}_{ij} \partial_a V \partial^a K}{4(-2+d)^4(4+d)} + \frac{(-3+d)(-1+d) r^2 \hat{x}_{ij} \partial_a \hat{W}^b{}_b \partial^a K}{2(-2+d)^2(4+d)} + \frac{(-1+d)^2 r^2 V \hat{x}_{ij} \partial_t V_a \partial^a V}{2(-2+d)^2(4+d)} \\
&+ \frac{(-3+d)(-1+d)^2(-2+3d) K r^2 \hat{x}_{ij} \partial_a V \partial^a V}{8(-2+d)^4(4+d)} - \frac{(-1+d)^3(-2+3d) r^2 V^2 \hat{x}_{ij} \partial_a V \partial^a V}{16(-2+d)^4(4+d)} - \frac{(-1+d)(-3+2d) r^2 \hat{W}^b{}_b \hat{x}_{ij} \partial_a V \partial^a V}{8(-2+d)^2(4+d)} \\
&- \frac{(-1+d)^2 r^2 V \hat{x}_{ij} \partial_a \hat{W}^b{}_b \partial^a V}{2(-2+d)^2(4+d)} - \frac{(-1+d)^2 r^2 \hat{x}_{ij} \partial_a \hat{X} \partial^a V}{(-2+d)^2(4+d)} - \frac{(-1+d) r^2 \hat{x}_{ij} \partial_a \hat{Z}^b{}_b \partial^a V}{(-2+d)(4+d)} \\
&+ \frac{(-3+d)(-1+d) r^2 \hat{W}^{ab} \hat{x}_{ij} \partial_b \partial_a K}{2(-2+d)^2(4+d)} - \frac{(-1+d)^2 r^2 V \hat{W}^{ab} \hat{x}_{ij} \partial_b \partial_a V}{2(-2+d)^2(4+d)} - \frac{(-1+d) r^2 \hat{x}_{ij} \hat{Z}^{ab} \partial_b \partial_a V}{(-2+d)(4+d)} \\
&+ \frac{2(-1+d) r^2 \hat{x}_{ij} \partial_a V_b \partial^b \hat{R}^a}{(-2+d)(4+d)} + \frac{2(-3+d) r^2 \hat{x}_{ij} \partial_b V_a \partial^b \hat{R}^a}{(-2+d)(4+d)} - \frac{(-3+d)(-1+d) r^2 V^a \hat{x}_{ij} \partial_a V_b \partial^b V}{(-2+d)^2(4+d)} \\
&- \frac{(-1+d) r^2 \hat{W}_{ab} \hat{x}_{ij} \partial^a V \partial^b V}{4(-2+d)^2(4+d)} + \frac{(-5+d)(-1+d) r^2 V^a \hat{x}_{ij} \partial_b V_a \partial^b V}{(-2+d)^2(4+d)} + \frac{(-1+d) r^2 \hat{x}_{ij} \partial_t \hat{W}_{ab} \partial^b V^a}{(-2+d)(4+d)} \\
&+ \frac{3(-1+d) r^2 V \hat{x}_{ij} \partial_a V_b \partial^b V^a}{2(-2+d)(4+d)} + \frac{(-1+d) r^2 V \hat{x}_{ij} \partial_b V_a \partial^b V^a}{2(-2+d)(4+d)} - \frac{r^2 \hat{x}_{ij} \partial_b \hat{W}^i{}_i \partial^b \hat{W}^a{}_a}{4(-2+d)(4+d)} \\
&+ \frac{r^2 \hat{x}_{ij} \partial_i \hat{W}_{ab} \partial^i \hat{W}^{ab}}{2(-2+d)(4+d)}.
\end{aligned}
$$

MQSII compact terms

$$\mathrm{MQSIIC}_{1\mathrm{PN}} = \frac{(-1+d) r^2 \hat{x}_{ij} \sigma}{4(-2+d)(4+d)}.$$

$$\mathrm{MQSIIC}_{2\mathrm{PN}} = \frac{(-1+d) r^2 V \hat{x}_{ij} \sigma}{(-2+d)^2(4+d)}.$$

$$\mathrm{MQSIIC}_{3\mathrm{PN}} = -\frac{2(-3+d)(-1+d) K r^2 \hat{x}_{ij} \sigma}{(-2+d)^3(4+d)} + \frac{2(-1+d) r^2 V^2 \hat{x}_{ij} \sigma}{(-2+d)^3(4+d)} + \frac{(-1+d) r^2 \hat{W}^a{}_a \hat{x}_{ij} \sigma}{2(-2+d)(4+d)}.$$

$$
\begin{aligned}
\mathrm{MQSIIC}_{4\mathrm{PN}} = &- \frac{8(-3+d)(-1+d) K r^2 V \hat{x}_{ij} \sigma}{(-2+d)^4(4+d)} + \frac{8(-1+d) r^2 V^3 \hat{x}_{ij} \sigma}{3(-2+d)^4(4+d)} + \frac{4(-1+d) r^2 V_a V^a \hat{x}_{ij} \sigma}{(-2+d)^2(4+d)} \\
&+ \frac{2(-1+d) r^2 V \hat{W}^a{}_a \hat{x}_{ij} \sigma}{(-2+d)^2(4+d)} + \frac{4(-1+d) r^2 \hat{X} \hat{x}_{ij} \sigma}{(-2+d)^2(4+d)} + \frac{2(-1+d) r^2 \hat{x}_{ij} \hat{Z}^a{}_a \sigma}{(-2+d)(4+d)}.
\end{aligned}
$$

MQSIII non-compact terms

$$\mathrm{MQSIIINC}_{3\mathrm{PN}} = -\frac{(-1+d)^2 r^4 \hat{x}_{ij} \partial_a V \partial^a V}{32(-2+d)^2(4+d)(6+d)}.$$

$$\mathrm{MQSIIINC}_{4\mathrm{PN}} = \frac{(-4+d)(-1+d)^2 r^4 \hat{x}_{ij}(\partial_t V)^2}{64(-2+d)^3(4+d)(6+d)} - \frac{(-1+d) r^4 V^a \hat{x}_{ij}\partial_t\partial_a V}{8(-2+d)(4+d)(6+d)} - \frac{(-1+d)^2 r^4 V \hat{x}_{ij}\partial_t^2 V}{32(-2+d)^2(4+d)(6+d)} + \frac{(-3+d)(-1+d)^2 r^4 \hat{x}_{ij}\partial_a V \partial^a K}{8(-2+d)^3(4+d)(6+d)} - \frac{(-1+d)^2(-2+3d) r^4 V \hat{x}_{ij}\partial_a V \partial^a V}{64(-2+d)^3(4+d)(6+d)} - \frac{(-1+d) r^4 \hat{x}_{ij}\partial_a \hat{W}^b{}_b \partial^a V}{16(-2+d)(4+d)(6+d)} - \frac{(-1+d) r^4 \hat{W}^{ab}\hat{x}_{ij}\partial_b\partial_a V}{16(-2+d)(4+d)(6+d)} + \frac{(-1+d) r^4 \hat{x}_{ij}\partial_a V_b \partial^b V^a}{8(-2+d)(4+d)(6+d)} + \frac{(-3+d) r^4 \hat{x}_{ij}\partial_b V_a \partial^b V^a}{8(-2+d)(4+d)(6+d)}.$$

MQSIII compact terms

$$\mathrm{MQSIIIC}_{2\mathrm{PN}} = \frac{(-1+d) r^4 \hat{x}_{ij}\sigma}{16(-2+d)(4+d)(6+d)}.$$

$$\mathrm{MQSIIIC}_{3\mathrm{PN}} = \frac{(-1+d) r^4 V \hat{x}_{ij}\sigma}{4(-2+d)^2(4+d)(6+d)}.$$

$$\mathrm{MQSIIIC}_{4\mathrm{PN}} = -\frac{(-3+d)(-1+d) K r^4 \hat{x}_{ij}\sigma}{2(-2+d)^3(4+d)(6+d)} + \frac{(-1+d) r^4 V^2 \hat{x}_{ij}\sigma}{2(-2+d)^3(4+d)(6+d)} + \frac{(-1+d) r^4 \hat{W}^a{}_a \hat{x}_{ij}\sigma}{8(-2+d)(4+d)(6+d)}.$$

MQSIV non-compact terms

$$\mathrm{MQSIVNC}_{4\mathrm{PN}} = -\frac{(-1+d)^2 r^6 \hat{x}_{ij}\partial_a V \partial^a V}{192(-2+d)^2(4+d)(6+d)(8+d)}.$$

MQSIV compact terms

$$\mathrm{MQSIVC}_{3\mathrm{PN}} = \frac{(-1+d) r^6 \hat{x}_{ij}\sigma}{96(-2+d)(4+d)(6+d)(8+d)}.$$

$$\mathrm{MQSIVC}_{4\mathrm{PN}} = \frac{(-1+d) r^6 V \hat{x}_{ij}\sigma}{24(-2+d)^2(4+d)(6+d)(8+d)}.$$

MQSV compact terms

$$\mathrm{MQSVC}_{4\mathrm{PN}} = \frac{(-1+d) r^8 \hat{x}_{ij}\sigma}{768(-2+d)(4+d)(6+d)(8+d)(10+d)}.$$

MQVI non-compact terms

$$\mathrm{MQVINC}_{\mathrm{2PN}} = -\frac{(-1+d)^2(2+d)\hat{x}_{ija}\partial_t V\partial_a V}{4(-2+d)^3(4+d)} - \frac{(-1+d)^2(2+d)\hat{x}_{ija}\partial_a V_b\partial^b V}{(-2+d)^2 d(4+d)}.$$

$$\begin{aligned}
&\mathrm{MQVINC}_{\mathrm{3PN}} = \\
&-\frac{(-1+d)^2(2+d)\hat{x}_{ija}\partial_t V\partial_t V_a}{(-2+d)^2 d(4+d)} + \frac{4(-1+d)(2+d)V^a\hat{x}_{ijb}\partial_t\partial_a V_b}{(-2+d)d(4+d)} - \frac{(-1+d)^2(2+d)V^a\hat{x}_{ija}\partial_t^2 V}{2(-2+d)^2 d(4+d)} \\
&+\frac{(-1+d)^2(2+d)V\hat{x}_{ija}\partial_t^2 V_a}{2(-2+d)^2 d(4+d)} + \frac{(-3+d)(-1+d)^2(2+d)\hat{x}_{ija}\partial_t V\partial_a K}{2(-2+d)^4(4+d)} + \frac{(-3+d)(-1+d)^2(2+d)\hat{x}_{ija}\partial_t K\partial_a V}{2(-2+d)^4(4+d)} \\
&-\frac{(-1+d)^3(2+d)V\hat{x}_{ija}\partial_t V\partial_a V}{4(-2+d)^4(4+d)} + \frac{(-1+d)^3(2+d)\Psi_{ijb}^{\partial_a V}\partial_t\partial_b V\partial_a V}{2(-2+d)^4(4+d)} - \frac{(-1+d)^2(2+d)V^a\hat{x}_{ijb}\partial_a V\partial_b V}{2(-2+d)^3(4+d)} \\
&+\frac{(-1+d)^3(2+d)\Psi_{ijb}^{\partial_a V}\partial_t V\partial_b\partial_a V}{2(-2+d)^4(4+d)} + \frac{2(-3+d)(-1+d)^2(2+d)\hat{x}_{ija}\partial_a V_b\partial^b K}{(-2+d)^3 d(4+d)} - \frac{(-1+d)^2(2+d)\hat{x}_{ija}\partial_t\hat{W}_{ab}\partial^b V}{(-2+d)^2 d(4+d)} \\
&+\frac{(-1+d)^3(2+d)V^a\hat{x}_{ija}\partial_b V\partial^b V}{2(-2+d)^3 d(4+d)} + \frac{2(-1+d)^3(2+d)\Psi_{ijb}^{\partial_a V}\partial_a V^i\partial_i\partial_b V}{(-2+d)^3 d(4+d)} + \frac{2(-1+d)(2+d)\hat{W}^{bi}\hat{x}_{ija}\partial_i\partial_b V_a}{(-2+d)d(4+d)} \\
&+\frac{2(-1+d)^3(2+d)\Psi_{ijb}^{\partial_a V}\partial_b\partial_a V_i\partial^i V}{(-2+d)^3 d(4+d)} + \frac{2(-1+d)(2+d)\hat{x}_{ija}\partial_a\hat{W}_{bi}\partial^i V^b}{(-2+d)d(4+d)} - \frac{2(-1+d)(2+d)\hat{x}_{ija}\partial_b\hat{W}_{ai}\partial^i V^b}{(-2+d)d(4+d)}.
\end{aligned}$$

$$\begin{aligned}
&\mathrm{MQVINC}_{\mathrm{4PN}} = \\
&-\frac{2(-1+d)^2(2+d)\hat{x}_{ija}\partial_t\hat{R}_a\partial_t V}{(-2+d)^2 d(4+d)} - \frac{(-1+d)^2(2+d)V^a\hat{x}_{ija}(\partial_t V)^2}{2(-2+d)^2 d(4+d)} + \frac{2(-3+d)(-1+d)^2(2+d)\hat{x}_{ija}\partial_t K\partial_t V_a}{(-2+d)^3 d(4+d)} \\
&-\frac{(-1+d)^3(2+d)V\hat{x}_{ija}\partial_t V\partial_t V_a}{(-2+d)^3 d(4+d)} - \frac{2(-1+d)(2+d)\hat{x}_{ija}\partial_t V_a\partial_t\hat{W}^b{}_b}{(-2+d)d(4+d)} + \frac{8(-1+d)(2+d)V^a\hat{x}_{ijb}\partial_t\partial_a\hat{R}_b}{(-2+d)d(4+d)} \\
&+\frac{8(-1+d)(2+d)\hat{R}^a\hat{x}_{ijb}\partial_t\partial_a V_b}{(-2+d)d(4+d)} + \frac{4(-1+d)^2(2+d)VV^a\hat{x}_{ijb}\partial_t\partial_a V_b}{(-2+d)^2 d(4+d)} - \frac{8(-1+d)^2(2+d)V^a\Psi_{iji}^{\partial_b V}\partial_t\partial_i\partial_a V_b}{(-2+d)^2 d(4+d)} \\
&+\frac{(-3+d)(-1+d)^2(2+d)V^a\hat{x}_{ija}\partial_t^2 K}{(-2+d)^3 d(4+d)} + \frac{(-1+d)^2(2+d)V\hat{x}_{ija}\partial_t^2\hat{R}_a}{(-2+d)^2 d(4+d)} - \frac{(-1+d)^2(2+d)\hat{R}^a\hat{x}_{ija}\partial_t^2 V}{(-2+d)^2 d(4+d)} \\
&-\frac{(-1+d)^3(2+d)VV^a\hat{x}_{ija}\partial_t^2 V}{2(-2+d)^3 d(4+d)} - \frac{(-3+d)(-1+d)^2(2+d)K\hat{x}_{ija}\partial_t^2 V_a}{(-2+d)^3 d(4+d)} + \frac{3(-1+d)^3(2+d)V^2\hat{x}_{ija}\partial_t^2 V_a}{4(-2+d)^3 d(4+d)} \\
&-\frac{(-1+d)(2+d)\hat{W}^b{}_b\hat{x}_{ija}\partial_t^2 V_a}{(-2+d)d(4+d)} + \frac{(-1+d)(2+d)\hat{W}_{ab}\hat{x}_{ija}\partial_t^2 V^b}{(-2+d)d(4+d)} + \frac{(-1+d)(2+d)V^a\hat{x}_{ijb}\partial_t^2\hat{W}_{ab}}{(-2+d)d(4+d)} \\
&-\frac{(-1+d)(2+d)V^a\hat{x}_{ija}\partial_t^2\hat{W}^b{}_b}{(-2+d)d(4+d)} - \frac{2(-1+d)^2(2+d)\Psi_{ijb}^{\partial_a V}\partial_t^2\partial_b\hat{R}_a}{(-2+d)^2 d(4+d)} - \frac{2(-1+d)^3(2+d)V\Psi_{ijb}^{\partial_a V}\partial_t^2\partial_b V_a}{(-2+d)^3 d(4+d)} \\
&-\frac{(-3+d)^2(-1+d)^2(2+d)\hat{x}_{ija}\partial_t K\partial_a K}{(-2+d)^5(4+d)} + \frac{(-3+d)(-1+d)^3(2+d)V\hat{x}_{ija}\partial_t V\partial_a K}{2(-2+d)^5(4+d)} - \frac{(-3+d)(-1+d)^3(2+d)\Psi_{ijb}^{\partial_a V}\partial_t\partial_b V\partial_a K}{(-2+d)^5(4+d)} \\
&+\frac{(-3+d)(-1+d)^3(2+d)V\hat{x}_{ija}\partial_t K\partial_a V}{2(-2+d)^5(4+d)} + \frac{(-3+d)(-1+d)^3(2+d)K\hat{x}_{ija}\partial_t V\partial_a V}{2(-2+d)^5(4+d)} + \frac{2(-1+d)^2(2+d)V^a\hat{x}_{ijb}\partial_t V_b\partial_a V}{(-2+d)^2 d(4+d)} \\
&-\frac{(-1+d)^2(2+d)\hat{x}_{ija}\partial_t\hat{X}\partial_a V}{(-2+d)^3(4+d)} - \frac{(-3+d)(-1+d)^3(2+d)\Psi_{ijb}^{\partial_a V}\partial_t\partial_b K\partial_a V}{(-2+d)^5(4+d)} + \frac{(-1+d)^4(2+d)V\Psi_{ijb}^{\partial_a V}\partial_t\partial_b V\partial_a V}{2(-2+d)^5(4+d)} \\
&+\frac{(-1+d)(2+d)\hat{x}_{ija}\partial_t\hat{W}_{bi}\partial_a\hat{W}^{bi}}{(-2+d)d(4+d)} - \frac{(-1+d)^2(2+d)\hat{x}_{ija}\partial_t V\partial_a\hat{X}}{(-2+d)^3(4+d)} + \frac{(-3+d)(-1+d)^2(2+d)V^a\hat{x}_{ijb}\partial_a V\partial_b K}{(-2+d)^4(4+d)} \\
&-\frac{4(-1+d)^2(2+d)V^a\hat{x}_{ijb}\partial_t V_a\partial_b V}{(-2+d)^3 d(4+d)} - \frac{2(-1+d)^3(2+d)\Psi_{ijb}^{\partial_a V}\partial_t^2 V_a\partial_b V}{(-2+d)^3 d(4+d)} + \frac{(-3+d)(-1+d)^2(2+d)V^a\hat{x}_{ijb}\partial_a K\partial_b V}{(-2+d)^4(4+d)} \\
&-\frac{(-1+d)^2(2+d)\hat{R}^a\hat{x}_{ijb}\partial_a V\partial_b V}{(-2+d)^3(4+d)} - \frac{(-1+d)^4(2+d)VV^a\hat{x}_{ijb}\partial_a V\partial_b V}{(-2+d)^4 d(4+d)} + \frac{(-1+d)^4(2+d)\Psi_{ijb}^{\partial_a V}\partial_t V\partial_a V\partial_b V}{2(-2+d)^5(4+d)}
\end{aligned}$$

$$
\begin{aligned}
&+ \frac{2(-4+d)(-1+d)^2(2+d)V^a\hat{x}_{ijb}\partial_t V\partial_b V_a}{(-2+d)^3 d(4+d)} - \frac{4(-1+d)(2+d)V^a\hat{x}_{ijb}\partial_a V^i\partial_b V_i}{(-2+d)d(4+d)} - \frac{8(-1+d)^2(2+d)\Psi^{\partial_a V}_{ijb}\partial_t\partial_i V_a\partial_b V^i}{(-2+d)^2 d(4+d)} \\
&- \frac{4(-1+d)^2(2+d)\hat{x}_{ija}\partial_a V^b\partial_b\hat{X}}{(-2+d)^2 d(4+d)} - \frac{(-3+d)(-1+d)^3(2+d)\Psi^{\partial_a V}_{ijb}\partial_t V\partial_b\partial_a K}{(-2+d)^5(4+d)} - \frac{(-3+d)(-1+d)^3(2+d)\Psi^{\partial_a V}_{ijb}\partial_t K\partial_b\partial_a V}{(-2+d)^5(4+d)} \\
&+ \frac{(-1+d)^4(2+d)V\Psi^{\partial_a V}_{ijb}\partial_t V\partial_b\partial_a V}{2(-2+d)^5(4+d)} + \frac{2(-3+d)(-1+d)^2(2+d)\hat{x}_{ija}\partial_t\hat{W}_{ab}\partial^b K}{(-2+d)^3 d(4+d)} + \frac{4(-3+d)(-1+d)^2(2+d)\hat{x}_{ija}\partial_a\hat{R}_b\partial^b K}{(-2+d)^3 d(4+d)} \\
&- \frac{2(-3+d)(-1+d)^3(2+d)V^a\hat{x}_{ija}\partial_b V\partial^b K}{(-2+d)^4 d(4+d)} - \frac{2(-1+d)^3(2+d)V\hat{x}_{ija}\partial_b V\partial^b\hat{R}_a}{(-2+d)^3 d(4+d)} + \frac{(-1+d)^2(2+d)\hat{W}_{ab}\hat{x}_{ija}\partial_t V\partial^b V}{2(-2+d)^3(4+d)} \\
&+ \frac{4(-1+d)^2(2+d)V^a\hat{x}_{ija}\partial_t V_b\partial^b V}{(-2+d)^2 d(4+d)} - \frac{(-1+d)^3(2+d)V\hat{x}_{ija}\partial_t\hat{W}_{ab}\partial^b V}{(-2+d)^3 d(4+d)} - \frac{4(-1+d)^2(2+d)\hat{x}_{ija}\partial_t\hat{Z}_{ab}\partial^b V}{(-2+d)^2 d(4+d)} \\
&+ \frac{2(-1+d)^2(2+d)\hat{W}_{bi}\hat{x}_{ija}\partial_a V^i\partial^b V}{(-2+d)^2 d(4+d)} + \frac{2(-1+d)^4(2+d)VV^a\hat{x}_{ija}\partial_b V\partial^b V}{(-2+d)^4 d(4+d)} + \frac{2(-1+d)^4(2+d)V^2\hat{x}_{ija}\partial_b V_a\partial^b V}{(-2+d)^4 d(4+d)} \\
&+ \frac{(-1+d)^3(2+d)V^a\Psi^{\partial_b V}_{iji}\partial_b V\partial_i\partial_a V}{(-2+d)^4(4+d)} - \frac{4(-3+d)(-1+d)^3(2+d)\Psi^{\partial_a V}_{ijb}\partial_a V^i\partial_i\partial_b K}{(-2+d)^4 d(4+d)} + \frac{4(-1+d)(2+d)\hat{W}^{bi}\hat{x}_{ija}\partial_i\partial_b\hat{R}_a}{(-2+d)d(4+d)} \\
&+ \frac{4(-1+d)^3(2+d)\Psi^{\partial_a V}_{ijb}\partial_a\hat{R}^i\partial_i\partial_b V}{(-2+d)^3 d(4+d)} + \frac{(-1+d)^3(2+d)V^a\Psi^{\partial_b V}_{iji}\partial_a V\partial_i\partial_b V}{(-2+d)^4(4+d)} + \frac{8(-1+d)(2+d)\hat{x}_{ija}\hat{Z}^{bi}\partial_i\partial_b V_a}{(-2+d)d(4+d)} \\
&- \frac{4(-3+d)(-1+d)^3(2+d)\Psi^{\partial_a V}_{ijb}\partial_b\partial_a V_i\partial^i K}{(-2+d)^4 d(4+d)} + \frac{4(-1+d)(2+d)\hat{x}_{ija}\partial_a\hat{W}_{bi}\partial^i\hat{R}^b}{(-2+d)d(4+d)} - \frac{4(-1+d)(2+d)\hat{x}_{ija}\partial_b\hat{W}_{ai}\partial^i\hat{R}^b}{(-2+d)d(4+d)} \\
&+ \frac{2(-1+d)^3(2+d)\Psi^{\partial_a V}_{ijb}\partial_t\partial_b\hat{W}_{ai}\partial^i V}{(-2+d)^3 d(4+d)} - \frac{2(-1+d)^2(2+d)V^a\hat{x}_{ijb}\partial_a\hat{W}_{bi}\partial^i V}{(-2+d)^2 d(4+d)} + \frac{(-1+d)^3(2+d)\Psi^{\partial_a V}_{ijb}\partial_a V\partial_b V_i\partial^i V}{(-2+d)^4(4+d)} \\
&+ \frac{4(-1+d)^3(2+d)\Psi^{\partial_a V}_{ijb}\partial_b\partial_a\hat{R}_i\partial^i V}{(-2+d)^3 d(4+d)} + \frac{2(-1+d)^4(2+d)\Psi^{\partial_a V}_{ijb}\partial_b V\partial_i V_a\partial^i V}{(-2+d)^4 d(4+d)} + \frac{2(-1+d)^2(2+d)V^a\hat{x}_{ijb}\partial_i\hat{W}_{ab}\partial^i V}{(-2+d)^2 d(4+d)} \\
&+ \frac{2(-1+d)^4(2+d)V\Psi^{\partial_a V}_{ijb}\partial_i\partial_b V_a\partial^i V}{(-2+d)^4 d(4+d)} - \frac{4(-1+d)(2+d)V^a\hat{x}_{ijb}\partial_b V_i\partial^i V_a}{(-2+d)^2(4+d)} + \frac{2(-1+d)^4(2+d)V\Psi^{\partial_a V}_{ijb}\partial_i\partial_b V\partial^i V_a}{(-2+d)^4 d(4+d)} \\
&+ \frac{4(-1+d)(2+d)V^a\hat{x}_{ijb}\partial_a V_i\partial^i V_b}{(-2+d)d(4+d)} + \frac{2(-1+d)^2(2+d)\hat{W}_{ai}\hat{x}_{ija}\partial^b V\partial^i V_b}{(-2+d)^2 d(4+d)} + \frac{8(-1+d)(2+d)\hat{x}_{ija}\partial_a\hat{Z}_{bi}\partial^i V^b}{(-2+d)d(4+d)} \\
&+ \frac{4(-1+d)(2+d)V^a\hat{x}_{ija}\partial_b V_i\partial^i V^b}{(-2+d)d(4+d)} - \frac{8(-1+d)(2+d)\hat{x}_{ija}\partial_b\hat{Z}_{ai}\partial^i V^b}{(-2+d)d(4+d)} - \frac{2(-1+d)(2+d)V^a\hat{x}_{ija}\partial_i V_b\partial^i V^b}{(-2+d)d(4+d)} \\
&- \frac{2(-1+d)(2+d)\hat{x}_{ija}\partial_t\hat{W}_{bi}\partial^i\hat{W}_a{}^b}{(-2+d)d(4+d)} + \frac{2(-1+d)^3(2+d)\Psi^{\partial_a V}_{ijb}\partial_t\hat{W}_{ai}\partial^i\partial_b V}{(-2+d)^3 d(4+d)} - \frac{4(-1+d)^2(2+d)\hat{W}^{ij}\Psi^{\partial_a V}_{ijb}\partial_j\partial_i\partial_b V_a}{(-2+d)^2 d(4+d)} \\
&- \frac{4(-1+d)^2(2+d)\Psi^{\partial_a V}_{ijb}\partial_b\partial_a\hat{W}_{ij}\partial^j V^i}{(-2+d)^2 d(4+d)} + \frac{4(-1+d)^2(2+d)\Psi^{\partial_a V}_{ijb}\partial_i\partial_b\hat{W}_{aj}\partial^j V^i}{(-2+d)^2 d(4+d)} - \frac{4(-1+d)^2(2+d)\Psi^{\partial_a V}_{ijb}\partial_a\hat{W}_{ij}\partial^j\partial_b V^i}{(-2+d)^2 d(4+d)} \\
&+ \frac{4(-1+d)^2(2+d)\Psi^{\partial_a V}_{ijb}\partial_i\hat{W}_{aj}\partial^j\partial_b V^i}{(-2+d)^2 d(4+d)} - \frac{4(-1+d)^2(2+d)\Psi^{\partial_a V}_{ijb}\partial_b\hat{W}_{ij}\partial^j\partial^i V_a}{(-2+d)^2 d(4+d)}.
\end{aligned}
$$

MQVI compact terms

$$
\mathrm{MQVIC}_{1\mathrm{PN}} = -\frac{2(-1+d)(2+d)\hat{x}_{ija}\sigma_a}{(-2+d)d(4+d)}.
$$

$$
\mathrm{MQVIC}_{2\mathrm{PN}} = \frac{2(-1+d)^2(2+d)V^a\hat{x}_{ija}\sigma}{(-2+d)^2 d(4+d)} + \frac{2(-5+d)(-1+d)(2+d)V\hat{x}_{ija}\sigma_a}{(-2+d)^2 d(4+d)}.
$$

$$
\begin{aligned}
&\mathrm{MQVIC}_{3\mathrm{PN}} = \\
&\frac{4(-1+d)^2(2+d)\hat{R}^a\hat{x}_{ija}\sigma}{(-2+d)^2 d(4+d)} - \frac{4(-3+d)(-1+d)^2(2+d)VV^a\hat{x}_{ija}\sigma}{(-2+d)^3 d(4+d)} - \frac{4(-5+d)(-3+d)(-1+d)(2+d)K\hat{x}_{ija}\sigma_a}{(-2+d)^3 d(4+d)}
\end{aligned}
$$

$$- \frac{(-5+d)^2(-1+d)(2+d)V^2\hat{x}_{ija}\sigma_a}{(-2+d)^3 d(4+d)} - \frac{4(-1+d)(2+d)\hat{W}_{ab}\hat{x}_{ija}\sigma^b}{(-2+d)d(4+d)} - \frac{4(-1+d)(2+d)V^a\hat{x}_{ijb}\sigma_{ab}}{(-2+d)d(4+d)}$$
$$- \frac{4(-1+d)(2+d)V^a\hat{x}_{ija}\sigma^b{}_b}{(-2+d)^2 d(4+d)} - \frac{4(-5+d)(-1+d)^2(2+d)\sigma^a\Psi^{\partial_a V}_{ijb}\partial_b V}{(-2+d)^3 d(4+d)} - \frac{4(-1+d)^3(2+d)\sigma\Psi^{\partial_a V}_{ijb}\partial_b V_a}{(-2+d)^3 d(4+d)}$$
$$- \frac{4(-1+d)^3(2+d)V^a\Psi^{\partial_a V}_{ijb}\partial_b\sigma}{(-2+d)^3 d(4+d)} - \frac{4(-5+d)(-1+d)^2(2+d)V\Psi^{\partial_a V}_{ijb}\partial_b\sigma_a}{(-2+d)^3 d(4+d)}.$$

$$\mathrm{MQVIC}_{4\mathrm{PN}} =$$
$$- \frac{4(-5+d)(-1+d)^2(2+d)\hat{R}^a V\hat{x}_{ija}\sigma}{(-2+d)^3 d(4+d)} + \frac{8(-3+d)^2(-1+d)^2(2+d)KV^a\hat{x}_{ija}\sigma}{(-2+d)^4 d(4+d)} - \frac{16(-1+d)^2(2+d)V^2V^a\hat{x}_{ija}\sigma}{(-2+d)^3 d(4+d)}$$
$$+ \frac{8(-1+d)^2(2+d)\hat{x}_{ija}\hat{Y}_a\sigma}{(-2+d)^2 d(4+d)} + \frac{4(-5+d)^2(-3+d)(-1+d)(2+d)KV\hat{x}_{ija}\sigma_a}{(-2+d)^4 d(4+d)}$$
$$- \frac{2(-1+d)(2+d)(53-15d-9d^2+3d^3)V^3\hat{x}_{ija}\sigma_a}{3(-2+d)^4 d(4+d)} + \frac{8(-5+d)(-1+d)(2+d)\hat{X}\hat{x}_{ija}\sigma_a}{(-2+d)^2 d(4+d)}$$
$$+ \frac{24(-1+d)(2+d)V^aV^b\hat{x}_{ija}\sigma_b}{(-2+d)d(4+d)} + \frac{4(-8+d)(-1+d)(2+d)V_aV^a\hat{x}_{ijb}\sigma_b}{(-2+d)^2 d(4+d)}$$
$$+ \frac{4(-5+d)(-1+d)(2+d)V\hat{W}_{ab}\hat{x}_{ija}\sigma^b}{(-2+d)^2 d(4+d)} - \frac{16(-1+d)(2+d)\hat{x}_{ija}\hat{Z}_{ab}\sigma^b}{(-2+d)d(4+d)} - \frac{8(-1+d)(2+d)\hat{R}^a\hat{x}_{ijb}\sigma_{ab}}{(-2+d)d(4+d)}$$
$$- \frac{16(-1+d)(2+d)VV^a\hat{x}_{ijb}\sigma_{ab}}{(-2+d)^2 d(4+d)} - \frac{8(-1+d)(2+d)\hat{R}^a\hat{x}_{ija}\sigma^b{}_b}{(-2+d)^2 d(4+d)} + \frac{8(-3+d)(-1+d)(2+d)VV^a\hat{x}_{ija}\sigma^b{}_b}{(-2+d)^3 d(4+d)}$$
$$+ \frac{8(-5+d)(-3+d)(-1+d)^2(2+d)\sigma^a\Psi^{\partial_a V}_{ijb}\partial_b K}{(-2+d)^4 d(4+d)} - \frac{8(-1+d)^3(2+d)\sigma\Psi^{\partial_a V}_{ijb}\partial_b\hat{R}_a}{(-2+d)^3 d(4+d)}$$
$$+ \frac{4(-5+d)(-1+d)^3(2+d)V^a\sigma\Psi^{\partial_a V}_{ijb}\partial_b V}{(-2+d)^4 d(4+d)} - \frac{32(-3+d)(-1+d)^2(2+d)V\sigma^a\Psi^{\partial_a V}_{ijb}\partial_b V}{(-2+d)^4 d(4+d)}$$
$$+ \frac{4(-5+d)(-1+d)^3(2+d)V\sigma\Psi^{\partial_a V}_{ijb}\partial_b V_a}{(-2+d)^4 d(4+d)} + \frac{8(-1+d)^2(2+d)\sigma^i{}_i\Psi^{\partial_a V}_{ijb}\partial_b V_a}{(-2+d)^3 d(4+d)}$$
$$+ \frac{8(-1+d)^2(2+d)\sigma_{ai}\Psi^{\partial_a V}_{ijb}\partial_b V^i}{(-2+d)^2 d(4+d)} - \frac{8(-1+d)^3(2+d)\hat{R}^a\Psi^{\partial_a V}_{ijb}\partial_b\sigma}{(-2+d)^3 d(4+d)} + \frac{4(-5+d)(-1+d)^3(2+d)VV^a\Psi^{\partial_a V}_{ijb}\partial_b\sigma}{(-2+d)^4 d(4+d)}$$
$$+ \frac{8(-5+d)(-3+d)(-1+d)^2(2+d)K\Psi^{\partial_a V}_{ijb}\partial_b\sigma_a}{(-2+d)^4 d(4+d)} - \frac{16(-3+d)(-1+d)^2(2+d)V^2\Psi^{\partial_a V}_{ijb}\partial_b\sigma_a}{(-2+d)^4 d(4+d)}$$
$$+ \frac{8(-1+d)^2(2+d)\hat{W}_{ai}\Psi^{\partial_a V}_{ijb}\partial_b\sigma^i}{(-2+d)^2 d(4+d)} + \frac{8(-1+d)^2(2+d)V^a\Psi^{\partial_a V}_{ijb}\partial_b\sigma^i{}_i}{(-2+d)^3 d(4+d)}$$
$$+ \frac{8(-1+d)^2(2+d)\sigma^a\Psi^{\partial_b V}_{iji}\partial_i\hat{W}_{ab}}{(-2+d)^2 d(4+d)} + \frac{8(-1+d)^2(2+d)V^a\Psi^{\partial_b V}_{iji}\partial_i\sigma_{ab}}{(-2+d)^2 d(4+d)}.$$

MQVI Surface terms

$$\mathrm{MQVISL}_{2\mathrm{PN}} = \frac{(-1+d)^2(2+d)VV_a}{2(-2+d)^2 d(4+d)}.$$

$$\mathrm{MQVISL}_{3\mathrm{PN}} = \frac{(-1+d)^2(2+d)\hat{R}_a V}{(-2+d)^2 d(4+d)} - \frac{(-3+d)(-1+d)^2(2+d)KV_a}{(-2+d)^3 d(4+d)} + \frac{(-1+d)^3(2+d)V^2V^a}{4(-2+d)^3 d(4+d)}$$
$$- \frac{(-1+d)(2+d)V^b\hat{W}_{ab}}{(-2+d)d(4+d)} + \frac{(-1+d)(2+d)V_a\hat{W}^b{}_b}{(-2+d)d(4+d)}.$$

$$\mathrm{MQVISL}_{4\mathrm{PN}} =$$

$$
\begin{aligned}
&-\frac{2(-3+d)(-1+d)^2(2+d)K\hat{R}_a}{(-2+d)^3d(4+d)}+\frac{(-1+d)^3(2+d)\hat{R}^aV^2}{(-2+d)^3d(4+d)}-\frac{(-3+d)(-1+d)^3(2+d)KVV^a}{(-2+d)^4d(4+d)}\\
&+\frac{(-1+d)(2+d)V^aV_bV^b}{(-2+d)^2(4+d)}-\frac{2(-1+d)(2+d)\hat{R}^b\hat{W}_{ab}}{(-2+d)d(4+d)}-\frac{(-1+d)^2(2+d)VV_b\hat{W}^{ab}}{(-2+d)^2d(4+d)}\\
&+\frac{2(-1+d)(2+d)\hat{R}_a\hat{W}^b{}_b}{(-2+d)d(4+d)}+\frac{(-1+d)^2(2+d)VV^a\hat{W}^b{}_b}{(-2+d)^2d(4+d)}+\frac{2(-1+d)^2(2+d)V_a\hat{X}}{(-2+d)^2d(4+d)}\\
&+\frac{2(-1+d)^2(2+d)V\hat{Y}_a}{(-2+d)^2d(4+d)}-\frac{4(-1+d)(2+d)V^b\hat{Z}_{ab}}{(-2+d)d(4+d)}+\frac{4(-1+d)(2+d)V_a\hat{Z}^b{}_b}{(-2+d)d(4+d)}.
\end{aligned}
$$

$$
\mathrm{MQVISD}_{3\mathrm{PN}}=\frac{2(-1+d)^2(2+d)\Psi^{\partial_bV}_{iji}\partial_i\partial_a\hat{R}_b}{(-2+d)^2d(4+d)}-\frac{2(-1+d)^2(2+d)\partial_a\Psi^{\partial_bV}_{iji}\partial^i\hat{R}^b}{(-2+d)^2d(4+d)}.
$$

$$
\mathrm{MQVISD}_{4\mathrm{PN}}=\frac{4(-1+d)^2(2+d)\Psi^{\partial_bV}_{iji}\partial_i\partial_a\hat{Y}_b}{(-2+d)^2d(4+d)}-\frac{4(-1+d)^2(2+d)\partial_a\Psi^{\partial_bV}_{iji}\partial^i\hat{Y}^b}{(-2+d)^2d(4+d)}.
$$

MQVII non-compact terms

$$
\begin{aligned}
\mathrm{MQVIINC}_{3\mathrm{PN}}=&-\frac{(-1+d)^2(2+d)r^2\hat{x}_{ija}\partial_tV\partial_aV}{8(-2+d)^3(4+d)^2}-\frac{(-1+d)^2(2+d)r^2\hat{x}_{ija}\partial_aV_b\partial^bV}{2(-2+d)^2d(4+d)^2}\\
&+\frac{(-1+d)^2(2+d)r^2\hat{x}_{ija}\partial_bV_a\partial^bV}{2(-2+d)^2d(4+d)^2}.
\end{aligned}
$$

$$
\begin{aligned}
&\mathrm{MQVIINC}_{4\mathrm{PN}}=\\
&-\frac{(-1+d)^2(2+d)r^2\hat{x}_{ija}\partial_tV\partial_tV_a}{2(-2+d)^2d(4+d)^2}+\frac{2(-1+d)(2+d)r^2V^a\hat{x}_{ijb}\partial_t\partial_aV_b}{(-2+d)d(4+d)^2}\\
&+\frac{(-1+d)^2(2+d)r^2V\hat{x}_{ija}\partial_t^2V_a}{2(-2+d)^2d(4+d)^2}+\frac{(-3+d)(-1+d)^2(2+d)r^2\hat{x}_{ija}\partial_tV\partial_aK}{4(-2+d)^4(4+d)^2}\\
&+\frac{(-3+d)(-1+d)^2(2+d)r^2\hat{x}_{ija}\partial_tK\partial_aV}{4(-2+d)^4(4+d)^2}-\frac{(-1+d)^3(2+d)r^2V\hat{x}_{ija}\partial_tV\partial_aV}{4(-2+d)^4(4+d)^2}\\
&-\frac{(-1+d)^2(2+d)r^2\hat{x}_{ija}\partial_a\hat{R}^b\partial_bV}{(-2+d)^2d(4+d)^2}-\frac{(-1+d)^2(2+d)r^2V^a\hat{x}_{ijb}\partial_aV\partial_bV}{2(-2+d)^3d(4+d)^2}\\
&+\frac{(-3+d)(-1+d)^2(2+d)r^2\hat{x}_{ija}\partial_aV_b\partial^bK}{(-2+d)^3d(4+d)^2}-\frac{(-3+d)(-1+d)^2(2+d)r^2\hat{x}_{ija}\partial_bV_a\partial^bK}{(-2+d)^3d(4+d)^2}\\
&+\frac{(-1+d)^2(2+d)r^2\hat{x}_{ija}\partial_bV\partial^b\hat{R}_a}{(-2+d)^2d(4+d)^2}-\frac{(-1+d)^2(2+d)r^2\hat{x}_{ija}\partial_t\hat{W}_{ab}\partial^bV}{2(-2+d)^2d(4+d)^2}\\
&-\frac{(-1+d)^3(2+d)r^2V\hat{x}_{ija}\partial_aV_b\partial^bV}{2(-2+d)^3d(4+d)^2}+\frac{(-1+d)^2(2+d)r^2V^a\hat{x}_{ija}\partial_bV\partial^bV}{4(-2+d)^3(4+d)^2}\\
&+\frac{(-1+d)^3(2+d)r^2V\hat{x}_{ija}\partial_bV_a\partial^bV}{2(-2+d)^3d(4+d)^2}+\frac{(-1+d)(2+d)r^2\hat{x}_{ija}\partial_b\hat{W}^i{}_i\partial^bV_a}{(-2+d)d(4+d)^2}\\
&+\frac{(-1+d)(2+d)r^2\hat{W}^{bi}\hat{x}_{ija}\partial_i\partial_bV_a}{(-2+d)d(4+d)^2}+\frac{(-1+d)(2+d)r^2\hat{x}_{ija}\partial_a\hat{W}_{bi}\partial^iV^b}{(-2+d)d(4+d)^2}\\
&-\frac{(-1+d)(2+d)r^2\hat{x}_{ija}\partial_b\hat{W}_{ai}\partial^iV^b}{(-2+d)d(4+d)^2}-\frac{(-1+d)(2+d)r^2\hat{x}_{ija}\partial_i\hat{W}_{ab}\partial^iV^b}{(-2+d)d(4+d)^2}.
\end{aligned}
$$

MQVII compact terms

$$
\mathrm{MQVIIC}_{2\mathrm{PN}}=-\frac{(-1+d)(2+d)r^2\hat{x}_{ija}\sigma_a}{(-2+d)d(4+d)^2}.
$$

$$\mathrm{MQVIIC}_{3\mathrm{PN}} = -\frac{4(-1+d)(2+d)r^2V\hat{x}_{ija}\sigma_a}{(-2+d)^2d(4+d)^2}.$$

$$\mathrm{MQVIIC}_{4\mathrm{PN}} = \frac{8(-3+d)(-1+d)(2+d)Kr^2\hat{x}_{ija}\sigma_a}{(-2+d)^3d(4+d)^2} - \frac{8(-1+d)(2+d)r^2V^2\hat{x}_{ija}\sigma_a}{(-2+d)^3d(4+d)^2} - \frac{2(-1+d)(2+d)r^2\hat{W}^b{}_b\hat{x}_{ija}\sigma_a}{(-2+d)d(4+d)^2}.$$

MQVIII non-compact terms

$$\mathrm{MQVIIINC}_{4\mathrm{PN}} = -\frac{(-1+d)^2(2+d)r^4\hat{x}_{ija}\partial_tV\partial_aV}{32(-2+d)^3(4+d)^2(6+d)} - \frac{(-1+d)^2(2+d)r^4\hat{x}_{ija}\partial_aV_b\partial^bV}{8(-2+d)^2d(4+d)^2(6+d)} + \frac{(-1+d)^2(2+d)r^4\hat{x}_{ija}\partial_bV_a\partial^bV}{8(-2+d)^2d(4+d)^2(6+d)}.$$

MQVIII compact terms

$$\mathrm{MQVIIIC}_{3\mathrm{PN}} = -\frac{(-1+d)(2+d)r^4\hat{x}_{ija}\sigma_a}{4(-2+d)d(4+d)^2(6+d)}.$$

$$\mathrm{MQVIIIC}_{4\mathrm{PN}} = -\frac{(-1+d)(2+d)r^4V\hat{x}_{ija}\sigma_a}{(-2+d)^2d(4+d)^2(6+d)}.$$

MQVIV compact terms

$$\mathrm{MQVIVC}_{4\mathrm{PN}} = -\frac{(-1+d)(2+d)r^6\hat{x}_{ija}\sigma_a}{24(-2+d)d(4+d)^2(6+d)(8+d)}.$$

MQTI non-compact terms

$$\mathrm{MQTINC}_{2\mathrm{PN}} = \frac{(-1+d)^2(2+d)\hat{x}_{ijab}\partial^aV\partial^bV}{8(-2+d)^2d(1+d)(6+d)}.$$

$$\mathrm{MQTINC}_{3\mathrm{PN}} = \frac{(-1+d)^2(2+d)\hat{x}_{ijab}\partial_tV^b\partial^aV}{(-2+d)^2d(1+d)(6+d)} - \frac{(-3+d)(-1+d)^2(2+d)\hat{x}_{ijab}\partial^aK\partial^bV}{2(-2+d)^3d(1+d)(6+d)} - \frac{(-1+d)(2+d)\hat{x}_{ijai}\partial_bV^i\partial^bV^a}{(-2+d)d(1+d)(6+d)} - \frac{(-1+d)(2+d)\hat{x}_{ijbi}\partial^bV^a\partial^iV_a}{(-2+d)d(1+d)(6+d)} + \frac{2(-1+d)(2+d)\hat{x}_{ijai}\partial^bV^a\partial^iV_b}{(-2+d)d(1+d)(6+d)}.$$

$$\mathrm{MQTINC}_{4\mathrm{PN}} = \frac{2(-1+d)(2+d)\hat{x}_{ijab}\partial_tV^a\partial_tV^b}{(-2+d)d(1+d)(6+d)} - \frac{2(-1+d)(2+d)V^a\hat{x}_{ijbi}\partial_t\partial_a\hat{W}_{bi}}{(-2+d)d(1+d)(6+d)}$$

$$
\begin{aligned}
&-\frac{(-1+d)^2(2+d)V\hat{x}_{ijab}\partial_t^2\hat{W}_{ab}}{2(-2+d)^2d(1+d)(6+d)}-\frac{2(-3+d)(-1+d)^2(2+d)\hat{x}_{ijab}\partial_tV^b\partial^aK}{(-2+d)^3d(1+d)(6+d)}\\
&+\frac{2(-1+d)^2(2+d)\hat{x}_{ijab}\partial_t\hat{R}^b\partial^aV}{(-2+d)^2d(1+d)(6+d)}+\frac{(-1+d)^3(2+d)V\hat{x}_{ijab}\partial_tV^b\partial^aV}{(-2+d)^3d(1+d)(6+d)}\\
&+\frac{(-1+d)^2(2+d)\hat{W}^{bi}\hat{x}_{ijbi}\partial_aV\partial^aV}{4(-2+d)^2d(1+d)(6+d)}+\frac{(-1+d)(2+d)\hat{x}_{ijab}\partial_a\hat{W}^{ij}\partial_b\hat{W}_{ij}}{2(-2+d)d(1+d)(6+d)}\\
&-\frac{(-1+d)(2+d)\hat{W}^{ab}\hat{x}_{ijij}\partial_b\partial_a\hat{W}_{ij}}{(-2+d)d(1+d)(6+d)}+\frac{(-3+d)^2(-1+d)^2(2+d)\hat{x}_{ijab}\partial^aK\partial^bK}{2(-2+d)^4d(1+d)(6+d)}\\
&+\frac{4(-1+d)(2+d)\hat{x}_{ijbi}\partial_aV^i\partial^b\hat{R}^a}{(-2+d)d(1+d)(6+d)}-\frac{4(-1+d)(2+d)\hat{x}_{ijai}\partial_bV^i\partial^b\hat{R}^a}{(-2+d)d(1+d)(6+d)}\\
&+\frac{(-1+d)^2(2+d)V^a\hat{x}_{ijab}\partial_tV\partial^bV}{(-2+d)^3d(1+d)(6+d)}+\frac{2(-1+d)^2(2+d)V^a\hat{x}_{ijbi}\partial_aV^i\partial^bV}{(-2+d)^2d(1+d)(6+d)}\\
&+\frac{(-1+d)^2(2+d)\hat{W}^i{}_i\hat{x}_{ijab}\partial^aV\partial^bV}{4(-2+d)^2d(1+d)(6+d)}-\frac{(-1+d)^2(2+d)\hat{W}_a{}^i\hat{x}_{ijbi}\partial^aV\partial^bV}{(-2+d)^2d(1+d)(6+d)}\\
&-\frac{2(-1+d)^2(2+d)V^a\hat{x}_{ijai}\partial_bV^i\partial^bV}{(-2+d)^2d(1+d)(6+d)}-\frac{2(-1+d)(2+d)\hat{x}_{ijbi}\partial_t\hat{W}_{ai}\partial^bV^a}{(-2+d)d(1+d)(6+d)}\\
&+\frac{2(-1+d)(2+d)\hat{x}_{ijai}\partial_t\hat{W}_{bi}\partial^bV^a}{(-2+d)d(1+d)(6+d)}+\frac{(-1+d)^2(2+d)\hat{x}_{ijab}\partial^aV\partial^b\hat{X}}{(-2+d)^2d(1+d)(6+d)}\\
&-\frac{4(-1+d)(2+d)\hat{x}_{ijbi}\partial^b\hat{R}^a\partial^iV_a}{(-2+d)d(1+d)(6+d)}+\frac{4(-1+d)(2+d)\hat{x}_{ijai}\partial^b\hat{R}^a\partial^iV_b}{(-2+d)d(1+d)(6+d)}\\
&+\frac{2(-1+d)^2(2+d)V^a\hat{x}_{ijai}\partial^bV\partial^iV_b}{(-2+d)^2d(1+d)(6+d)}-\frac{(-1+d)(2+d)\hat{x}_{ijab}\partial_i\hat{W}^j{}_j\partial^i\hat{W}_{ab}}{(-2+d)d(1+d)(6+d)}\\
&-\frac{2(-1+d)(2+d)\hat{x}_{ijab}\partial_b\hat{W}_{ij}\partial^j\hat{W}_a{}^i}{(-2+d)d(1+d)(6+d)}+\frac{(-1+d)(2+d)\hat{x}_{ijab}\partial_i\hat{W}_{bj}\partial^j\hat{W}_a{}^i}{(-2+d)d(1+d)(6+d)}\\
&+\frac{(-1+d)(2+d)\hat{x}_{ijab}\partial_j\hat{W}_{bi}\partial^j\hat{W}_a{}^i}{(-2+d)d(1+d)(6+d)}.
\end{aligned}
$$

MQTI compact terms

$$
\mathrm{MQTIC}_{\mathrm{2PN}}=\frac{(-1+d)(2+d)\hat{x}_{ijab}\sigma_{ab}}{(-2+d)d(1+d)(6+d)}.
$$

$$
\mathrm{MQTIC}_{\mathrm{3PN}}=\frac{4(-1+d)(2+d)V\hat{x}_{ijab}\sigma_{ab}}{(-2+d)^2d(1+d)(6+d)}.
$$

$$
\begin{aligned}
\mathrm{MQTIC}_{\mathrm{4PN}}=&-\frac{8(-3+d)(-1+d)(2+d)K\hat{x}_{ijab}\sigma_{ab}}{(-2+d)^3d(1+d)(6+d)}+\frac{8(-1+d)(2+d)V^2\hat{x}_{ijab}\sigma_{ab}}{(-2+d)^3d(1+d)(6+d)}\\
&+\frac{2(-1+d)(2+d)\hat{W}^a{}_a\hat{x}_{ijbi}\sigma_{bi}}{(-2+d)d(1+d)(6+d)}.
\end{aligned}
$$

MQTII non-compact terms

$$
\mathrm{MQTIINC}_{\mathrm{3PN}}=\frac{(-1+d)^2(2+d)r^2\hat{x}_{ijab}\partial^aV\partial^bV}{16(-2+d)^2d(1+d)(4+d)(6+d)}.
$$

$$
\mathrm{MQTIINC}_{\mathrm{4PN}}=\frac{(-1+d)^2(2+d)r^2\hat{x}_{ijab}\partial_tV^b\partial^aV}{2(-2+d)^2d(1+d)(4+d)(6+d)}-\frac{(-3+d)(-1+d)^2(2+d)r^2\hat{x}_{ijab}\partial^aK\partial^bV}{4(-2+d)^3d(1+d)(4+d)(6+d)}
$$

$$- \frac{(-1+d)(2+d)r^2\hat{x}_{ijai}\partial_b V^i \partial^b V^a}{2(-2+d)d(1+d)(4+d)(6+d)} - \frac{(-1+d)(2+d)r^2\hat{x}_{ijbi}\partial^b V^a \partial^i V_a}{2(-2+d)d(1+d)(4+d)(6+d)}$$
$$+ \frac{(-1+d)(2+d)r^2\hat{x}_{ijai}\partial^b V^a \partial^i V_b}{(-2+d)d(1+d)(4+d)(6+d)}.$$

MQTII compact terms

$$\mathrm{MQTIIC}_{3\mathrm{PN}} = \frac{(-1+d)(2+d)r^2\hat{x}_{ijab}\sigma_{ab}}{2(-2+d)d(1+d)(4+d)(6+d)}.$$

$$\mathrm{MQTIIC}_{4\mathrm{PN}} = \frac{2(-1+d)(2+d)r^2 V\hat{x}_{ijab}\sigma_{ab}}{(-2+d)^2 d(1+d)(4+d)(6+d)}.$$

MQTIII non-compact terms

$$\mathrm{MQTIIINC}_{4\mathrm{PN}} = \frac{(-1+d)^2(2+d)r^4\hat{x}_{ijab}\partial^a V \partial^b V}{64(-2+d)^2 d(1+d)(4+d)(6+d)^2}.$$

MQTIII compact terms

$$\mathrm{MQTIIIC}_{4\mathrm{PN}} = \frac{(-1+d)(2+d)r^4\hat{x}_{ijab}\sigma_{ab}}{8(-2+d)d(1+d)(4+d)(6+d)^2}.$$

Bibliography

[1] T. Marchand, L. Blanchet & G. Faye; «Gravitational-wave tail effects to quartic non-linear order»; Class. Quant. Grav. **33**, p. 244 003 (2016)arXiv:1607.07601[gr-qc]. ix, 44, 50, 62

[2] T. Marchand, L. Bernard, L. Blanchet & G. Faye; «Ambiguity-Free Completion of the Equations of Motion of Compact Binary Systems at the Fourth Post-Newtonian Order»; Phys. Rev. **D97**, p. 044 023 (2018). 1707.09289. ix, 32, 85, 102, 151

[3] L. Bernard, L. Blanchet, G. Faye & T. Marchand; «Center-of-Mass Equations of Motion and Conserved Integrals of Compact Binary Systems at the Fourth Post-Newtonian Order»; Phys. Rev. **D97**, p. 044 037 (2018). 1711.00283. ix, 103, 120, 143, 157

[4] T. Marchand, G. Faye & L. Blanchet; «Hadamard regularization of the mass quadrupole moment of compact binary systems at the fourth post-Newtonian order, in prep»; . ix

[5] A. Einstein; «The Foundation of the General Theory of Relativity»; Annalen der Physik (1916). 1

[6] A. Einstein; «Approximative Integration of the Field Equations of Gravitation»; Sitzunber. Preuss. Akad. Wiss. Berlin (Math. Phys.) p. 688–696 (1916). 1

[7] A. Einstein; «On Gravitational Waves»; Sitzunber. Preuss. Akad. Wiss. Berlin (Math. Phys.) p. 154–167 (1918). 1

[8] A. S. Eddington; «The propagation of gravitational waves»; Proc. Royal. Soc. Lond. **A102**, p. 268–282 (1922). 1

[9] D. Kennefick; «Controversies in the History of the Radiation Reaction problem in General Relativity»; (1997). 1

[10] H. Bondi; «Plane gravitational waves in general relativity»; Nature **179**, p. 1072–1073 (1957). 1

[11] F. P. H. Bondi & I. Robinson; «Gravitational waves in general relativity 3. Exact plane waves»; Proc. Royal. Soc. Lond. **A251**, p. 519–533 (1959). 1

[12] F. Pirani; «Invariant formuation of gravitational radiation theory»; Phys. Rev. **105**, p. 1089–1099 (1957). 1

[13] H. Lorentz & J. Droste; *The motion of a system of bodies under the influence of their mutual attraction, according to Einstein's theory*; p. 330 (Nijhoff, The Hague) (1937); versl. K. Akad. Wet. Amsterdam **26**, 392 and 649 (1917). 1, 31

[14] S. Chandrasekhar & F. Esposito; «The 5/2-post-Newtonian equations of hydrodynamics and radiation reaction in general relativity»; Astrophys. J. **160**, p. 153–179 (1970). 2

[15] W. Burke & K. Thorne; «Gravitational Radiation Damping»; dans M. Carmeli, S. Fickler & L. Witten (rédacteurs), «Relativity», p. 209–228 (Plenum Press, New York and London) (1970). 2

[16] W. Burke; «Gravitational radiation damping of slowly moving systems calculated using matched asymptotic expansions»; J. Math. Phys. **12**, p. 401 (1971). 2

[17] L. Blanchet; «Gravitational radiation from post-Newtonian sources and inspiralling compact binaries»; Living Rev. Rel. **17**, p. 2 (2014)arXiv:1310.1528[gr-qc]. 2, 92, 123

[18] T. Damour & N. Deruelle; «Radiation reaction and angular momentum loss in small angle gravitational scattering»; Phys. Lett. A **87**, p. 81 (1981). 2

[19] R. Hulse & J. Taylor; «Discovery of a pulsar in a binary system»; Astrophys. J. **195**, p. L51 (1975). 2, 11

[20] M. Maggiore; *Gravitational waves. Volume 1: theory and experiments* (Oxford University Press) (2008). 2, 7

[21] L. Blanchet & B. R. Iyer; «Third post-Newtonian dynamics of compact binaries: Equations of motion in the center-of-mass frame»; Class. Quant. Grav. **20**, p. 755 (2003)gr-qc/0209089. 11

[22] J. M. Weisberg, D. J. Nice & J. H. Taylor; «Timing Measurements of the Relativistic Binary Pulsar PSR B1913+16»; Astrophys. J. **722**, p. 1030–1034 (2010). 1011.0718. 12, 13

[23] J. Weber; «Evidence for Discovery of Gravitational Radiation»; Phys. Rev. Lett. **22**, p. 1320–1324 (1969). https://link.aps.org/doi/10.1103/PhysRevLett.22.1320. 15

[24] J. Weber; «Gravitational-Wave-Detector Events»; Phys. Rev. Lett. **20**, p. 1307–1308 (1968). https://link.aps.org/doi/10.1103/PhysRevLett.20.1307. 15

[25] J. Aasi *et al.*; «Advanced LIGO»; Class. Quant. Grav. **32**, p. 074 001 (2015). 1411.4547. 16

[26] B. Abbott *et al.*; «Observation of Gravitational Waves from a Binary Black Hole Merger»; Phys. Rev. Lett. **116**, p. 061 102 (2016)arXiv:1602.03837[gr-qc]. 16, 19, 25

[27] B. P. Abbott *et al.*; «GW150914: The Advanced LIGO Detectors in the Era of First Discoveries»; Phys. Rev. Lett. **116**, p. 131 103 (2016). 1602.03838. 17

[28] K. Somiya; «Detector configuration of KAGRA: The Japanese cryogenic gravitational-wave detector»; Class. Quant. Grav. **29**, p. 124 007 (2012). 1111.7185. 17

[29] P. Amaro-Seoane *et al.* 1702.00786. 17

[30] M. Armano *et al.*; «Sub-Femto- g Free Fall for Space-Based Gravitational Wave Observatories: LISA Pathfinder Results»; Phys. Rev. Lett. **116**, p. 231 101 (2016). 17

[31] J. A. Faber & F. A. Rasio; «Binary Neutron Star Mergers»; Living Rev. Rel. **15**, p. 8 (2012). 1204.3858. 20

[32] M. Shibata & K. Taniguchi; «Coalescence of Black Hole-Neutron Star Binaries»; Living Rev. Rel. **14**, p. 6 (2011). 20

[33] J. Kormendy & D. Richstone; «Inward bound: The Search for supermassive black holes in galactic nuclei»; Ann. Rev. Astron. Astrophys. **33**, p. 581 (1995). 20

[34] M. C. Begelman, R. D. Blandford & M. J. Rees; «Massive black hole binaries in active galactic nuclei»; Nature **287**, p. 307–309 (1980). 20

[35] J. R. Gair, S. Babak, A. Sesana, P. Amaro-Seoane, E. Barausse, C. P. L. Berry, E. Berti & C. Sopuerta; «Prospects for observing extreme-mass-ratio inspirals with LISA»; J. Phys. Conf. Ser. **840**, p. 012 021 (2017). 1704.00009. 21

[36] C. D. Ott; «The Gravitational Wave Signature of Core-Collapse Supernovae»; Class. Quant. Grav. **26**, p. 063 001 (2009). 0809.0695. 21

[37] B. P. Abbott *et al.*; «First narrow-band search for continuous gravitational waves from known pulsars in advanced detector data»; Phys. Rev. **D96**, p. 122 006 (2017). 1710.02327. 21

[38] F. Pretorius; «Evolution of binary black hole spacetimes»; Phys. Rev. Lett. **95**, p. 121 101 (2005)gr-qc/0507014. 23

[39] M. Campanelli, C. O. Lousto, P. Marronetti & Y. Zlochower; «Accurate evolutions of orbiting black-hole binaries without excision»; Phys. Rev. Lett. **96**, p. 111 101 (2006). gr-qc/0511048. 23

[40] J. G. Baker, J. Centrella, D.-I. Choi, M. Koppitz & J. van Meter; «Gravitational wave extraction from an inspiraling configuration of merging black holes»; Phys. Rev. Lett. **96**, p. 111 102 (2006). gr-qc/0511103. 23

[41] J. Healy, C. O. Lousto, Y. Zlochower & M. Campanelli; «The RIT binary black hole simulations catalog»; Class. Quant. Grav. **34**, p. 224 001 (2017). 1703.03423. 23

[42] A. Buonanno & T. Damour; «Effective one-body approach to general relativistic two-body dynamics»; Phys. Rev. D **59**, p. 084 006 (1999)gr-qc/9811091. 24

[43] B. P. Abbott *et al.*; «Localization and broadband follow-up of the gravitational-wave transient GW150914»; Astrophys. J. **826**, p. L13 (2016). 1602.08492. 25

[44] B. Abbott *et al.*; «GW170817: Observation of Gravitational Waves from a Binary Neutron Star Inspiral»; Phys. Rev. Lett. **119**, p. 161 101 (2017)arXiv:1710.05832[gr-qc]. 26, 27

[45] L. Blanchet, G. Faye, B. R. Iyer & S. Sinha; «The third post-Newtonian gravitational wave polarisations and associated spherical harmonic modes for inspiralling compact binaries in quasi-circular orbits»; Class. Quant. Grav. **25**, p. 165 003 (2008)arXiv:0802.1249[gr-qc]. 30, 67, 68, 144

[46] A. Einstein, L. Infeld & B. Hoffmann; «The Gravitational Equations and the Problem of Motion»; Ann. Math. **39**, p. 65–100 (1938). 31

[47] V. Fock; «On motion of finite masses in general relativity»; J. Phys. (Moscow) **1**, p. 81–116 (1939). 31

[48] T. Ohta, H. Okamura, T. Kimura & K. Hiida; «Physically acceptable solution of Einstein's equation for many-body system»; Prog. Theor. Phys. **50**, p. 492–514 (1973). 31

[49] H. Okamura, T. Ohta, T. Kimura & K. Hiida; «Perturbation calculation of gravitational potentials»; Prog. Theor. Phys. **50**, p. 2066–2079 (1973). 31

[50] T. Ohta, H. Okamura, T. Kimura & K. Hiida; «Higher-order gravitational potential for many-body system»; Prog. Theor. Phys. **51**, p. 1220–1238 (1974). 31

[51] T. Ohta, H. Okamura, T. Kimura & K. Hiida; «Coordinate Condition and Higher Order Gravitational Potential in Canocical Formalism»; Prog. Theor. Phys. **51**, p. 1598–1612 (1974). 31

[52] T. Damour; «Problème des deux corps et freinage de rayonnement en relativité générale»; C. R. Acad. Sc. Paris **294**, p. 1355 (1982). 31

[53] T. Damour; «Gravitational radiation and the motion of compact bodies»; dans N. Deruelle & T. Piran (rédacteurs), «Gravitational Radiation», p. 59–144 (North-Holland Company, Amsterdam) (1983). 31

[54] T. Damour & N. Deruelle; «Lagrangien généralisé du système de deux masses ponctuelles, à l'approximation post-post-newtonienne de la relativité générale»; C. R. Acad. Sc. Paris **293**, p. 537 (1981). 31

[55] T. Damour & N. Deruelle; «Radiation reaction and angular momentum loss in small angle gravitational scattering»; Phys. Lett. A **87**, p. 81 (1981). 31

[56] N. Deruelle; *Sur les équations du mouvement et le rayonnement gravitationnel d'un système binaire en Relativité Générale*; Thèse de doctorat; Université Pierre et Marie Curie; Paris (1982). 31

[57] S. Kopeikin; «The equations of motion of extended bodies in general-relativity with conservative corrections and radiation damping taken into account»; Astron. Zh. **62**, p. 889–904 (1985). 31

[58] L. Grishchuk & S. Kopeikin; «Equations of motion for isolated bodies with relativistic corrections including the radiation reaction force»; dans J. Kovalevsky & V. Brumberg (rédacteurs), «Relativity in Celestial Mechanics and Astrometry», p. 19–33 (Reidel, Dordrecht) (1986). 31

[59] L. Blanchet, G. Faye & B. Ponsot; «Gravitational field and equations of motion of compact binaries to 5/2 post-Newtonian order»; Phys. Rev. D **58**, p. 124 002 (1998)gr-qc/9804079. 31

[60] Y. Itoh, T. Futamase & H. Asada; «Equation of motion for relativistic compact binaries with the strong field point particle limit: Formulation, the first post-Newtonian order, and multipole terms»; Phys. Rev. D **62**, p. 064 002 (2000)gr-qc/9910052. 32

[61] Y. Itoh, T. Futamase & H. Asada; «Equation of motion for relativistic compact binaries with the strong field point particle limit: The second and half post-Newtonian order»; Phys. Rev. D **63**, p. 064 038 (2001)gr-qc/0101114. 32

[62] M. Pati & C. Will; «Post-Newtonian gravitational radiation and equations of motion via direct integration of the relaxed Einstein equations. II. Two-body equations of motion to second post-Newtonian order, and radiation-reaction to 3.5 post-Newtonian order»; Phys. Rev. D **65**, p. 104 008 (2002)gr-qc/0201001. 32, 122, 123

[63] P. Jaranowski & G. Schäfer; «Radiative 3.5 post-Newtonian ADM Hamiltonian for many body point - mass systems»; Phys. Rev. D **55**, p. 4712–4722 (1997). 32

[64] P. Jaranowski & G. Schäfer; «Third post-Newtonian higher order ADM Hamilton dynamics for two-body point-mass systems»; Phys. Rev. D **57**, p. 7274–7291 (1998)gr-qc/9712075. 32

[65] P. Jaranowski & G. Schäfer; «Binary black-hole problem at the third post-Newtonian approximation in the orbital motion: Static part»; Phys. Rev. D **60**, p. 124 003 (1999)gr-qc/9906092. 32

[66] P. Jaranowski & G. Schäfer; «The binary black-hole dynamics at the third post-Newtonian order in the orbital motion»; Ann. Phys. (Berlin) **9**, p. 378–383 (2000)gr-qc/0003054. 32

[67] T. Damour, P. Jaranowski & G. Schäfer; «Dynamical invariants for general relativistic two-body systems at the third post-Newtonian approximation»; Phys. Rev. D **62**, p. 044 024 (2000)gr-qc/9912092. 32

[68] T. Damour, P. Jaranowski & G. Schäfer; «On the determination of the last stable orbit for circular general relativistic binaries at the third post-Newtonian approximation»; Phys. Rev. D **62**, p. 084 011 (2000)gr-qc/0005034. 32

[69] T. Damour, P. Jaranowski & G. Schäfer; «Dimensional regularization of the gravitational interaction of point masses»; Phys. Lett. B **513**, p. 147–155 (2001)gr-qc/0105038. 32

[70] T. Damour, P. Jaranowski & G. Schäfer; «Equivalence between the ADM-Hamiltonian and the harmonic-coordinates approaches to the third post-Newtonian dynamics of compact binaries»; Phys. Rev. D **63**, p. 044 021 (2001)Erratum Phys. Rev. D **66**, 029901(E) (2002); gr-qc/0010040. 32

[71] T. Damour, P. Jaranowski & G. Schäfer; «Poincaré invariance in the ADM Hamiltonian approach to the general relativistic two-body problem»; Phys. Rev. D **62**, p. 021 501(R) (2000)Erratum Phys. Rev. D **63**, 029903(E) (2000); gr-qc/0003051. 32

[72] L. Blanchet & G. Faye; «General relativistic dynamics of compact binaries at the third post-Newtonian order»; Phys. Rev. D **63**, p. 062 005 (2001)gr-qc/0007051. 32, 91

[73] L. Blanchet & G. Faye; «Lorentzian regularization and the problem of point-like particles in general relativity»; J. Math. Phys. **42**, p. 4391–4418 (2001)gr-qc/0006100. 32, 91

[74] L. Blanchet & G. Faye; «Equations of motion of point-particle binaries at the third post-Newtonian order»; Phys. Lett. A **271**, p. 58 (2000)gr-qc/0004009. 32, 91, 137, 138, 139

[75] L. Blanchet & G. Faye; «Hadamard regularization»; J. Math. Phys. **41**, p. 7675–7714 (2000)gr-qc/0004008. 32, 91, 141

[76] V. de Andrade, L. Blanchet & G. Faye; «Third post-Newtonian dynamics of compact binaries: Noetherian conserved quantities and equivalence between the harmonic-coordinate and ADM-Hamiltonian formalisms»; Class. Quant. Grav. **18**, p. 753–778 (2001)gr-qc/0011063. 32

[77] L. Blanchet, G. Faye, B. R. Iyer & B. Joguet; «Gravitational-wave inspiral of compact binary systems to 7/2 post-Newtonian order»; Phys. Rev. D **65**, p. 061 501(R) (2002)Erratum *Phys. Rev. D*, 71:129902(E), 2005; gr-qc/0105099. 32, 67

[78] Y. Itoh & T. Futamase; «New derivation of a third post-Newtonian equation of motion for relativistic compact binaries without ambiguity»; Phys. Rev. D **68**, p. 121 501(R) (2003)gr-qc/0310028. 32

[79] Y. Itoh; «Equation of motion for relativistic compact binaries with the strong field point particle limit: Third post-Newtonian order»; Phys. Rev. D **69**, p. 064 018 (2004)gr-qc/0310029. 32

[80] Y. Itoh; «Third-and-a-half order post-Newtonian equations of motion for relativistic compact binaries using the strong field point particle limit»; Phys. Rev. D **80**, p. 024 003 (2009)arXiv:0911.4232[gr-qc]. 32, 122, 123

[81] S. Foffa & R. Sturani; «Effective field theory calculation of conservative binary dynamics at third post-Newtonian order»; Phys. Rev. D **84**, p. 044 031 (2011)arXiv:1104.1122[gr-qc]. 32, 33

[82] B. Iyer & C. Will; «Post-Newtonian gravitational-radiation reaction for two-body systems»; Phys. Rev. Lett. **70**, p. 113–116 (1993). 32, 122, 123

[83] B. Iyer & C. Will; «Post-Newtonian gravitational radiation reaction for two-body systems: Nonspinning bodies»; Phys. Rev. D **52**, p. 6882–6893 (1995). 32, 122, 123

[84] C. Will & A. Wiseman; «Gravitational radiation from compact binary systems: Gravitational waveforms and energy loss to second post-Newtonian order»; Phys. Rev. D **54**, p. 4813–4848 (1996)gr-qc/9608012. 32

[85] C. Will; «Generation of Post-Newtonian Gravitational Radiation via Direct Integration of the Relaxed Einstein Equations»; Prog. Theor. Phys. Suppl. **136**, p. 158–167 (1999). 32

[86] M. Pati & C. Will; «Post-Newtonian gravitational radiation and equations of motion via direct integration of the relaxed Einstein equations: Foundations»; Phys. Rev. D **62**, p. 124 015 (2000)gr-qc/0007087. 32

[87] P. Jaranowski & G. Schäfer; «Towards the fourth post-Newtonian Hamiltonian for two-point-mass systems»; Phys. Rev. D **86**, p. 061 503(R) (2012)arXiv:1207.5448[gr-qc]. 32

[88] P. Jaranowski & G. Schäfer; «Dimensional regularization of local singularities in the 4th post-Newtonian two-point-mass Hamiltonian»; Phys. Rev. D **87**, p. 081 503(R) (2013)arXiv:1303.3225[gr-qc]. 32

[89] P. Jaranowski & G. Schäfer; «Derivation of the local-in-time fourth post-Newtonian ADM Hamiltonian for spinless compact binaries»; Phys. Rev. D **92**, p. 124 043 (2015)arXiv:1508.01016[gr-qc]. 32

[90] T. Damour, P. Jaranowski & G. Schäfer; «Non-local-in-time action for the fourth post-Newtonian conservative dynamics of two-body systems»; Phys. Rev. D **89**, p. 064 058 (2014)arXiv:1401.4548[gr-qc]. 32, 85, 97, 102

[91] T. Damour, P. Jaranowski & G. Schäfer; «On the conservative dynamics of two-body systems at the fourth post-Newtonian approximation of general relativity»; Phys. Rev. D **93**, p. 084 014 (2016)arXiv:1601.01283[gr-qc]. 32, 102

[92] L. Bernard, L. Blanchet, A. Bohé, G. Faye & S. Marsat; «Fokker action of non-spinning compact binaries at the fourth post-Newtonian approximation»; Phys. Rev. D **93**, p. 084 037 (2016)arXiv:1512.02876[gr-qc]. 32, 85, 86, 87, 88, 97, 143, 151, 157

[93] L. Bernard, L. Blanchet, A. Bohé, G. Faye & S. Marsat; «Energy and periastron advance of compact binaries on circular orbits at the fourth post-Newtonian order»; Phys. Rev. D **95**, p. 044 026 (2017)arXiv:1610.07934[gr-qc]. 32, 85, 97, 119, 151, 157

[94] L. Bernard, L. Blanchet, A. Bohé, G. Faye & S. Marsat; «Dimensional regularization of the IR divergences in the Fokker action of point-particle binaries at the fourth post-Newtonian order»; Phys. Rev. **D96**, p. 104 043 (2017). 1706.08480. 32, 85, 97, 98, 99, 101, 102, 120, 121, 143, 145, 151, 157

[95] S. Foffa, P. Mastrolia, R. Sturani & C. Sturm; «Effective field theory approach to the gravitational two-body dynamics at fourth post-Newtonian order and quintic in the Newton constant»; Phys. Rev. D **95**, p. 104 009 (2017)arXiv:1612.00482[gr-qc]. 33

[96] S. Foffa & R. Sturani; «Tail terms in gravitational radiation reaction via effective field theory»; Phys. Rev. D **87**, p. 044 056 (2013)arXiv:1111.5488[gr-qc]. 33

[97] S. Foffa & R. Sturani; «The dynamics of the gravitational two-body problem in the post-Newtonian approximation at quadratic order in the Newton's constant»; Phys. Rev. D **87**, p. 064 011 (2013)arXiv:1206.7087[gr-qc]. 33

[98] C. R. Galley, A. K. Leibovich, R. A. Porto & A. Ross; «Tail effect in gravitational radiation reaction: Time nonlocality and renormalization group evolution»; Phys. Rev. D **93**, p. 124 010 (2016)1511.07379. 33, 102

[99] W. Tulczyjew; «On the energy-momentum tensor density for simple pole particles»; Bull. Acad. Polon. Sci. **5**, p. 279 (1957). 33

[100] W. Tulczyjew; «Motion of multipole particles in general relativity theory»; Acta Phys. Polon. **18**, p. 37 (1959). 33

[101] M. Mathisson; «Republication of: New mechanics of material systems»; General Relativity and Gravitation **42**, p. 1011–1048 (2010). 33

[102] A. Papapetrou; «Spinning test-particles in general relativity. I»; Proc. R. Soc. London A **209**, p. 248 (1951). 33

[103] W. G. Dixon; «Extended bodies in general relativity: their description and motion»; dans J. Ehlers (rédacteur), «Isolated Gravitating Systems in General Relativity», p. 156–219 (1979). 33

[104] T. Damour, P. Jaranowski & G. Schäfer; «Hamiltonian of two spinning compact bodies with next-to-leading order gravitational spin-orbit coupling»; Phys. Rev. D **77**, p. 064 032 (2008). 34

[105] J. Hartung & J. Steinhoff; «Next-to-next-to-leading order post-Newtonian spin-orbit Hamiltonian for self-gravitating binaries»; Annalen der Physik **523**, p. 783–790 (2011)arXiv:1104.3079[gr-qc]. 34

[106] J. Hartung, J. Steinhoff & G. Schäfer; «Next-to-next-to-leading order post-Newtonian linear-in-spin binary Hamiltonians»; Annalen der Physik **525**, p. 359 (2013). 1302.6723. 34

[107] G. Faye, L. Blanchet & A. Buonanno; «Higher-order spin effects in the dynamics of compact binaries I. Equations of motion»; Phys. Rev. D **74**, p. 104 033 (2006)gr-qc/0605139. 34

[108] S. Marsat, A. Bohé, G. Faye & L. Blanchet; «Next-to-next-to-leading order spin-orbit effects in the equations of motion of compact binary systems»; Class. Quant. Grav. **30**, p. 055 007 (2013)arXiv:1210.4143[gr-qc]. 34, 135, 136

[109] A. Bohé, S. Marsat, G. Faye & L. Blanchet; «Next-to-next-to-leading order spin-orbit effects in the near-zone metric and precession equations of compact binary systems»; Class. Quant. Grav. **30**, p. 075 017 (2013)arXiv:1212.5520[gr-qc]. 34

[110] R. A. Porto; «Next-to-leading-order spin orbit effects in the motion of inspiralling compact binaries»; Class. Quant. Grav. **27**, p. 205 001 (2010)arXiv:1005.5730[gr-qc]. 34

[111] M. Levi; «Next-to-leading order gravitational spin-orbit coupling in an effective field theory approach»; Phys. Rev. D **82**, p. 104 004 (2010)arXiv:1006.4139[gr-qc]. 34

[112] A. Bohé, G. Faye, S. Marsat & E. Porter; «Quadratic-in-spin effects in the orbital dynamics and gravitational-wave energy flux of compact binaries at the 3PN order»; Class. Quant. Grav. **32**, p. 195 010 (2015)arXiv:1501.01529[gr-qc]. 34

[113] J. Hartung & J. Steinhoff; «Next-to-next-to-leading order post-Newtonian spin(1)-spin(2) Hamiltonian for self-gravitating binaries»; Ann. Phys. **523**, p. 919 (2011)arXiv:1107.4294[gr-qc]. 34

[114] R. A. Porto & I. Z. Rothstein; «Next to leading order spin(1)spin(1) effects in the motion of inspiralling compact binaries»; Phys. Rev. **78**, 044013 (2008). 0804.0260. 34

[115] M. Levi & J. Steinhoff; «Equivalence of ADM Hamiltonian and Effective Field Theory approaches at next-to-next-to-leading order spin1-spin2 coupling of binary inspirals»; J. Cosmo. Astropart. **1412**, p. 003 (2014). 1408.5762. 34

[116] R. A. Porto & I. Z. Rothstein; «Spin(1)Spin(2) Effects in the Motion of Inspiralling Compact Binaries at Third Order in the Post-Newtonian Expansion»; Phys. Rev. **D78**, p. 044 012 (2008). 0802.0720. 34

[117] M. Levi; «Binary dynamics from spin1-spin2 coupling at fourth post-Newtonian order»; Phys. Rev. **D85**, p. 064 043 (2012). 1107.4322. 34

[118] S. Hergt & G. Schäfer; «Higher-order-in-spin interaction Hamiltonians for binary black holes from source terms of Kerr geometry in approximate ADM coordinates»; Phys. Rev. **D77**, p. 104 001 (2008). 0712.1515. 34

[119] S. Marsat; «Cubic order spin effects in the dynamics and gravitational wave energy flux of compact object binaries»; Class. Quant. Grav. **32**, p. 085 008 (2015)arXiv:1411.4118[gr-qc]. 34

[120] R. A. Porto, A. Ross & I. Z. Rothstein; «Spin induced multipole moments for the gravitational wave flux from binary inspirals to third Post-Newtonian order»; JCAP **1103**, p. 009 (2011). 1007.1312. 34

[121] R. A. Porto, A. Ross & I. Z. Rothstein; «Spin induced multipole moments for the gravitational wave amplitude from binary inspirals to 2.5 Post-Newtonian order»; JCAP **9**, 028 (2012). 1203.2962. 34

[122] L. Blanchet, A. Buonanno & G. Faye; «Higher-order spin effects in the dynamics of compact binaries II. Radiation field»; Phys. Rev. D **74**, p. 104 034 (2006)Erratum *Phys. Rev. D*, 75:049903, 2007; gr-qc/0605140. 34

[123] A. Bohé, S. Marsat & L. Blanchet; «Next-to-next-to-leading order spin-orbit effects in the gravitational wave flux and orbital phasing of compact binaries»; Class. Quant. Grav. **30**, p. 135 009 (2013)arXiv:1303.7412[gr-qc]. 34

[124] S. Marsat, A. Bohé, L. Blanchet & A. Buonanno; «Next-to-leading tail-induced spin-orbit effects in the gravitational radiation of compact binaries»; Class. Quant. Grav. **31**, p. 025 023 (2013)arXiv:1307.6793[gr-qc]. 34

[125] A. Buonanno, G. Faye & T. Hinderer; «Spin effects on gravitational waves from inspiraling compact binaries at second post-Newtonian order»; Phys. Rev. **D87**, p. 044 009 (2013). 1209.6349. 34

[126] K. Arun, A. Buonanno, G. Faye & E. Ochsner; «Higher-order spin effects in the amplitude and phase of gravitational waveforms emitted by inspiraling compact binaries: Ready-to-use gravitational waveforms»; Phys. Rev. D **79**, p. 104 023 (2009)arXiv:0810.5336. 34

[127] K. Thorne; «Multipole expansions of gravitational radiation»; Rev. Mod. Phys. **52**, p. 299–339 (1980). 39, 63

[128] G. Faye, S. Marsat, L. Blanchet & B. R. Iyer; «The third and a half post-Newtonian gravitational wave quadrupole mode for quasi-circular inspiralling compact binaries»; Class. Quant. Grav. **29**, p. 175 004 (2012)arXiv:1204.1043[gr-qc]. 41, 67, 68, 144

[129] L. Blanchet & T. Damour; «Radiative gravitational fields in general relativity. I. general structure of the field outside the source»; Phil. Trans. Roy. Soc. Lond. A **320**, p. 379–430 (1986). 42, 43, 46, 47, 51, 59, 77

[130] L. Blanchet; «Quadrupole-quadrupole gravitational waves»; Class. Quant. Grav. **15**, p. 89–111 (1998)gr-qc/9710037. 43, 47, 48

[131] L. Blanchet & T. Damour; «Hereditary effects in gravitational radiation»; Phys. Rev. D **46**, p. 4304–4319 (1992). 44, 47

[132] L. Blanchet; «Gravitational-wave tails of tails»; Class. Quant. Grav. **15**, p. 113–141 (1998)gr-qc/9710038. 44, 50, 51, 56, 57, 58, 62, 63, 67, 68, 71

[133] G. Faye, L. Blanchet & B. R. Iyer; «Non-linear multipole interactions and gravitational-wave octupole modes for inspiralling compact binaries to third-and-a-half post-Newtonian order»; Class. Quant. Grav. **32**, p. 045 016 (2015)arXiv:1409.3546[gr-qc]. 65, 67, 68

[134] L. Blanchet, T. Damour, B. R. Iyer, C. M. Will & A. G. Wiseman; «Gravitational radiation damping of compact binary systems to second post-Newtonian order»; Phys. Rev. Lett. **74**, p. 3515–3518 (1995)gr-qc/9501027. 67

[135] L. Blanchet, T. Damour, G. Esposito-Farèse & B. R. Iyer; «Gravitational radiation from inspiralling compact binaries completed at the third post-Newtonian order»; Phys. Rev. Lett. **93**, p. 091 101 (2004)gr-qc/0406012. 67, 127

[136] T. Tanaka, H. Tagoshi & M. Sasaki; «Gravitational Waves by a Particle in Circular Orbit around a Schwarzschild Black Hole: 5.5 Post-Newtonian Formula»; Prog. Theor. Phys. **96**, p. 1087–1101 (1996)gr-qc/9701050. 67, 73

[137] R. Fujita; «Gravitational radiation for extreme mass ratio inspirals to the 14th post-Newtonian order»; Prog. Theor. Phys. **127**, p. 583 (2012)arXiv:1104.5615[gr-qc]. 67, 73

[138] R. Fujita; «Gravitational Waves from a Particle in Circular Orbits around a Schwarzschild Black Hole to the 22nd Post-Newtonian Order»; Prog. Theor. Phys. **128**, p. 971 (2012)arXiv:1211:5535[gr-qc]. 67, 73

[139] L. Blanchet, G. Faye & B. Whiting; «Half-integral conservative post-Newtonian approximations in the redshift factor of black hole binaries»; Phys. Rev. D **89**, p. 064 026 (2014)arXiv:1312.2975[gr-qc]. 67

[140] L. Blanchet, B. R. Iyer & B. Joguet; «Gravitational waves from inspiralling compact binaries: Energy flux to third post-Newtonian order»; Phys. Rev. D **65**, p. 064 005 (2002)Erratum *Phys. Rev. D*, 71:129903(E), 2005; gr-qc/0105098. 68, 144

[141] I. Gradshteyn & I. Ryzhik; *Table of Integrals, Series and Products* (Academic Press) (1980). 70

[142] E. Poisson; «Gravitational-radiation from a particle in circular orbit around a black-hole. I. Analytical results for the nonrotating case»; Phys. Rev. D **47**, p. 1497–1510 (1993). 73

[143] H. Tagoshi & T. Nakamura; «Gravitational waves from a point particle in circular orbit around a black hole: Logarithmic terms in the post-Newtonian expansion»; Phys. Rev. D **49**, p. 4016–4022 (1994). 73

[144] M. Sasaki; «Post-Newtonian expansion of the ingoing-wave Regge-Wheeler function»; Prog. Theor. Phys. **92**, p. 17–36 (1994). 73

[145] H. Tagoshi & M. Sasaki; «Post-Newtonian expansion of gravitational-waves from a particle in circular orbit around a Schwarzschild black-hole»; Prog. Theor. Phys. **92**, p. 745–771 (1994)gr-qc/9405062. 73

[146] S. Mano, H. Susuki & E. Takasugi; «Analytic Solutions of the Teukolsky Equation and their Low Frequency Expansions»; Prog. Theor. Phys. **95**, p. 1079 (1996)gr-qc/9603020. 73

[147] S. Mano, H. Susuki & E. Takasugi; «Analytic Solutions of the Regge-Wheeler Equation and the Post-Minkowskian Expansion»; Prog. Theor. Phys. **96**, p. 549 (1996)gr-qc/9605057. 73

[148] S. Mano & E. Takasugi; «Analytic Solutions of the Teukolsky Equation and their Properties»; Prog. Theor. Phys. **97**, p. 213 (1997)gr-qc/9611014. 73

[149] F. Messina & A. Nagar; «Parametrized-4.5PN TaylorF2 approximants and tail effects to quartic nonlinear order from the effective one body formalism»; Phys. Rev. **D95**, p. 124 001 (2017). [Erratum: Phys. Rev.D96,no.4,049907(2017)]; 1703.08107. 73

[150] L. Blanchet; «Time asymmetric structure of gravitational radiation»; Phys. Rev. D **47**, p. 4392–4420 (1993). 78, 80, 96, 123

[151] O. Poujade & L. Blanchet; «Post-Newtonian approximation for isolated systems calculated by matched asymptotic expansions»; Phys. Rev. D **65**, p. 124 020 (2002)gr-qc/0112057. 78, 80, 81, 82

[152] L. Blanchet; «Second post-Newtonian generation of gravitational radiation»; Phys. Rev. D **51**, p. 2559–2583 (1995)gr-qc/9501030. 80

[153] L. Blanchet; «On the multipole expansion of the gravitational field»; Class. Quant. Grav. **15**, p. 1971–1999 (1998)gr-qc/9801101. 80, 82, 83, 84

[154] T. Damour, P. Jaranowski & G. Schäfer; «Conservative dynamics of two-body systems at the fourth post-Newtonian approximation of general relativity»; Phys. Rev. **D93**, p. 084 014 (2016). 1601.01283. 85, 97

[155] E. Poisson & C. M. Will; *Gravity, Newtonian, Post-Newtonian, Relativistic* (Cambridge University Press) (2014). 90

[156] L. Blanchet, T. Damour & G. Esposito-Farèse; «Dimensional regularization of the third post-Newtonian dynamics of point particles in harmonic coordinates»; Phys. Rev. D **69**, p. 124 007 (2004)gr-qc/0311052. 91, 92, 94, 140, 141

[157] L. Blanchet, T. Damour, G. Esposito-Farèse & B. R. Iyer; «Dimensional regularization of the third post-Newtonian gravitational wave generation of two point masses»; Phys. Rev. D **71**, p. 124 004 (2005)gr-qc/0503044. 94, 127

[158] L. Blanchet & A. Le Tiec; «First Law of Compact Binary Mechanics with Gravitational-Wave Tails»; Class. Quant. Grav. **34**, p. 164 001 (2017)1702.06839[gr-qc]. 121

[159] C. Königsdörffer, G. Faye & G. Schäfer; «The binary black-hole dynamics at the third-and-a-half post-Newtonian order in the ADM-formalism»; Phys. Rev. D **68**, p. 044 004 (2003)astro-ph/0305048. 122, 123

[160] S. Nissanke & L. Blanchet; «Gravitational radiation reaction in the equations of motion of compact binaries to 3.5 post-Newtonian order»; Class. Quant. Grav. **22**, p. 1007 (2005)gr-qc/0412018. 122, 123

[161] L. Blanchet & T. Damour; «Tail-transported temporal correlations in the dynamics of a gravitating system»; Phys. Rev. D **37**, p. 1410 (1988). 123

[162] L. Blanchet; «Gravitational radiation reaction and balance equations to post-Newtonian order»; Phys. Rev. D **55**, p. 714–732 (1997)gr-qc/9609049. 123

[163] L. Blanchet & B. R. Iyer; «Hadamard regularization of the third post-Newtonian gravitational wave generation of two point masses»; Phys. Rev. D **71**, p. 024 004 (2004)gr-qc/0409094. 133

[164] J. M. Martín-García, A. García-Parrado, A. Stecchina, B. Wardell, C. Pitrou, D. Brizuela, D. Yllanes, G. Faye, L. Stein, R. Portugal & T. Bäckdahl; «xAct: Efficient tensor computer algebra for Mathematica»; (GPL 2002–2012); http://www.xact.es/. 135

[165] L. Blanchet, G. Faye & B. Whiting; «High-order half-integral conservative post-Newtonian coefficients in the redshift factor of black hole binaries»; Phys. Rev. D **90**, p. 044 017 (2014)arXiv:1405.5151[gr-qc]. 140

Tanguy MARCHAND **15 Juin 2018**

Sujet : Études des ondes gravitationnelles des binaires compactes à l'approximation post-newtonienne.

Résumé : La détection ainsi que l'analyse des ondes gravitationnelles émises par les systèmes binaires d'objets compacts reposent sur notre capacité à faire des prédictions précises au sein de la théorie de la relativité générale. Dans cette thèse, nous utilisons la théorie post-newtonienne (PN), et en particulier le formalisme connu sous le nom de Blanchet-Damour-Iyer, afin d'étudier de tels systèmes. La finalité des différents calculs réalisés au sein de cette thèse est d'obtenir la phase du signal gravitationnel à l'ordre 4,5PN, et les résultats que nous présentons nous rapprochent fortement de cet objectif. Tout d'abord, nous calculons les sillages d'ondes à l'ordre 3 dans le champ radiatif, ce qui nous permet d'obtenir le coefficient 4,5PN du flux d'énergie émis par des systèmes binaries compacts sans spin dans le cas d'orbites circulaires. Puis, nous calculons la dernière ambiguité apparaissant dans les équations du mouvement de deux corps compacts sans spin à l'ordre 4PN, ce qui nous permet d'obtenir la première dérivation à partir de principes fondamentaux de ce résultat. Nous étudions alors en détail les différentes quantités conservées générées par cette dynamique. Enfin, nous présentons un premier résultat préliminaire du quadrupôle de masse source à l'ordre 4PN, ce qui constitue l'une des étapes cruciales dans l'obtention de la phase à l'ordre 4.5PN.

Mots clés : théorie post-newtonienne, ondes gravitationnelles, système binaire compact

Subject : Studying gravitational waves of compact binary systems using post-Newtonian theory.

Abstract: The detection and the analysis of gravitational waves emitted by compact binary systems rely on our ability to make accurate predictions within general relativity. In this thesis, we use the post-Newtonian (PN) formalism, and in particular the Blanchet-Damour-Iyer framework, to study the dynamics and the emission of gravitational waves of such systems. The different computations that we performed are motivated by our aim to obtain the phase of the gravitational wave signal at the 4.5PN order. In that regard, crucial steps have been achieved within this thesis. First of all, we compute the third-order tail effects in the radiation field, yielding the 4.5PN coefficient of the energy flux for binaries of non-spinning objects in circular orbits. Besides, we determine the remaining ambiguity of the 4PN Lagrangian of two spinless compact bodies. This result completes the first derivation from first principles of the 4PN equations of motion. Then we comprehensively study the conserved quantities of the 4PN dynamics. Finally, we provide a preliminary result of the 4PN source mass quadrupole, which constitutes one of the crucial steps towards the computation of the 4.5PN phase.

Keywords : Post-newtonian theory, gravitational waves, compact binary system